Elucidating the role of mTOR kinase in chronic lymphocytic leukaemia cell migration

Ailsa Holroyd

University of Glasgow

College of Medical, Veterinary & Life Sciences

PhD thesis

Abstract

Chronic lymphocytic leukaemia is a mature B cell neoplasm which, despite recent focused research attention, remains incurable. It is the commonest leukaemia in the Western world and affects around 3,500 patients per annum in the UK and with the median age of those diagnosed at around 70 years it poses a specific challenge in disease management with standard chemoimmunotherapy being potentially too toxic for many patients. Treatments targeting the B cell receptor (BCR)-mediated signals including ibrutinib and idelalisib which target BTK and PI3K respectively, have pronounced clinical effects with improvement in progression-free and overall survival for significant patient numbers and are becoming more widely available. However, issues of disease resistance mutations and clonal evolution leave scope for novel targets of BCR and related signalling pathways. My hypothesis is that the serine/threonine protein kinase mechanistic target of rapamycin (mTOR) signalling which is located downstream of BTK and PI3K and downstream of BCR signalling offers a promising therapeutic target in CLL and may complement existing therapies that have proven clinical efficacy. Furthermore, dual mTORC1/2 inhibition offers a potential mechanism for overcoming the negative feedback loop which internally regulates mTOR kinase thus may offer potential for an improvement on the mTORC1 inhibitors already tested in clinical trial.

Project Aims

1. To explore the molecular effects of mTOR inhibition on CLL cell migration *in vitro*.

2. To investigate the functional effects of mTOR kinase inhibition on CLL cell migration.

3. To examine the regulation of CLL cell migration by small GTPases and the effects of mTOR inhibition.

Table of Contents

List of Tables

List of Figures

List of Primary CLL samples

Sample ID	Age	Sex	Binet stage	Cytogenetics	ZAP70
8	65	F	A	11q-	-
9	76	F	B	N	-
12	65	F	B	13q-	-
16	82	F	A	N	+
18	67	F	B	11q-	+
28	75	F	A	17p-	+
32	61	F	A	N	+
42	80	F	B	N	+
44	69	F	A	N	-
46	58	F	A	N	+
52	84	F	B	11q-	-
57	78	M	C	N	+
69	50	M	A	N	+
72	52	F	A	N	+
76	52	F	A	6q-	+
77	67	M	A	N	-
80	62	M	C	17p-	-
85	63	F	A	11q-	N/A
86	68	F	A	11q-	+
88	43	F	A	N	-
90	67	F	B	N	+
92	78	M	C	11q-	+
93	68	M	C	17p-	+
95	74	M	A	N	N/A
98	71	M	B	17p-	-
104	68	M	A	N	-
106	57	M	B	N	+
108	66	F	C	N	+
109	N/A	M	B	17p-	N/A
113	50	F	C	17p-	+
114	62	M	B	N	+
116	69	M	A	N	+
118	68	M	B	11q-	+
119	67	F	B	17p-	N/A
120	60	M	C	N	+
122	64	M	B	17p-	-
126	69	M	B	N	+
130	58	F	B	N	N/A
132	71	F	B	17p-	+
133	59	F	C	N	-

136	46	M	C	11q-	+
137	73	M	B	N	-
138	66	F	B	N	+
139	54	F	B	11q-	-
140	62	F	C	trisomy 12	-
142	65	F	B	N	+
143	58	F	C	11q-	+
144	73	M	B	17p-	-
147	74	M	C	N	+
148	48	M	B	11q-	-
149	62	M	B	17p-	N/A
152	62	M	B	N	-
153	74	M	B	11q-	-
154	60	M	C	N	+
155	49	M	B	11q-	N/A
157	64	M	B	11q-	N/A
158	74	M	C	N	N/A
159	67	M	C	N	N/A
160	66	M	C	trisomy 12	N/A

M = Male, F = Female, + positive, - negative, N/A = not available

List of Antibodies for Western blot

Specificity	Species	Dilution	Manufacturer
AKT	rabbit	1:1000	Cell Signalling Technology ®
p-AKT (Ser473)	rabbit	1:1000	Cell Signalling Technology ®
GAPDH	rabbit	1:1000	Cell Signalling Technology ®
MCL-1	rabbit	1:1000	Cell Signalling Technology ®
NDRG1	rabbit	1:1000	Cell Signalling Technology ®
pNDRG1 (Thr346)	rabbit	1:1000	Cell Signalling Technology ®
S6	mouse	1:1000	Cell Signalling Technology ®
pS6 (Ser235/236)	rabbit	1:1000	Cell Signalling Technology ®
4EBP1	rabbit	1:1000	Cell Signalling Technology ®
p4EBP1 (Ser65)	rabbit	1:1000	Cell Signalling Technology ®
anti-rabbit goat IgG, HRP-linked	rabbit	1:2000	Cell Signalling Technology ®
anti-mouse horse IgG, HRP-linked	mouse	1:2000	Cell Signalling Technology ®
IRDye® 680RD goat IgG (H + L)	mouse	1:15000	Li-Cor®
IRDye® 680RD goat IgG (H + L)	rabbit	1:15000	Li-Cor®
BCL-2-like Protein 11	rabbit	1:1000	Cell Signalling Technology ®
BCL-2-like Protein 1	rabbit	1:1000	Cell Signalling Technology ®
BCL-2	mouse	1:1000	Cell Signalling Technology ®
Rap1	mouse	1:1000	Santa Cruz Biotechnology
Rap1	rabbit	1:1000	Cell Signalling Technology ®
Rac1	mouse	1:1000	Merck Millipore
Rac1	mouse	1:1000	ThermoFisher Scientific
pFOXO1 (Thr24)	rabbit	1:1000	Cell Signalling Technology ®
FOXO1A	rabbit	1:1000	Cell Signalling Technology ®
pS6K1 (Thr389)	rabbit	1:1000	Cell Signalling Technology ®
S6K1	rabbit	1:1000	Cell Signalling Technology ®
PARP	rabbit	1:1000	Cell Signalling Technology ®

List of Antibodies for Immunofluorescence

Specificity	Species	Dilution	Manufacturer
Rap1	rabbit	1:200	Santa Cruz
Phalloidin	toxin	1:200	Invitrogen Ltd.
Anti-rabbit	goat	1:200	Invitrogen Ltd.
Anti-rabbit	goat	1:200	Invitrogen Ltd.
Anti-mouse	goat	1:200	Invitrogen Ltd.
EEA-1	mouse	1:100	Abcam Plc.
LAMP-1	mouse	1:20	Abcam Plc.

List of Antibodies for Flow Cytometry

Description	Reactivity	Clone	Format	Isotype	Manufacturer
CD5	Human	UCHT2	FITC	Mouse IgG1, κ	BD Biosciences
CD11a	Human	HI111	BV510	Mouse IgG1, κ	BD Biosciences
CD19	Human	SJ25-C1	APC-Cy7	Mouse IgG1, κ	BD Biosciences
CD19	Human	SJ25C	PE-Cy7	Mouse IgG1, κ	BD Biosciences
CD38	Human	HIT2	V450	Mouse IgG1, κ	BD Biosciences
CD44	Human	G44-26	APC	Mouse IgG2b, κ	BD Biosciences
CD49d	Human	9F10	APC	Mouse IgG1, κ	BD Biosciences
CD62L	Human	DREG-56	PE	Mouse IgG1, κ	BD Biosciences
CD184 (CXCR4)	Human	12G-5	PE-Cy7	Mouse IgG2a, κ	BD Biosciences
CD185 (CXCR5)	Human	RF8-B2	PerCP-Cy5.5	Rat IgG2b, κ	BD Biosciences
CD184 (CXCR4)	Mouse	2B11/CXCR4	PE	Rat IgG2b, κ	BD Biosciences
CD19	Mouse	1D3	APC-Cy7	Lewis IgG2a, κ	BD Biosciences
CD19	Mouse	1D3	PE-Cy 7	Lewis IgG2a, κ	BD Biosciences

List of Manufacturers and Distributors

Manufacturer name	Distributor	Address
Abcam	Abcam Plc	Cambridge, UK
BD Biosciences	BD Biosciences	Wokingham, UK
BioRad	BioRad Laboratories Ltd	Watford, UK
Biolegend	BioLegend UK Ltd	London, UK
Bioline	Bioline Reagents Ltd	London, UK
Carl Zeiss Microscopy	Carl Zeiss Ltd	Cambridge, UK
CoStar	Sigma-Aldrich Company Ltd	Gillingham, UK
Cell Signalling	New England BioLabs Ltd	Hitchin, UK
eBiosciences	Fisher Scientific - UK Ltd	Loughborough, UK
Gibco	Fisher Scientific - UK Ltd	Loughborough, UK
Greiner	Greiner Bio-One Ltd	Stonehouse, UK
Hendley	C.A. Hendley Ltd	Essex, UK
Invitrogen	Fisher Scientific - UK Ltd	Loughborough, UK
Jackson ImmunoResearch	Stratech Scientific Ltd	Ely, UK
Li-Cor	Li-Cor Biotechnology UK Ltd	Cambridge, UK
Merck	Merck Chemicals Ltd	Nottingham, UK
Merck Millipore	Millipore Laboratories UK	Watford, UK
Peprotech	Peprotech EC Ltd	London, UK
Pierce	Fisher Scientific - UK Ltd	Loughborough, UK
Santa Cruz	Santa Cruz Biotechnology, Inc.	Heidelberg, Germany
Sigma-Aldrich	Sigma-Aldrich Company Ltd	Gillingham, UK
Scientific Laboratory Supplies	Scientific Laboratory Supplies Ltd	Newhouse, UK
Thermofisher	Fisher Scientific - UK Ltd	Loughborough, UK

Acknowledgements

I would like to express my thanks to my supervisors Dr. Alison Michie and Dr. Alison McCaig for their consistent support and advice throughout the course of my studies. Dr. Alison McCaig has offered me guidance with experimental design and has been a steady source of advice in relation to my experimental findings and data analysis. Both Dr. Alison McCaig and Dr. Mike Leach have provided me with clinical samples to facilitate the experiments described in this thesis. Dr. Alison Michie has been an excellent tutor and has given me a robust training in scientific thought and writing. She has taught me to design experiments and to evaluate the scientific work of others critically, assisting me to develop an understanding of my own work in the wider context to which it belongs. I'd like to thank her for her assistance with the writing and review of this manuscript. Also, I wish to thank Dr. Heather Jørgensen and Dr. Helen Wheadon for their advice and support. I am grateful to Prof. Tessa Holyoake and Prof. Mhairi Copland for their guidance and career support. Next, I would like to express my gratitude to the Kay Kendall Leukaemia Fund and to the University of Glasgow for providing the funding support for these experiments. I'd also like to thank both current and former members of Dr. Michie's research group, including Dr. Jodie Hay, Dr. Emilio Cosimo, Dr. Anuradha Tarafdar, Dr. Odette Middleton, PhD students Natasha Malik and Michael Moles, Jennifer Cassels, Karen Dunn and all of the staff at the Paul O' Gorman Leukaemia Research Centre for their advice in relation to experimental design, for their assistance with the completion of experiments and for their advice with regard to data analysis. I'd like to thank the thesis submission support team at the University of Glasgow, namely, Blair Thompson, for providing IT support.

Lastly, I would like to highlight the contribution of my friends and family for their invaluable support for me in the completion of my PhD studies. In particular, I'd like to thank my husband, David Holroyd, my mother, Una Neil and my father, James Neil.

Author's Declaration

I declare that this thesis and the work presented in it are my own work which has been generated by me as a result of my own original research.

Ailsa Holroyd

November 2018

Definitions/abbreviations

Activation-induced cytidine deaminase	AID
Autoimmune haemolytic anaemia	AIHA
Aicardi-Goutieres syndrome	AGS
Allogeneic stem cell transplantation	AlloSCT
Absolute lymphocyte count	ALC
A proliferation-inducing ligand	APRIL
Ataxia telangiectasia mutated	ATM
B cell activating factor	BAFF
Baculoviral IAP repeat containing 3	BIRC3
B cell lymphoma 2	BCL-2
BCL-2 like protein 1	BCL2L1
BCL-2 like protein 11	BCL2L11
B cell receptor	BCR
B cell linker protein	BLNK
Bone Marrow	BM
B-Raf proto-oncogene	BRAF
Bruton's tyrosine kinase	BTK
C-C motif chemokine ligand 3	CCL3
C-C motif chemokine ligand 4	CCL4
Chromatin immunoprecipitation sequencing	ChIP-Seq
Chronic Lymphocytic Leukaemia	CLL
Cluster of differentiation	CD
Cytomegalovirus	CMV
Class switch recombination	CSR
Complete remission	CR
Computed tomography scan	CT
C-X-C chemokine receptor type 4	CXCR4
C-X-C chemokine receptor type 5	CXCR5
C-X-C motif chemokine 12	CXCL12
Direct Antiglobulin	DAT
Deoxyribonucleic acid	DNA
Diffuse Large B Cell Lymphoma	DLBCL
Epstein-Barr virus	EBV
Early Growth Response 2 gene	EGR2
Focal adhesion kinase	FAK
Flow Cytometry	FC
^{18}Fluorodeoxyglucose	^{18}FDG
Fluorescent In Situ Hybridisation	FISH
Follicular lymphoma	FL
Germinal centre	GC
Guanosine diphosphate	GDP
Guanosine triphosphate	GTP
Genome wide association study	GWAS

Hyaluronic acid	HA
High count monoclonal B cell lymphocytosis	HC-MBL
Hodgkin Lymphoma	HL
Harakiri	HRK
Inhibitors of apoptosis	IAP
Immunoglobulin heavy chain	IgV_H
Immunoglobulin class D	IgD
Immunoglobulin class M	IgM
Immunohistochemistry	IHC
Immunoreceptor tyrosine-based activation motif	ITAM
Immune thrombocytopenic purpura	ITP
Low count monoclonal B cell lymphocytosis	LC-MBL
Lactate dehydrogenase	LDH
Lymph node	LN
Mucosa-associated lymphoid tissue	MALT
Monoclonal B cell lymphocytosis	MBL
Myeloid cell leukaemia 1	MCL-1
Multiple myeloma	MM
Messenger ribonucleic acid	mRNA
Micro ribonucleic acid	miRNA
Minimal residual disease	MRD
Marginal zone lymphoma	MZL
Non-relapse mortality	NRM
Nuclear factor kappa-light-chain-enhancer	NFkβ
Overall survival	OS
Phosphatidylinositol (4,5)-triphosphate	PIP3
Phosphoinositide 3'-kinase	PI3K
Peripheral Blood	PB
Programmed Death Ligand 1	PD-L1
Positron emission tomography/computed tomography	PET-CT
Progression-free survival	PFS
Phospholipase gamma C 2	PLCγ2
Protein kinase C	PKC
Polymerase Chain Reaction	PCR
Protector of Telomeres 1 gene	POT1
p53 upregulated modulator of apoptosis	PUMA
Partial remission	PR
Receptor Tyrosine Kinase Like Orphan Receptor 1	ROR1
Roswell Park Memorial Institute - 1640 medium	RPMI-1640 medium
Ribonucleic acid	RNA
Richter's Syndrome	RS
Stromal cell-derived factor 1	SDF-1
Splicing factor 3b subunit 1	SF3B1
Src homology 2	SH2

Somatic hypermutation	SHM
Small lymphocytic lymphoma	SLL
B cell linker protein/BLNK	SLP-65
single nucleotide polymorphism	SNP
Spleen tyrosine kinase	SYK
Regulatory T cells	Treg
T cell leukaemia/lymphoma 1 gene	TCL-1
Telomere repeat binding factor 2	TERF2IP
Tumour protein p53	TP53
Untranslated region	UTR
Vascular Cell Adhesion Molecule 1	VCAM-1
Exportin 1 gene	XPO1
Zeta-associated protein - 70 kD	ZAP-70

Chapter 1 Introduction

1.1 CLL epidemiology

1.1.1 Disease incidence and prevalence

Chronic lymphocytic leukaemia (1) is the most frequently occurring leukaemia in the Western world, with an incidence of 4-5/100000 each year in countries such as the UK, USA, Ireland and Australia and with around 3500 new cases in the UK alone (2, 3). Also, with reference to the UK's data on CLL, the disease accounts for around 1% of all new cancer cases however less than 1% of all cancer deaths are attributable to CLL. Each year there are around 1000 deaths from the disease in the UK alone. CLL is a disease which shows a male predominance; there is a lifetime risk of the disease of 1/155 for men and around 1 in 260 for women (3). CLL rates have increased by 14% since the 1990s which represents an increase for male and female patients and for both genders together (4). As with other cancers, CLL incidence increases with age and this is most likely due to the associated acquisition of DNA damage and cumulative exposure to disease risk factors. It is of note that age-specific incidence increases markedly from age 45-49 with the gender differences in incidence being most marked in this age category. Some families display multiple members with the CLL or with related lymphomas therefore CLL has been attributed as one of the most heritable cancers (5). There do not appear to be any significant differences in clinical features of so-called "familial CLL" from sporadic cases and the search is underway for specific predisposing germline mutations (6). It seems that the risk of solid tumours is not increased in association with CLL from the original cohort of study of familial CLL cases however it has since been concluded that CLL does increase the risk of a second malignancy and of skin tumours in particular (5, 7).

1.1.2 Demographic distribution of CLL patients

CLL rates show a strong age correlation with 4 in 10 cases being diagnosed in people aged 75 or older. Of interest, 5-11% of affected individuals are <55 years of age and this patient population were historically believed to have a poorer prognosis although this was derived from early studies predating many advances in CLL care (2). It is now known that CLL in younger patients carries a preponderance of high-risk features which may explain the poorer outcome,

based on a large-scale study of biomarkers (8). Furthermore, CLL median survival is in the order of 5 to 10 years, dependent upon risk factor status, and comorbid disease incidence increases with age, such that younger patients are significantly more likely to die of their disease (4). Of recent new UK cases diagnosed in 2014, 63% were in male patients as opposed to 37% in female patients and the mortality rates do not differ significantly for gender. The mainstay of CLL patients are from countries such as the UK, USA, Ireland and Australia and the disease displays a predilection for people of Caucasian origin. There is a paucity of cases in people of Asian descent; rates are 5 to 10-fold lower than those of Caucasians, which suggests that the disease is a product of both genetic and environmental risk factors. However, it is notable that the relative lower disease incidence in Asians is not affected by geographical migration of individuals to higher-risk regions (9).

1.2 Clinical features of CLL

CLL is defined as a malignant B cell neoplasm which differs from its counterpart, small lymphocytic lymphoma (SLL), due to the circulating lymphocyte population in the peripheral blood (PB). The patient's clinical history is an important feature for evaluation at diagnosis and at clinical review which, which may comprise frequent infections and which may indicate the existence of lymphadenopathy or splenomegaly which may be confirmed upon clinical examination. In addition to clinical history-taking and physical examination, the diagnostic procedure commonly involves the evaluation of the lymphocyte count, PB smear and immunophenotyping characterisation of the aberrant lymphoid population.

1.2.1 Lymphocytosis: immunophenotypic and morphological features

The clinical diagnosis of CLL requires the presence of monoclonal B cell populations at >5 X 10^9/l in the PB with characteristic immunophenotypic features which consists of CD5, CD19, CD22 and CD23 positivity, FMC7 negativity and weak expression (+/-) of surface immunoglobulin (SmIg). A diagnostic score has been developed to incorporate 5 of these markers with high sensitivity for the diagnosis of CLL. The diagnostic score is based on the probability of a PB

specimen conforming to the diagnostic entity of CLL, to aid distinction of CLL from conditions such as mantle cell or marginal zone lymphoma. The features of the CLL score are described in Table 1-1 and a score of at least 4/5 is found to be a feature of 87% of cases of CLL. A high CLL score has been shown to correlate strongly with the typical morphological features of CLL and where 3/5 of the listed conditions are present an alternative diagnosis should be sought (10). A range of alternative markers have been proposed as providing an alternative diagnostic score however none to date have superseded the Matutes score (11, 12).

Table 1-1 Scoring system for CLL
An immunophenotypic score based on flow cytometric analysis of peripheral blood whereby a score of >/= 4/5 is indicative of a diagnosis of CLL and a score of </= 3/5 should encourage consideration of an alternative diagnosis (10).

Cell surface marker	1 point	0 point
Surface immunoglobulin	Weak	moderate/strong
CD5	Positive	Negative
CD22 /CD79b	Negative	Positive
CD23	Positive	Negative
FMC7	Negative	Positive

In cases of atypical CLL there may be modifications to the immunophenotype and in practice 92% of CLL cases score 4 or 5, 6% score 3 and 2% score 1 or 2 (13).

CLL displays characteristic features on examination of PB smear: a population of lymphoid cells is visible; these are small and monotypic with a dense nucleus containing visible nucleoli and some chromatin aggregation, with a small border of cytoplasm. CLL cells are more fragile than the non-malignant lymphocyte population and on preparation of PB films for examination there may be the pathognomonic finding of “smudge” or “smear cells” whose appearance is

attributable to the cytoplasmic fragments which are breakdown products of CLL cells.

1.2.2 **Hypogammaglobulinaemia and immune deficit**

Mature B cell malignancies such as CLL share clinical features of immune system compromise which are mainly attributable to the associated loss of γ–globulin production. The process of CLL cell malignant transformation requires subversion of normal cellular functions such as production of immunoglobulin. As the malignant B cell population gradually out-competes the healthy B cell population with and through immune dysregulation by mechanisms that are not yet clearly defined, there is immune paresis. One consequence of the malignant clonal progression in CLL is the reduction in serum γ–globulin levels, sufficient to impair humoral immunity.

1.2.3 **Autoimmune features and associations**

There are widely recognised associations between CLL and autoimmune disease, in particular, autoimmune haemolytic anaemia (AIHA) and immune thrombocytopenic purpura (14). The biological basis for the association is complex and not yet fully understood but is believed to be based upon the ability of CLL cells to promote the production of polyclonal autoantibody. CLL cells may interact with T cells in the disease microenvironment by presenting autologous red blood cell antigens; the T cell population expands and interacts with normal B cells to provoke the production of antibody (15). Despite some CLL cells retaining the ability to produce immunoglobulin, it is rare that an autoreactive clone produces sufficient autoantibody to cause clinical disease; although limited in repertoire it is more usual for CLL cells to secrete polyclonal antibody; the biological basis for the majority of immune manifestations of CLL (16). CLL therapy with fludarabine may be complicated by AIHA and fludarabine is avoided as a therapeutic strategy in patients with AIHA as the drug may worsen the haemolysis. It is not fully understood as to how fludarabine may worsen haemolysis in CLL however it may be that fludarabine acts to remove the suppression of a pre-existing red cell autoantibody (17). The finding of a low platelet count in untreated CLL patients requires further investigation to delineate ITP from bone marrow infiltration as the latter carries a significantly

poorer prognosis and will require monitoring and follow up (18). Although patients with autoimmune cytopenias are typically believed to have a worse prognosis than those without, there are conflicting reports as to the impact on overall patient prognosis and association with other risk factors (14, 19). AIHA has been found in association with an unmutated immunoglobulin heavy chain (IgV_H) and with a positive direct antiglobulin test, but as only patients requiring CLL therapy are likely to have had screening for prognostic markers, there may have been bias introduced with this finding (20). Furthermore, the same population studied for ITP associations found no association between ITP and IgV_H mutational status (21). Hypothetically, the basis for AIHA as a cause of worse overall outcomes in CLL is that the individual likelihood of CLL cell exposure to red cell antigen increases, for example in the shared environment of the spleen, which may be enlarged. The presence of AIHA may therefore correlate with advanced disease stage in CLL which in turn confers a poorer prognosis. All cytopenias in CLL require careful consideration in their diagnosis and management to promote the overall health of the patient and to permit safe and successful completion of CLL therapy.

1.2.4 **Richter's syndrome**

In around 5% of patients affected by CLL, their clinical course includes the potential for high-grade transformation of disease known as Richter's syndrome (RS) (22). This, rare and often intractable condition, manifests most commonly as non-Hodgkin Diffuse Large B Cell Lymphoma (DLBCL) (90%) but may alternatively be similar in pathology to Hodgkin lymphoma (HL) in 10% of cases (23). Investigation for RS is indicated in response to clinical presentation of the patient with "night sweats" or weight loss, known as "B symptoms", a rapid increase in palpable lymph node (LN) number and/or size and a marked increase in serum Lactate Dehydrogenase (LDH) on PB sampling. Patients are investigated further by PET CT where available and positive findings include a demonstrable increase in ^{18}Fluorodeoxyglucose (^{18}FDG)-avidity in regions of disease transformation, relative to the background activity of CLL-affected nodes (24). Histopathological findings on LN biopsy in affected nodes typically include effacement of LN architecture by a monomorphic B cell population which carries a high Ki67% on immunohistochemistry with concomitant background of the original CLL which differs by its largely low Ki67% index and by CD5 positivity.

Management of RS is dependent upon histological subtype and clinical trial entry should be sought where suitable trials are available. Median survival of patients with RS is currently <1 year therefore this remains an area in need of directed research effort (25). For patients able to achieve a remission with chemoimmunotherapy for Richter's syndrome, salvage with allogeneic stem cell transplantation (AlloSCT) may be an option.

1.3 Disease monitoring and identification of relapse

1.3.1 Disease staging and prognostication

There is a spectrum of disease presentation in CLL from disease which is mainly confined to the PB, to that which manifests as bulky lymphadenopathy. Associations between CLL immunophenotype and cytogenetic subset have been identified in relation to LN involvement. Moderate splenomegaly is a common clinical feature but medical imaging may be required to identify subtle enlargement. The underlying aetiology of splenomegaly may be uncertain in the context of an AIHA, also splenomegaly may be associated with splenic pooling of platelets which in turn causes thrombocytopenia. SLL requires histopathological assessment of LN biopsy. Clinical features of lymphadenopathy and splenomegaly are present in SLL but the PB lymphocyte count should not reach measurement levels of >5 x 10^9/l (26). Because investigation, management and monitoring of SLL is equivalent to CLL, these diagnostic entities shall be regarded as synonymous hereinafter.

The clinical course of CLL varies widely from an almost indolent disorder to a rapidly progressive condition which leads to an early death. In general, CLL is a disease which follows a relapsing and remitting course; it is largely an incurable disease, except for the intervention of AlloSCT, an intensive therapy restricted to patients with a low level of comorbidity. The overwhelming majority of patients with CLL are therefore ineligible for curative therapy, thus the aim of their treatment is to prolong their progression-free (PFS) or overall survival (OS). Individual patient prognosis may be classified using a disease-based risk score derived from either of the Rai and Binet scoring systems (27, 28). The Binet staging system is in more widespread use in the UK and it integrates clinical features as described in Table 1-2.

Table 1-2 Binet staging system.
Disease stage relates to survival with stage A median patient survival duration at >10 years, stage B at >8 years and with stage C at approximately 6.5 years.

Stage	Clinical features
A	Lymphocytosis, does not meet criteria for stages B and C
B	>/= 3 areas of lymphadenopathy, does not meet criteria for stage C
C	Anaemia (Hb <10 g/dL) or thrombocytopenia (platelets <100 x 10^9/L)

Patients of Binet stage A CLL may be characterised as having greater longevity, fewer relapses and are less likely to require CLL therapy. Negative outcomes increase in frequency from stage A to B with stage C disease conferring the poorest prognosis in terms of PFS and OS. In addition to disease-specific markers, the presence or absence of which define patient prognosis and shall be discussed in section 1.6, clinical trials are in progress to create and refine prognostic tools and markers and this shall be discussed. Evaluation of the patient with CLL at the time of diagnosis is performed with attention to available national guidelines with the aim of establishing the timing and indication for therapy. In addition to the armamentarium of investigational tests below, the patient's clinical condition may dictate the necessity for treatment in the absence of any other indication. Terms used to describe responses to therapy find their origin in clinical trial protocols but their use may be extended to routine clinical practice, such terms include partial (PR) or complete (CR) response. Estimation of prognostic markers such as Zeta-associated-protein kinase 70 (ZAP-70) and Fluorescence *In Situ* Hybridisation studies do not represent an indication for therapy so shall be dealt with separately (29).

1.3.2 **Physical examination**

Once a diagnosis of CLL has been established, patients should be evaluated for cervical, axillary and inguinal lymphadenopathy with measurement of maximal LN size in each region in 2 dimensions, and the presence and extent of hepato- or splenomegaly should be recorded.

1.3.3 **Peripheral Blood sampling and Bone Marrow biopsy**

After diagnostic blood counts and evaluation of prognostic parameters, serial PB sampling is performed to monitor disease progression. Disease progression in need of treatment may not always be discernible from the absolute lymphocyte count however lymphocyte doubling time of </= 1 yr may be indicative of a need to start CLL therapy (30). BM aspirate and biopsy sampling is recommended prior to the initiation of myelosuppressive therapy and either to monitor treatment response, in the context of clinical trials, as per protocol, or in the investigation of cytopenias.

1.3.4 **Minimal residual disease monitoring by flow cytometry and PCR**

Recent advances in the understanding of CLL biology have contributed to the development of techniques to monitor low levels of disease which remain after completion of therapy; these levels are referred to as “minimal residual disease” or MRD. The monitoring of MRD requires the existence of a disease-specific marker and requires the ready availability of an assay to permit routine clinical testing at pre-specified time-points in line with clinical trial protocols. The benefits of MRD negativity were demonstrated first with the use of alemtuzumab which showed an improved survival with MRD eradication (31). The assays for monitoring MRD were developed further for use in monitoring of response to chemoimmunotherapy regimens (32). Some of the earliest trial data on MRD arose from the CLL8 study which established the superiority of chemoimmunotherapy over chemotherapy alone (33). MRD was found to predict OS and PFS independently of other parameters and MRD negativity associated more strongly with the chemoimmunotherapy arm (33). Monitoring may be performed to establish MRD status in CR or it may be employed as a tool to detect relapse at an early stage. Optimal schedules of monitoring for MRD and

clinical implications are the subject of current clinical trials to enable a schedule for testing that may be applied universally. Flow cytometry (FC) may be used to determine the presence of cells with a disease-specific immunophenotype. Allele-specific primers may facilitate disease monitoring by polymerase chain reaction (PCR) and markers may be screened for using either PB or BM sampling and the site of MRD testing and test positivity has implications for patient prognosis. In general, a threshold of 10^4 is used as the limit of detection however this may be lowered as the sensitivity of assays are improved. Recent study has confirmed an association between MRD negativity and improved PFS in CLL, incorporating data from a number recent trials including CLL8, CLL10 and CLL11 to establish MRD as a primary end point in randomised clinical trials (34).

1.3.5 **CT/ PET-CT scanning**

Clinical staging of CLL is not reliant upon CT scan findings however CT scanning is often utilised by clinical trials as a means of assessing disease response. Where CT scans are in use, one scan is to be performed prior to the initiation of therapy and a subsequent scan is indicated at the end of therapy if abnormalities were detected at the outset. PET CT scanning is not routinely indicated in CLL except as part of the diagnostic workup for suspected cases of Richter's syndrome (RS).

1.4 CLL disease management

Individual cases and their relative eligibility for therapy are assessed using parameters such as the CLL International Prognostic Index (CLL-IPI) in Table 1-3 which aid clinical decision-making relation to timing and intensity of therapy.

Table 1-3 The CLL International Prognostic Index (CLL-IPI).
A risk score may be calculated for each patient, based upon integrated CLL-IPI parameters to aid prediction of time to first treatment in CLL (35).

Variable	Adverse factor	Grading
(17p)/TP53	Deleted and/or mutated	4
IGHV mutation status	Unmutated	2
B2M, mg/L	>3.5	2
Clinical stage	Binet B/C or Rai I-IV	1
Age	>65 years	1
	Prognostic score	**0-10**

1.4.1 **Chemoimmunotherapy**

The current standard of care in CLL first-line regimen for "fit" patients is a combination of purine analogue fludarabine, alkylating agent cyclophosphamide and monoclonal anti-CD20 antibody, rituximab (FCR). The original study which established fludarabine as first-line alkylating agent contrasted the PFS of CLL patients on fludarabine as a single agent with that of chlorambucil-treated patients (36). Later, as reported by the CLL4 trial, fludarabine in combination with cyclophosphamide was found to have greater PFS than either fludarabine or cyclophosphamide alone (37). The development of chimeric monoclonal antibodies directed at the CD20 changed the landscape of combination therapy for all types of B cell malignancy. CLL has a relatively low CD20 expression and high lymphocyte counts compared with other B cell malignancies such that responses to a single agent rituximab regimen were poor, but when introduced in addition to FC demonstrated superior PFS and OS to the chemotherapy-only regimen as part of the CLL8 trial (38, 39).

Limitations to FCR as a treatment approach include its toxicity; median age of patients in the CLL8 trial was 61 years which is relatively young as a CLL population and current UK guidance no longer recommend FCR for use in patients of >70 years in age. As mentioned previously, patients with a 17p deletion as part of their disease phenotype fare particularly poorly. Furthermore, in the context of early disease relapse (*i.e.* <3 years from first-line FCR) patients receiving repeat FCR have poorer OS than those who achieve a greater initial response duration (40). For those younger patients with few comorbid diseases assessed to be unfit for FCR the regimen of bendamustine in

combination with rituximab is offered (BR). Bendamustine is an alkylating agent with properties shared with those of purine analogues. The original study contrasted its impact with that of chlorambucil to demonstrate a significant improvement in PFS (41). The use of BR as a combination yielded significant responses in the first-line and relapsed/refractory settings (42) however under comparison with FCR in the CLL10 study it gave a significantly lower PFS overall and in the patient age group >65 years there was no significant benefit of FCR over BR, most likely due to the increased toxicity associated with the regimen often experienced by this patient group.

Chlorambucil is largely reserved for those patients unfit for either of the above regimens and has been trialled in combination both with rituximab (R-Clb) and with an alternative anti-CD20 antibody: obinutuzumab (G-Clb). Obinutuzumab differs from rituximab in that it maps its CD20 epitope in 3 dimensions with a glyco-engineered Fc region with enhanced antibody-dependent cellular cytotoxicity and apoptosis in relation to rituximab. G-Clb resulted in more partial and complete responses than R-Clb, with both superior to chlorambucil alone, and PFS of G-Clb was greatest (43). Obinutuzumab therapy tends to result in a greater frequency and severity of infusion-related reactions than rituximab, which may influence treatment decisions in some patients (43).

1.4.2 **Treatment algorithm**

The optimal sequencing of therapies in CLL has been altered greatly by the introduction of novel agents as described below, and numerous alternative therapeutic algorithms have been proposed. The results of ongoing clinical trials including CLARITY, FLAIR and the planned successor trials which have already been planned will alter the therapeutic order of established chemoimmunotherapeutic regimens as will the introduction of novel combinations as more information is acquired from such trials. At present, it is considered as good clinical practice for patients requiring therapy to be entered into a clinical trial where a suitable trial is available.

1.4.3 **Novel agents in clinical practice**

BTK inhibitors have been in widespread clinical use since the development of ibrutinib and second-generation acalabrutinib and others (GS-4059, BGB-3111, CC-292). The phase 1b demonstration of safety and efficacy with this orally-administered irreversible BTK-binding agent established ibrutinib's tolerability and its ability to produce durable remissions that transcend prognostic sub-classification (44). At three years' follow up ibrutinib demonstrated high response rates as a single agent in both treatment-naïve and relapsed/refractory settings (45). Since this study, an increase in the incidence of atrial fibrillation and the development of minor haemorrhagic complications have been reported in recipients of ibrutinib; bleeding diatheses have been attributable to an off-target platelet function defect (46). Only modest toxicity featured in this patient group with grade 3 cytopenias, infections and fatigue observed. The kinetics of treatment-related lymphocytosis was observed in some patients at >1 yr with no adverse effect on those patients experiencing such an elevation (45). Ibrutinib is being compared with ofatumumab in the phase 3 RESONATE trial and interim results are available with 74% of patients on ibrutinib being progression-free at 24 months. PFS appears to be consistent across patient subgroups except for a reduction in PFS with those carrying both 17p deletion and TP53 mutation and so far RESONATE reports ongoing safety and efficacy consistent with the earlier evidence (47).

Another, irreversible but more selective, BTK inhibitor has been developed which has no effect on epidermal growth factor receptor (EGFR), tyrosine kinase expressed in hepatocellular carcinoma (TEC) and interleukin-2-inducible T-cell kinase (48). Acalabrutinib (ACP-196) offers greater selectivity which may accommodate a greater dose range and has been trialled in relapsed CLL in a phase I/II study with evidence of safety and efficacy in patient groups including the 17p deletion subset (49).

Idelalisib, the first-in-class PI3Kδ inhibitor was first evaluated in combination with rituximab in the relapsed/refractory setting. This heavily pre-treated patient group experienced significant responses in comparison with the rituximab and placebo combination with an impact on PFS and OS (50, 51). Idelalisib has also been compared with ofatumumab in a phase 3 trial but as a

combination with ofatumumab compared with ofatumumab alone (52). The relapsed/refractory nature of those cases enrolled in the trial were amenable to the drug combination and displayed improved PFS independently of prognostic risk categories. Idelalisib has also been used in the treatment-naïve setting in combination with rituximab. Durable responses were observed in this phase II study in all prognostic categories with the main side effect of diarrhoea/colitis observed at grade 3 with some patients requiring cessation of therapy as a result (53). Phase III study of idelalisib in combination with rituximab in relapsed/refractory patients demonstrated improvement in PFS, Overall Response Rates (ORR) and OS across the risk categories at interim analysis (51), with long-term results awaited. Second-generation duvelisib (IPI-145) which targets both PI3Kγ and PI3Kδ holds promise in the targeting of additional microenvironmental signals as PI3Kγ is expressed not only by malignant B cells but by T cells and other aspects of the innate immune system (54). There appear to be apoptotic effects *in vitro* in addition to anti-migratory and chemotaxis effects and the drug is in phase I study (55).

Direct targeting of the BCL-2 protein was first explored as a therapeutic strategy in CLL with the development of BH3 mimetics such as ABT-737 and ABT-263 (navitoclax). Prior to this, the only mode of BCL-2 inhibition was with the use of antisense molecules such as Oblimersen and SPC2996 (56, 57). BH3 mimetics are thus named as they share an ability to bind the hydrophobic groove on anti-apoptotic BCL-2 proteins directly. As non-specific BCL-2 inhibitors target both BCL-2 and BCL2L1 effectively with significant apoptotic effects *in vitro* on primary CLL samples, they were first investigated as potential agents for combination use in CLL. However ABT-737 did not graduate to clinical studies and ABT-263 did not progress beyond phase I in CLL trials due to the impact of off-target platelet effects on drug tolerability, mediated by BCL-XL (58). Fortuitously, an agent with capacity to directly target BCL-2 whilst sparing platelet number was developed in the same year and was progressed quickly to clinical trial evaluation (59). Venetoclax phase I studies were able to demonstrate 79% ORR as a single agent and with a maximal dose of 400mg and CR in 20% of cases confirmed with MRD negativity. Even as monotherapy venetoclax can achieve 16 months' PFS in the 17p deletion subgroup. Phase 1b

studies are maturing with 24 months' PFS at 82% in combination with rituximab (60).

Safety and tolerability concerns were raised over the development of tumour lysis syndrome (TLS) relating to the exquisite sensitivity of CLL to BCL-2 inhibition. Two fatalities were recorded and three cases of acute renal failure were recorded, leading to the introduction of a sub-therapeutic dose escalation phase prior to a plateau at the therapeutic level to permit gradual disease debulking. Other adverse reactions recorded which limit therapeutic utility of venetoclax include neutropenia and there are concerns as to the degree of the depletion of innate immune cells, given the ubiquity of BCL-2 in normal cells. Challenges to BCL-2 inhibition as a therapeutic strategy include the functional redundancy of BCL-2 family members such that multiple family members may need to be targeted concurrently for long-term response, also the occasional upregulation of myeloid cell leukaemia 1 (MCL-1) and other anti-apoptotic proteins as a consequence of BCL-2 inhibition.

Combination therapy with the eagerly-anticipated MCL-1 inhibitors may provide a fail-safe in circumstances of venetoclax resistance. Microenvironment modification has been targeted as a means of therapy and knowledge of the role of the Programmed Death-1 (PD-1) and Programmed Death Ligand-1 (PD-L1) axis in interactions between CLL cells and immune effector cells has been exploited with the development of PD-1/PD-L1 pathway inhibitors (48). Patients have been treated for relapsed CLL using PD-1 blockade as a therapeutic strategy after progression on ibrutinib and in the context of Richter transformation, showing promise in setting of RS.

1.4.4 **Role of allogeneic stem cell transplantation**

AlloSCT remains the only known cure for CLL and its application is limited to those with an available donor who are without significant comorbidity and in general, <70 years old. A recent European Society for Blood and Marrow Transplantation (EBMT) multicentre study confirmed long-term survival (OS) in 35% of patients at 10 years with an even contribution from disease relapse and other causes in impact on survival (61). There was a sharp gradient in treatment-related mortality (NRM) in older patients (>65) with an increase from 14% to 47%

in 5-year survival with age-matched controls as anticipated with such an intensive procedure. In another study, individual centre experience of supporting allogeneic procedures varied widely however the event-free survival was found to be 37% at 5 years (1). Ten year follow-up data for AlloSCT in CLL was published from the CLL3X trial by the German Lymphoma Study Group (GCLLSG) with PFS of 34% in a study of 90 patients, indicating that AlloSCT does not always offer a cure for those patients that are eligible (62). Non-myeloablative is the preferred option for transplant conditioning, lending support to the procedure as a reduced-intensity version. In this patient cohort above many others, patient selection is key to optimising outcome in allogeneic stem cell transplantation. Work is ongoing to optimise the procedure and to find its position in the CLL treatment algorithm in the era of novel agents, as the role of ibrutinib is explored as an alternative and as a bridge to transplantation.

1.5 Normal B cell lymphopoiesis

Normal B cell development involves transition through stages of cellular maturation, each of which may be distinguished by cell surface receptor profile and by the maturation status of the B cell Receptor (BCR). B cell development is tightly regulated both temporally and anatomically to create a magnitude of diversity in immune responses to pathogens without error which may lead to neoplastic changes. B cell antigen specificity and diversity is created by the BCR; these steps are highly regulated to permit a sufficient diversity of BCR and to eliminate autoreactive cells. B cell diversity is created in one of three ways: by the negative selection of B cells with initiation of cell death, by inactivation of B cells to induce anergy, and by BCR editing.

1.5.1 B Cell Receptor: structure and function

The BCR is a multivalent transmembrane molecule which displays affinity to a range of antigenic molecules which it may bind reversibly with varying avidity, according to its specificity. The cell surface structure depends upon the class of antibody being expressed, which on mature B cells is either IgD or IgM. The cell surface structure consists of two heavy chain immunoglobulin (IgV_H) molecules which are associated each with a light chain molecule (IgV_L). The structure may be further subdivided into a fragment crystallisable (Fc) region which is

associated with the plasma membrane and the portion responsible for antigen-binding, known as the fragment antigen binding (Fab). The antibody isotype is largely dictated by the Fc region and the Fab fragment has both constant and variable regions with the antigen-binding specificity determined by the variable region. The identical arms of the Fab fragment and their variable regions on both heavy chain molecules possess areas which provide additional antigen specificity, known as heavy chain complementarity regions (HCDR1,2,3) (63). Membrane-bound immunoglobulin (Ig) molecules do not transmit signals directly but are linked to transmembrane CD79A/CD79B heterodimers which signal via their Immunoreceptor Tyrosine-based Activation Motif (ITAM) (see Figure 1-1 B cell receptor structure).

The BCR exists as a discrete oligomeric structure which differs according to the specific class of IgV_H molecule (64). The BCR exerts its function in the regulation of B cell development to mediate cell fate decisions, and in antigen processing to confer cellular immunity. Upon BCR ligation by antigen, either a cascade of signal transduction is commenced, resulting in receptor oligomerisation, with BCR internalisation of the bound antigen to permit antigen processing and antigen presentation to T cells. The various mechanisms of BCR activation and their subversion in CLL will be discussed.

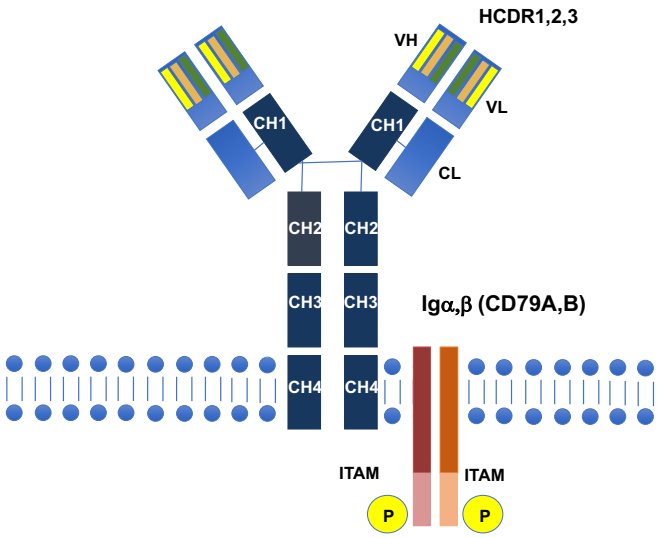

Figure 1-1 B cell receptor structure
The BCR molecule consists of antigen-binding heavy chains (VH, CH1-4) containing heavy chain complementarity determining region 3 (HCDR3) and light chains (VL, CL). The transmembrane molecules Igα and β transmit the BCR signal via phosphorylation of immunoreceptor tyrosine activation motifs (ITAM).

1.5.2 **B cell development and regulation**

Our understanding of B cell development and differentiation has progressed significantly since the earliest, almost linear representations of the B cell hierarchy (65). We now know that there are multiple well-defined stages which have transition phases, tightly-regulated by chemokine-ligand interactions with persistence of fluidity in developmental potential at all stages to mediate response to infection and to populate the growing organism as shown in Figure 1-2 (66). The first class of antibody to appear on the cell surface is IgM; the formation of pre-B cells requires the rearrangement of the immunoglobulin molecule at both variable- and joining-regions to form a primitive BCR constructed from μ chain molecules. Pre-B cells have a pre-BCR which is formed from 2 light chains attached to 2 μ chains which then insert into the plasma membrane. As the diagram in Figure 1-3 illustrates, the mature BCR defines the immature B cell stage, the latest stage which is confined to the BM which then emigrate to the spleen or LN to become transitional or marginal zone B cells.

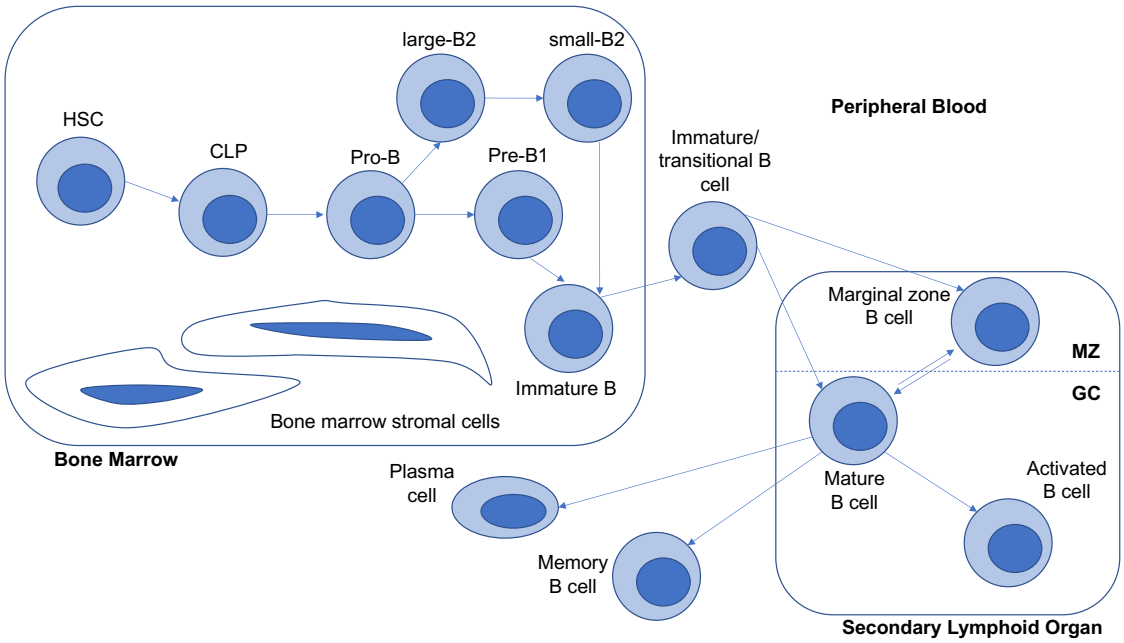

Figure 1-2 Stages of B cell development
Maturation initiates in the bone marrow microenvironment with the most primitive precursor, the haematopoietic stem cell (HSC), followed by common lymphoid precursor (CLP) to progenitor B cell (Pro-B). At this point there is a divergence into B-1 and B-2 subtypes; B-1 transitional cells may populate the spleen but have terminal differentiation stages in the body serous cavities. Cells move through from marginal zone (MZ) to germinal centre (GC) in the secondary lymphoid organs to terminal stages of differentiation which circulate in the peripheral blood. Mature B cells which populate B cell follicles are thought to have different cellular origins to MZ and B-1 phenotyped cells (66).

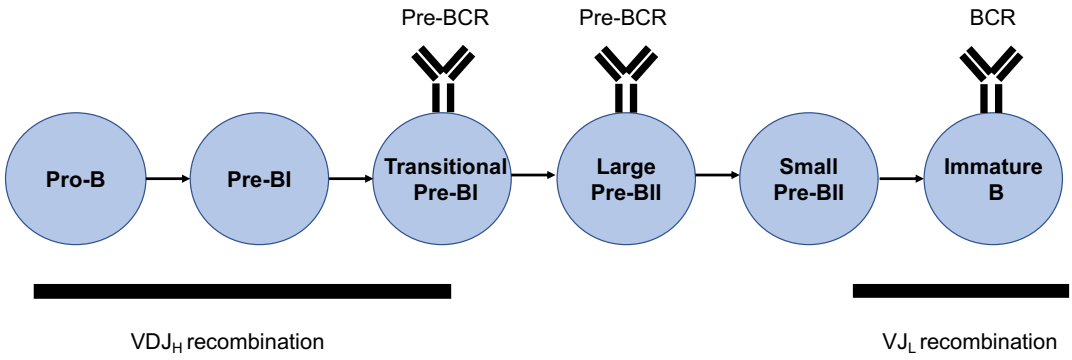

Figure 1-3 Stages of BCR maturation
The diagram above illustrates the stages of B cell maturation with a specific focus on BCR maturation and with delineation of stages of heavy and light chain recombination which demarcate maturation stages. The stages of maturation are also delineated by cell marker surface expression. Regulation of VDJ recombination is by RAG gene expression which occurs at all stages up to the immature B cell stage. B cell development is tightly regulated by transcription factors, including IKAROS family transcription factors, followed by STAT5, E2A and EBF1. There is an underlying dependence upon RUNX1 function in early B cell development (67). Later, PAX5 and BLNK are pivotal regulators of B cell development. Overexpression of developmental regulatory factors such as RUNX1 are frequently implicated in developing leukaemias of immature B cell origin (68).

B cells are categorised as B-1 or B-2 cells which is a phenotypic characterisation largely based upon the presence or absence of surface expression of CD5. They may be further subdivided into B-1a (CD5+) and B-1b (CD5-) cells which share other phenotypic features (69). B-2 cells are largely negative for CD5 expression although surface expression on these cells may be induced and as there is some surface phenotype overlap of B-1 cells and activated B cells therefore cell surface phenotype-based definitions should be applied with caution (69). The major B cell subset responsible for populating the spleen and LN is known as the B-2 cell stage and these cells may progress from transitional stages T1 to T2, reliant upon basal BCR signals, with maintenance of T2 cells receiving a contribution from external signals. A third transitional phase from T2 to the mature Follicular stage is responsible for the generation of the anergic B cell population (70). The transition from T2 to follicular/marginal zone B cells is regulated both by BAFF and NF-κB2 and by a stronger BCR signal at this stage. B cell development is critically dependent upon BCR signalling as where there is disruption of the BCR signal this results in a differentiation block. The BCR is required for mature B cell development even before the stage of antigenic exposure. The B-1 cell stage transitions independently of BAFF but with greatest reliance upon the BCR signal and other signals; B-1 cells are responsible for populating the body's serous cavities. Localisation of B lymphocytes plays a part in regulation of cellular development by means of microenvironmental variations in factors such as BAFF signalling (66). Regulation of B cell development appears also to be influenced by features of the BCR such as its antigen specificity and density of cell surface distribution (71).

1.5.3 **Immunoglobulin gene rearrangement**

As stated previously, BCR comprises both heavy and light chain Ig molecules, these are encoded on chromosome 14 in the case of the heavy chain molecule or chromosomes 2 and 22 for kappa (κ) and lambda (λ) chains respectively. Each heavy and light chain gene is split into constant segments (Cμ,Cδ) with variable (V) and joining (J) segments, and only at the IgV_H locus, diversity (D) segments. In early B cell differentiation in the BM, there is reorganisation of the gene segments to create a wide array of Ig molecules; with D and J regions recombining before V and DJ. Initiation of somatic recombination is performed by protein products of the recombinase-activating gene (RAG) family (72). RAG1

and RAG2 proteins exist in a complex which creates DNA double-strand breaks which are then repaired by non-homologous end joining (NHEJ) by enzymes including terminal deoxynucleotidyl transferase (TdT). Once a functional IgV_H molecule has been created there is elimination of the alternate allele from recombination attempts by a process known as allelic exclusion. The IgV_H molecule undergoes the described recombination process before the light chains, which are restricted to either κ or λ in any given B cell.

1.5.4 **Somatic hypermutation and class switch recombination**

Once a functional IgV_H molecule has been created, the cell may proceed to maturation and migrates into the germinal centre (GC) of the spleen and LN to undergo affinity maturation by a process known as somatic hypermutation (73) (74, 75). As B cells respond to pathogens via antigen-presenting cells, the V regions accumulate point mutations at 10^6 –fold increased frequency than the background DNA mutation rate. Although SHM generates mutations at random and may not even generate coding sequences, the selection of mutated molecules which bind antigen with greater affinity occurs later in the GC. Also in response to antigen-binding, B cells engage in isotype switching known as class switch recombination (CSR), from production of low affinity IgM to high affinity IgG, IgA and IgE antibodies. In CLL, cells express a similar class of immunoglobulin molecule to naïve B cells, both IgM and IgD however some cases may undergo isotype class switching and may express terminally differentiated isotypes (76, 77). The mechanism of CSR is one of DNA deletion and recombination in the IgV_H gene at the switch regions which results in exchange of $C\mu/C\delta$ regions for $C\gamma$, $C\alpha$ and $C\varepsilon$ regions (78). Activation-induced cytidine deaminase (AID), a single-strand DNA cytidine deaminase, exhibits increased levels of expression in activated germinal centre B cells and is key to the mechanistic basis for B cell diversity, playing a role in both SHM and CSR (79). Both SHM and CSR require transcription to occur and at this point the DNA helix is opened up and single strand DNA is generated which may be deaminated by AID to form mismatched base pairs. The processes of SHM and CSR harness the normal cellular processes of base excision repair and mismatch repair to convert deaminated sites to mutations and/or double-strand breaks. In SHM, there is an increased occurrence of mutations in the complementarity-determining regions of the immunoglobulin molecule; the regions which bind antigen directly. The

mutation rate is amplified by regions where AID is more active, relative to other areas of the V genes (80). In CSR, transcription occurring upstream of the switch region of the first constant domain opens the DNA helix to facilitate AID activity. The normal functioning of the processes of SHM and CSR are essential to create a diversity of B cells which can respond to a wide range of pathogens, with fail-safe mechanisms to reduce autoreactivity and prevent the unregulated proliferation of a clonal population. Both SHM and CSR may be subverted in CLL and have implications for disease features and heterogeneity and response to therapy (81, 82).

1.6 CLL pathogenesis

1.6.1 Monoclonal B cell lymphocytosis

It is now recognised that individual cases of CLL typically begin with a precursor syndrome known as monoclonal B cell lymphopoiesis (MBL)(83). MBL is a diagnostic entity which comprises <5 X 10^9/l circulating clonal lymphocytes, often with a CLL-specific immunophenotyped, and no evidence of extramedullary disease (26). Study of peripheral blood samples using flow cytometry or molecular analysis confirmed the existence of a pre-diagnostic clone in 44/45 CLL cases, leading to the understanding of MBL as a precursor condition of CLL (84).There is a distinction to be made between low count (LC) and high count (HC) as these conditions carry differing risk of progression to CLL. HC-MBL is regarded as indistinguishable from CLL and many of the CLL-specific mutations may be seen in this condition as found in CLL. Hypogammaglobulinaemia is a feature of HC but not LC-MBL, consequently patients with HC-MCL are more vulnerable to infections such as Epstein-Barr virus (EBV) and Cytomegalovirus (CMV), or infection by encapsulated organisms such as *streptococcus pneumoniae*.

It is known that T cells are increased overall in CLL, with a greater number of T cells which are phenotypically activated; there is an increased activated phenotype compartment correlates with advanced disease stage in CLL (85). T cell compartment differences also exist between MBL and CLL with T regs being reduced in HC-MBL in relation to CLL. LC-MBL was also found to have the cytogenetic abnormalities as seen in CLL although progression rates are low,

therefore the rate of LC-MBL in the general population remains fairly constant over time (86). T cell clones have been found in association with LC-MBL (86). Interestingly, recent work has shown an increase in T cell exhaustion relative to age-matched controls with a reduction in immune synapse function as B cell clone expands, whereas this capacity of T cells remains unchanged in stable LC-MBL. The pathogenesis of MBL is of interest in the efforts to elucidate the mechanisms of CLL, and debate is ongoing as to the role of infection in its aetiology. Up to 50% of patients with MBL experience significant infections and these infections may predate the incidence of CLL (87). Large-scale association studies have shown a link between pneumonia and subsequent CLL but whether this is a function or basis of the disease remains unknown (88). There appears to be no increased risk of hospitalisation with infection in HC-MBL in contrast with LC-MBL when correction is applied for patient age. Studies have also shown the risk of non-haematological malignancies with HC-MBL is increased relative to their inherent risk of CLL, indicating the importance of immune surveillance as mechanism of protection against oncogenesis (89).

1.6.2 **Immunoglobulin heavy chain mutation in CLL**

The delineation of prognostic subgroups based on patient immunoglobulin heavy chain mutational status not only provided the basis for an awareness of the role of SHM in CLL pathogenesis but also gave elucidation to theories on the cell of origin in CLL (90). Further exploration of the phenomenon of SHM led researchers to hypothesise that cases of CLL where the original malignant cell has passed through the GC have mutated immunoglobulin genes, therefore arise from a more mature B cell than those which have IgV_H that are yet to undergo SHM.

Theories regarding populations with differential IgV_H mutational status have been investigated, first by using gene expression microarray data which displayed only minor differences between IgV_H mutational subgroups (91). An appreciation of the contribution of epigenetic regulation to cancer pathogenesis has provided an alternative approach to disease theories. In general, it appears that CLL is a disease of widespread DNA hypomethylation and although overall DNA methylation does not appear to relate to gene expression levels, specific gene body CpG dinucleotide methylation status was found to correlate more strongly

with gene expression (92). On analysis of the epigenetic signature of each subpopulation it was discovered that unmutated CLL DNA methylation patterns resemble those of naïve B cells whereas mutated CLL bears more similarity to that of memory B cells. These data suggest that unmutated CLL is derived from a pre-germinal centre origin, with a germinal centre-experienced cell as the basis for mutated CLL (92).

The original study which identified IgV_H mutational status as an independent risk factor compared IgV_H genes with the nearest germline gene and found 2 subsets; 45.2% of patients each possessing >/= 98% sequence homology to the nearest germline gene and a subset comprising 54.8% of patients, each of whom displayed somatic mutations in their IgV_H gene. These populations showed distinct differences in CLL disease stage, atypical CLL morphology, between use of specific variable regions in the IgV_H molecule and with prognostic measures such as OS to conclude that an unmutated IgV_H confers a worse prognosis by all of these measures, independently of known effects of disease karyotype on prognosis (90). Recent evidence has clarified that it is the absolute percent deviation from germ-line sequence rather than the previously assigned threshold of 98% which is the indicator of prognosis and response to chemoimmunotherapy (93). Furthermore, IgV_H mutational status was found to have a surrogate marker in ZAP70, as high levels correlate with unmutated status. This finding had positive implications for disease risk stratification of CLL populations, given the practical difficulties with IgV_H sequencing in routine clinical laboratories. From gene expression profiling studies, expression of ZAP-70, a tyrosine kinase with increased expression in a diversity of lymphoid populations was increased at the messenger RNA (mRNA) level in those patients with unmutated IgV_H genes in 93% of cases (94).

The role of AID in determination of CLL IgV_H mutational status has been explored (95). It is known that the AID regulation of processes of SHM and CSR are dissociated in unmutated CLL, in which the disease retains the capacity to switch class of immunoglobulin. However, CLL unmutated IgV_H is known to have increased levels of AID. It is hypothesised that build-up of an AID splice variant leads to functional inactivation of AID but there may other, as yet undetermined, mechanisms at play (95).

1.6.3 IgV_H gene stereotypy and HCDR3

Understanding of CLL disease biology has been enhanced by an awareness of the presence and function of stereotyped IgV_H sequences, which may be found in up to a third of cases of CLL (13). Stereotypy in immunoglobulin gene sequence may co-segregate with properties ranging from patient characteristics and disease biological properties, discernible at the clonal level. The shared characteristics of stereotyped IgV_Hs have contributed to an understanding of CLL biology with the applications extending to and beyond those cases which have stereotyped clones. Theories of CLL pathogenesis which incorporate immunological response to foreign and self-antigens are supported by the finding of IgV_H stereotypy as CLL cells use a restricted range of IgV_Hs (96, 97), some of which are specific to CLL but there are others which are non-specific (98). Indeed, 9/19 major CLL-like sequences have been discovered at different stages of B cell development in normal precursor cells (13). Presence of stereotyped IgV_H rearrangements are thought to be linked to B cell tolerance, as mechanisms such as deletion and receptor editing are employed by the CLL pathogenic processes to limit diversity of the IgV_H. Infection-based theories of CLL are supported by the presence of IgV_H stereotypy as the frequency of a limited range of sequences which are described as stereotyped in CLL may have originated as an individual's response to a particular infectious agent, for example *streptococcus pneumoniae* or *haemophilus influenza (99)*.

Stereotyped IgV_H rearrangements have been studied in normal B cell populations by ultra-deep next generation sequencing in an attempt to map CLL ontogeny with some evidence of restriction of stereotype subset restriction to developmental stages and with some light chain restriction in individual subsets. It also appears that CLL-like stereotyped sequences are present at their highest frequency in young adults, with frequency declining over time, linking diversity of IgV_H to the ageing process (100). In addition to a predilection for use of specific IgV_H subsets there is a restricted range of HCDR3 sequences deployed by the pathogenic process in CLL. Findings in relation to HCDR3 specificity give additional credence to antigenic exposure theories of CLL as these are the main determinants of antigen recognition by the BCR. As it seems that neither HCDR3 nor IgV_H are sufficient to confer an adequate range of diversity in the antigenic

response process, it seems unsurprising that both immune mechanisms may be hijacked in CLL pathogenesis (101).

1.6.4 **CD38 and cell surface abnormalities**

With the advent of IgV_H mutational status subclassification was another of the earliest discoveries in relation to prognostic delineation of CLL, that of CD38 and its role (102). The role of specific cell surface immunophenotypic markers in CLL pathogenesis, in particular, that of the single-chain type II transmembrane glycoprotein CD38, was found to vary in its cellular expression by cell differentiation and activation status. Patients with high CD38 expression share features of a more aggressive disease and have associated bulk LN disease, low haemoglobin, hepatomegaly and high beta-2 microglobulin levels (103). As a result, patient population outcomes such as OS are poorer where CD38 expression features in individuals with CLL (104). Investigation for the basis of the differential outcomes by CD38 expression have uncovered an increased migratory potential for CD38+ CLL cells and with the discovery of CD49d as an independent negative prognostic determinant, the mechanism of migration control was partially elucidated. CD49d plays a role in adhesion to fibronectin, part of the extracellular matrix with its binding of vascular cell adhesion molecule 1 (VCAM-1) influencing cellular binding in the CLL microenvironment. CD49d promotes CLL cell survival by allowing CLL cells to evade apoptosis and its expression is associated with that of CD38 (105).

1.6.5 **Cytogenetic aberrations**

A large proportion (~80%) of CLL cases are defined by one of a small group of frequently recurring cytogenetic anomalies, each with their own biological and phenotypic associations. The most prevalent defect is a loss of genetic material at the 13q14 locus, occurring in 55% of all CLL cases, which confers a better outcome in terms of disease progression and survival (PFS and OS) in comparison to those cases where no cytogenetic abnormality may be identified. The next most frequently occurring defect is of a deletion at the 11q23 region, which is notable as the site of genes responsible for the regulation of lymphocyte development *e.g. ATM, KMT2A*. First discovered as a distinct subgroup in the late 1990s, CLL patients harbouring the 11q deletion were defined as having

poor prognostic parameters such as low OS and PFS and with the characteristic clinical finding of extensive bulky nodal disease (106). Specific morphological abnormalities are present in CLL affected by trisomy of chromosome 12; these patients have an indeterminate prognosis in comparison with cases which have a normal karyotype, but share an association with *NOTCH1* mutation and CD49d positivity, the implications of which shall be discussed (107). Although its impairment or disruption is ubiquitous in cancer, in CLL, the genomic guardian TP53 along with additional chromosome 17p material is commonly deleted to confer the poorest prognosis of all chromosomal subgroups with low PFS, OS and resistance to fludarabine chemotherapy; a key component of current standard chemoimmunotherapy regimens (108). Other cytogenetic abnormalities are less commonly observed, *e.g.* 6q del., 2p gain, but may confer additional cellular phenotypic and clinical properties. Complex karyotype profiles incorporating at least three cytogenetic defects confer a particularly poor outlook independently of CLL International Prognostic Index (CLL-IPI) scores underlining the importance of identifying all detectable abnormalities (109).

1.6.6 **Somatic mutations contributing to CLL**

As well as loss of chromosomal loci, CLL may be stratified by alterations which are limited to the level of a single transcript, conferring characteristic clinical properties to mutational subgroups. Mutations in the gene affected in ataxia telangiectasia, *ATM,* were one of the first to be discovered in CLL and may be found in isolation or in association with loss of the corresponding chromosomal region on the opposite chromosome; locus 11q23 (110, 111). Mutations in the *ATM* gene tend to result in a partial or complete loss of protein function with consequent impairment in DNA damage response and appears to form part of the pathogenic mechanism of affected CLL cases, occurring at the pre-germinal centre phase of differentiation (112). Cases affected by *ATM* mutations may have more aggressive disease with poorer PFS, similar to those affected by 11q deletion as a sole abnormality.

The tumour suppressor TP53, a DNA damage repair pathway gene encoded on chromosome 17p13 and is recurrently implicated in CLL, as it is in many other cancers and cancer syndromes. Of all frequently occurring mutations in CLL it confers the poorest outcomes with demonstrable resistance to standard

chemoimmunotherapy inherent to affected cases (108). *TP53* mutation is an independent prognostic risk factor in CLL and European recommendations apply the requirement for a minimum of Sanger sequencing of exons 4-9 of the gene in all cases of CLL prior to therapy (113).

Mutations in the *BIRC3* gene provide a biological explanation for the chemo-refractoriness of a subset of CLL patients and may be present as an isolated anomaly or in association with *TP53* disruption (114). The protein BIRC3, a member of the inhibitors of apoptosis family (IAP), acts as an E3 ubiquitin-protein ligase to regulate both canonical and non-canonical signalling of the NF-kappa-β signalling pathway. The 10-year survival of those harbouring a *BIRC3* lesion is estimated at 29%, equivalent to that of *TP53* mutation carriers.

Other recurrent abnormalities which confer a poor prognosis independently of all other abnormalities are those lesions which target the spliceosome function and its catalytic component, *SF3B1.* Cases of mutated *SF3B1* may be considered to have an indeterminate prognosis and investigative strategies have employed integrated transcriptome and functional analysis (115). Mutational changes may be activating coding or non-coding mutations and are found in association with subtle changes in DNA telomerase, with inhibitory effects on NOTCH signalling. It appears that SF3B1 is mainly a subclonal event with somatic mutations which lead to the progression of an affected subclone which then leads to overall disease progression.

Mutations in *NOTCH1* play a role independently of spliceosome responses in that NOTCH1, NOTCH2 and their ligands are constitutively activated as part of the pathogenesis of CLL (116). NOTCH PEST-domain activating mutations are a source of upregulated NOTCH activity and such mutations were found to be present in a subset of CLL cases and were found to cluster with cases displaying trisomy 12. The trisomy 12-associated NOTCH–mutated population have demonstrable increases in integrin signalling via upregulated expression of CD38 and CD49d (107). The increased migratory capacity of the described subset shall be discussed later; it appears that the increased capacity for tissue homing associated with the trisomy 12 subgroup relays a more aggressive disease phenotype. The contribution of NOTCH1-mutation to CLL cases carried prognostic significance, independent of other risk factors for CLL progression and

these mutations did not co-segregate with TP53 mutations (117). Known pathways for inhibition of the NOTCH signal including γ-secretase inhibitors have been exploited with therapeutic efficacy in CLL (118). Other recurrent somatic mutations have been observed at a lower frequency and shall not be discussed here as their prognostic value is less clearly established.

1.6.7 **Germline mutations contributing to CLL**

Large scale genome-wide association studies (GWAS) aimed at elucidating inherited traits which render individuals as susceptible to CLL are in progress to decipher the genetic basis of the disease. Based upon the observation that there is a relative 7.52-fold increase in risk of CLL for first degree relatives of affected patients (5), a single-nucleotide polymorphism study was conducted by candidate gene studies and with the use of Sanger sequencing, enlisting 206 families with no discernible associations found. Susceptibility loci were then determined using GWAS with p-value set at $<10^{-8}$ for novel loci. Individual alleles predisposing to CLL were found to have weak association in isolation but acting in concert there were strong associations with an enrichment for genes associated with open chromatin (119). GWAS findings were progressed to techniques such as chromatin immunoprecipitation sequencing (ChIP-seq) to develop an understanding of associations with gene function which led to the discovery of a causal variant at 15q15.1 in the *RelA* gene associated with decreased B cell lymphoma 2- modifying factor (BMF) binding (120). Furthermore, whole exome sequencing was used to identify familial CLL genes and led to the discovery of loss of function mutations in POT1; 3.5% of CLL has somatic mutations in POT1, part of the shelterin gene complex responsible for maintaining DNA integrity (121). The POT1 findings are supported by the finding that mutations are associated with other cancers including malignant melanoma and glioma and TERF2IP shelterin genes are mutated in other CLL families, providing direct evidence for inherited susceptibility towards CLL (122).

Studies are ongoing to find overlap between susceptibility loci and genes with functions known to be implicated in oncogenesis. Information from whole genome sequencing has also contributed to our understanding of CLL heritability in the study of an individual with the congenital autoimmune disease Aicardi-Goutieres syndrome (123). It is known for *SAMHD1* to be mutated in AGS; it is

the gene which codes for deoxynucleoside triphosphate triphosphohydrolase, a protein involved in DNA damage repair pathways. A patient with germ-line mutated *SAMHD1* developed CLL at the early age of 24, commencing the retrospective screening of CLL samples for SAMDH1 expression and variant allele frequency, found to be at around 11% in CLL patients requiring therapy (124). Whilst not directly implicating *SAMHD1* in the heritability of CLL, this case serves to describe a predisposing factor thought to be one of the early events in CLL development and to illustrate the discovery of clinically significant mutations with a low frequency of occurrence.

1.6.8 **BCL-2 and apoptotic regulators**

The discovery of B cell lymphoma-2 (*BCL-2*) was grounded in the study of the recurrent t(14;18) chromosomal translocations which are integral to the development of follicular lymphoma (FL). Using recombinant DNA probes to characterise the breakpoint from patients affected by FL it was established that rearrangements in chromosome 18 were limited to a short region of the chromosome (125, 126). Northern blotting was used to generate multiple variant transcripts with subsequent determination of the DNA sequence of *BCL-2* and the protein sequence of the encoded *BCL-2* product (127). Multiple protein members of the BCL-2 family have since been discovered, some of which are anti-apoptotic and some structurally similar proteins which have pro-apoptotic actions. BCL-2-family proteins play central roles in regulation of CLL cell death and may be categorised structurally based on the presence or absence of single or multiple domains with homology to BCL-2 (BH domains).

The original family-member, BCL-2, measuring at around 26 kDa, resides in the mitochondrial membrane and participates in oncogenesis by the prevention of apoptosis, facilitating the accumulation of malignant cells; oncogenes were hitherto known as pro-proliferative in mechanism of action. A range of pro-survival molecules known to act similarly to BCL-2 include MCL-1, BCL2L1 (also known as BCL-XL) and BCL2A1 (BFL1) and knowledge of these proteins with overlapping functions has informed the drug development process. The unique importance of BCL-2 to CLL pathogenesis is corroborated by the fact that it is overexpressed in CLL cells, and by the evidence that potent and selective BCL-2 inhibitor ABT-199 leads to MRD negativity and spares patient platelet counts

unlike the BCL-2 inhibitors which were developed earlier and which also inhibit BCL-XL. The first identified regulator of BCL-2, the pro-apoptotic BAX, exists together with BCL-2 in homeostatic equilibrium until the event of cellular injury at which point BAX undergoes conformational change and oligomerisation, thereby creating a channel in the mitochondrial membrane. The next step is the initiation of caspase cascade and apoptotic processes via the escape of cytochrome *c* from the mitochondria and into the cytoplasm. Pro-apoptotic functions are shared by BCL-2 family members BAX and BAK, however a third group of BH3 domain-only members (BID, BAD, BIK, BIM, BMF, HRK, NOXA, and PUMA) act as a ligand between other BCL-2 family-members and may be targeted in cancer therapy by BH3-mimetic agents (128).

1.6.9 **miRNAs in CLL pathogenesis**

The discovery that genetic alteration in noncoding genomic regions can be initiating events in malignant transformation led to a paradigm shift in cancer biology. MicroRNAs (miRNAs) are regulatory RNAs implicated in a range of cellular processes including DNA methylation, cellular growth, differentiation and programmed cell death. These small noncoding sequences have been associated with several types of cancer and much of the original surrounding data were derived from familial studies, from studies using solid organ tumours and from the biology of mouse models with deletion of the 13q14 region which encodes DLEU2/miR-15a/16-1 (129-131).

Prior to any CLL-specific study, understanding of the functions of were miR15a and 16-1 limited to transcriptional processing with responsibility for activation of apoptosis in tumour cells. Their proximity on 13q14.3, which is also commonly disrupted in cancer, led to suspicions that these miRNAs were the target of events in the process of cellular transformation. Hypotheses involving miR-15a and miR-16-1 as tumour suppressors were augmented by the rare finding that the loss of miR-16-1 function via an inactivating mutation leads to CLL (132). These discoveries were confirmed as integral to CLL biology by the finding that BCL-2 expression inversely correlated with miR-15a and miR-16-1. The role of miR-15a and miR-16-1 in regulation of homeostatic levels of BCL-2 may be key to their loss in oncogenic processes but also may be required for cancer drug response to DNA damaging agents such as fludarabine (133).

Receptor tyrosine kinase-like orphan receptor 1 (ROR1) positive CLL cells differ from ROR1 negative with respect to miR-15a/miR-16-1 positivity. It was found that miR-15a/miR-16-1 and miR365-3p target 3' untranslated (UTR) region of ROR1 which was predicted by nanoscan software and confirmed by luciferase assay with the co-transfection of HEK-203 cells (134). In support of the contribution of ROR1 to CLL progression, ROR1 is low or deficient in cases of CLL with chromosomal deletion of 13q; this and earlier findings lay the foundations for the therapeutic targeting of ROR-1 in combination with BCL-2, the therapeutic implications of which shall be discussed in (1.13.2). The second most common alteration in miRNA found in CLL targets the activation of TCL-1. MicroRNA miR3676 targets 28 bp repeats in the Tcl-1 3'UTR and its 17p13 localisation means that it is co-deleted with TP53 (135). It was later found miR3676 is not a microRNA as originally believed but is a short transfer RNA, cleaved by RNAse Z and with IL-2 binding capacity, however its role in histone-binding is to silence gene expression; functioning as micro-RNA (136).

1.6.10 CLL clonal evolution

The existence of clonal proliferation was established in the heavy water labelling study of CLL birth and death rates which formed the biological basis for the existence of clonal evolution. With the advent of Next Generation Sequencing (NGS) it became possible to study a variety of abnormalities simultaneously and to track their progression within clones and subclones of CLL. These studies provided the information on the properties of genomic abnormalities commonly observed in CLL; as to whether they exist as "driver" or "passenger" mutations in an individual (137, 138). It has been realised that subclonal mutations are worthy of study and their response to CLL therapies is of relevance to disease prognosis. In particular, clonal and subclonal *TP53* mutations are of equal importance and carry similar negative prognostic value to mutations affecting whole clones of CLL. Patients with subclonal *NOTCH1* mutations also carry similar outcomes as to clonal mutations (139, 140). Subclonal architecture in the context of disease relapse may inform the choice of second or subsequent-line therapy and the disease profile at relapse of patient treated with novel agents in CLL may help to characterise the mutations that promote disease resistance and relapse. With recent studies we have a greater understanding of the complexity of CLL; reflective of the contribution of

several clones and subclones, each with differing properties. Therapeutic strategies may be tailored in light of the above knowledge to prevent the unchecked proliferation of a single clone or subclone.

1.7 B cell migration

1.7.1 CLL microenvironment

The significant contribution of both LN and BM microenvironments has given rise to investigation of disease pathogenesis. Dameshek first described CLL in 1967 as an "accumulative disease of immunologically incompetent lymphocytes" (141) however we now have evidence of CLL clonal proliferation ranging from 0.1-1% per day (142). CLL cells undergo unregulated cell division in proliferation centres also known as pseudofollicules which are demarcated on histopathological assessment of the CLL node. Molecular interactions between CLL cells and the BM and or LN cells have been implicated in CLL cell survival, proliferation and clonal evolution. In LN affected by CLL, cells evade immune destruction and proliferate with aid from survival signals acquired from the microenvironment which have a function in normal B cell development. BCR activation is enlisted in the pathogenic process, along with signals such as CD40 ligand (CD154), BAFF, and APRIL (143, 144). Mesenchymal BM stromal cells have also been found to be protective of CLL cells with contributions from T cells via SDF-1 and CD49d and VCAM-1 interactions and from CD68+ nurse-like cells among others (145, 146).

1.7.2 Chemokine-ligand regulation of B cell positioning and migration

Cancer cell rehoming and the mechanisms by which it is governed are central to tumour spread and clonal expansion. The processes of cytoskeletal protein assembly, actin remodelling and integrin formation are amongst a range of individual events that precede cellular migration and are tightly regulated by chemokine and adhesion molecule interactions. In normal lymphocyte migration, selectin and integrin binding of lymphocytes at the vascular endothelium initiates lymphocyte rolling, arrest and firm adhesion. Subsequent transendothelial migration is triggered by integrin activation and chemokine receptor/ ligand binding as the lymphocyte is exposed to local chemokine release from the vascular lumen (147). B cell positioning within the LN GC is

determined by chemokine surface receptor expression of CXCR4 and CXCR5 and secretion of ligands CXCL12, CXCL13 and CCL19/CCL21 by the LN stromal cells. B cells migrate along chemokine gradients to the appropriate microanatomical site where they mature through phases of SHM and clonal selection on the basis of antigen affinity.

1.7.3 **Chemokine signalling in CLL**

In CLL, the pathophysiological process hijacks the innate properties of normal B cells not only to retain the function of recognised surface markers which interact with chemokines to regulate migration such as CXCR4 – CXCL12 and CXCR5 – CXCL13, but also to utilise the enhanced expression of these markers, facilitating increased migration to the secondary lymphoid organs. Understanding the regulation of these events offers potential candidates for *in vitro* study of oncogenic signalling: molecules of interest in CLL can be broadly categorised as chemokine receptors, adhesion molecules and other transmembrane signalling molecules.

CXCR4 surface molecule function is preserved in CLL cells with high expression of CXCR4 on CLL cells in PB and downregulated expression after migration underneath a stromal cell layer (148). Also, CXCR5 surface expression is found to be present and functional on CLL cells (149). The molecule CD49d, which is the α4 component of the $\alpha4\beta1$ integrin complex, has been implicated in CLL cell migration for some time (150) and its expression has been found to co-segregate with prognostic entities that have a tendency for increased migration (107, 151). Interestingly, those cells carrying trisomy 12 in association with the poor prognostic marker *NOTCH1* mutation display further upregulation of integrin signalling by way of increased $\beta2$ signalling (107). The surface marker CD38 is established as a marker of negative prognostic significance and this could be in part due to increased BCR signalling and tendency for cellular migration to the LN (152). CD44 interaction with its extracellular matrix ligand hyaluronan (HA) plays a role in cell positioning within the secondary lymphoid organs to receive pro-survival signals, which have been implicated in cell activation, migration and tissue retention of CLL cells. Properties of the CLL microenvironment including the presence of CCL21 secretion and the strength of CD40-CD40L interactions with T cells determine the balance of the equilibrium of CD44-HA binding; CCL21

induces motility whereas CD40L stimulation shifts the balance towards tissue retention of CLL cells (153). The surface receptor CD62L is implicated in homing of CLL cells and is upregulated in cells localised to LN and BM tissue (154). A similar pattern of increased expression of MMP9 on cells localised to the LN and BM formed the basis of studies of MMP9 in lymphocyte homing and egress. *In vitro* modelling of CLL migration demonstrated an upregulation in MMP9 with increased migration under regulation by $\alpha4\beta1$ integrin and PI3K/AKT signalling (155).

More recent studies of cellular migration have described surface changes in chemokine receptor profile and have derived an emigrant lymphocyte phenotype ($CXCR4^{dim}/CD5^{hi}$) (156). Proliferation studies have established a 2-compartment model of CLL with those cells in the PB demonstrating a low proliferation rate and those with a higher birth rate being derived from the secondary lymphoid tissue. Cells traffic between compartments and display distinct surface immunophenotype along with gene expression profile (157). Studies that demonstrate the immunophenotypic differences employed deuterium labelling of resting and proliferative fractions of CLL cells (158) whereas later work examined paired fine needle aspirates and CLL PB samples and used functional assays to demonstrate phenotypic differences. An *in vitro* circulation system of migration was utilised to lend further support to the proposed model of migration in which the CLL microenvironment exerts a phenotype upon cells according to their positioning (156).

1.8 BCR signalling

CLL cells resident in LN and BM display activation of BCR signalling and this, coupled with profound clinical responses elicited by treatment with BCR signalling inhibitors, has focused CLL drug development. Therefore the next subsections detail the BCR signalling process and the various methods by which signalling may be aberrantly active in B cell malignant disease.

1.8.1 **BCR signalling pathway**

Further evidence for migratory effects as part of the neoplastic process can be derived from recent advances in CLL therapy and the function of inhibitors which act downstream of the BCR signalling cascade. It has long been understood that the ability of B cells to respond to antigenic binding of BCR molecules is retained in CLL but the reliance on differential methods of activation of signalling downstream of the BCR varies by B cell malignancy. Both antigen-dependent and autonomous BCR signalling are at play in CLL and recruit similar downstream effectors in signal mediation which shall be discussed (159). Antigen binding of the BCR molecule, through the surface immunoglobulin leads to Igα/β (CD79A/B) phosphorylation of tyrosine residues on immune-receptor tyrosine-based activation motifs (ITAM) by Src-family kinases, such as LYN, FYN or BLK. Binding of tandem Src homology 2 (SH2) domains within the spleen tyrosine kinase (SYK) molecule, a non-receptor tyrosine kinase, allows further propagation of the signal by recruitment of BLNK to the phosphorylated tyrosine residues. BLNK, the B cell linker protein also known as SLP-65, acts as a substrate for SYK to recruit proteins such as the enzyme phospholipase C gamma 2 (PLC$\gamma 2$) and TEC family kinase Bruton's tyrosine kinase (BTK) to the signalling complex (Figure 1-4). Active PI3K generates phosphatidylinositol (3,4,5) triphosphate (PIP_3) to enable membrane recruitment of oncogenic serine/threonine kinase AKT, BTK and PLC$\gamma 2$ and permit signal transduction to the nucleus (160).

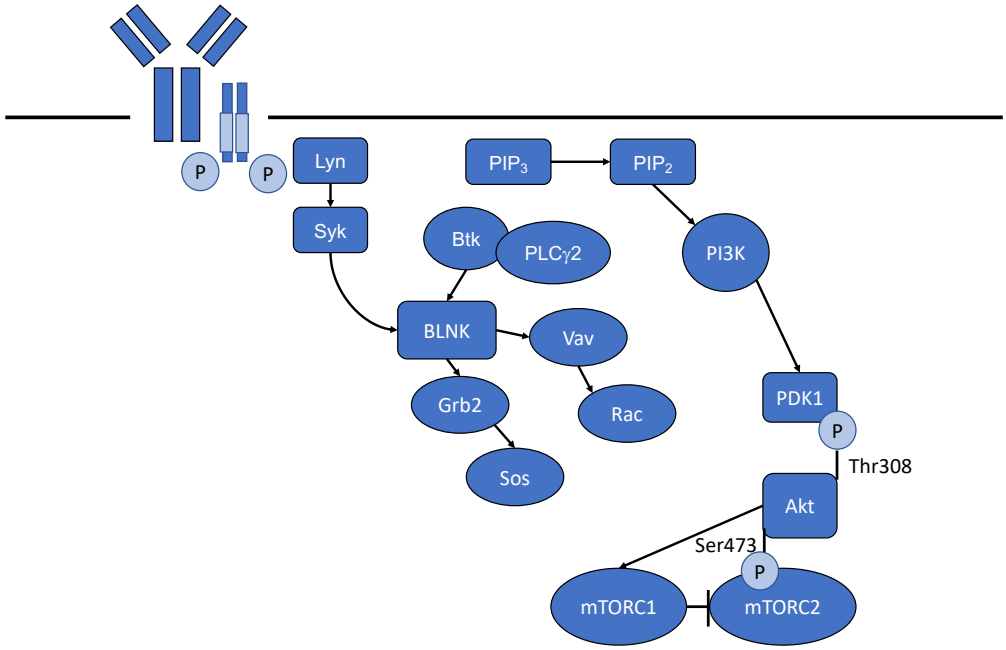

Figure 1-4 BCR signalling pathway
A diagram to summarise the intracellular molecular interactions downstream of the BCR signalling pathway is shown with a focus on the positioning of the mTOR signalling complex.

1.8.2 **BCR signalling in CLL pathogenesis**

Signalling by the pre-BCR complex may be disrupted in malignant transformation; evidence for this resides in the ability of the pre-BCR to promote the accumulation of lymphocytes which are undergoing maturation and light chain rearrangement/restriction. The pre-BCR contains 2 functional IgV_H μ molecules which associate with precursor light chain molecules and the immunoglobulin heterodimer CD79A/CD79B (161). As the pre-B cells develop, there is auto-aggregation of pre-BCR molecules on the cell surface and ligand-independent activation of signalling. Aberrant enhancement of the pre-BCR signal may form part of the malignant process, as in precursor B cell leukaemia, or may facilitate transformation in the case of mature B cell neoplasms. The study of defects in pre-B cell signalling has formed our understanding of the cellular origins of CLL and of the earliest events in the neoplastic process. Immunophenotyping and transcriptional profiling of CLL samples identified mutations which were present in multiple sorted cellular fractions with a focus on the progenitor compartment. The mutations which associated most frequently in the early compartment included those which were already known to feature frequently in CLL pathogenesis, including *NOTCH1, XPO1, SF3B1, TP53, BRAF* and *EGR2*. The BRAF-MAPK-EGR2 signalling pathway is directly

involved in pre-BCR signalling, with *BRAF*-G2469R responsible for constitutive phosphorylation of ERK and activation of EGR2 transcription factor in BaF3 cells. These data may be an indication that the individual genetic lesions described are responsible for the development of CLL and may be supported by future comparisons with the mutation rate in healthy haematopoietic precursors (162).

To confirm these findings, 2 GFP-expressing constructs were inserted into mouse models $BRAF^{wt}$ and *BRAF*-G469R to show that the mutated construct increased endogenous levels of EGR2 by QRT-PCR (EGR2/ABL) and resulted in a downstream increase in pERK by Western blot, concluding that BRAF-G469R affects B cell differentiation *in vivo*. After 5 weeks to allow B cell differentiation in transplanted mice there was a reduction of B cells in BM in *BRAF*-mutated B220IgM+ cells. EGR2-E356K, a mutant which affects transcription of target genes due to impairment of DNA-binding capacity was introduced to immunodeficient mice to study the relationship of EGR2 to the BCR signal by gene expression analysis. The importance of EGR2 to B cell receptor activation was established as EGR2-E356K mutant and BCR activation signatures display overlap of 239 differentially regulated genes; 15 of these are downregulated and of those overexpressed genes there are 168 identifiable as direct EGR2 targets (162).

Another study traced the origins of CLL-specific cellular defects back to haematopoietic precursor cells in the pursuit of the earliest oncogenic events in CLL initiation. Firstly, FACS analysis of the BM of patients with CLL was used to enumerate cell fractions at each stage of B cell differentiation with the discovery of clonal expansion at the pro-B cell stage. Analysis of the haematopoietic stem cell (HSC) subpopulations of CLL BM samples did not reveal any abnormalities at this stage so the investigation proceeded to evaluate the IgV_H gene rearrangement status in BM precursors. The purified HSC compartment, isolated from CLL patients were found to possess clonal IgV_H gene rearrangement however the pro-B cell population exhibited polyclonal rearrangement of IgV_H genes, indicating that clonal selection occurs after the stage of pro-B cell differentiation and cannot be attributed to CLL-HSCs (163).

To characterise the CLL-initiating cell population, xenotransplantation experiments were performed, transplanting CLL cells purified from the BM or PB

of patients into NSG mice. There was failure of engraftment of human CLL in the mice, indicating that CLL cells do not possess the engraftment potential of normal HSCs, hence the next step was to attempt engraftment of purified CLL-HSCs. As with the study of human CLL BM, differentiation was skewed toward the B cell lineage in the xenotransplanted mice. CD19+ B cells originating from CLL-HSCs also co-expressed CD5, an immunophenotypic characteristic of human CLL and a feature not present in B cells derived from normal HSCs. Furthermore, in mice possessing CD5+ B cells clones there was co-expression of surface IgM, CD20 and CD23 with absence of CD10. However, the experimental results from the CLL-HSC xenotransplantation should be considered with caution in the absence of supportive studies to date (163).

The study of mouse xenotransplantation models permits study of haematopoiesis and generation of clonal populations within normal and healthy cells. When contrasted with xenotransplanted B cells derived from normal control HSCs, there appear to be normal polyclonal IGH rearrangement from pro-B cells derived from both normal HSCs and CLL-HSCs. Notably, mature B cells appear to have undergone clonal selection even in the disease-supportive environment of the xenogeneic transplant model. In the analysis of mouse xenotransplantation models it was revealed that IGH-VDJ combinations of cells derived from CLL-HSC differ from the original transplanted disease in their IgV_H gene use. Interestingly, there appeared to be a predilection for the use of VH1, VH3 and VH4 by the disease xenograft. Further study of disease populations was performed by serial transplantation experiments confirming that CLL-HSCs are capable of self-renewal and produce distinct and independently-derived clones. Unlike normal HSCs, therefore, CLL-HSCs are able to develop monoclonal or oligoclonal B cell disease *in vivo*, tracing the origins of CLL to the most primitive stage, the self-renewing HSC (163).

DNA methylation changes are a feature of CLL and are known to confer prognostic information (92) however, another study corroborated the diversity of DNA methylation patterns between samples and established that the methylation changes are likely to be acquired stochastically by the developing clone and their study may contribute to our understanding of clonal evolution. Furthermore, these methylation changes appear to be more frequent in genomic regions where there is a relative absence of genes and those genomic areas

which replicate later, indicating that methylation variations occur as the developing clone proliferates, as a function of the error which is inherent to cancer cell proliferation. It is interesting to note, therefore, that these changes may also be tracked as early on as the HSC compartment (164).

Mature B cell receptor signalling may be activated by a range of modalities and each of these may be exploited by the process of malignant transformation. Inherent activation of the BCR pathway was discovered using transfection of TKO cells deficient in BLNK/SLP-65 with receptors derived from B cell malignancies and a tamoxifen-inducible ERT2-SLP65 fusion protein. Using the artificial system designed for *in vitro* BCR study, it was discovered that BCRs from a range of malignancies including multiple myeloma (MM), marginal zone lymphoma (MZL) and FL require BCR crosslinking to display activation via calcium flux assays whereas CLL-derived BCRs possess autonomous signalling capacity (165). It appears that this signalling is HCDR3-dependent, as a separate experiment which involved CLL-secreted BCRs did not activate those TKO cells with cell-surface BCRs of their own. Therefore, it is believed that autonomous BCR signalling in CLL is reliant upon structures intrinsic to the BCR. The role of autonomous BCR signalling in more aggressive B cell malignancies such as DLBCL and MALT lymphoma appears to be ill-defined at present. Some tumours may display antigenic specificity but it is difficult to prove an interaction between antigen and BCR to be directly responsible for tumour progression. Other lymphomas and their reliance on the antigen-activated BCR signal has been studied in a mouse model with forced expression of a BCR with specificity directed to a ubiquitously expressed self-antigen. There was an increase in lymphomagenesis with disease bearing greater morphological resemblance to CLL than to a MYC-dependent lymphoma, reflective of the inherent role of chronic antigen dependent BCR activity in CLL (166).

Behaviour of CLL B cells has been likened to anergic normal B cells and shared features in relation to the antigen-binding and processing by B cells have been demonstrated. The phenomenon of anergy in B cells is defined by an impaired response of cells to BCR stimulation; anergy is exploited by the pathogenic process in CLL to promote disease survival. A subset of CLL was characterised by expansion of an anergic cell population, which featured constitutive activation of ERK1/2 and nuclear factor of activated T cells c1 (NFAT-c1) and which evade

apoptosis induction (167). In normal BCR cell receptor signalling, binding of the receptor instigates internalisation of the molecule, permitting antigen processing via acidified endosomes. It appears that the leukaemic cell internalises the BCR molecule more readily than normal B cells and this internalisation occurs independently of the CD79b molecule, giving rise to the conclusion that BCR-ligand on the CLL cell surface is uncoupled from downstream signalling (168).

To recapitulate, either BCRs may be activated by auto-crosslinking or by antigen-triggered interactions however the established awareness of low-level "basal" signal, transmitted by the BCR, has been augmented by an appreciation of its aberrant deployment in B cell neoplasia. It has been shown that ablation of the BCR leads to apoptosis of normal B cells (169) indicating that there is a basal signal dependency of all B cells. Furthermore, naïve B cells may signal through IgM or IgD molecules, both of which transmit tonic signals via the ITAMs situated on the CD79A/CD79B heterodimer (170). The tonic signal is also transmitted via the intracytoplasmic tails of the immunoglobulin molecules after class switching to IgG or IgE with other qualitative differences in the signal after class switching, delineating some of the factors determining the reliance upon IgM signalling by B cell malignancies with further work required to appreciate the utilisation by either class of molecule in the misappropriation of the tonic BCR signal by the neoplastic process.

1.8.3 **Downstream targets of the BCR**

BCR signal transduction may be modified by downstream signalling molecules with the aim of therapeutic targeting being the diminution of signal output in malignancies reliant upon the BCR signal. One such target was first identified as the underlying cause of congenital immunodeficiency syndrome "Bruton's agammaglobulinaema" with the disrupted target as the Bruton's tyrosine kinase (*BTK*) gene encoded on chromosome Xq22.1; the protein product of which is essential for B lymphocyte production and development. Targeting the enzymatic activity of the BTK protein was first attempted using *in vivo* models of autoimmune disease and B cell lymphoma using PCI-32765 or ibrutinib with promising clinical responses (171). Using field-specific *in vitro* and *in vivo* models of human CLL, PCI-32765 was confirmed as an agent with efficacy and

selectivity against CLL with their mode of action to be discussed in the next section (172).

The PI3K family of enzymes can be subdivided into three classes according to their biological structure and substrate classification and they are known to regulate cell growth, differentiation and survival. Phosphoinositide 3-kinases (PI3K) are a family of lipid kinases which are involved in the regulation of cell growth, differentiation and survival. Class I enzymes, commonly activated by cell surface receptors, may be subdivided further into IA and IB. Class IA are heterodimers comprising a 110 kDa regulatory domain which are either termed α, β, γ or δ depending upon the splice variant of their associated 85 kDa regulatory domain. Dysregulation of class IA PI3K is the most common to be implicated in human disease, including the isoform PI3Kδ whose expression is restricted to haemopoietic cells and is involved in the pathogenesis of B cell malignancies (173). PI3K is possibly plays a less critical role than BTK as a moiety in BCR signal transduction because BTK may also function as an adaptor protein, modifying any enhanced signalling to originate from the PI3K molecule. The positioning of BTK in relation to PI3K may have consequences for the relative efficacy of therapeutic targeting of each molecule.

Spleen tyrosine kinase (SYK), a member of the SYK/ZAP70 family of non-receptor tyrosine kinases is positioned proximally, downstream of the BCR signalling complex and is found to be disrupted in autoimmune disease and in B cell malignancies. The SYK molecule is required for the pre-BCR signal therefore its loss of function is associated with failure of B cell development at an early stage. Given the dependence of both mature and malignant B cells on normal SYK functioning, the prodrug SYK inhibitor fostamatinib (R788) was trialled in CLL and B cell lymphomas with displayed preferential targeting of cancer cells *in vivo* (174). Thus, it has been tested more widely in clinical trials however its greatest utility has been demonstrated in the therapy of autoimmune disease such as rheumatoid arthritis (175).

1.8.4 **BCR signalling inhibitors and CLL migration**

Ibrutinib, fostamatinib and idelalisib, which target BTK, SYK and PI3Kδ respectively, all affect CLL cell migration mediated by tissue-specific

expression of chemokines and ligands; modulating processes of cellular adhesion, transendothelial migration and tissue retention via effects on integrins and adhesion molecules (176-178). Normal lymphocyte migration processes have been discussed already in 1.7.2. These inhibitors, as well as targeting BCR-mediated signals, also have effects on microenvironmental signalling out-with the BCR signalling pathway. Paracrine secretion of chemokines CCL3 and CCL4 by CLL cells is blocked, reducing support from monocyte-derived nurse-like cells and accessory T cells (176, 177). Pre-clinical studies of BCR signalling inhibitors detail a striking lymphocytosis effect with individual therapies in terms of plasma chemokine levels and surface receptor expression. Using primary CLL samples De Rooij *et al*. demonstrated a reduction in signalling via CXCL12, CXCL13 and CCL19 upon ibrutinib treatment, with a reduction in adhesion and migration of CLL cells (178). In parallel studies of ibrutinib, Ponader *et al*. identified a reduction in migration toward CXCL12 and CXCL13, which inhibited CCL3 and CCL4 secretion. Targeting of SYK with fostamatinib also displayed an inhibitory effect on CCL3 and CCL4 secretion in primary disease samples, with a reduction in homing towards CXCL12 and CXCL13 and a reduction in CLL cell adhesion to VCAM-1 (177, 179). Our group investigated the effects of LYN kinase inhibition with dasatinib revealing inhibitory effects on the CXCR4-CXCL12 signalling axis in CLL samples *in vitro* (180). PI3Kδ inhibition with idelalisib revealed a downregulation of chemokine levels *in vitro*, a finding that was corroborated by data from patients treated with the drug during clinical trial. Chemokine levels in patient plasma samples exhibited a reduction in secretion of CCL3, CCL4 and CXCL13 and a concomitant surge in the lymphocyte count in the PB (176).

1.9 Modelling CLL *in vivo*

Cellular migration has not only been studied *in vitro* as summarised in the experimental work described above but also in the more physiological environment of the murine models of CLL. The array of available murine models represents the wide heterogeneity in human disease phenotype and shall be discussed with a focus on the model developed in our laboratory and employed in experiments described herein.

1.9.1 **PKCαKR construct and mouse model**

The PKCαKR mouse model developed in our laboratory utilises a catalytically inactive version of the protein kinase Cα (PKCα) molecule to transform murine cells, resulting in disease with an aggressive CLL-like phenotype (181). Phenotypic characterisation of the PKCαKR mouse model is still in progress for this mouse that represents an exciting prospect for the *in vivo* modelling of CLL cell migration (182). On further interrogation of our model the PKCαKR expressing cells exhibit activation of ERK-MAPK-mTOR signalling, a basis for the proliferative capacity of these cells. The PKCα-KR model expresses predominantly unmutated IgV_H genes with longer CDR3 regions and an upregulation of ZAP-70, all shared features of poor prognostic CLL. The inherent downregulation of PKCα is also visible in our CLL patient cohort with elevation of PKCβII as a mechanism of disease progression. The PKCαKR construct also mediates upregulation of PKCβII; PKCβII has been identified as a downstream regulator of the BCR signal and also features in CLL pathogenesis with demonstrable increase in its activity in BCR-dependent CLL (183).

1.9.2 **Other models**

The Tcl-1 mouse model is analogous to poor prognostic CLL and relies on the deregulated expression of the oncogene *T cell leukaemia/lymphoma 1* (*Tcl-1*) in B lineage cells. Developed as a model for use in drug development, the Tcl-1 model was shown to express relevant therapeutic targets with demonstrable sensitivity to fludarabine (184). The Tcl-1 model requires PKCβ for development, however deletion of PKCβII leads to an increase in CLL cell survival and PKCβII expression was unchanged with our *in vitro* studies using this model, with a downregulation of PKCα. The Tcl-1 model also expresses predominantly unmutated IgV_H genes however the absence of ZAP-70 from the model offers insight into the distinction between models and potentially is reflective of disease onset at a later stage of differentiation than the PKCα-KR model, supported by the greater latency of the Tcl-1 model. Other models which have been less frequently employed include a 13q14 deletion model which targets the region encoding DLEU2/miR15a/16-1; New Zealand Black mice which are histopathologically CLL-like but differ in immunophenotype from CLL and the

APRIL mouse indolent model that produces a disease phenotypically like CLL but without CLL-like effects on survival. Interferon regulatory factor 4 (IRF4) is a transcriptional regulator and plays a role in B cell development. As murine CLL is derived from B-1 cell populations, an IgV_H subset Vh11 unique to B-1 cells may be employed in an ($IRF4^{-/-}$Vh11) knock-in to elicit a CLL-like disease. Characterisation of the disease model will aid in understanding its utility as a model of human CLL but also has implications for our understanding of the role of IRF4 in CLL pathogenesis and the mechanism by which it appears to suppress the onset of CLL (185).

1.9.3 *In vivo* models in migration studies

Pre-clinical data on ibrutinib and fostamatinib in the Tcl-1 model showed *in vivo* effects of an initial increase in lymphocytosis with therapy and a reduction in lymphadenopathy although the molecular mechanisms have not been elucidated (186, 187). LYN kinase, proximal to BCR signalling, has been targeted using dasatinib, and in the Tcl-1 model regulates haematopoietic cell-specific Lyn substrate (HS1) cytoskeletal formation, critical to the migration process (188). Based on the observation that the GTPase *Rho* knockout in the Tcl-1 mouse model displays a delayed disease onset, further work with this model revealed a reduction in homing of cells to the BM with a reduction in interactions with CXCL12 and CXCL13 and a reduction in the polarisation of phosphorylated focal adhesion kinase (FAK) with defective integrin function (189).

1.10 mTOR signalling pathway

1.10.1 mTOR kinase complexes: structure and function

Mechanistic target for rapamycin (mTOR) resides in two distinct signalling complexes mTORC1 and mTORC2, which integrate growth factor and nutrient signals to promote cell survival, growth and proliferation (190). mTORC1 contains RAPTOR, mLST8, PRAS40 and DEPTOR and mTORC2 contains RICTOR, mLST8, mSIN1 and DEPTOR (190-193). Originally defined in yeast (194, 195), the 250kDa protein kinase is both growth factor- and nutrient-sensitive with respect to mTORC1 however the “rapamycin-insensitive” mTORC2 responds only to growth factor signals and its existence explains the evident mTOR activity upon treatment with rapamycin (196). Positioned downstream of the

phosphatidylinositol-3-kinase (PI3K)-mediated signalling, mTOR integrates signals from binding of chemokine receptors, such as CXCR4 and CXCR5, and BCR-mediated signals in addition to the more frequently reported metabolic and growth factor responses ((197) & Figure 1-5).

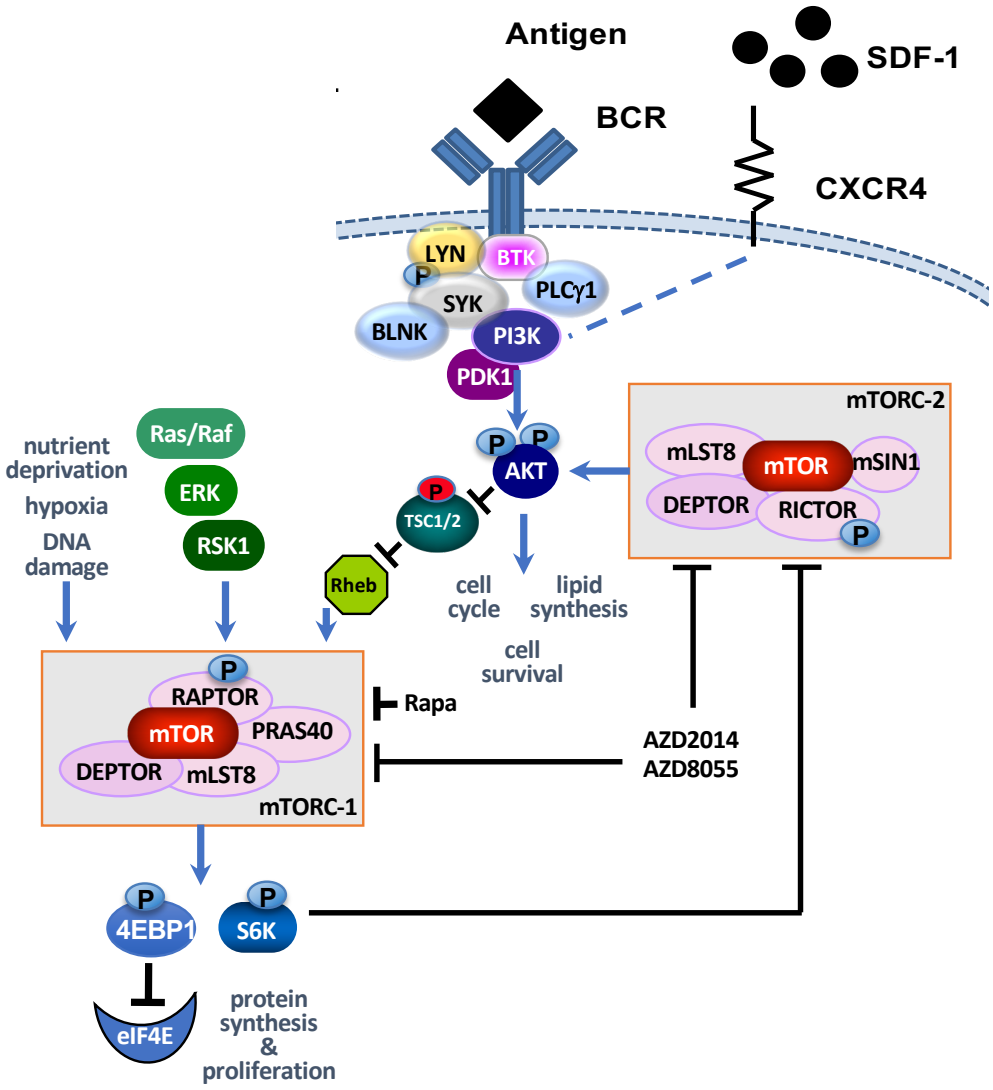

Figure 1-5 Diagram of B cell receptor signal transduction cascade with indication of relationship to chemokine receptor signalling in normal B cells
The mTOR kinase complex described earlier is demonstrated with its positioning downstream of the extracellular BCR and SDF-1 signals. The mTORC1 and dual mTORC1/2 inhibitors rapamycin and AZD8055/AZD2014 are displayed with their site of action within the mTOR complex shown.

The tuberous sclerosis (TSC1-TSC2) protein complex acts as an intermediary between the PI3K/AKT and mTOR signal, and its phosphorylation by AKT causes disassociation of the complex from GTPase Rheb which permits mTOR activation (198). Alternatively, in conditions of oxidative stress, hypoxia or starvation, mTOR may be inhibited by TSC1/2, activated by the conversion of Rheb-GTP to Rheb-GDP by 5'adenosine monophosphate-activated protein kinase (AMPK). While mTORC1 phosphorylates p70S6kinase (S6K) and eukaryotic initiation factor 4E-binding protein 1 (4EBP1) to increase protein synthesis, mTORC2 directly phosphorylates AKT^{S473}, enhancing its kinase activity 5–10 fold to promote cell

survival and initiate cell cycle (199, 200). Through AKT regulation, mTORC2 is considered to play a role in migration, however the precise molecular mechanisms have yet to be elucidated (200, 201). The activation of mTORC1 may be further regulated by localisation of the complex; mTOR is largely cytoplasmic but can associate with cellular organelle membranes, affecting its ability to phosphorylate S6K1. The functions of mTORC1 involve regulation of cellular proliferation, cell size, ribosomal biogenesis and angiogenesis by phosphorylation of S6K1 and 4E-BP1, which are directly responsible for mRNA translation (202). After mTORC1 activation, S6K1 triggers protein synthesis by phosphorylating PDCD4, marking it for degradation with secondary effects of binding and preventing elF4A helicase from fulfilling its function in mRNA unwinding. S6K1 can also function to dampen signalling via PI3K by inhibition of insulin receptor substrate 1 (IRS1) and 2 (IRS2) expression, providing a negative feedback loop within the mTORC1 side of the complex, thus explaining the non-aggressive nature of the hamartomatous tuberous sclerosis syndrome, a product of mutations in *tsc1/2* (203). Upon phosphorylation by mTORC1, 4E-BP1 is released from inhibiting the elongation initiation factor 4E (eIF4E).

mTORC2 plays a major role in signalling via the PI3K/AKT pathway, through phosphorylation and activation of AKT making it of interest as a therapeutic target in blocking the AKT signal, as mTORC2 has been demonstrated to be necessary for the development of activated PI3K signalling in tumours (204). Of note, an inhibitory feedback loop exists between mTORC1 and mTORC2, enabling an upregulation in AKT signalling with the removal of the mTORC1 signal, suggesting a complex regulatory role for mTOR in AKT-dependent malignancies (205, 206).

1.11 mTOR inhibitors

1.11.1 mTORC1 inhibitors

mTOR kinase was discovered by virtue of research gaining an understanding of the pharmacological activity of rapamycin (207). Originally discovered in the soil of Easter Island and derived from *Streptomyces Hygropicus,* this macrolide was found to possess both immunosuppressive and anti-neoplastic properties (208, 209). The two mTOR complexes are defined by their differential responses to

rapamycin; mTORC1 binds rapamycin allosterically by its association with FKBP12 whereas mTORC2 was first thought to be rapamycin-insensitive thus making mTORC1 the obvious choice as a drug development target. Thereafter, CCI-779 (temsirolimus) and RAD001 (everolimus) which have greater clinical tolerability than rapamycin, were developed for clinical use and have been trialed as therapies in both solid organ and haematological cancers with some efficacy (210-213). In CLL, everolimus elicited similar lymphocyte redistribution effects to that of PI3K and BTK inhibitors however overall clinical responses were not as promising (213), potentially due the existence of the negative feedback loop allowing preservation of AKT signalling in the absence of mTORC1 signal (205, 206).

1.11.2 Dual mTORC1/2 inhibitors

Dual mTOR inhibitors can be divided into two broad categories (Table 1). Firstly, there are small molecules that selectively inhibit both mTORC1 and mTORC2. First-in-class drug AZD8055 and its formulation for clinical use AZD2014 (Vistusertib) is an ATP-competitive inhibitor of mTOR, which selectively blocks phosphorylation of mTOR substrates (214). Dual mTOR inhibitors are ATP-competitive inhibitors and their superior clinical results and depth of mTORC1/2 inhibition was originally attributed to their ability to inhibit mTORC2 however some of their properties may a result of their ability to block rapamycin-resistant components of mTORC1. Upon inhibition of PRAS40 phosphorylation by dual mTOR inhibitors, this protein has enhanced binding of the RAPTOR/mTOR complex with resultant inhibition of the mTORC1/4EBP1 signal (215). Furthermore, there are differential effects upon cyclin D1 and D3 by rapamycin and dual mTOR inhibitors, with a reduction in protein expression of these and an increase in p27 with dual mTOR inhibition (216).

1.11.3 Dual mTORC1/2 inhibitors with overlapping functions

Pitfalls with these agents include the development of drug resistance, or the existence of alternative activating signals or negative feedback loops. Other types of dual mTOR inhibitor aim to overcome the potential deficiencies of specific inhibitors and inhibit PI3K signals as well as mTOR (Table 1-4); these have the advantage of inhibiting the three proto-oncogenic kinases PI3K, AKT

and mTOR, closing some of the feedback loops. Concerns regarding their effects on normal non-malignant cells have not prevented their use however overall clinical effects have been modest thus far. Compounds such as SAR245409 and PF-04691502 fared well in pre-clinical tests in comparison with specific pan-PI3K inhibitors in CLL however clinical data is awaited (217, 218).

Table 1-4 Dual mTOR inhibitors in current clinical trials
Agents currently under evaluation in clinical trials are indicated; their respective molecular target, phase of investigation and disease of study are shown.

Drug	Generic name	Inhibitor target	Phase	Disease
AZD2014	VISTUSERTIB	Dual mTOR kinase	I-II	AST, GBM, HCC, Lymphomas
OSI-027		Dual mTOR kinase	I	AST, Lymphomas
PF-04691502		PI3K-mTOR	I-II	Breast, Endometrial, AST
SAR245409	VOXTALISIB	PI3K-mTOR	I-II	AST, GBM, Ovarian, Breast
CC-115 CC-223 MLN0128 (TAK228) VS-5584		Dual mTOR/DNA-PK Dual mTOR kinase Dual mTOR kinase PI3K-mTOR	I-II I-II I-II I	AST, GBM, AML NSCLC, NHL, MM Prostate, thyroid, breast, liver Metastatic cancer, lymphomas

1.11.4 mTOR inhibition in CLL *in vitro*

One dedicated study used CXCL12-transwell migration studies to demonstrate the ability of PI3K/mTOR inhibitor SAR245409 to reduce chemokine-mediated migration (218). Using vascular cell adhesion molecule-1 (VCAM-1) coated plates, CLL cells were pre-treated with 1 μM SAR245409, BYL719 (PI3Kα inhibitor), or idelalisib, and allowed to migrate towards 100ng/ml CXCL12 through a polycarbonate membrane. Relative migration was significantly lower in SAR245409-treated cells than untreated control cells (approximately 80% compared to 100%) with a lesser effect by idelalisib and no migration impairment by BYL719. The transwell assay was utilised again, this time with 200 ng/mL CXCL12 to assess migration on CLL cells treated with PF-04691502 at a dose range of 1.25-2.5 μM to show a significant inhibition of migration by the PI3K/mTOR inhibitor (217). To augment the approach to mTOR inhibition further, CC-115, mTOR and DNA damage pathway inhibitor, has shown promise using *in vitro* assessment of caspase-dependent cell killing, proliferation and BCR signalling in comparison to specific mTOR inhibitor CC-223 and BTK inhibitor CC-

229 and the compound has progressed further to preliminary clinical testing (219).

1.12 mTOR and cellular migration

1.12.1 mTORC1

To delineate the relative contribution of mTOR complexes to the cellular migration process we still refer to evidence from studies utilising rapamycin. The regulation of migration by inhibition of S6K1 and 4EBP1 has been shown in a variety of cell types, by the administration of rapamycin, to delineate the mechanisms by which control is exerted, including formation of the F-actin cytoskeleton, extracellular matrix remodelling (e.g. MMP9) focal adhesion formation, and Rho GTPase activation all regulated via S6K1 (220-222). Furthermore, there is evidence derived from inhibitor studies that support both mTORC1 and mTORC2 as regulators of cell adhesion (223). Extracellular matrix changes and GTPase activity are also regulated by 4EBP1 with evidence that it also regulates VEGF/TGFβ levels in a rapamycin-sensitive manner in mouse models of solid organ tumours and metastasis (224). Rapamycin appears to exert its effect downstream of S6K1 and 4EBP1 via regulation of small GTPase RhoA activation (225).

1.12.2 mTORC2

In contrast, mTORC2 mainly modulates the actin cytoskeleton to regulate migration (226, 227). Downstream effectors appear to be species and cell-type specific. PKA and Ras signalling pathways appear to be pivotal in amoebae (228), while, in mammals PKC, PKA signalling and Rac/RhoA are the main regulators of mTORC2-mediated migration (229). Studies using amoebae demonstrate that TORC2 exerts its influence via AKT and PKA regulation of adenylyl cyclase–based production of cyclic AMP (230). In mammalian systems, it appears that mTORC2 regulates neutrophil chemotaxis by regulation of F-actin polarisation and myosin II phosphorylation, again regulated by cAMP production but via PKC in a RhoA/ROCK dependent fashion (231). There are also putative mTORC2-independent effects of RICTOR on migration that have yet to be fully explored (232).

1.12.3 Downstream mediators of mTOR kinase and migration control

It is hypothesised that mTORC1/2 inhibitors would also have effects on cytoskeletal formation with downstream effects of cAMP production mediated by PKC and GTPases and this is supported by studies from a variety of model organisms and cell types. Indeed, the first description of the RICTOR homologue pianissimo in *Dictyostelium discoidieum* is as a regulator of chemokine and GTPase signals. In the described piaA knock-out model, cells are unresponsive to chemokine stimulation or GTPγS activation, defects that are restored with constitutive activation of piaA (233). Cytoskeletal regulation was attributed to TORC2 in *Saccharomyces cerevisiae* and amoebae through regulation of the Rho GTPase family and downstream mediators including pkc1 (234). In mammalian systems, a link between RICTOR and PKCα was established first (227) followed by a link between mTORC2 and RhoA family in regulation of neutrophil chemotaxis via mechanisms which are independent of actin cytoskeletal reorganisation (235). It appears that Rac/cdc42 GTPases are responsible for actin cytoskeleton formation and these effects are driven by RICTOR-mediated inhibition of Rho-GDP dissociation inhibitor 2 (231, 236).

GTPases are also dysregulated in CLL cell migration, elucidated by two studies with a specific focus on Rap1 GTPase and its role. Chemokine-induced transendothelial migration has been shown to be defective in CLL and pathological B cells lose their chemokine-responsiveness in the disease. GTP-loading of Rap1 fails due to impaired endosomal recycling to the plasma membrane and this has been attributed to defective activation of phospholipase D1 and Arf1, its regulator (237). Additionally, chemokine-induced activation of integrin clustering fails due to an inability to polar clustering of αLβ2 integrin which is Rap1-induced. Binding of α4β1, VEGF and chemokine are all needed for αLβ2 activation, as a result of failure to GTP-load Rap1 in CLL cells (238). Studies are ongoing as to the relationship between mTOR signalling and Rap1 activity.

Chapter 2 Materials and methods

2.1 CLL samples

Patient CLL samples were provided after requesting informed consent of the patients of the Beatson West of Scotland Cancer Centre, for which local research ethics committee approval was obtained. Primary CLL cells were removed from liquid nitrogen storage and placed in a water bath at 37°C until almost thawed. The CLL cell suspension was diluted in DAMP solution (DNAseI 5000U, 1M $MgCl_2$, 0.155M Trisodium citrate, 20% Human Serum Albumin, Dulbecco's Phosphate-buffered saline (PBS)) added dropwise to a total of 10 ml over 10 min. Cells were centrifuged at 350 *g* for 5 min then washed in RPMI-1640 supplemented with 10% fetal calf serum and 10mM L-glutamine, 10000 units/ml penicillin and streptomycin 10000 μg/ml (hereafter referred to as complete media) then centrifuged at 350 *g* and resuspended in complete media in preparation for use. Sample purity was confirmed by FACS evaluation (Figure 2-1). Flow cytometry data were acquired using a FACSCantoII flow cytometer (BD Biosciences) using the FACS Diva software package.

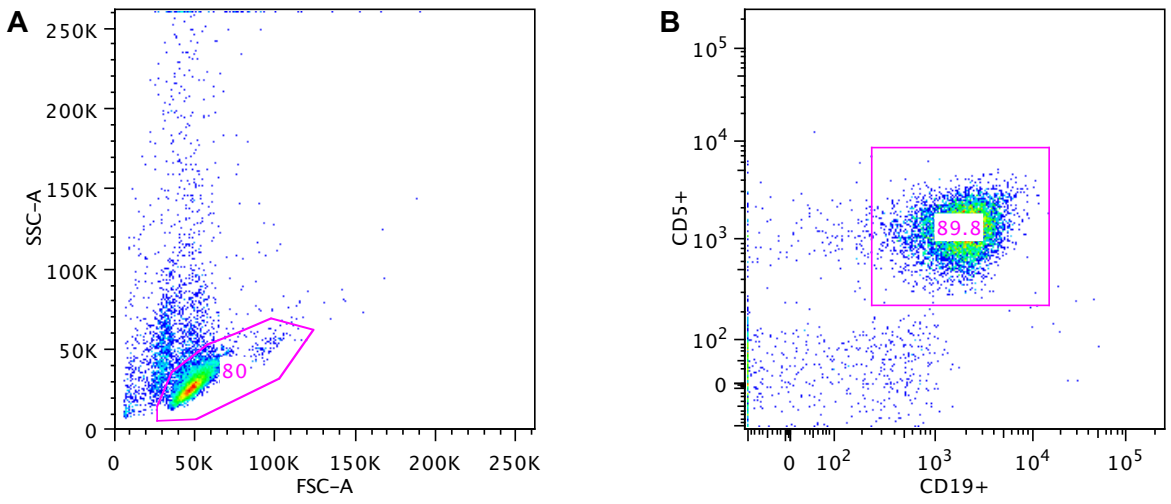

Figure 2-1 CLL cell purity by FACS analysis
Representative FACS plot displaying (A) live cell gating for assessment of (B) CD19+ and CD5+ cell surface staining using a patient sample which harbours a normal karyotype (CLL116).

2.1.1 Cell counting using a haemocytometer

An aliquot of CLL cell suspension was added at a dilution of 1:10 in 1X trypan blue solution into a 500 ul Eppendorf. Using a glass haemocytometer (Neubauer),

10 μl of the diluted cells was dispersed under the coverslip for viewing at X40 magnification by microscope (Nikon). A cell count was obtained from the 4 corner squares and the middle square of the counting chamber. To obtain the final count an average count of 5 squares was calculated with this number then multiplied by the dilution factor and by a correction factor for the cell chamber volume (10^4), to obtain a final cell count to be expressed per millilitre of original cell suspension.

2.1.2 **Cryopreservation of primary CLL samples**

Cell freezing mix was prepared by adding 10% dimethyl sulfoxide (DMSO) to fetal calf serum and used at room temperature. DMSO is used to prevent the formation of ice crystals which would destroy the cells during the freezing process. Cells were centrifuged at 350 *g* for 5 min then resuspended in cell freezing mix at a concentration of either 50 x 10^6 or 100 x 10^6 cells per millilitre in individual cryovials (Greiner). The cryovials were placed in a Mr. Frosty™ freezing container (Thermo Fisher Scientific) to allow gradual acclimatisation to -80°C before eventual storage at -180°C in liquid nitrogen storage tanks.

2.1.3 **Short-term stimulation with SDF-1**

Cells were rested in 1 ml of media prepared from RPMI-1640, 500 ml stock containing 10mM L-glutamine, 50000 units/ml penicillin and streptomycin 50000 μg/ml and 0.5% Bovine Serum Albumin (BSA) (Sigma-Aldrich Ltd., RPMI/BSA) for 2 h prior to the experiment. Cells were counted and placed into wells containing 1 x 10^6 cells and incubated in the presence or absence of inhibitors at 37 °C for 30 min. Cells were placed in a waterbath at 37 °C and SDF-1 (Peprotech Ltd.) was added at a concentration of 100 ng/ml. Experimental samples were removed from the waterbath and the reaction stopped by the addition of 1 ml ice-cold PBS at time points 0, 3 and 10 min.

2.1.4 **Short-term BCR stimulation with αIgM and avidin**

Primary CLL cells were incubated with drug inhibitors at 37°C for 30 min prior to BCR stimulation. Cells were transferred to a 1.5 ml Eppendorfs and placed on ice with the addition of αIgM (BD Biosciences) at 10 μg/ml. After 20 min, the cells were spun at 350 *g* for 5 min and avidin was added for a final concentration of

25 μg/ml. Cells were removed after 1 h and the reaction stopped with ice-cold PBS.

2.1.5 BCR stimulation with αIgM F(ab')$_2$ fragments

Primary CLL cells were incubated in complete medium with drug inhibitors at 37°C for 30 min prior to BCR stimulation. Soluble F(ab')$_2$ fragments (Jackson ImmunoResearch Laboratories, Inc.) at 10 μg/ml were added to mimic continuous antigen exposure of CLL cells and a range of incubations at 37°C were performed from 1 h to 48 h in duration.

2.2 Migration Assays

2.2.1 M2-10B4 cell proliferation in culture

The murine cell line M2-10B4 was found to secrete factors such as SDF-1 which may be used in co-culture experiments with human haematopoietic cells *in vitro* (239). A cryovial of M2-10B4 cells was thawed using DAMP as per CLL samples, resuspended in complete media and placed in a flask for adherent cell culture in an incubator at 37°C. Twice weekly, cells were checked for confluence and media was replenished to prevent exhaustion. Once confluent, the media was discarded and cells were washed in 5 ml of PBS. Then 1 ml trypsin was added to the flask and incubated at room temperature for 5 min, after which cells were removed, resuspended in 5 ml complete media and centrifuged at 350 *g* for 5 min. The pellet was resuspended again in 5 ml media and according to the extent of cell layer confluence, 1-4 ml of this suspension was discarded and supplemented with complete media to create a final volume of 10 ml. Cells were placed in a fresh flask and returned to an incubator for culture at 37°C.

2.2.2 Pseudoemperipolesis

The pseudoemperipolesis assay exploits the ability of CLL cells to transmigrate beneath a cellular layer along a chemokine gradient (148). In preparation, plates were coated with rat-tail collagen I (Invitrogen Ltd.) at 3 mg/ml concentration. Stromal M2-10B4 cells were placed in a 24-well plate at 1.5 x 10^5 cells per well and incubated at 37°C for 48 h until confluent. On a separate 24-well plate, primary CLL cells were plated at 2 x 10^6/well and were placed under drug

conditions: control, 100 nM AZD8055, 300 nM AZD8055, 10 nM rapamycin, 1 μM ibrutinib in the presence and absence of B cell receptor stimulation. Each well was prepared in duplicate and the plate was incubated for 15 h at 37°C prior to the start of the assay. Next, the M2-10B4 cell suspension was removed and CLL cells placed on top of the layer of cells in each well then incubated at 37°C for 5 h. After removal from the incubator, the cell suspension in each well was removed and wells were each washed 3 times with PBS to ensure removal of non-migrated CLL cells. Stromal cells were then trypsinised and stained using a $CD45^+/CD19^+$ fluorescent antibody to permit counting by flow cytometer. Cells were counted at high flow for 20 sec for each well and a sample of the initial CLL cell suspension was enumerated to provide a comparison. Negative controls containing empty stroma or CLL cells incubated to migrate for 5 min were washed in the same way as other wells and were established as containing <0.05% transmigrated cells.

2.2.3 Transwell migration assay: primary CLL cell sample preparation

After counting primary CLL cells, 5×10^5 were set aside per condition. Cells were rested in RPMI/BSA for 2 h prior to commencement of the assay and subsequently placed in drug conditions for 30 min at 37°C as follows: control, 100 nM AZD8055, 300 nM AZD8055, 10 nM rapamycin, 1 μM ibrutinib. Next, BCR stimulation was added using anti-IgM $F(ab')_2$ fragments for 1 h at 37 °C at a concentration of 10 μg/ml.

2.2.4 Transwell migration assay: murine PKC-αKR sample preparation

Murine fetal liver cells retrovirally transduced with the PKC-αKR construct (181) were prepared in culture over a layer of OP9 cells in Minimum Essential Media (MEM) alpha (Thermofisher Scientific). Each media unit (500ml) was supplemented with 50 mM HEPES, 5 mM sodium pyruvate, and 10 μg/ml gentamicin (HSG) and 1.25 mM 2-mercaptoethanol; 50,000 units of penicillin, streptomycin 50000 μg/ml, and 10 mM L-glutamine (2-PG) (Gibco®). Also, 20% fetal calf serum was the supplemental nutrient and 10 μg/ml of IL-7 (Peprotech EC Ltd, London) was added to promote proliferation. At the same time, control

MIEV-empty vector cells were cultured over OP9 cells. After 14 days, αKR and MIEV cells were counted and 3 x 10^5 per condition were set aside. Cells were rested in Dulbecco's Modified Eagle's Medium (DMEM) (Thermofisher Scientific) with 0.5% BSA for 2 h prior to commencement of the assay and subsequently placed in drug conditions for 30 min at 37°C as follows: control, 100 nM AZD8055, 10 nM rapamycin, 3 μM ibrutinib and 20 μM enzastaurin. Figure 2-2 confirms that PKC-αKR transduced cells, which are GFP positive, possess cell surface positivity for B cell marker, CD19.

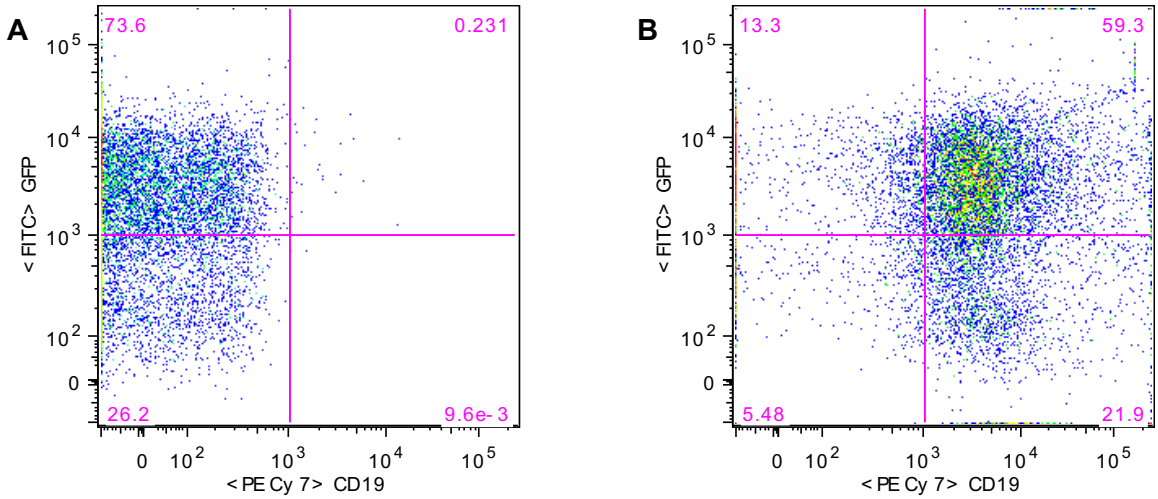

Figure 2-2 *In vitro* culture of PKCα-KR transduced cells
FACS plot of cells sampled from day 9 *in vitro* murine PKCα-KR cells in culture. Comparison with (A) unstained and cells stained for (B) PE-Cy7 CD19 highlights a discrete GFP+CD19+ population indicative of CLL-like disease.

2.2.5 **Transwell migration assay**

Cells in a volume of 100 μL were transferred to the upper chamber of a 6.5 mm-diameter, pore diameter 5 μm transwell culture insert (Costar®) and placed above 600 μL of media containing 150 ng/ml SDF-1. Each well was performed in duplicate with negative control containing media without SDF-1 and a positive control with direct insertion of CLL cell suspension to the lower chamber. The plate was placed at 37°C to allow transwell migration, and after 4 h the inserts were removed and after mixing the wells, 3 x 150 μl aliquots removed from each well for enumeration by flow cytometry. Cells were counted at high flow for 20 sec for each aliquot.

2.2.6 **Actin polymerisation by FACS analysis**

CLL cells were counted and 1 x 10^6 were set aside per condition; cells were rested in RPMI-1640/ 0.5% BSA for 2 h prior to 30 min drug incubation at 37^{o}C. Cells were placed in a water bath at 37^{o}C and 100 μL samples removed immediately prior to and at 15, 60, 300 and 600 sec post-addition of 100 ng/ml SDF-1 and placed directly into 250 μL of fixation/ permeabilisation buffer at 4^{o}C for 15 min. Each sample was then centrifuged at 350 *g* for 5 min then washed in 2 ml perm/wash buffer and then stained with 66 nM Alexa Fluor 488® phalloidin antibody (Invitrogen Ltd.) for 10 min at 4^{o}C. Samples were washed and centrifuged at 350 *g* for 5 min then analysed by flow cytometry, measuring 10,000 events recorded in the FITC (FL1) channel (gated on live cells by FSC/SSC).

2.3 Sodium dodecyl sulphate-polyacrylamide gel electrophoresis (SDS-PAGE) and Western blotting

2.3.1 **Sample preparation**

CLL cells were washed in PBS and the supernatant was aspirated. 1:10 dilution of stock of Protease and phosphatase inhibitors (13) were prepared by using 1 tablet of each to 1 millilitre of ddH_2O and allowed to dissolve, to make a 10X stock. Thereafter, lysis buffer prepared was from 1% NP-40, 10% glycerol, 20nM Tris (pH 7.5) and 137mM NaCl with a 1:10 dilution of protease and phosphatase inhibitors and 30μl was added with mixing to each cell pellet, with vortexing before and after. The tubes with cells and lysis buffer were placed on ice for 15 min, then centrifuged at 21000*g* for 20 min. Samples were stored at -20 ^{o}C in preparation for use.

2.3.2 **SDS-PAGE**

Samples were thawed and the protein concentration was estimated using the bichinchoninic acid assay (Pierce). Resolving gel was prepared as per protocol for a 12% acrylamide gel containing bis-acrylamide, double distilled water (ddH_2O), 10% sodium dodecyl sulphate (SDS), 0.5M Tris (pH 6.5), 10% ammonium persulphate and 1,2-bis(dimethylamino)ethane and allowed to set for 20 min. Stacking gel was prepared using the above reagents with the substitution of 1.5M

Tris (pH 8.5) and left to set for 30 min with a gel comb in place. Wells were washed thoroughly with ddH_2O and gels placed in a gel tank (Bio-Rad Laboratories) with immersion in running buffer (34.7 mM SDS, 245.6mM Tris, 2M glycine, ddH_20). Samples were prepared using PBS to supplement sample volume with DTT and loading buffer and were denatured using a heated plate for 10 min at 70 ^oC. Samples were loaded alongside a protein ladder (hyperPAGE II, Bioline) and electrophoresis commenced using 80 mV for 30 min then 180 mV until samples had run to the bottom of the gel. PVDF (polyvinylfluoridine) membranes were cut to gel size and prepared by immersion in 100% methanol for 30 sec prior to transfer. Gels and membranes were sandwiched between sheets of 1mm paper and immersed in transfer buffer (5% NuPAGE transfer buffer (25 mM Bicine 25 mM Bis-Tris (free base) 1 mM EDTA, pH 7.2), 10% methanol, ddH_2O) inside the X Cell II blot module (Invitrogen Ltd.) and electrophoresis performed using 30 mV for 1 h.

2.3.3 **Western blotting**

Blots were washed in TBS-T (10 mM Tris, 50 mM NaCl, ddH_2O, Tween 20 (Sigma-Aldrich Ltd.)) for 5 min and were blocked in 5% milk for 1 h. Blots were washed again for 5 min in TBS-T and primary antibody was added according to manufacturer's instruction, prepared either in 5% BSA or 5% milk. After overnight incubation at 4 ^oC blots were washed 3 x 5 min in TBS-T and secondary antibody applied according to the specificity of the primary antibody in use. After 1 h incubation at room temperature (RT) blots were washed for a further 3 x 5 min in TBS-T and treated with 700 μL Millipore chemiluminescent HRP substrate with measurement of chemiluminescence using the Molecular Imager® Chemi-Doc XRS™ imaging system (Bio-Rad Laboratories) or the Li-Cor Odyssey® Fc Imaging System. With the use of fluoresecent secondary antibodies there was a 1 h incubation period at room temperature (RT) with 3 x 5 min washes in TBS-T prior to measurement of fluorescence using the Li-Cor system.

2.3.4 **Densitometry analysis**

Images measured by the LiCor system were generated in Image Studio™ software with densitometry performed according to the manufacturer's instructions using Image Studio™ Lite v 5.2.5. Where images from a dataset had been generated in

2 different types of software (Molecular Imager® Chemi-Doc XRS™ and Li-Cor Odyssey® Fc Imaging System) analysis, images were converted to 8-bit tagged image file format for analysis using Image J v1.48.

2.4 Cell staining for flow cytometry analysis

2.4.1 Cell viability staining

After processing of whole blood samples, the success of the isolation process was assessed via cell surface marker staining for CLL-specific markers. Prior to use in our experiments, primary CLL samples, either fresh or thawed, were assessed for cellular viability. Representative FACS plot of staining for FITC/APC-conjugated Annexin V and 7-amino-actinomycin D (7AAD) viability markers are shown in Figure 2-3. A stock solution containing Annexin V 5μL, 7AAD 2.5μL (BD Biosciences) and 92.5μL Hank's Balanced Salt Solution (HBSS) (Gibco®) (12.6 mM $CaCl_2$, 4.9 mM $MgCl_2$, 4.1 mM $MgSO_4$ 53.3 mM KCl 4.4 mM KH_2PO_4 1379 mM NaCl 3.36 mM Na_2HPO_4, 55.5mM Dextrose) per experimental condition was prepared. Cells (0.5 -1 x 10^6/condition) were washed in FACS buffer and 100 μL of the antibody solution was added per condition and cells were left in the dark at RT for 20 min to allow staining. The antibody-cell binding reaction was quenched with 1 ml HBSS and cells were resuspended in 300 μL after washing in preparation for flow cytometry.

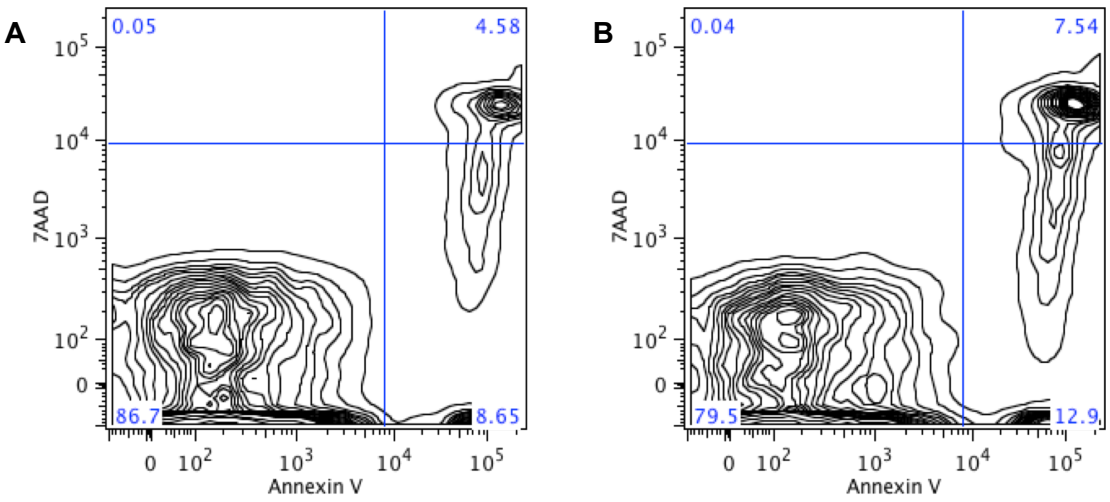

Figure 2-3 Contour FACS plots of fresh primary patient samples
CLL 159, a patient sample with a normal karyotype after 48 h incubation with (A) non-drug control and (B) 100 nM AZD8055. Apoptotic cells are delineated by their positivity for Annexin V which binds to phosphatidylserine on the outer leaflet of the plasma membrane. Live cells stain Annexin V$^-$7AAD$^-$ and are localised to Q3 whereas late apoptotic cells in Q2 are positive for both markers.

2.4.2 Flow cytometry surface antibody staining

CLL cells (1 x 10^6/ tube) were washed in HBSS and antibody stock solution was prepared using volumes of fluorescent antibody (BD Biosciences) according to the manufacturer's labelled instructions. Stock solution was adjusted using the addition of HBSS and aliquots of 20 μL were added per tube with subsequent incubation of cells at 4 °C for 15 min. The reaction was quenched with 1 ml of FACS buffer and cells were resuspended in 300 μL after washing in preparation for flow cytometry.

2.5 Immunofluorescence staining

2.5.1 Slide and sample preparation

Multispot slides (Hendley, Essex Ltd.) were coated with 0.01% poly-L-lysine for 2 h at 4 °C, removed and washed twice with PBS. In the preparation of cells for stimulation there was 1.5 h prior incubation in RPMI/BSA at 37 °C. Cells at a concentration of 3 x 10^6 /ml were incubated with drug conditions: control, 100 nM AZD8055, 10 nM rapamycin, 1 μM ibrutinib for 30 min at 37 °C prior to placement on slide spots with a further 30 min incubation.

2.5.2 **Rap1 activity assay by immunofluorescence staining**

Each drug condition was either left unstimulated or treated with 10 μg/ml EPAC agonist 8-(4-Chlorophenylthio)-2'-O-methyladenosine 3',5'-cyclic monophosphate monosodium hydrate (Sigma-Aldrich Ltd.) or 100 ng/ml SDF-1 for 5 min before removal of cells with a tissue and fixation each with 30 μl 4.2% formaldehyde at RT for 10 min. Spots were washed three times with PBS and permeabilised with 30 μl 0.5% Triton in PBS for 15 min. A further wash step was performed then cells were blocked with 5% BSA/ 0.2% Triton/ 1% ovalbumin for 1 h at RT. Cells were either individually stained with Rap1 (1:200) (Santa Cruz Biotechnology) or co-stained with LAMP-1 (1:20) or EEA-1 (1:100) antibodies for endosomal colocalisation (Abcam Plc.) prepared in 5% BSA block and incubated in the dark overnight at 4 °C in a moisture-containing chamber. Spots were washed twice and incubated with anti-rabbit Alexa Fluor 488® (Invitrogen Ltd.) or Rap1 single staining and for colocalisation a combination of anti-rabbit Alexa Fluor 594® and anti-mouse secondary Alexa Fluor 488® (Invitrogen Ltd.) at a concentration of 1:200 in 5% block for 1-2 h at RT. Slides were then washed three times in PBS and allowed almost to air-dry before placement of coverslip using ProLong™ Diamond Antifade Mountant with DAPI (Thermo Fisher Scientific) and storage of slides in the dark at RT prior to analysis.

2.5.3 **Actin polymerisation immunofluorescence staining**

Actin cytoskeletal formation was further evaluated by preparation of cells for immunofluorescence staining as above but in this case 2% BSA block was used and incubated for 30 min with stained with Alexa Fluor 488 phalloidin at 4 °C for 30 min in the dark. Slides were washed twice in PBS and allowed almost to air-dry before placement of coverslip using DAPI and storage of slides in the dark prior to analysis.

2.5.4 **Immunofluorescence staining: BCR stimulation technique**

Slides were first coated with 0.01% poly-L-lysine as before but after washing with PBS, αIgM or IgGκ1 isotype control (BD Biosciences) at a concentration of 10 μg/ml PBS were added to slide spots and incubated at 4 °C overnight. The following day the antibody was removed and slides were blocked with 10%

BSA/RPMI for 15 min at 37 °C before continuing with the protocol for immunofluorescence staining at the drug incubation step.

2.5.5 **Fluorescent microscopy**

Images were taken using Zeiss Axio Observer Imager M1 (Carl Zeiss Microscopy, LLC, United States) which is a microscope for multi-channel fluorescent acquisition. Epifluorescence microscopy illuminates the whole sample at once, but detects both in-focus and out-of-focus light which has implications for spatial resolution of cellular structures. To permit the use of a microscope system as a tool to evaluate colocalisation of two fluorophores, a variety of conditions must be met (240). For widefield fluorescent microscopy to be used in evaluation of colocalisation, images require deconvolution (240). Deconvolution uses data generated by an optical system to localise fluorescence more accurately, bringing images from a Z-stack into focus. In the experiments described herein, Z-stack distance was set at 0.55 μm with constant camera light exposure duration set in red, green and blue fluorescence channels for each spot under comparison. A range from between 8 and 12 images per Z-stack were taken using the motorised AxioCam camera and data from each combined using AxioVision v4.8.1 deconvolution software.

2.5.6 **Quantitative analysis of immunofluorescence**

Analysis of high power fluorescent microscope images was conducted using CellProfiler™ v2.2.0 software using .JPEG format grayscale images from FITC and DAPI channels. A single pipeline was generated to separate analysis by drug and BCR stimulation conditions and >200 cells per sample and condition were evaluated in each case. Figure 2-4 shows the method of immunofluorescence analysis performed using CellProfiler™ software.

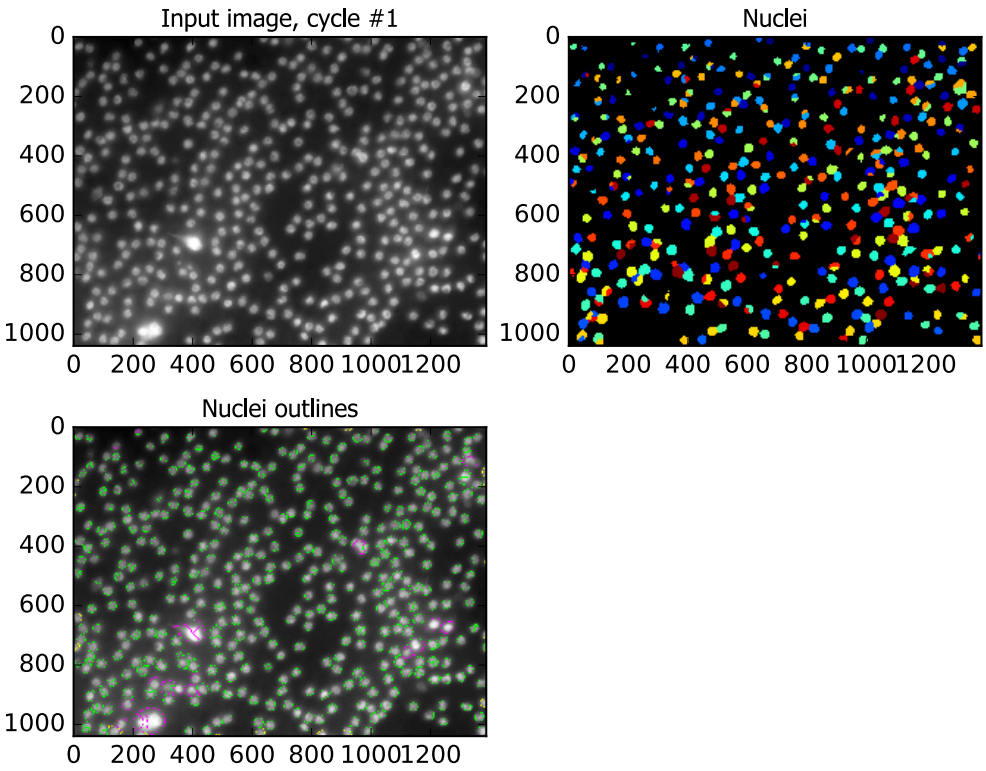
Input image, cycle #1
Nuclei
Nuclei outlines
0
200
400
600
800
1000
0 200 400 600 800 10001200

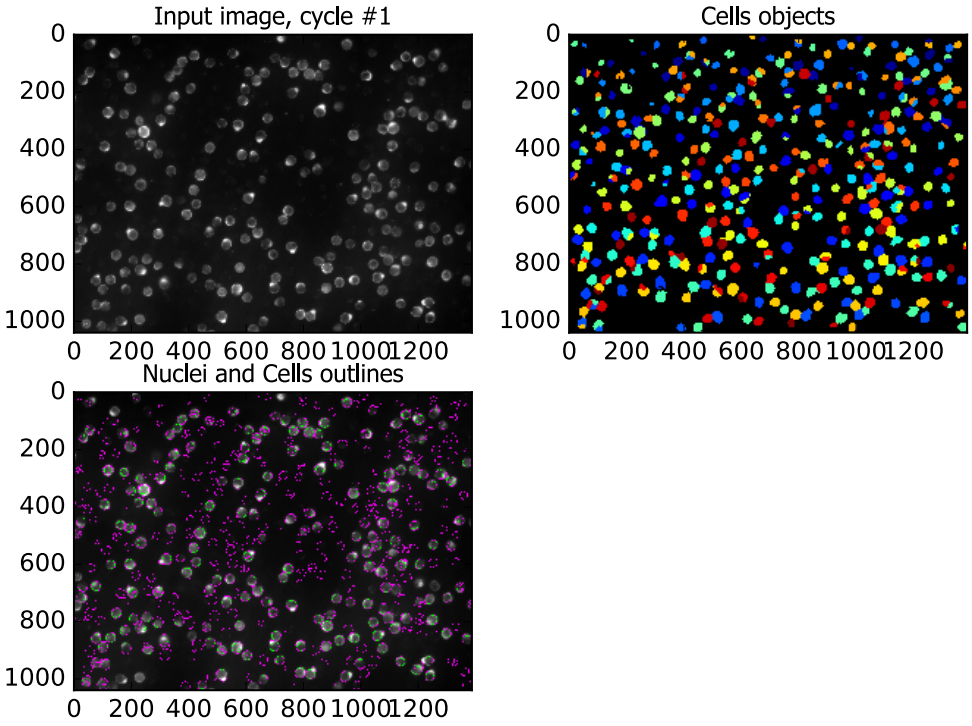
Input image, cycle #1
Cells objects
Nuclei and Cells outlines
0
200
400
600
800
1000
0 200 400 600 800 10001200

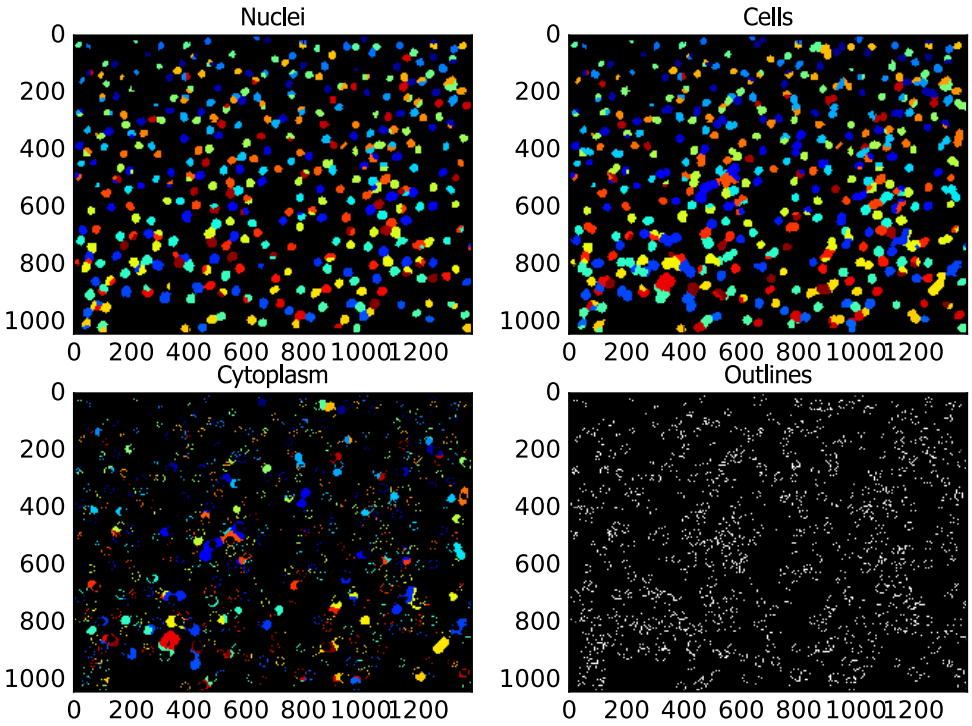

Figure 2-4 CellProfiler™ analysis of actin polymerisation
Representative cycles from CellProfiler™ analysis of images of phalloidin staining of CLL143 for assessment of actin polymerisation. Microscopic fields are pictured at x 40 magnification with automatic selection by the software of cell outline, nuclear outline and subsequent characterisation of fluorescence of cellular and subcellular structures.

2.6 GTPase activity assays

2.6.1 Rap1 activity assay: sample preparation

Primary CLL samples were rested in RPMI/BSA for 2 h prior to the experiment. Cells at a concentration of 2 x 10^7 were incubated for 30 min under the conditions: control, 100 nM AZD8055, 10 nM rapamycin, 1 μM ibrutinib then with or without stimulation using 100 ng/ ml SDF-1 and a separate positive control with EPAC agonist at 10 μg/ml for 5 min. To terminate the reaction, 1 ml ice-cold PBS was added to cells in media and then were spun at 100 *g* for 5 min. The pellet was resuspended and washed in ice-cold PBS for 5 min. After removal of PBS conditions were treated with 0.5 ml ice-cold 1 X lysis/binding wash buffer (Active Rap1 Detection Kit, Cell Signalling Technology®) and 1mM phenylmethanesulfonyl fluoride (PMSF) (Cell Signalling Technology®) with vortexing and placement on ice for 5 min. Samples were microcentrifuged at 16000 *g* at 4 °C for 15 min and the supernatant was removed for use in the immunoprecipitation assay.

2.6.2 **Rac1 activity assay: sample preparation**

Primary CLL samples were rested in RPMI/BSA for 2 h prior to the experiment. Cells at a concentration of 2 x 10^7 were incubated for 30 min under the conditions: control, 100 nM AZD8055, 10 nM rapamycin, 1 μM ibrutinib then with or without stimulation using 100 ng/ml SDF-1 or 10 μg/ml F(ab')$_2$ for 30 min. To terminate the reaction, 1 ml ice-cold PBS was added to cells in media and then were spun at 100*g* for 5 min. The pellet was resuspended and washed in ice-cold PBS for 5 min. After removal of PBS conditions were treated with 0.5 ml ice-cold 1 X lysis/binding wash buffer (Active Rac1 Pull-Down and Detection Kit, Thermofisher Scientific) and 1 X protease inhibitors (13) with vortexing and placement on ice for 5 min. Samples were microcentrifuged at 16000 *g* at 4 °C for 15 min and the supernatant was removed for use in the immunoprecipitation assay.

2.6.3 **GTPase activity assays: control steps**

As a control for the immunoprecipitation procedure, 500 μl control lysates were prepared adding 10 μl 0.5M EDTA pH 8.0 and vortexed and either 5 μl of 10 nM GTPγS or 5 μl of 100 mM GDP was added with vortexing. Samples were then agitated and placed at 30°C with termination of the reaction after 15 min using 32 μl of 1M $MgCl_2$.

2.6.4 **Rac1/Rap1 activity assay**

A spin cup per collection tube was set up with 100 μl of 50% glutathione resin added, centrifuging at 6000 *g* for 30 sec. Flow-through was discarded and 400 μl of 1 X lysis/binding/wash buffer was added to each spin cup with resin and after gently inverting the tubes, they were centrifuged at 6000 *g* for 30 sec and with flow-through discarded. Then, 20 μg GST-RalGDS-RBD (Active Rap1 Detection Kit) or GST-human Pak1-PBD (Active Rac1 Pull-Down and Detection Kit, Thermofisher Scientific) beads were added to the spin cup along with 700 μl of the cell lysate and after vortexing the spin cup cap was sealed and samples agitated at 4°C for 1 h. Samples were again centrifuged at 6000 *g* for 30 sec and spin cups transferred to a new collection tube. Two wash steps were performed, each with 400 μl of 1 X lysis/binding/wash buffer and centrifugation at 6000 *g*

for 30 sec after which a further collection tube was used. Reducing sample buffer containing 0.1 M dithiothreitol (DTT) added to 2 X SDS sample buffer to a final concentration of 50 mM DTT and 50 μl of buffer was added to each tube with vortexing and incubation at RT for 2 min. After centrifuging the tube at 6000 *g* for 2 min, spin cups were removed and discarded and eluted samples were heated at 95°C for 5 min.

2.6.5 **Western blot: Rap1 activity assay**

Western blot analysis was performed as described previously and after transfer, PVDF membrane was washed with 25 ml TBS for 5 min at RT then blocked with 25 ml TBS containing 0.1% Tween-20 (T-BST) and 5% BSA for 1 h at RT. Wash step was performed 3 times for 5 min with T-BST and membrane incubated with Rap1 rabbit antibody in T-BST overnight at 4 °C. After removal of primary antibody 3 x wash steps were performed and the membrane was incubated for 1 h with anti-rabbit antibody in TBS-T with 5% milk, then washed x 3 and developed as above.

2.6.6 **Western blot: Rac1 activity assay**

Western blot and transfer was performed as for Rap1 activity assay with block for 1 h using 25 ml TBS containing T-BST and 3% BSA at RT. Wash step was performed for 5 min with T-BST and membrane incubated with anti-Rac1 mouse antibody in T-BST with 3% BSA and 0.1% NaN_3 overnight at 4 °C. After removal of primary antibody 5 x wash steps were performed and the membrane was incubated for 1 h with anti-mouse antibody in TBS-T with 5% milk, then washed x 5 and developed as above.

2.6.7 **GTPase assays: loading controls**

To obtain an assessment of the total protein levels obtained by cell lysis of each drug and stimulation condition, the eluate from the immunoprecipitation step was retained and stored at -20°C. Once Western blot for active GTPase levels was performed, a second blot using the retained eluate was also performed and probed for total GTPase level (Rac1/Rap1) and a separate housekeeping protein such as GAPDH (241). The protocol for Western blot was performed as for active GTPase levels.

2.7 Statistical analysis

Data were analysed using Microsoft® Excel and a statistical software package (GraphPad v6 Software Inc., La Jolla, CA, USA) to perform a range of tests including the paired student's t-test and in each case to test goodness-of-fit, Kolgomorov-Smirnov test of normality were employed to generate K^2 for groups of samples. Where samples did not fit a normal distribution, non-parametric tests such as the Mann-Whitney U-test were used. P values were assigned the symbol * to indicate statistical significance where * is representative of $p < 0.05$ and $p > 0.01$, ** of $p < 0.01$ and $p > 0.001$, *** of $p < 0.001$ and $p > 0.0001$ and **** of $p < 0.0001$. Flow cytometry data were analysed using the FlowJo software package (Tree Star, Inc., Ashland, OR, USA).

Chapter 3 Molecular effects of mTOR inhibition on CLL cell migration *in vitro*

3.1 Introduction

The mechanisms underlying the lymphocyte redistribution effect demonstrated by BCR signalling inhibitors including mTOR inhibitors are worthy of study, initially in confirmation of this phenomenon as a *bona fide* means of drug effect. Based upon the relative absence of any apoptotic effect by BCR signalling inhibitors, it was speculated that the effects of microenvironmental displacement with subsequent loss of survival signals by CLL cells was for the most part responsible for the clinical activity of such drugs (242). The molecular processes and the downstream molecular signalling output of such drugs were not immediately apparent thus triggering intensive study as to the molecular control of migration. From already existing data, we have identified mTOR kinase as a target of interest however its study, in tandem with the examination of the effects of existing BCR signalling inhibitors, may yield information as to the differential mechanisms of each. Furthermore, the use of *in vitro* techniques to investigate the molecular effects of mTOR inhibitors may elucidate novel therapeutic targets.

AZD8055 is a novel, ATP-competitive inhibitor of mTOR signalling which binds the active site of mTOR kinase (214). Not only does it differ in its capacity for dual mTOR inhibition as opposed to mTORC1 inhibition alone, but, unlike the allosteric inhibitor rapamycin it is a direct inhibitor, binding to the mTOR kinase protein itself. Rapamycin is an allosteric inhibitor of mTOR; allosteric regulation is where an effector binds at a distant allosteric site which exerts functional regulation. Rapamycin binds FKBP12 and the resultant complex inhibits mTORC1 activity (243). AZD8055 is orally administered when applied *in vivo* with a maximum tolerated dose of 90 mg, administered twice daily, thus we elected to use concentration ranges from 30 - 300 nM for *in vitro* experiments. AZD8055 has an IC_{50} of 0.8 nM and its selectivity for mTOR kinase complexes has been confirmed *in vitro* (214). The clinical grade analogue of AZD8055, AZD2014 has an almost identical chemical structure but has greater oral bioavailability than AZD8055 due to its lower rate of hepatic metabolism (244). However, for *in vitro* testing we have selected AZD8055 as it was the original version of the compound

and is in widespread use for *in vitro* experimentation (244). Rapamycin is a highly potent allosteric inhibitor of mTORC1 with effectiveness at low concentration levels therefore I elected to use concentration ranges from 0.1 nM to 10 nM (207).

3.1.1 **CLL cell viability**

Our initial approach was to conduct cell viability studies to provide an overall assessment of the performance of mTOR inhibitors. This section focuses on the optimisation of our experimental approach followed by the study of short and long-term incubation with drug inhibitors, with *in vitro* BCR and chemokine-ligand stimulation to simulate the tissue microenvironment.

Cell viability was tested using both fresh and thawed primary CLL cells. Cells were cryopreserved either using histopaque which enriches for B cells or using RosetteSep™ which employs a negative selection method utilising crosslinking of cells which bind to specific cell surface markers to red blood cells, with separation via a density gradient such that B cells are separated from all other leukocytes as they do not possess the target markers, using the technique as described by Laprevotte *et al.* (245).

The effects of cryopreservation and thawing on cell viability are long-established and an applicable immunology study of peripheral blood mononuclear cell recovery demonstrated a range of cell sample viability from 1 - 96% on thawing of 54 samples from cryopreservation. The median cell viability was 70% which provided early evidence in identification of the threshold for adequate recovery of lymphocyte function, as assessed by cellular proliferation assays (246).

Techniques in cell cryopreservation have developed since the earliest studies and the introduction of DNase treatment to cell thawing procedures has reduced the incidence of cell clumping, which leads to reduced cell recovery and may lead to alterations in cell function and phenotype (247). Advances in cryopreservation methodology may thus improve the range of samples to retain viability and function, increasing the availability of samples for experimental use. According to their availability, fresh CLL samples were preferred as their baseline viability was generally greater than for those samples which had

undergone the cryopreservation and thawing process. A representative fresh patient sample shown in Figure 3-1 displays a 50 % reduction in cell viability (Q3) and a significant increase in apoptosis (Q2) at 48 h incubation. To account for differences in cellular recovery, viability studies were performed on a mixture of both fresh and thawed samples.

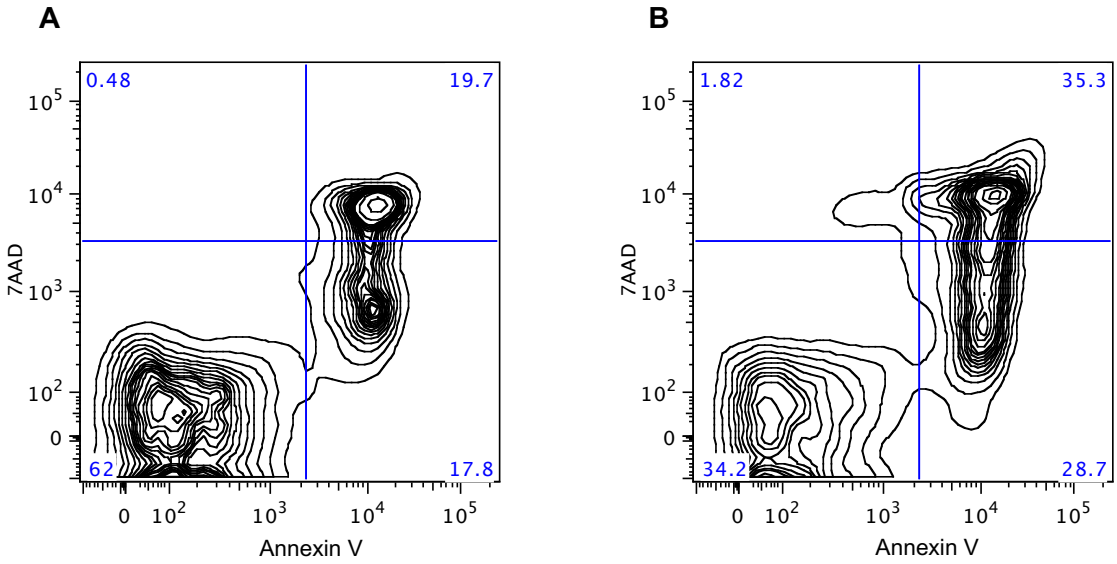

Figure 3-1 Comparison by FACS analysis of fresh and thawed CLL cell viability
Annexin V/7AAD staining after 48 h incubation of patient sample CLL12 taken either fresh (A) or thawed (B). FACS plots are size gated for comparison of viability markers.

3.1.2 Serial FCS dilution experiment – optimisation of media

Apart from the BCR and SDF-1 signalling axes already described in 1.7 and 1.8, mTOR is activated by growth factor signals and is nutrient-responsive (248), therefore we investigated a range of media serum dilutions for use in our experiments. CLL samples were incubated for 48 h in a range of serum concentrations from 0 – 10 % with determination of cellular viability level by staining and flow cytometry for Annexin V and 7AAD. The cell viability was determined for a range of samples with variation in viability shown in Figure 3-2 A. Figure 3-2 B displays individual viability results for each serum concentration demonstrating the rising trend to maximal or near-maximal viability represented by the 10 % FCS incubations for each sample. Normalised viability was calculated for a sample set extended from that in Figure 3-2 A to include CLL with a normal karyotype in Figure 3-2 C with control value set at the viability for those samples incubated in 10% FCS. Individual raw values for the dataset in Figure 3-2 C and their distribution are plotted on the axes for Figure 3-2 D. In Figure 3-3 A&B

there is demonstration of an AZD8055 or rapamycin-dependent dose-dependent trend in inhibition with increasing media serum concentration. With AZD8055 (Figure 3-3 C) there is a significant reduction in normalised cell viability which is greatest at the 10 % FCS concentration, however with rapamycin (Figure 3-3 D) these figures represent only a trend which correlates with serum concentration.

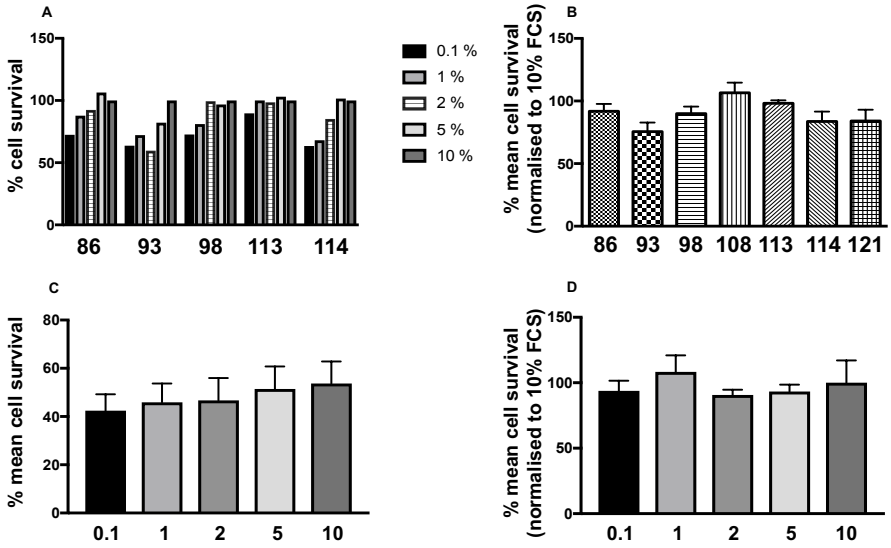

Figure 3-2 CLL cell viability across a range of serum concentrations
Cell viability studies over 48 h of patient samples across a distribution of prognostic markers with individual serum concentrations shown (A, n=5), also, demonstration of mean and SEM combining a range of serum concentrations (B, n=7). Percentage of viable cells was calculated using flow cytometry measurement of Annexin V/ 7AAD. Mean cell viability with SEM for individual serum concentrations is demonstrated for 7 samples in (C) with these data presented after normalisation in (D).

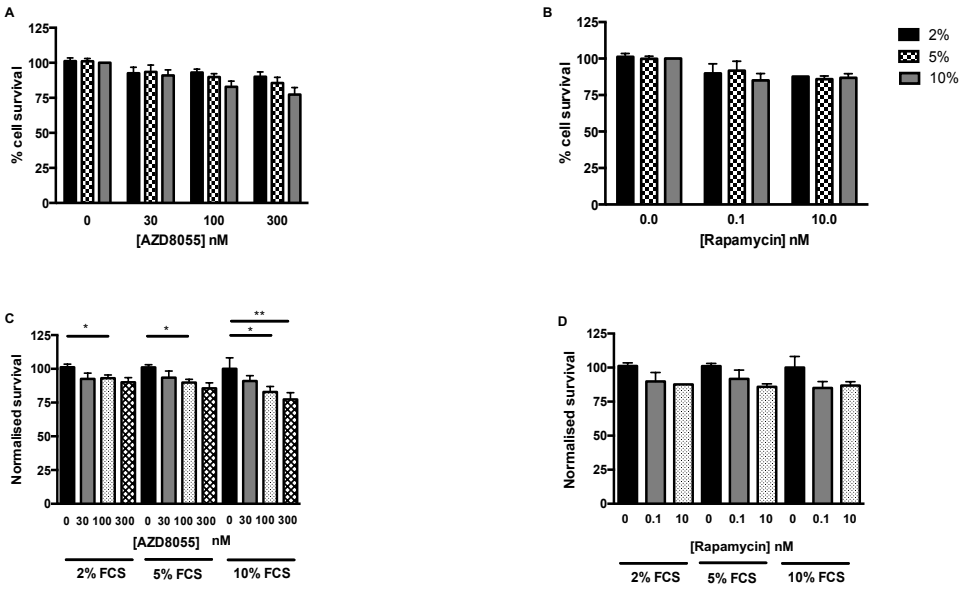

Figure 3-3 Effects of mTOR inhibition on CLL cell viability with variation in serum concentration
CLL samples were rested in their respective serum concentrations for 2 h then treated for 48 h with AZD8055 (A&C) and rapamycin (B&D). Normalised data values (A&B) including mean and SEM are shown. *=p≤0.05; **=p≤0.01; ***=p≤0.001; ****=p≤0.0001.

The experiments to investigate the role of media serum concentration were extended to incorporate mTOR inhibitors to provide data on the effects of mTOR inhibition on CLL cells in combination with a range of serum concentrations, to inform our later experiments. Figure 3-5 displays the effects on primary CLL samples of a range of AZD8055 concentrations from 0 – 300 nM (A) and rapamycin 0 – 10 nM (B) with 48 h incubation at each drug concentration after suspension in their respective FCS concentrations. Figure 3-5 C demonstrates the significant dose-related reduction in CLL cell viability with AZD8055 which is most prominent at the 10% FCS concentration at 48 h. The experiment was extended to 96 h (Figure 3-5), where similar patterns of drug effect persist with both AZD8055 (A) and rapamycin (B).

The effects of CLL cell suspension in 10 % serum display the greatest effects on cell survival with the addition of mTOR inhibitors, with significance shown at 48 and 96 h incubation with both AZD8055 at all concentrations from 30 nM - 300 nM and rapamycin 0.1 nM. It may be that the greater effect at the higher serum concentration may be a result of greater protein phosphatase activity at low serum concentrations. Phosphatases may remove the inhibitory effect of the drugs at low serum concentrations with the experiments performed at higher serum concentration demonstrating a greater effect of mTOR inhibition.

There is an appreciable but low rate of apoptosis upon treatment with AZD8055 or rapamycin (Figure 3-4). Rates of apoptosis appear to be dose-related for both drugs and although their overall ability to induce apoptosis is low, there is a significant increase in apoptosis with an increased FCS concentration from 2 to 5 % and from 2 to 10% with 300 nM AZD8055 and from 2 to 10% at 100 nM AZD8055. These findings confirm that the serum concentration of 10% is optimal for experimental evaluation of the effects of mTOR inhibitors on CLL cells *in vitro* thus media containing 10% FCS was selected for use in further experiments.

Increasing concentrations of AZD8055 and rapamycin show an incremental impact on survival over 48 h and 96 h of CLL cells *in vitro*. Figure 3-5 establishes decrease in viability with increasing concentration of (A) AZD8055 on CLL cell viability over both time points; the effects upon rapamycin treatment are lesser (B).

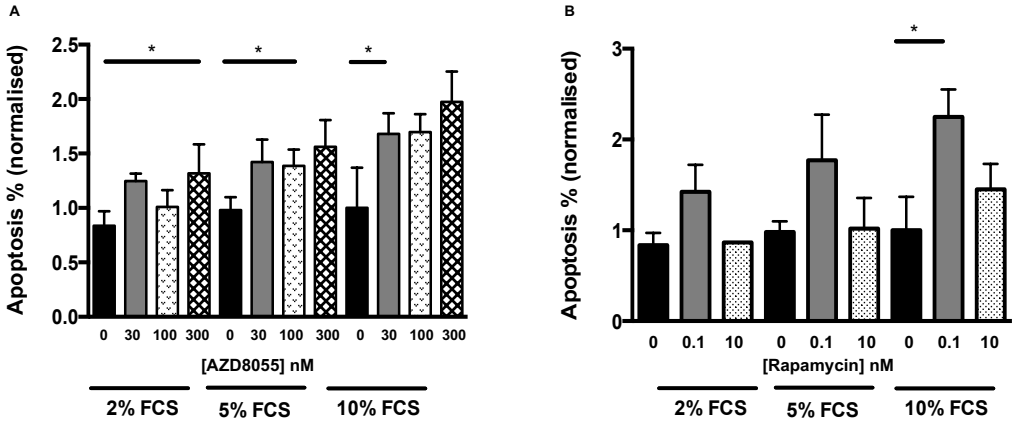

Figure 3-4 Effects of mTOR inhibition and FCS concentration on CLL cell apoptosis
Cells were prepared in their respective serum concentrations for 2 h then treated with mTOR inhibitors for 48 h. Apoptosis was determined by FACS analysis for Annexin V and 7AAD staining. Quadrant Q2 defines the late apoptotic cell populations and percentages of each sample (n=7) were normalised to 1 with mean and SEM displayed for (A) AZD8055 and (B) rapamycin. *=p≤0.05; **=p≤0.01; ***=p≤0.001; ****=p≤0.0001.

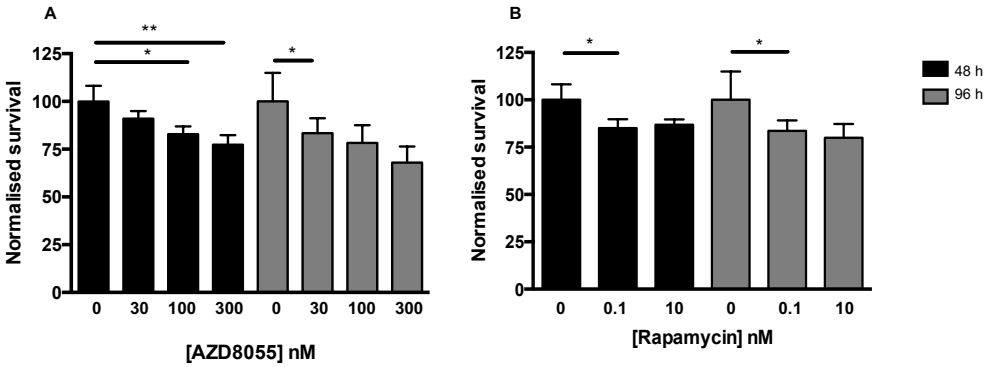

Figure 3-5 Effects of mTOR inhibition on CLL cell viability at 48 and 96 h
CLL cell viability is compared between samples incubated with increasing doses of (A) AZD8055 and (B) rapamycin at 10 % FCS concentration. Data are normalised with mean and SEM shown for each drug concentration (n=7). *=p≤0.05; **=p≤0.01; ***=p≤0.001; ****=p≤0.0001.

3.1.3 Impact of mTOR inhibition on CLL cell viability with SDF-1 stimulation

SDF-1 is produced in a tightly regulated manner by BM stroma and cells of the LN, a feature which is hijacked by the malignant process in CLL. The spatial regulation of SDF-1 and consequent concentration gradient of the ligand which results is responsible for cellular survival as well as being implicated in CLL migration. The application of SDF-1 to CLL experimentation *in vitro* exploits the cell surface overexpression of its receptor, CXCR4, by CLL cells (148) and FACS plots of viability experiments are shown in Figure 3-6.

Our initial approach was to incubate cells for 48 h with inhibitors and 100 ng/ml SDF-1 although this approach was found to be flawed as serum starvation could not be employed over this duration, limiting the size of SDF-1 effect that could be demonstrated. Figure 3-6 demonstrates non-significant inhibition of 48 h viability with AZD8055 at 300 nM and rapamycin 10 nM with only moderate effects of SDF-1 on CLL cell viability being demonstrable. The CXCR4/CXCL12 axis has been studied with specific reference to its effects on mTORC1 substrate p70S6K, indicating that the optimal time point for study of SDF-1 reactions is significantly earlier than 48 h, most likely due to exhaustion of the cellular reaction to the chemokine (249). The reaction appears to plateau by 30 min and is approaching termination by 1 h, giving a framework on which to base further experiments. As it has been discussed previously, mTOR kinase is activated by range of signals with many of these being of key importance to cellular metabolism. Furthermore, the mTOR signalling pathway has been shown to signal downstream of CXCL12 in regulation of cellular migration of T cells (250), whilst the influence of CXCL12 on CLL cell migration remains relatively underexplored. Therefore, our revised approach was to expose primary CLL cells to a period of serum starvation prior to our experiments involving SDF-1, aiming to enhance the demonstration of SDF-1 stimulation effects, other than viability effects, with our study to be limited to a shorter duration of exposure to chemokine as in section 3.2.5.

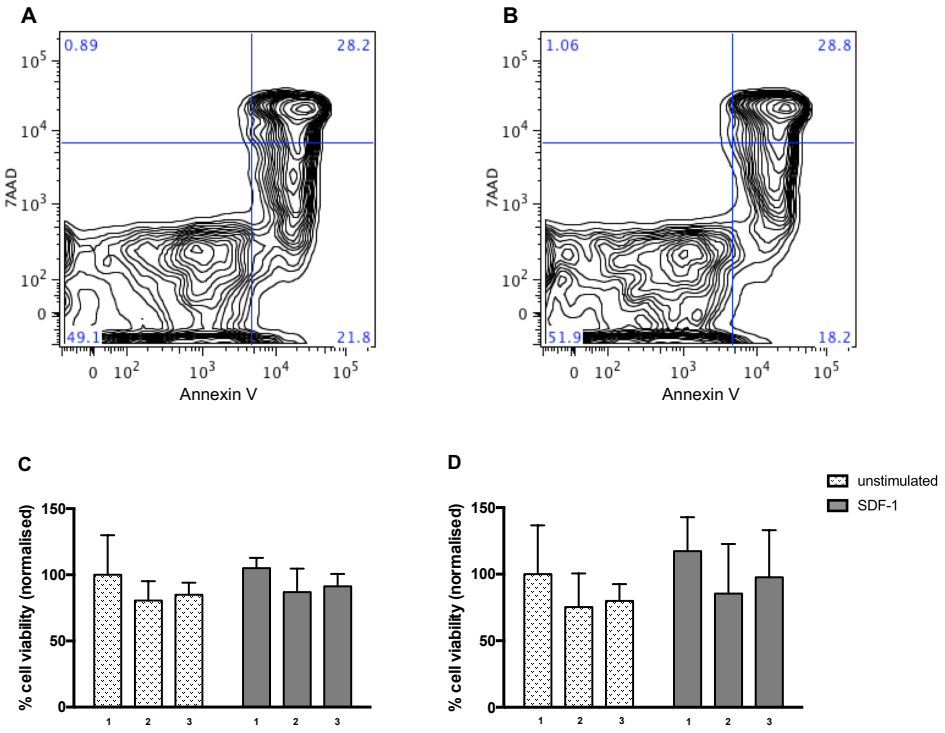

Figure 3-6 CLL cell viability effects of long term SDF-1 incubation
Normal karyotype CLL patient sample CLL126 was incubated with 100 ng /ml SDF-1 (B) for 48 h and viability was compared with an unstimulated sample (A). Normalised mean and SEM viability effects of mTOR inhibition and +/- SDF-1 stimulation are also shown (C & D). CLL cells were incubated for 30 min with mTOR inhibitors then treated with SDF-1 for 48 h. Viability was determined by FACS calculation of percentage viable cells of on CLL samples (n=10) over (C) 48 h and (D) 96 h with drug conditions: 1 = NDC, 2 = AZD8055 300 nM and 3 = Rapamycin 10 nM.

3.1.4 Optimisation of F(ab')$_2$ vs anti-IgM and effects on viability

The effects of BCR stimulation on the microenvironment in CLL may be modelled *in vitro* using various methods, either by soluble or bound anti-IgM or by use of F(ab')$_2$ fragment stimulation. Data relating to chemokine expression of CLL cells have yielded contrasting results and some of these differences have been attributed to the utilisation of varying methods of BCR stimulation; either immobilised or soluble and through F(ab')$_2$ fragment stimulation or anti-IgM stimulation, with BCR cross-linking (251, 252). There has been support in the published literature for either method however the apparent differences in response of CLL cell to the variations in BCR stimulation methodology led the authors of one study to comment that there is "no standardized (sic) method of BCR stimulation" (253). With the aim of providing clarity over the issue of BCR stimulation, there has been dedicated study of each method in parallel by Rombout *et al* (254). The type of stimulation utilised, whether soluble or immobilised anti-IgM, was shown to have differential effects on CLL cell mRNA and protein expression of genes related to a BCR-activation signature with some differential effects on 48 h – 72 h cell survival (254). However, in this study, there appeared to be no significant differences elicited between anti-IgM or F(ab')$_2$ fragment stimulation. My work incorporates the use of soluble BCR stimulation, either anti-IgM stimulation with the addition of avidin crosslinking, or F(ab')$_2$ fragment stimulation. Where possible I have performed comparisons between these methods using the same patient sample to confirm my findings. To investigate the short-term effects of BCR stimulation, I performed a series of experiments, each conducted over 24 h, to examine the effects of mTOR inhibition and BCR stimulation on cell viability and apoptotic regulators. Figure 3-7 indicates minimal difference in the effects of BCR stimulation by various methods when conducted over 1 h as compared with 24 h. Figure 3-8 indicates that the 48 h stimulation effects of either F(ab')$_2$ fragment stimulation or anti-IgM stimulation promote a significant improvement in viability when compared with unstimulated cells or anti-IgM stimulation alone.

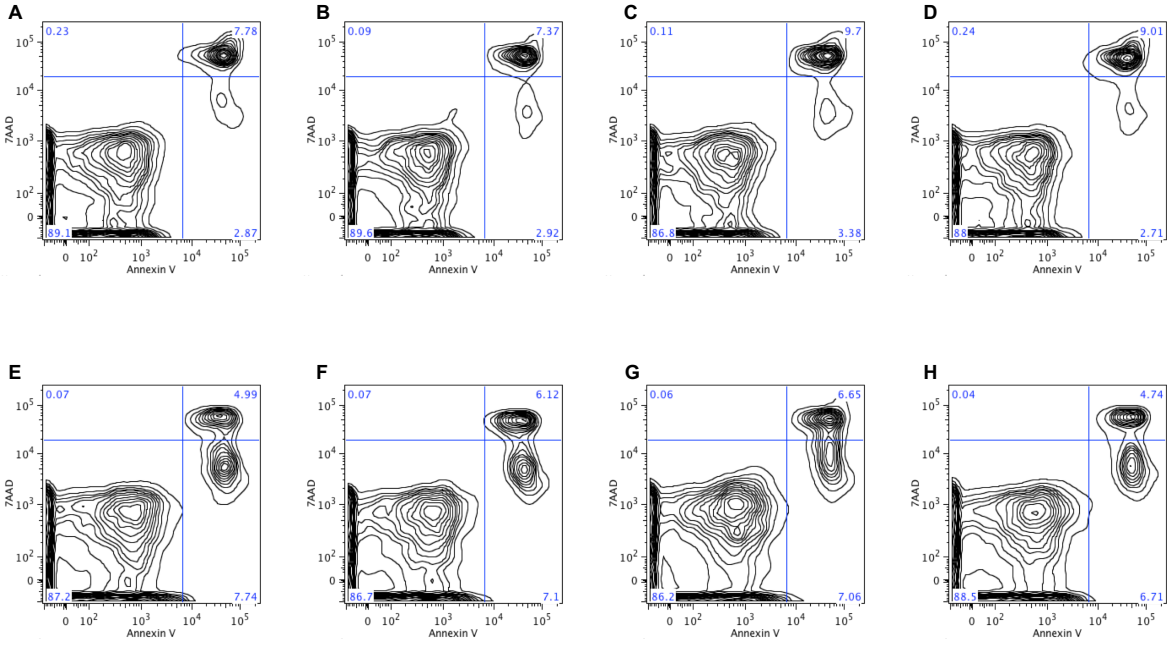

Figure 3-7 Modality of BCR stimulation and effects on short-term CLL cell viability
Cellular viability studies of CLL57 (normal karyotype CLL) by FACS at 1 h incubation with (A) no stimulation (B) 10 μg/ml anti-IgM antibody (C) 10 μg/ml anti-IgM antibody for 20 min, then washing, then then 25 μg/ml avidin and (D) 10 μg/ml F(ab')$_2$ fragments. Conditions were extended for 24 h shown in (E) no stimulation (F) 10 μg/ml anti-IgM antibody (G) 10 μg/ml anti-IgM antibody for 20 min, then washing, then 25 μg/ml avidin and (H) 10 μg/ml F(ab')$_2$ fragments.

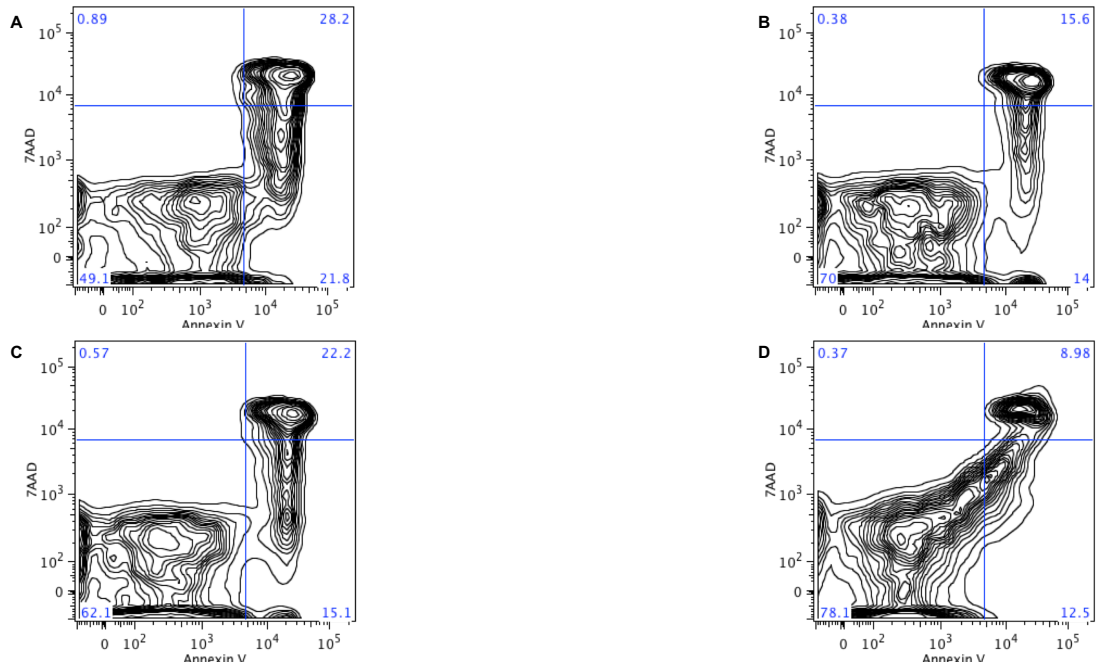

Figure 3-8 Long-term CLL cell viability effects of BCR stimulation
FACS plots to compare viability of cells from a normal karyotype CLL sample (CLL126) when incubated at 37°C for 48 h with either (A) no stimulation (B) 10 μg/ml F(ab')$_2$ fragments (C) 10 μg/ml anti-IgM antibody and (D) 10 μg/ml anti-IgM antibody for 20 min, then washing, then 25 μg/ml avidin.

3.1.5 Effects of mTOR inhibition and BCR stimulation on CLL viability

BCR stimulation is one of the key survival signals received by CLL cells in the disease microenvironment and the well-documented effects of BCR stimulation *in vitro* are exploited in our experimental strategy (254). To mimic this aspect of the CLL cell microenvironment, we stimulated the CLL cells by ligating the BCR, with either $F(ab')_2$ fragments or biotinylated anti-IgM crosslinked with avidin and incubated the cells for 48 and 96 h. Preliminary experiments were conducted to show a limited effect of shorter durations of mTOR inhibition upon CLL viability in the presence and absence of BCR stimulation. Figure 3-9 shows the BCR stimulation effects at 24 h incubation on a single CLL sample, with and without dual mTOR inhibition using AZD8055.

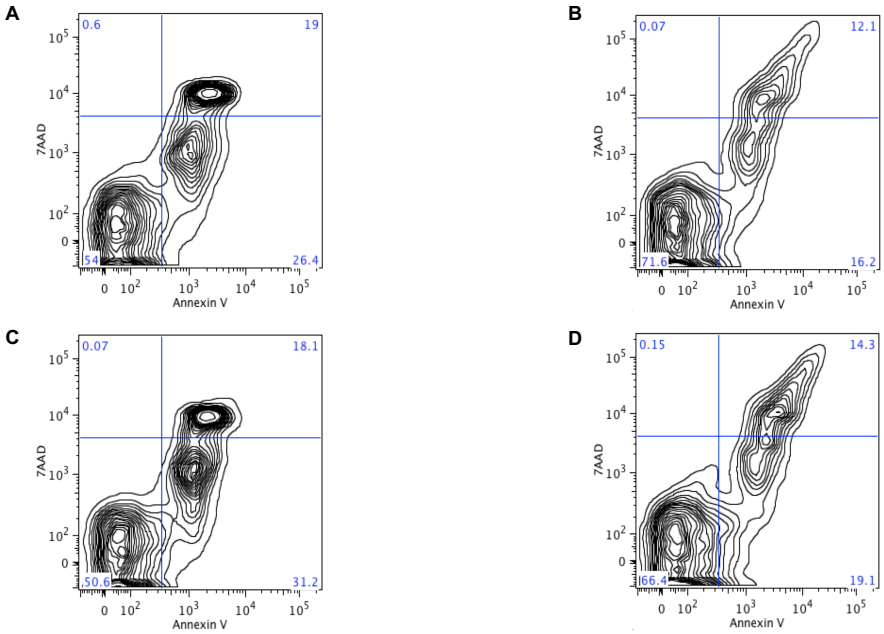

Figure 3-9 Short-term viability effects of dual mTOR inhibition with BCR stimulation Cellular viability studies of CLL77 (normal karyotype CLL) by FACS at 24 h incubation with the conditions: (A) untreated control (B) 10 μg/ml anti-IgM stimulation for 20 min with washing of CLL samples followed by 25 μg/ml avidin crosslinking (C) AZD8055 100 nM alone (D) AZD8055 100 nM and subsequent 10 μg/ml anti-IgM stimulation for 20 min with washing of CLL samples followed by 25 μg/ml avidin crosslinking.

Figure 3-10 illustrates the significant reductions in cell viability seen upon treatment of CLL cells with mTOR inhibitors in the presence or absence of BCR stimulation. For drug treatment, CLL cells were pre-treated for 30 min with mTOR inhibitors, as indicated. CLL cell viability is reduced by both AZD8055 and rapamycin over 48 h (A) and 96 h (B) incubation periods. Dual mTORC-1/2 inhibition offers a more robust impact on CLL cell viability over that of mTORC-1

inhibition *in vitro*, even after accounting for the effects of BCR stimulation. The addition of F(ab')$_2$ and anti-IgM stimulation enhanced the effect of drug inhibitors at 48 h and 96 h, as did crosslinking with avidin to a lesser degree. However, the overall effects of crosslinking with avidin were to increase relative viability of CLL cells at both 48 h and 96 h, when compared with unstimulated cells and those stimulated with anti-IgM alone, although this did not reach significance. The concentrations of 300 nM AZD8055 and 10 nM rapamycin are the highest doses that we have used and in these experiments they were used with the aim of achieving maximal mTOR inhibition for these initial experiments. However, our concentration range was extended to include a clinically attainable concentration of 100 nM with concurrent assessment of viability effects of ibrutinib at 1 μM. Figure 3-11 displays the effects of BCR stimulation on untreated CLL cells (A) with a significant increase in viability with the addition of either F(ab')$_2$ or anti-IgM stimulation with avidin crosslinking. The effects of BCR stimulation are evaluated in the context of drug conditions, and with data normalisation with significance demonstrated in the AZD8055 300 nM condition, also the rapamycin and ibrutinib conditions (Figure 3-11 B). There was a significant reduction in cellular viability with AZD8055 at both concentrations in the presence and absence of BCR stimulation, as with both rapamycin and ibrutinib (Figure 3-11 C).

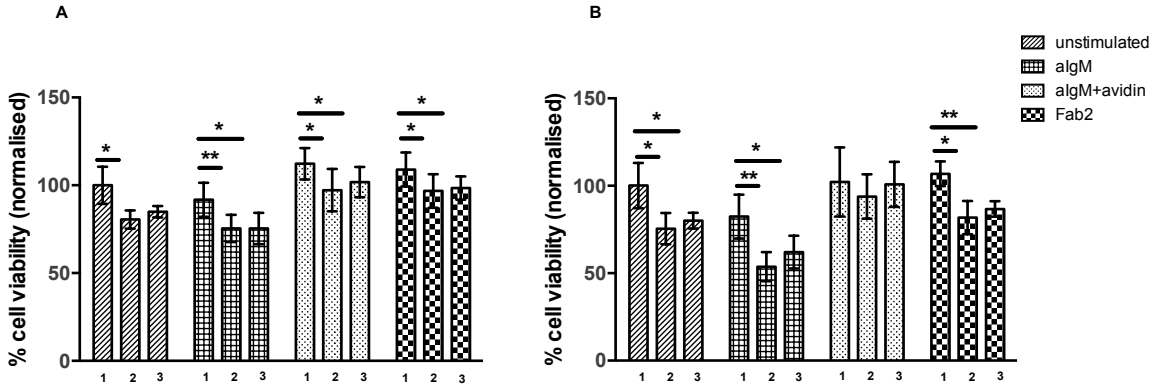

Figure 3-10 Effects of long term BCR stimulation and mTOR inhibition on CLL cell viability Impact of mTOR inhibition and method of BCR, either 10 μg / ml F(ab')$_2$ stimulation or 10 μg / ml anti-IgM alone or with 25 μg / ml avidin crosslinking, on cellular viability for CLL samples at (A) 48 h incubation and (B) 96 h incubation. Drug conditions are denoted: 1 = NDC (Non-drug control), 2 = AZD8055 300 nM and 3 = Rapamycin 10 nM. FACS analysis of Annexin V and 7AAD staining were used to calculate percentage viability with mean +/- SEM values as shown (n = 8). *=p≤0.05; **=p≤0.01; ***=p≤0.001; ****=p≤0.0001.

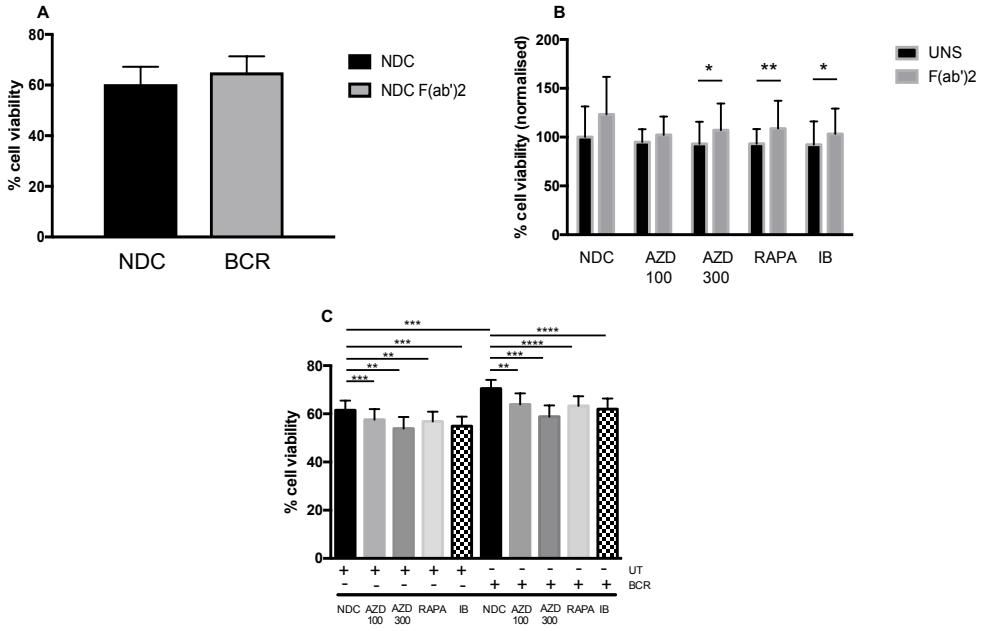

Figure 3-11 Cell viability over 48 h drug incubation with mTOR inhibitors
Evaluation of percentage of viable untreated cells as determined by FACS evaluation reveals significant effects of BCR stimulation (A) which persist in the presence of drug conditions (B). Normalised percentage cell viability is inhibited significantly over 48 h by AZD8055 (AZD), rapamycin (RAPA) and ibrutinib (IB) when compared with the non-drug control (NDC), an effect which is overcome by the addition of BCR stimulation (C). Mean +/- SEM data are shown (n=23). *=p≤0.05; **=p≤0.01; ***=p≤0.001; ****=p≤0.0001.

3.1.6 Impact of BCR stimulation on pro- and anti-apoptotic proteins

Changes in the expression of pro- and anti-apoptotic proteins after 48 h stimulation in the presence or absence of drug treatment are shown (Figure 3-12). The expression of BCL-2 which is fundamental to CLL pathogenesis remains constant, whereas MCL-1 levels are modulated with AZD8055 and ibrutinib treatment (Figure 3-12 A). The addition of BCR stimulation serves to increase MCL-1 levels which may be abrogated by AZD8055 and ibrutinib and to a lesser extent, rapamycin. At 48 h BCR incubation there is an upregulation in the Bim 15 kDa isoform with the addition of AZD8055 and ibrutinib; Bim_L levels also appear to be downregulated with BCR stimulation (Figure 3-12 B). There appears to be a relative enhancement of the Bim_{EL} level with AZD8055 and ibrutinib in the BCR stimulated cells however Bim_S levels appear relatively unchanged (Figure 3-12 B). These blots confirm that GTPase Rap1 and Rac1 levels are relatively unchanged over 48 h mTOR inhibition with or without BCR stimulation which shall be discussed further in Chapter 5 (Figure 3-12 A&C). Changes in overall protein levels of GTPase protein families are therefore not an anticipated feature of drug inhibition, but were studied nevertheless, to confirm consistent overall protein levels. The levels of BCL-xL are upregulated by BCR stimulation and there are inhibitory effects with AZD8055, and ibrutinib and rapamycin in the presence of BCR stimulation, to a lesser extent. Once loading correction has been applied, the trend to significance in BCL-xL level changes persist with AZD8055 inhibition in the presence of BCR stimulation. Poly (ADP-ribose) polymerase (PARP) levels and relative size of cleaved and uncleaved fractions are indicative of pro-apoptotic activity by the drug inhibitors. Figure 3-12 B demonstrates induction of apoptosis by AZD8055 as assessed by the relatively increased quantity of PARP cleavage product when compared with the uncleaved protein. These effects persist with BCR stimulation, with a relatively smaller proportion of cleaved PARP with both rapamycin and ibrutinib. The viability effects of short-term BCR stimulation by FACS as shown in Figure 3-10 are supported by Western blot experiments, studying apoptotic regulators. Figure 3-13 shows the less pronounced effects of mTOR inhibition on markers such as MCL-1 and PARP over 24 h.

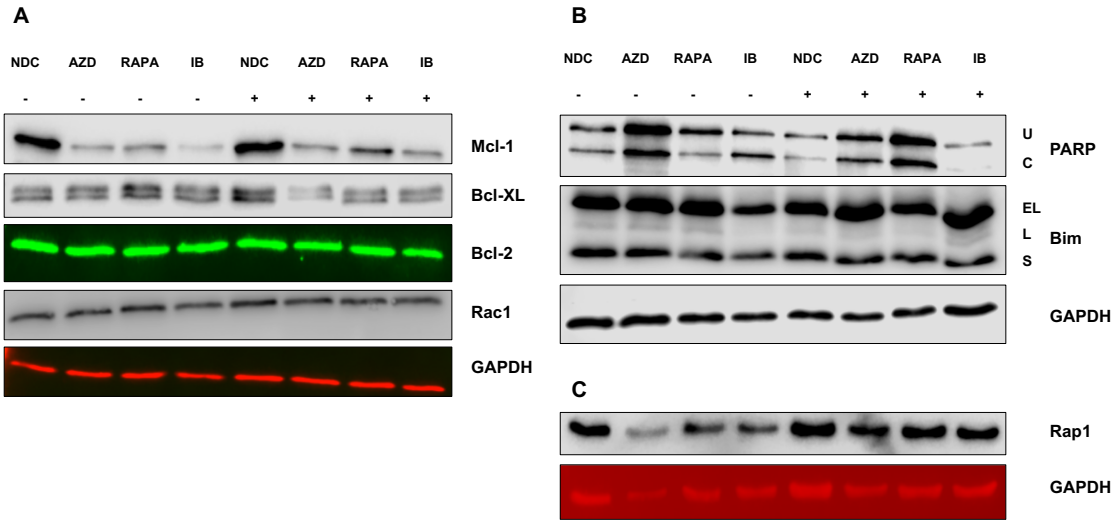

Figure 3-12 Long-term effects of mTOR inhibition on apoptotic proteins
Western blot for protein levels of apoptotic regulators and effectors at 48 h incubation with demonstrated effects of non-drug control (NDC), 100 nM AZD8055 (AZD), 10 nM rapamycin (RAPA) and 1 μM ibrutinib (IB) +/- BCR stimulation in primary CLL samples (A) CLL157 (11q deletion) (B) CLL18 (11q deletion) and (C) CLL140 (normal karyotype). Western blot identification of proteins demonstrated are based upon estimated molecular weights: MCL-1 (40 kDa), BCL-XL (30 kDa), BCL-2 (26 kDa), Rac1 (21 kDa), GAPDH (36 kDa), PARP uncleaved (116 kDa) and cleaved (89 kDa), Bim_{EL} (23 kDa), Bim_L (15 kDa) and Bim_S (12 kDa) and Rap1 (23 kDa).

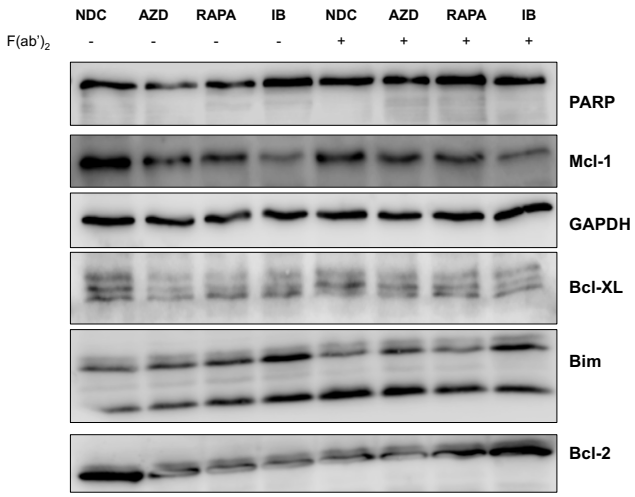

Figure 3-13 Short-term effects of mTOR inhibition on apoptotic proteins
CLL143, a CLL sample known to harbour an 11q deletion, was treated with incubation with control (NDC), 100 nM AZD8055 (AZD), 10 nM rapamycin (RAPA) and ibrutinib 1 μM (IB) for 30 min, +/- BCR stimulation for 24 h, demonstrating the effects of mTOR inhibitors and ibrutinib on apoptotic regulators at this time point.

Densitometry analysis was performed on combined results from Western blotting of individual CLL patients for apoptotic regulators at 48 h incubation with drug inhibitors in the presence or absence of BCR stimulation. The blots were analysed using Image Studio software as all long-term BCR stimulation images

were generated using the Li-Cor system. Figure 3-14 demonstrates the significant inhibition of anti-apoptotic MCL-1 protein by AZD8055 in cells which have been stimulated via the BCR. There are inhibitory effects of rapamycin and ibrutinib on MCL-1 however these are not statistically significant. The pro-survival BCL-2 family member BCL-xL also displayed significant inhibitory effects by AZD8055 in BCR-stimulated cells compared with untreated control (Figure 3-15). Densitometry of cleaved PARP levels as shown in Figure 3-16 demonstrate the apoptotic effects of AZD8055 and ibrutinib in Figure 3-16 A&B with consistent effects after controlling for protein loading. With the addition of BCR stimulation, both AZD8055 and ibrutinib display apoptotic effects. Rapamycin also exhibits some apoptotic activity in the experiments using 4 samples in the context of BCR stimulation alone (Figure 3-16 B). Densitometry values could be obtained for Western blot from two samples probed for Rac1 and one sample for Rap1 GTPase, each demonstrating minimal changes in GTPase levels with mTOR inhibition in the presence and absence of BCR stimulation (Figure 3-17 A&B).

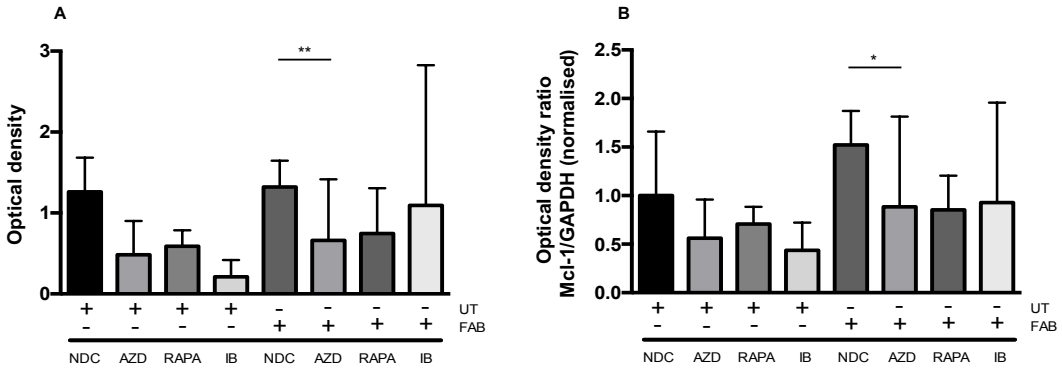

Figure 3-14 Densitometry analysis of MCL-1 expression by Western blot
Densitometry values of mean and SEM MCL-1 levels with the effects of non-drug control (NDC), AZD8055 100 nM (AZD), rapamycin 10 nM (RAPA) and ibrutinib 1 μM (IB) +/- BCR stimulation (A) and with loading correction applied (B) (n=6). Statistical comparison is performed using the paired Student's t test. *=p≤0.05; **=p≤0.01; ***=p≤0.001; ****=p≤0.0001.

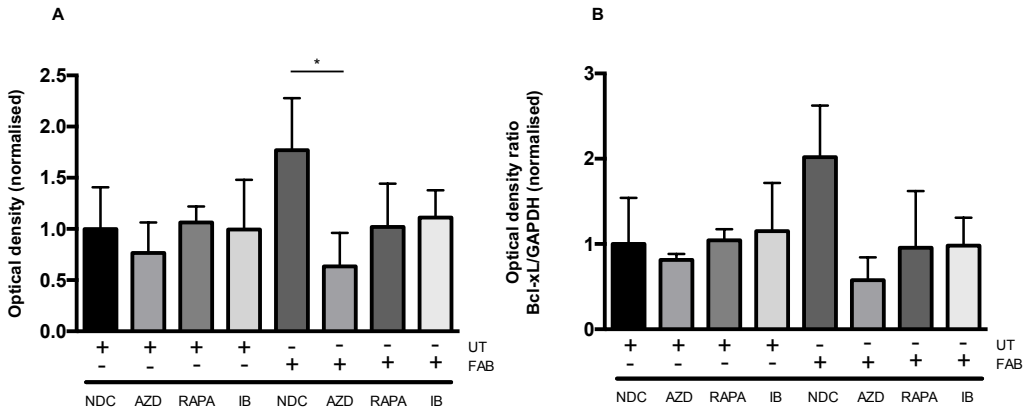

Figure 3-15 Densitometry analysis of BCL-xL expression by Western blot
Normalised mean and SEM BCL-xL levels with the effects of non-drug control (NDC), AZD8055 100 nM (AZD), rapamycin 10 nM (RAPA) and ibrutinib 1 μM (IB) +/- BCR stimulation (A) and with loading correction applied (B) (n=5). Statistical comparison is performed using the paired Student's t test. *=p≤0.05; **=p≤0.01; ***=p≤0.001; ****=p≤0.0001.

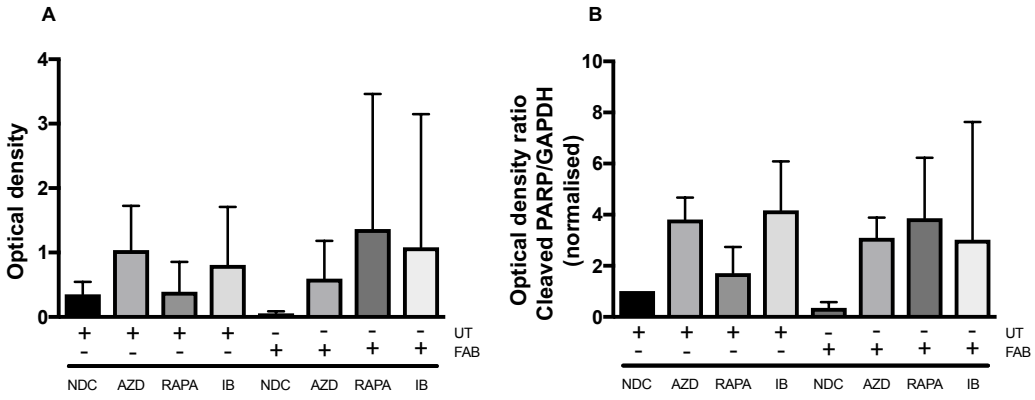

Figure 3-16 Densitometry analysis of cleaved PARP expression by Western blot
Normalised mean and SEM cleaved PARP levels are shown and the relative effects of non-drug control (NDC), AZD8055 100 nM (AZD), rapamycin 10 nM (RAPA) and ibrutinib 1 μM (IB) +/- BCR stimulation (A). Once loading correction has been applied, the effects of mTOR inhibitors persists (B) (n=4).

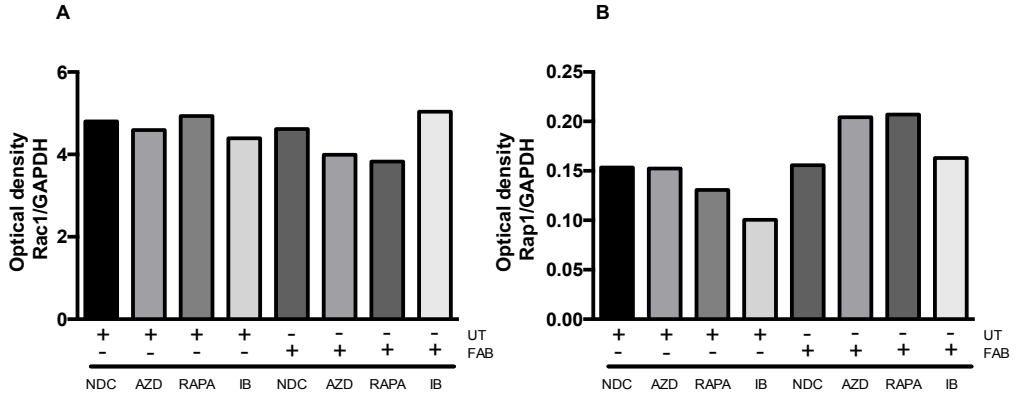

Figure 3-17 Densitometry analysis of GTPase protein expression by Western blot
Total mean Rac1 (A, n=2) and Rap1 (B, n=1) levels are shown with relative effects of non-drug control (NDC), AZD8055 100 nM (AZD), rapamycin 10 nM (RAPA) and ibrutinib 1 μM (IB) +/- BCR stimulation. Rac1 and Rap1 levels are displayed with correction for protein loading.

3.2 Protein expression of chemokine receptor and adhesion markers

As the chemokine receptor and adhesion molecule profile of cells in our CLL cell bank has not been studied, the surface expression of CXCR4, CXCR5, CD62L, CD44, CD11a, CD38 and CD49d markers were determined in freshly isolated CLL samples. CXCR4 and CXCR5 are responsible for migration along a chemokine gradient to the BM and LN niches and CD62L and CD44 are responsible for CLL cell positioning within the microenvironment (148, 149, 153, 154). CD11a is an adhesion molecule found in the early stages of CLL (148, 149, 153, 154, 255). CD38 and CD49d are independent negative prognostic risk parameters and form part of macromolecular complexes required for CLL cell homing (152, 256).

We found a wide range of variability in the expression of markers between CLL samples (Figure 3-18) and CXCR4, CD62L and CD44 were selected for further study in view of their consistent elevation. CXCR5 was selected, although less highly expressed, for its importance in migration and in view of the existing data with this molecule (149). CD38 and CD49d antibodies stained with low mean fluorescence in most samples and although we explored alternative antibodies, no significant increase in mean fluorescence was noted with these antibodies.

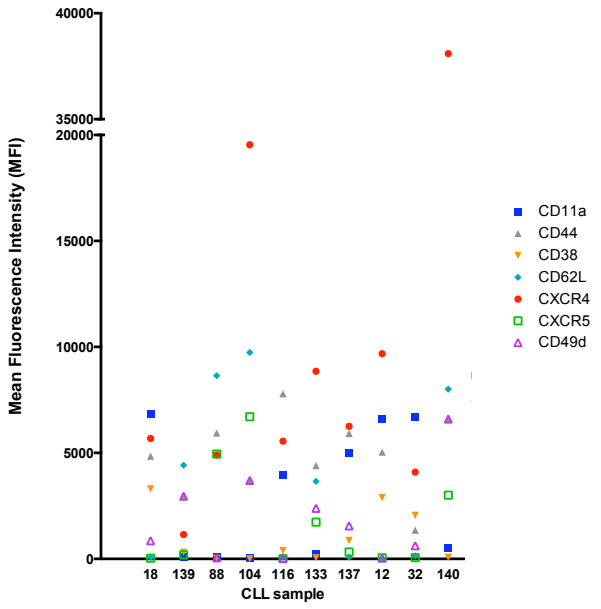

Figure 3-18 Flow cytometry analysis of fluorescence by antibody bound to cell surface adhesion markers
CLL samples were incubated with antibody to CD11a, CD44, CD38, CD62L, CXCR4, CXCR5 and CD49d with known functions in cell adhesion and migration. After 20 min, cells were washed and resuspended in HBSS to allow FACS analysis of fluorescence intensities. CLL18 and CLL139 are samples with 11p deletion, CLL12 has 13q deletion, CLL32 has 6p deletion and CLL140 has trisomy 12 chromosomal abnormality. All other samples possess a normal karyotype.

3.2.1 Short-term response of chemokine and adhesion molecule expression to BCR stimulation by flow cytometry

To facilitate selection of patient samples for use in migration studies discussed in chapter 4, we measured surface expression of key proteins CXCR4, CXCR5 and CD62L by fluorescent antibody staining in primary CLL samples after 1 h BCR stimulation, mirroring the transwell assay design. Data shown in Figure 3-19 support a reduction in CXCR4 and CD62L in response to BCR stimulation, consistent with existing published data, and only minimal responses of CXCR5 (252). Further analysis of 1 h BCR responses with stratification of samples by type of BCR stimulation, either $F(ab')_2$ stimulation or anti-IgM with avidin crosslinking, demonstrated that CD62L levels were significantly reduced with $F(ab')_2$ stimulation (Figure 3-20 A&B). The effects of cryopreservation and thawing on cellular surface marker expression have been examined with minor differences to be observed in the percentage expression of CLL phenotypic markers in comparison with that of fresh CLL cells (257). To account for differences in protein levels with cellular recovery, cell surface marker expression studies were performed on both fresh and thawed samples from the

same patient wherever possible, to confirm my findings. Further analysis with sample stratification by fresh and thawed sample sources displayed similar trends within these subgroups (Figure 3-20 C&D).

Chemokine receptor responses to short-term BCR-stimulation were re-grouped by prognostic categories, either by disease karyotype (Figure 3-21) or by non-receptor tyrosine kinase, ZAP70 expression (Figure 3-22) to determine whether surface expression was altered in distinct prognostic subsets. Trends to reduction in chemokine and adhesion marker surface levels were maintained even with the low sample number represented in some subgroups. The trends to reduction in surface expression of both CXCR4 and CD62L featured both in negative prognostic subgroups (17p deletion, 11q deletion, ZAP70 positive) and normal karyotype/ZAP70 negative groups alike. Statistical analyses were performed between samples grouped by prognostic parameters with no demonstrable significance in any of the subgroups.

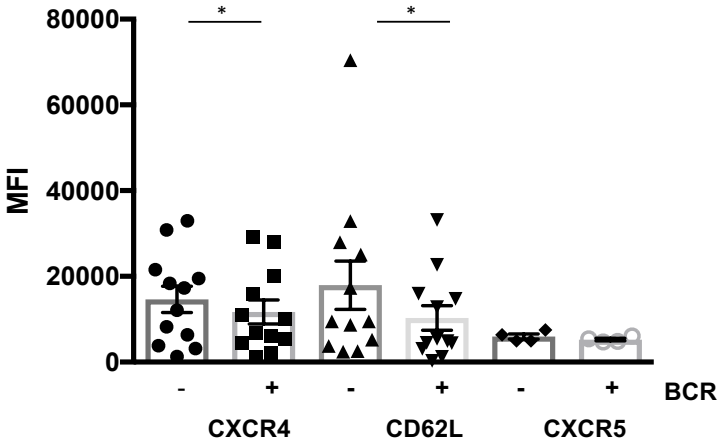

Figure 3-19 Impact of BCR stimulation on chemokine receptor and adhesion molecule cell surface profile
Mean fluorescence intensity measured for CXCR4 (n=11), CXCR5 (n=4) and CD62L (n=11) for a range of CLL samples, treated for 1 h with either F(ab')$_2$ stimulation or α-IgM with avidin crosslinking prior to antibody staining. *=p≤0.05; **=p≤0.01; ***=p≤0.001; ****=p≤0.0001.

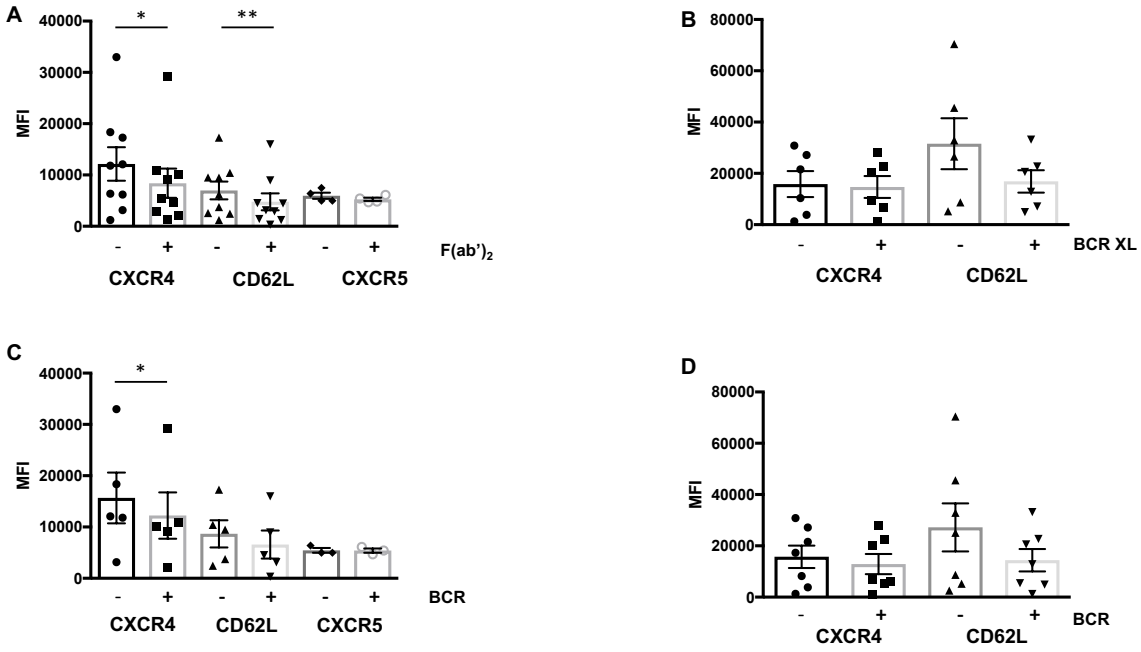

Figure 3-20 Chemokine receptor and adhesion molecule levels by BCR stimulation and sample type
Mean fluorescence intensity measured for CXCR4, CXCR5 and CD62L for a range of CLL samples, treated for 1 h with (A, n=8) F(ab')$_2$ stimulation (B, n=6) α-IgM with avidin crosslinking with samples stimulated with either type of BCR stimulation but stratified as to whether they were used (C, n=5) fresh or (D, n=7) thawed. *=p≤0.05; **=p≤0.01; ***=p≤0.001; ****=p≤0.0001.

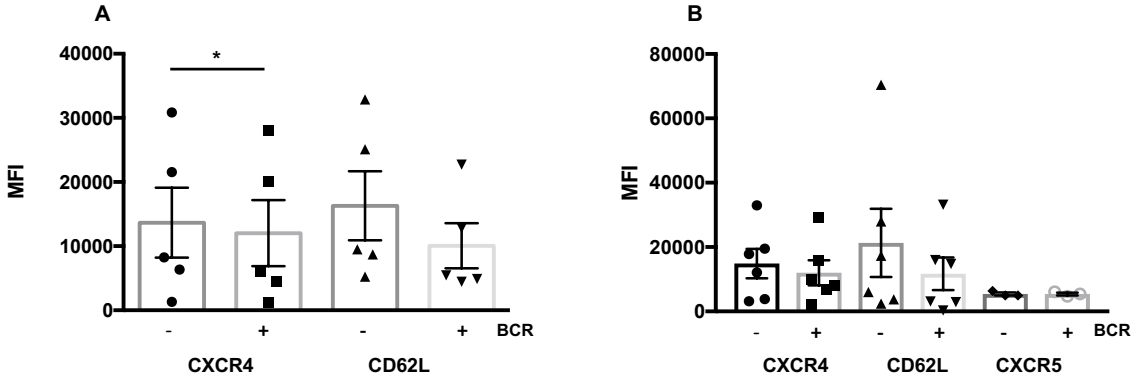

Figure 3-21 Chemokine receptor and adhesion molecule levels by sample karyotype
Mean fluorescence intensity measured for CXCR4, CXCR5 and CD62L for a range of CLL samples (n=11), with samples characterised by (A) either 17p or 11q deletion (n=5) or (B) normal karyotype (n=6). *=p≤0.05; **=p≤0.01; ***=p≤0.001; ****=p≤0.0001.

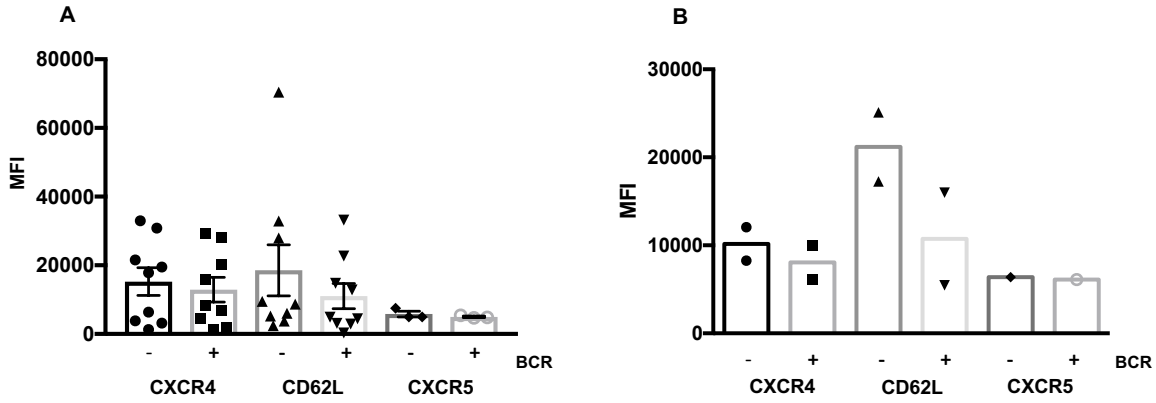

Figure 3-22 Chemokine receptor and adhesion molecule levels by sample ZAP70 status0 Mean fluorescence intensity measured for chemokine receptors CXCR4, CXCR5 and CD62L for a range of CLL samples (n=11), with samples characterised by (A) ZAP70 positive (n=9) (B) ZAP70 negative (n=2) prognostic marker status.

The cell markers CXCR4, CXCR5, CD62L and CD44 were also studied after long-term incubation with BCR stimulation to distinguish the direct effects of BCR stimulation on local signal transduction visible over 1 h from putative effects which may be mediated by signal transduction to the cell nucleus with consequent alteration of gene expression of surface markers. Consistent with existing published data, Figure 3-23 shows a significant reduction in CXCR4 whereas there was only a trend to reduction in CXCR5, with less pronounced changes in CD62L and CD44 (252).

Over 48 h drug incubation no significant changes on chemokine receptor expression were observed in the absence of BCR stimulation (Figure 3-24 A,C&E), however with the addition of BCR stimulation (Figure 3-24 B,D&F) there were significant changes in CXCR4 (B), indicating that the reduction in chemokine receptor levels that are normally seen with BCR were lost upon AZD8055 and ibrutinib drug treatment. This may provide an insight into the mechanism of action of these drugs, as it is already known that ibrutinib may overcome the impact of negative prognostic conditions by negating the component of BCR signalling and its contribution to disease survival and evolution, in those clones for which upregulated BCR signalling is a prominent feature of the disease pathogenesis (258).

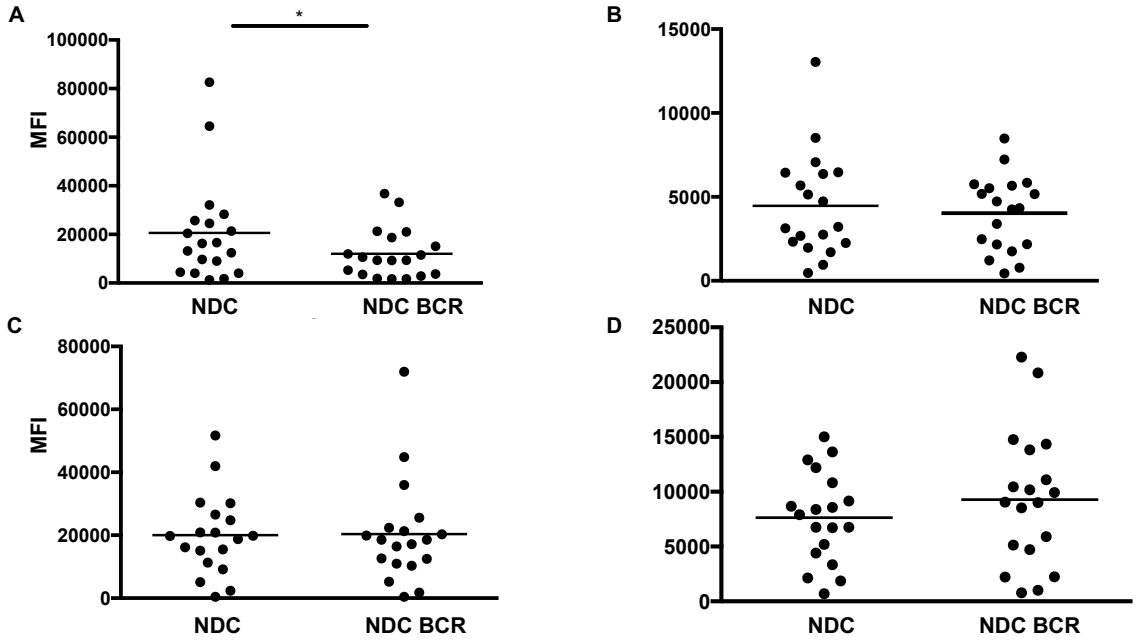

Figure 3-23 Chemokine receptor and adhesion molecule responses to BCR stimulation Cells were incubated for 48 h in the presence or absence of BCR stimulation with sample staining with fluorescent antibody to CXCR4 (A) CXCR5 (B) CD62L (C) CD44 (D) (n=18). Stained samples were analysed by flow cytometry to quantify relative levels of cell marker surface expression. CLL12, 28, 44, (fresh and thawed) 77, 80, 90, 92, 93, 95 (fresh and thawed), 106, 113, 118, 138 (fresh and thawed), 139, 140, 142. Samples were grouped for additional analysis by method of BCR stimulation however no significant differences were observed. *=p≤0.05; **=p≤0.01; ***=p≤0.001; ****=p≤0.0001.

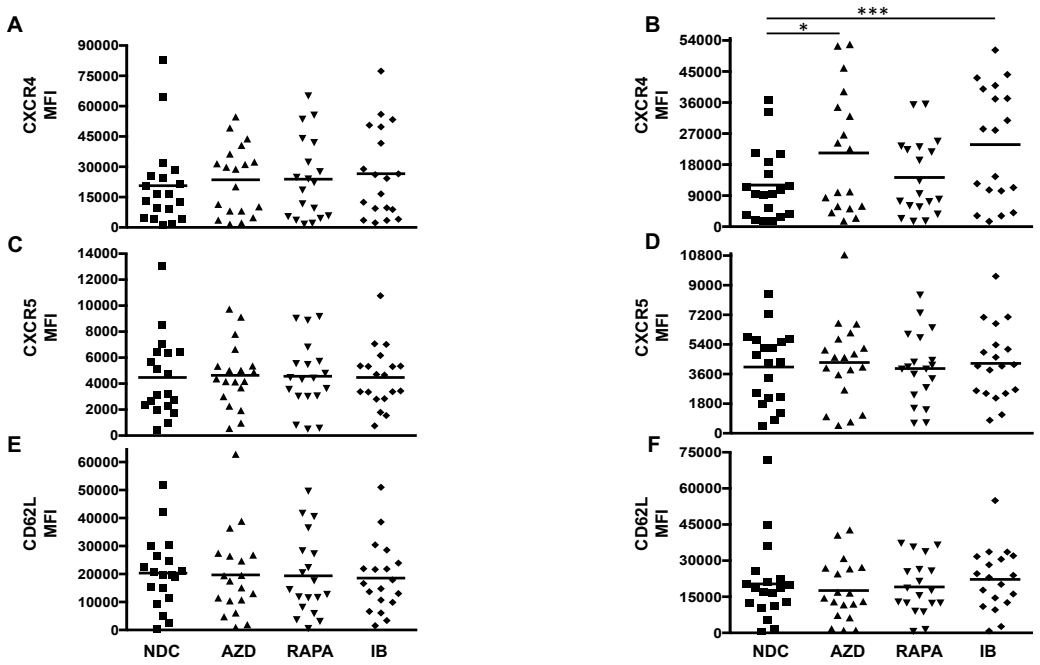

Figure 3-24 Long-term effects on cell surface profile with mTOR inhibitors and BCR stimulation
The same CLL samples used in figure 3.24 (n=19) were incubated for 48 h with 30 min prior drug inhibition with non-drug control (NDC), 300 nM AZD8055 (AZD), 10 nM rapamycin (RAPA), 1 μM ibrutinib (IB). Graphs show mean fluorescence intensity (MFI) by FACS analysis for CXCR4 (A & B) CXCR5 (C & D) CD62L (E & F). Graphs A, C & E represent unstimulated cells with drug conditions only whereas graphs B, D & F represent samples exposed to BCR stimulation for 48 h. *=p≤0.05; **=p≤0.01; ***=p≤0.001; ****=p≤0.0001.

3.2.2 Promotion of LN-emigrant phenotype with the addition of SDF-1

It is known that CLL surface immunophenotype varies according to cellular positioning, either in migration towards or away from the LN niche (156). We performed experiments to assess the *in vitro* effects of chemokine ligand on cell surface immunophenotype, in the presence or absence of inhibitors.

Three patient samples, CLL3, CLL44 and CLL122 were incubated for 48 h after pre-treatment with inhibitors. Although no effects on cell viability could be demonstrated after 48 h incubation with SDF-1, the conditions were replicated as for the viability experiments to assess CXCR4 and CD5 expression by FACS. An example of the effect of SDF-1 on untreated CLL cells harbouring a LN emigrant phenotype ($CXCR4^{dim}CD5^{hi}$) is displayed (Figure 3-25). A significant increase in the percentage of $CXCR4^{dim}CD5^{hi}$ cells was observed with untreated, 300 nM AZD8055 or 1 μM ibrutinib-treated cells with the addition of SDF-1. Relative proportions of $CXCR4^{dim}CD5^{hi}$ cells were compared in the SDF-1-treated

conditions, demonstrating significant inhibition of these cells by 100 nM AZD8055, but only a trend to significance with ibrutinib and rapamycin (Figure 3-26).

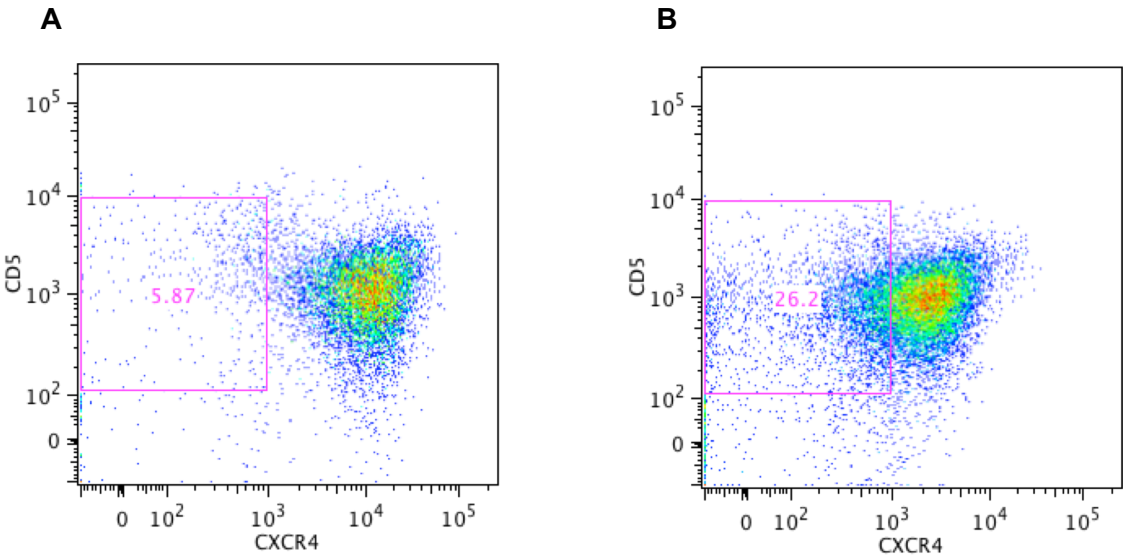

Figure 3-25 Changes in CLL cell surface phenotype with long-term SDF-1 stimulation
Flow cytometry analysis of patient sample CLL44, a normal karyotype CLL sample after 48 h incubation and staining for CD5 and CXCR4 (A) NDC (B) NDC + 100 ng/ml SDF-1.

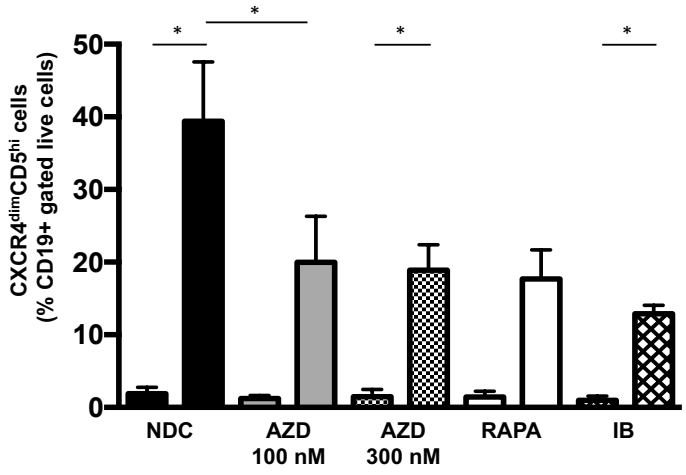

Figure 3-26 "LN emigrant" phenotyped CLL cells and changes with SDF-1 stimulation
Flow cytometry quantification of $CXCR4^{dim}CD5^{hi}$ cells expressed as a proportion of all live cells after gating on CD19+. Cells were placed in drug conditions: Non-drug control (NDC), 100 nM and 300 nM AZD8055 (AZD), 10 nM rapamycin (RAPA), 1 μM ibrutinib (IB) for 48 h +/- 100 ng/ml SDF-1 (n=3). *=p≤0.05; **=p≤0.01; ***=p≤0.001; ****=p≤0.0001.

3.2.3 *In vivo* ibrutinib – CLL120

Study of the lymphocyte-redistribution phenomenon was extended to *in vivo* examination of lymphocyte response and chemokine effects in a BCR-signalling-inhibitor-naive patient with 17p deletion CLL on initiation of ibrutinib monotherapy. Figure 3-27 outlines the effects of ibrutinib administered at a daily dose of 420 mg, commencing at day 0 with serial peripheral blood sampling performed up to 3 months following the initiation of therapy. There is an early rise in surface CXCR4 levels with a second, larger, peak in CXCR4 levels which corresponds to a minor rise in the lymphocyte count which tails off along with the lymphocytosis (Figure 3-27 B). Other chemokine receptors more closely map the second peak of lymphocytosis whereas there are no rises alongside the initial lymphocyte peak count (Figure 3-27 C-G). The cell surface marker trends should be interpreted with caution given the single sample represented by these data and given the minor overall changes in lymphocyte count compared with many other samples however it appears that in this patient sample the CXCR4 level changes appear to precede the lymphocyte redistribution effects which may occur with ibrutinib therapy and after the drop in lymphocyte count, cells appear to have a low CXCR4 level, more in keeping with a LN emigrant phenotype. Other cell surface marker changes occur after the rise in lymphocyte count which may reflect a role in relation to the ongoing effect of ibrutinib once the lymphocyte redistribution has occurred, possibly reflecting a role in the prevention of LN re-entry by the evacuated CLL cells, rendering cells susceptible to a method of cell death resembling *anoikis* (259).

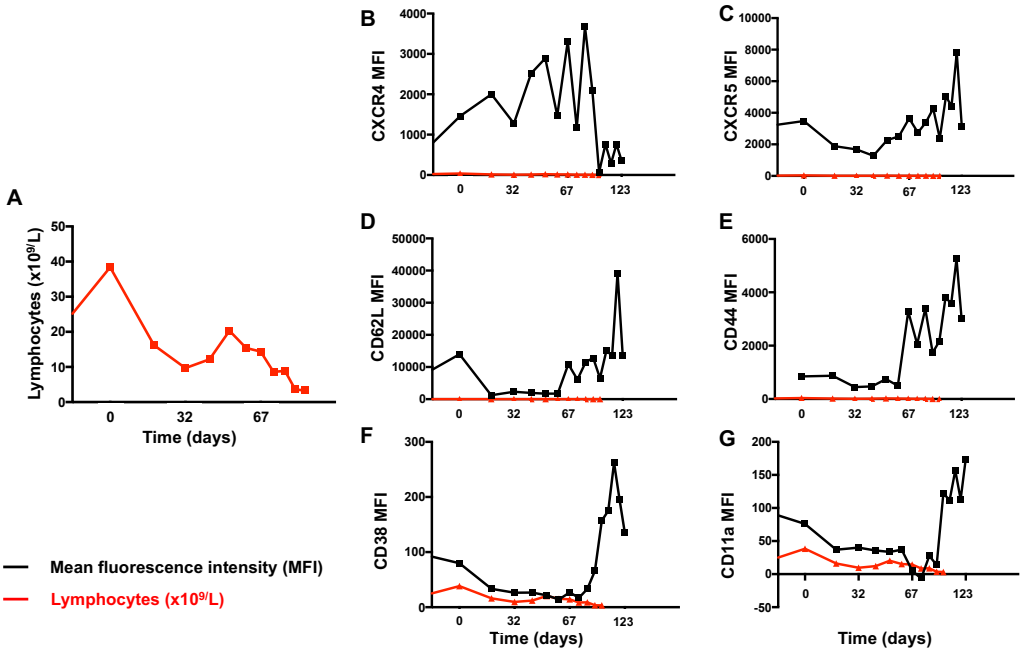

Figure 3-27 Changes in cell surface profile and lymphocyte count with ibrutinib therapy *in vivo*

Samples from patient CLL120 at the point of commencing ibrutinib with distribution over time of measurements of (A) peripheral blood lymphocytes and mean fluorescence intensity of chemokines and adhesion molecules by FACS staining for (B) CXCR4 (C) CXCR5 (D) CD62L (E) CD44 (F) CD38 (G) CD11a.

3.2.4 Short-term response of mTOR kinase substrate to BCR stimulation by protein expression

The effects of mTOR inhibitors *in vitro* may be monitored by study of their specific effects on mTORC1 and mTORC2 substrates and their impact on protein phosphorylation status. Figure 3-28 displays representative blots of the impact of BCR stimulation and mTOR inhibition on mTOR substrates after 1 h stimulation. BCR stimulation acts to increase phosphorylation levels of mTOR substrates such as AKT^{S473} and $S6^{S235/236}$ as shown in Figure 3-28. With mTOR inhibition by AZD8055 there is a reduction in the AKT^{S473} phosphorylation consistent with mTORC2 inhibition which was not observed with rapamycin. Indeed, in the patient sample shown (CLL149), which was found to harbour a 17p deletion, there appears to be an elevation in AKT^{S473} phosphorylation upon rapamycin treatment, suggesting the release of a negative feedback loop upon inhibition of mTORC1 only (Figure 3-28 B). Ibrutinib treatment reduced AKT phosphorylation as previously reported (186). The positioning of mTORC2, targeted by AZD8055 specifically, downstream of BTK, were delineated by Western blot for Rictor phosphorylation. The S6K target Rictor, a component of the mTORC2 kinase complex, is phosphorylated at threonine 1135 upon stimulation of BCR for 1 h. The inhibitory effects of AZD8055 on $Rictor^{Thr1135}$ phosphorylation are visible most clearly with the addition of BCR stimulation whereas there are minimal effects of rapamycin and of ibrutinib (Figure 3-28 A).

The mTORC1-specific effects were studied using p4EBP1 as an indicator and pS6 as, although not a direct target it is phosphorylated by protein S6K which is a direct target of mTORC1. The limited availability of a suitable antibody for S6K led us to the preference for blotting for pS6 instead. Phosphorylation of the eukaryotic translation initiation factor protein target, $4EBP1^{Thr37/46}$, is reduced with dual mTORC1/2 inhibition but is less affected by rapamycin whereas pS6 is targeted by rapamycin. Ibrutinib has inhibitory effects on both mTORC1 substrates, pS6 and p4EBP1. To delineate the mechanisms of mTORC1/2 inhibition in CLL we studied FOXO1 phosphorylation status after 1 h BCR stimulation in our samples. Forkhead box protein 01 (FOXO1) is a transcription factor which is modulated/inhibited by the signalling output of mTORC2 in B cells. This places FOXO1 downstream of the AKT signal, with its inhibition by AKT being conferred by phosphorylation at threonine residue 24 (260). At 1 h BCR

stimulation, a reduction in FoxO1^{T24} phosphorylation is observed with AZD8055 and ibrutinib treatment (Figure 3-28 B), indicative of mediation of the FOXO1 signal by mTOR and in support of the tumour suppressor functions of FOXO1 in CLL.

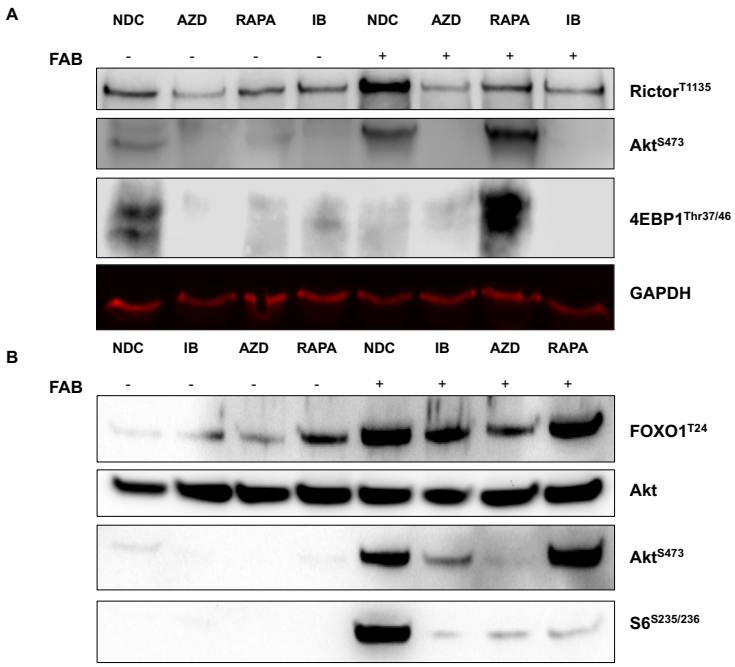

Figure 3-28 Protein expression effects of mTOR inhibitors with short-term BCR stimulation Western blot images are obtained from protein lysates of patient sample (A) CLL159 (normal karyotype CLL) and (B) CLL149 which is known to harbour a 17p deletion to demonstrate the effects of 1 h BCR stimulation and non-drug control (NDC), AZD8055 100 nM (AZD), rapamycin 10 nM (RAPA) and ibrutinib 1 μM (IB) +/- BCR stimulation on mTOR substrates. Expected molecular weight of mTOR and its effectors are as follows: Rictor 200 kDa, FOXO1 78-82 kDa, AKT 60 kDa, S6 32 kDa, 4EBP1 15-20 kDa. GAPDH is predicted at 36 kDa.

Effects of AZD8055 and ibrutinib on the BCR-stimulated AKT^{S473} phosphorylation signal were highly significant and there was also a strongly significant effect on untreated BCR-stimulated cells (Figure 3-29 A). The effects on AKT^{S473} phosphorylation persisted despite correction for protein loading, with significant inhibition by both AZD8055 and ibrutinib with the addition of BCR-stimulation (Figure 3-30 A). Densitometry analysis of 4EBP1$^{Thr37/46}$ revealed significant inhibition by AZD8055-alone with and without the addition of BCR stimulation which persisted when adjusted for protein loading, as assessed by GAPDH levels (Figure 3-29 B & Figure 3-30 B). Analysis of S6$^{S235/236}$ revealed significant effects of rapamycin and ibrutinib in the presence of BCR-stimulation using the measured protein expression (Figure 3-29 C). A significant rise in the S6$^{S235/236}$ signal could be demonstrated with the addition of BCR stimulation and after correction for protein loading there was a significant inhibitory effect by AZD8055 and ibrutinib upon stimulation with BCR (Figure 3-30 C). Densitometry analysis of FOXO1^{T24} revealed non-significant decreases in FOXO1^{T24} phosphorylation with AZD8055 and once loading control correction is applied there is an increase in FOXO1^{T24} signal with rapamycin, relative to the signal generated in untreated control conditions (Figure 3-29 D & Figure 3-30 D).

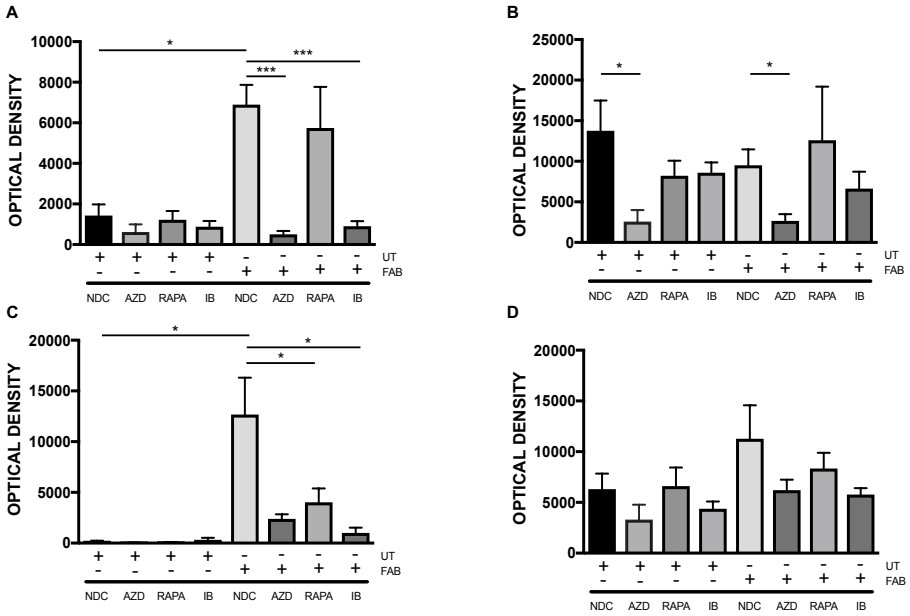

Figure 3-29 Short-term BCR stimulation and mTOR inhibition densitometry analysis Densitometry analysis of Western blot for mTOR substrates (A) AKT^{S473} (n=7) (B) $4EBP1^{Thr37/46}$ (n=7) (C) $S6^{S235/236}$ (n=5) (D) $FOXO1^{T24}$ (n=5) following 30 min drug pre-treatment with either non-drug control (NDC), 100 nM AZD8055 (AZD), 10 nM rapamycin (RAPA) or 1 μM ibrutinib (IB) and subsequent 1 h BCR stimulation. *=p≤0.05; **=p≤0.01; ***=p≤0.001; ****=p≤0.0001.

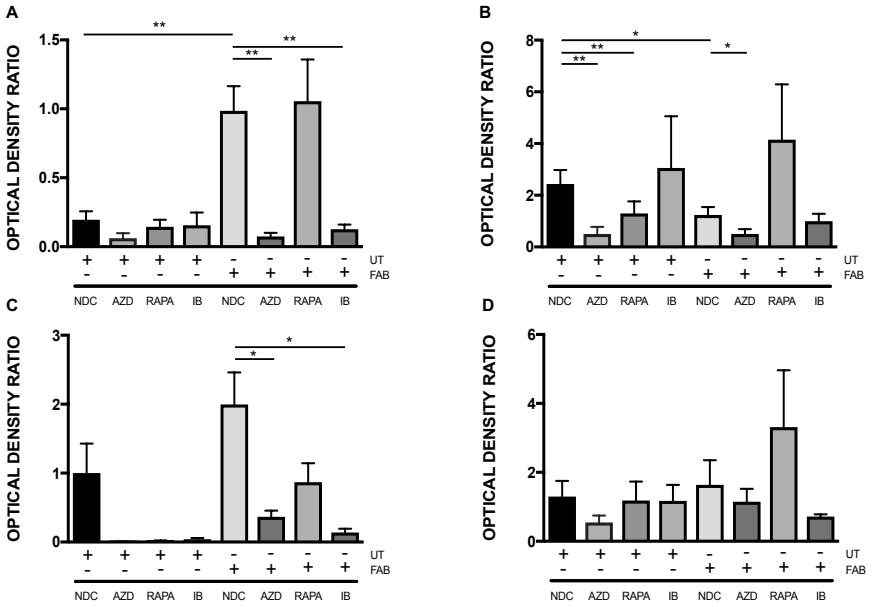

Figure 3-30 Short-term BCR stimulation and mTOR inhibition densitometry analysis with loading correction

Densitometry analysis of Western blot for mTOR substrates with GAPDH correction expressed as a density ratio for substrates: (A) AKT^{S473} (n=7) (B) $4EBP1^{Thr37/46}$ (n=7) (C) $S6^{S235/236}$ (n=5) (D) $FOXO1^{T24}$ (n=5) following 30 min drug pre-treatment with either non-drug control (NDC), 100 nM AZD8055 (AZD), 10 nM rapamycin (RAPA) or 1 μM ibrutinib (IB) and subsequent 1 h BCR stimulation. *=p≤0.05; **=p≤0.01; ***=p≤0.001; ****=p≤0.0001.

3.2.5 **Effects of SDF-1 stimulation on mTOR activity**

The effects of inhibitors on mTOR substrates after 30 min SDF-1 stimulation of CLL cells are shown (Figure 3-31). As expected, SDF-1 increased the phosphorylation of mTORC1 downstream substrates $S6^{S235/236}$ and $Rictor^{T1135}$, and mTORC2 downstream substrates AKT^{S473} and FOXO1, while $4EBP1^{T37/46}$ phosphorylation was not elevated, as assessed by Western blotting. Phosphorylation of AKT^{S473} is targeted by AZD8055 and ibrutinib whereas this is relatively unaffected by rapamycin, indicative of mTORC2 inhibition (Figure 3-31 A). Confirmation of mTORC2 inhibition by AZD8055 and delineation of its effects as downstream of ibrutinib's target are shown with differential phosphorylation status of $Rictor^{T1135}$ in the presence of AZD8055 as opposed to ibrutinib (Figure 3-31 A). The inhibition of mTOR kinase activity using phosphorylation of $4EBP1^{T37/46}$ as a marker of mTORC1 effects is visible in Figure 3-31 B where activity is reduced with dual mTORC1/2 inhibition but is relatively spared by rapamycin. There is inhibition of $S6^{S235/236}$ by both rapamycin and AZD8055, visible in Figure 3-31 A&B, reflective of the differential inhibitory effects on S6K and 4EBP1 phosphorylation by rapamycin. Ibrutinib has inhibitory effects on phosphorylation of both mTORC1 substrates, S6 and 4EBP1 however FOXO1 appears relatively unaffected by drug inhibitors under SDF-1 stimulation (Figure 3-31 B).

Phosphorylation of FOXO1 by AKT is an inhibitory event in transcriptional regulation of its targets, so an increase in its phosphorylation levels correlates with the increase in PI3K/mTOR/AKT signalling activity induced by BCR and SDF-1 stimulation. As increased phosphorylation can sometimes equate to a reduction in the tumour suppressor activity of FOXO1 in CLL, inhibition of phosphorylation by AZD8055 and rapamycin may represent their therapeutic activity. Further work is required to delineate whether FOXO1 phosphorylation is the underlying method of functional control or whether regulation of nuclear translocation is the mainstay of FOXO1 activity regulation.

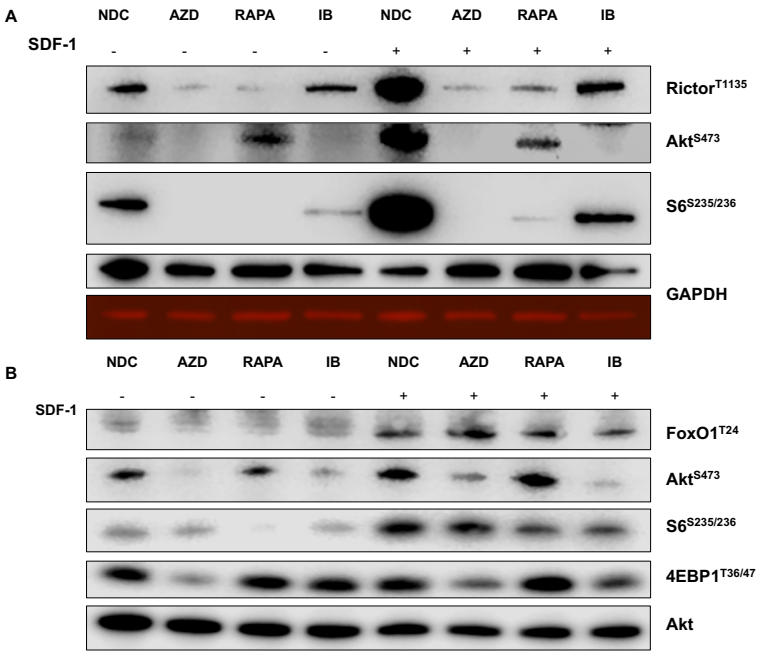

Figure 3-31 Protein expression effects of mTOR inhibitors with short-term SDF-1 stimulation Western blot images are obtained from protein lysates of patient sample (A) CLL152 (normal karyotype CLL) and (B) CLL143 which is known to harbour an 11q deletion to demonstrate the effects of 30 min SDF-1 stimulation and non-drug control (NDC), AZD8055 100 nM (AZD), rapamycin 10 nM (RAPA) and ibrutinib 1 μM (IB) on mTOR substrates. Expected molecular weight of mTOR and its effectors are as follows: Rictor 200 kDa, FOXO1 78-82 kDa, AKT 60 kDa, S6 32 kDa, 4EBP1 15-20 kDa. GAPDH is predicted at 36 kDa.

Densitometry analysis of AKT^{S473} revealed an increase in phosphorylation upon SDF-1 stimulation compared with untreated controls (Figure 3-32 A). The pattern of drug inhibitor effects with AZD8055 were in keeping with the activity against mTORC1/2, displaying significant inhibition on AKT^{S473} phosphorylation, followed by effects of ibrutinib with no effect in AKT^{S473} phosphorylation with rapamycin treatment (Figure 3-32 A). An increase in the S6$^{S235/236}$ signal could be demonstrated with the addition of SDF-1 stimulation with an inhibitory effect by AZD8055 and ibrutinib on S6$^{S235/236}$ phosphorylation, where cells were also stimulated using SDF-1 (Figure 3-32 B). Densitometry analysis of 4EBP1$^{T37/46}$ revealed inhibition by AZD8055 and ibrutinib in the presence and absence of SDF-1 stimulation (Figure 3-32 C). Effects upon the phosphorylated FOXO1 signal follow the pattern of AKT^{S473} phosphorylation with relatively small inhibitory effects of rapamycin but with most striking effects visible with AZD8055 and ibrutinib treatments, exhibited both with and without SDF-1 stimulation.

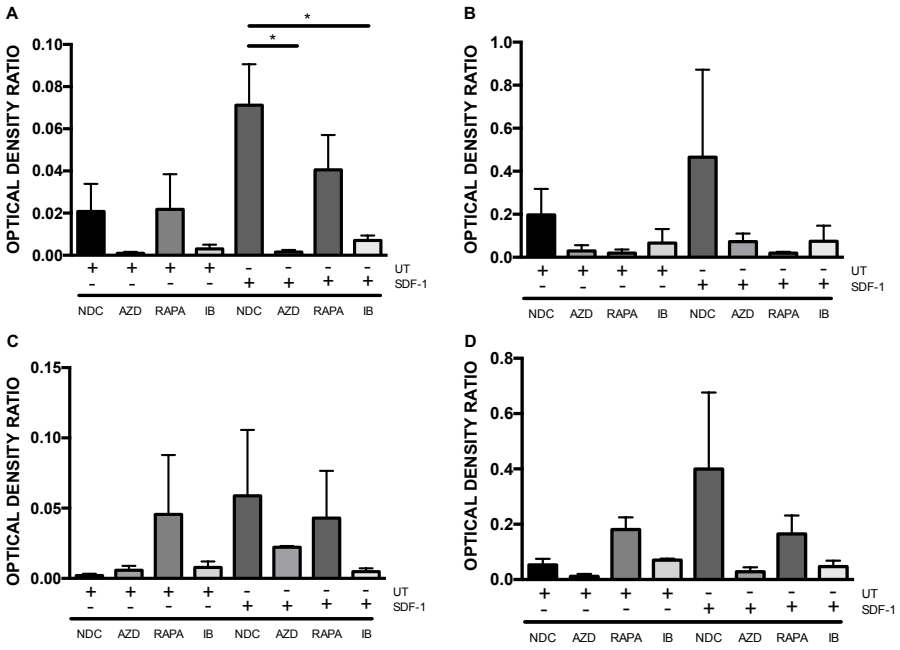

Figure 3-32 Densitometry analysis of protein expression effects of SDF-1 stimulation and mTOR inhibition

Densitometry analysis of Western blot for mTOR substrates with GAPDH correction expressed as a density ratio for substrates: (A) AKT^{S473} (n=6) (B) $S6^{S235/236}$ (n=4) (C) $4EBP1^{T37/46}$ (n=3) (D) $FOXO1^{T24}$ (n=3) following 30 min drug pre-treatment, either non-drug control (NDC), 100 nM AZD8055 (AZD), 10 nM rapamycin (RAPA) or 1 μM ibrutinib (IB) and subsequent 30 min SDF-1 stimulation. *=p≤0.05; **=p≤0.01; ***=p≤0.001; ****=p≤0.0001.

3.3 Summary of findings

The experimental settings were optimised for assessment of the molecular effects of mTOR inhibitors using *in vitro* methods in demonstration of effects on primary CLL cell viability over the 48 h time-point. I identified that 10 % FCS as the optimal serum concentration for the cellular viability experiments. The impact of AZD8055 on viability was greater than that of rapamycin, some of which may be attributable to a greater capacity to induce apoptosis, and which was greater than that of the control drug, ibrutinib. Effects on cellular markers of apoptosis over long-term inhibition with mTOR inhibitors and ibrutinib were studied with dual mTOR inhibitor AZD8055 demonstrating greatest impact on anti-apoptotic regulators such as BCL-xL and MCL-1. These findings are of significance for future work as further exploration of the efficacy of the control drug, ibrutinib and its mode of action is required to set the parameters for study of novel agents which act via inhibition of the BCR signal. The next chapter addresses the functional effects of mTOR inhibition *in vitro* as an alternative means of study of mTOR kinase effects on CLL cell migration. I introduced microenvironmental stimuli to my experimental approach, which required optimisation of the time-points for use in SDF-1 experiments to amplify the viability changes observed with my focus on mTOR inhibition. I examined the variability introduced by the combination of using fresh and thawed CLL samples in viability and in evaluation of chemokine receptor profiles and found this to be a valid approach. I also evaluated methods of BCR stimulation and found that in our cells there were no significant differences with the use of either $F(ab')_2$ stimulation or anti-IgM with avidin cross-linking, and that these approaches could also be combined without confounding my study.

The chemokine receptor and adhesion molecule profile of CLL cells were relatively heterogenous at baseline however the response to BCR stimulation could be measured in terms of changes in mean fluorescence intensity by FACS, with significant effects on CXCR4 and CD62L to downmodulate their levels with short-term exposure to BCR stimulation. Sample populations were stratified by well-characterised risk factors for CLL progression and whilst no increase in statistical significance was observed, changes persisted in high-risk CLL subgroups, highlighting the importance of these findings. The chemokine receptor experiments were extended to the 48 h time-point to assess whether

the observed changes were transient or could potentially be affected by changes at the level of the cell nucleus and gene expression changes. Only the significant reduction in CXCR4 levels could be replicated over 48 h which draws attention to the pivotal importance of CXCR4 to the migration process in CLL. Inhibitors were introduced to the 48 h BCR stimulation experiments with CLL samples exposed to BCR stimulation exhibiting significantly higher levels of CXCR4 in AZD8055 and ibrutinib conditions. These effects may be interpreted as a drug action to overcome the normal response of the cell to BCR stimulation in downmodulation of CXCR4. It is possible that these are methods utilised by the CLL cell in emigration from the LN.

CLL cell phenotype changes were explored further by use of CXCR4 and CD5 surface staining and response of these markers to SDF-1 stimulation. A marked increase in $CXCR4^{lo}CD5^{hi}$ population was observed with the addition of SDF-1, which was reduced by all inhibitors tested and was significantly overcome with the addition of AZD8055. It is possible that the response to a chemokine gradient is being thwarted in response to mTOR inhibition or BTK inhibition and that by these means that CLL cells are expelled into the peripheral blood, away from the protective niche which has the highest concentration of chemokine ligand.

These studies were correlated with the observation of *in vivo* effects on ibrutinib on one of the first patients in our centre to receive the drug. Changes in chemokine receptor and adhesion molecule levels were mapped over a 3-month period. Again, CXCR4 was identified as a critical component of regulation of migration of CLL cells with changes on other markers occurring much later than with CXCR4. A *caveat* exists that these effects were studied in a single patient, who was heavily pre-treated with anti-CD52 (alemtuzumab) and experienced only modest lymphocyte counts at the peak of the redistribution effect, therefore this effect merits study in other ibrutinib recipients.

Effects of mTOR inhibition on mTOR substrate expression were studied over a short-term time point selected at 1 h for BCR stimulation effects and 30 min for SDF-1 effects. The dual mTOR inhibitor displayed greatest efficacy of inhibition the mTOR kinase and fared favourably when compared with positive control, ibrutinib. Further work is required to examine the downstream effects of mTOR inhibition which is the focus of chapter 5.

Chapter 4 Functional effects of mTOR kinase inhibition on CLL cell migration

4.1 Introduction

The evaluation of drug inhibitors and their impact on functional assays offers a complementary approach to the molecular assays already described as the information provided may confirm the impact of molecular changes on cellular migration. Functional assays also provide a means of attributing individual chemokine ligand and receptor changes to overall changes in migration effects, for example the CXCR4-CXCL12 or CXCR5-CXCL13 axes. In some cases, the assays offer visualisation of migration effects to provide strong evidence of the direct impact of drug inhibitors on cellular events relating to migratory function. Normal ymphocyte migration is discussed in 1.7.2, with comparison to CLL migration in 1.7.3. Based upon an understanding of the mechanisms which regulate migration it may be hypothesised that CLL cells may display variability in migration potential, based upon the surface immunophenotype of the CLL cell and whether it is peripheral or nodal in origin.

I used two types of timed migration assay to assess the capacity of our primary CLL samples to migrate *in vitro*. The discovery of stromal-derived factor as a growth factor with activity in haematopoietic system development is now 30 years old and the concept of using CXCL12 or stromal-derived factor (SDF-1) to elicit B cell migration *in vitro* followed, 10 years later (261, 262), with its discovery made in the mouse haematopoietic system and with the first experiments performed in sorted murine bone marrow cells. These findings led to the development the pseudoemperipolesis assay which is the study of transmigration of CLL cells beneath a stromal layer to exploit the property of upregulated surface expression of CXCR4, a pathognomonic feature of CLL (148). The assay developed subsequently utilises the adherent murine cell line M2-10B4, known for their ability to secrete CXCL12 in a spontaneous and self-sustaining fashion, along with other haematopoietic growth factors such as stem cell factor (239). I did not perform any assay to quantitate CXCL12 production by M2-10B4 cells as the secretion of chemokine ligand is an established feature of these cells and the production of other, accessory, chemokine ligands by the cell line would potentially confound any such analysis. Instead, I controlled the

experimental conditions with reference to the cell count of M2-10B4 cells, with cell suspension aliquots of equal volume to be used in each experimental plate and well.

The transwell migration assay also utilises SDF-1, this time as an addition to serum-starved media placed in wells below a polycarbonate permeable membrane, through which CLL cells are able to migrate along a chemokine ligand gradient. There are existing data to support the use of the transwell assay as a way of measuring the impact of novel therapeutic approaches (176, 186) and our group has also published data in the use of the transwell assay (180).

Actin polymerisation is a tightly regulated cellular function which may be deployed in a variety of processes within the cell, including cytokinesis, cellular motility and vesicle endocytosis and trafficking. Phalloidin staining, used in our approach, is known to bind not only actin filaments but hWASp-VCA and Arp2/3 which are involved in the stable actin-binding complex. Fluorescent phalloidin stabilises actin filaments and allows visualisation of the products of the actin polymerisation reaction, providing a cross-sectional approach to the dynamic cellular mobilisation processes. The fluorescence intensity from labelled phalloidin staining may permit evaluation by either FACS measurement or by microscopic imaging of fluorescent cell structures for visual assessment of actin localisation and for quantitative analysis.

4.2 The effects of mTOR inhibition on CLL cell pseudoemperipolesis

The pseudoemperipolesis phenomenon is observed in Figure 4-1, with bunched CLL cells which have transmigrated through and underneath the cellular layer of M2-10B4 cells. The foci of CLL cells are visible through the translucent M2-10B4 cell stroma and with the large stromal cell nuclei visible, dispersed throughout the microscopic field. The pseudoemperipolesis experimental protocol was optimised for the drug conditions as the initial experimental conditions, each performed in duplicate wells with triplicate FACS measurements of each, incorporated a 1 h drug incubation period before commencing the pseudoemperipolesis stage of the experiment.

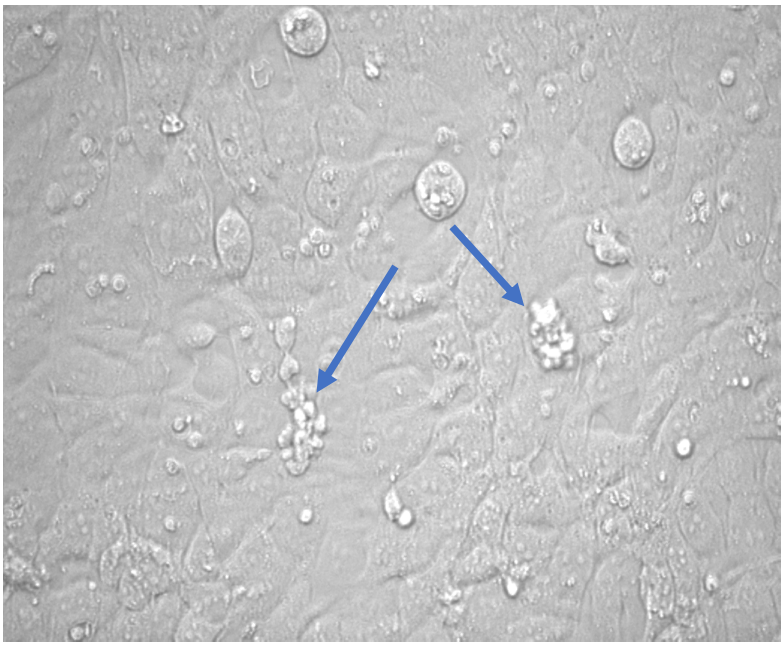

Figure 4-1 CLL cell pseudoemperipolesis
High power (x40) microscopic image of M2-10B4 stromal cell layer with evidence of pseudoemperipolesis exhibited by patient sample CLL132 (17p deletion). The arrows indicate two groups of CLL cells which have undergone pseudoemperipolesis.

Figure 4-2 compares the effect of 1 h incubation with 100 nM AZD8055 on CLL cell pseudoemperipolesis with the transmigratory capacity of untreated control cells. Consistent with published examples of the assay, the negative control level of pseudoemperipolesis was <0.05% however there was no difference between drug-treated and untreated cells. These findings led us to adapt our approach to incorporate an overnight incubation step to expose CLL cells to drug inhibitors demonstrated in Figure 4-2. There is no overall change in pseudoemperipolesis at either 100 nM AZD8055 or 1 nM rapamycin when compared with the untreated control cells, which may be attributable to the limited time period of exposure to the drug inhibitors. Overnight exposure to AZD8055 100 nM of CLL cells prior to pseudoemperipolesis reveals a trend to significant reduction in migration with the drug, with no clear effects on rapamycin. Differential effects of rapamycin may be anticipated however, given its potential for upregulation of AKT signalling.

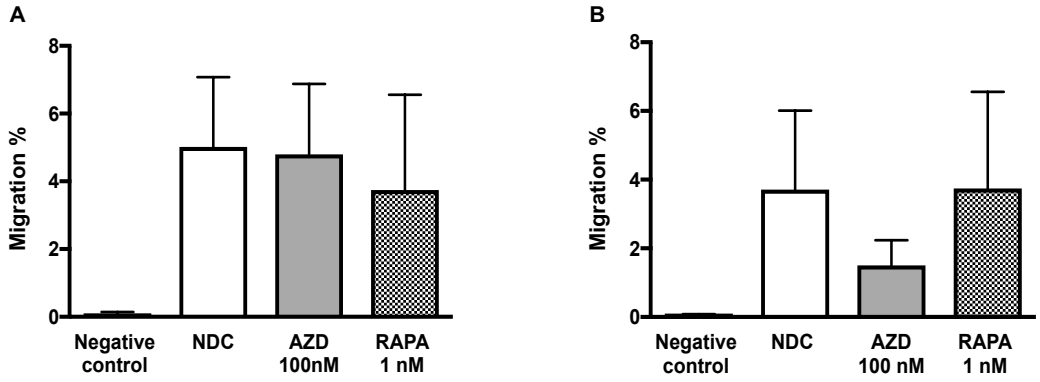

Figure 4-2 Effect of duration of drug incubation prior to pseudoemperipolesis experiments Raw data comparing mean and SEM pseudoemperipolesis of n=4 samples. CLL cells were prepared by 1 h exposure to non-drug control (NDC), AZD8055 100 nM (AZD) and rapamycin 10 nM (RAPA) then with pseudoemperipolesis conducted over 5 h (A). Extension of the drug incubation period to 15 h reveals greater inhibition of pseudoemperipolesis effects by AZD8055 after this time point (n=6) (B).

A potential *caveat* to extending our incubation period from 1 h to the overnight incubation with drug inhibitors and BCR stimulation would be that any drug effects may be erroneously attributed to migration effects, rather than CLL cell viability effects which may be the actual mechanism of drug activity. However, we have already shown that even over 24 h incubation with dual mTOR inhibitor AZD8055 there are minimal effects upon CLL cell viability, using viability studies (Figure 3-13) and markers of apoptosis (Figure 3-16).

Next, the influence of BCR stimulation may be examined using the pseudoemperipolesis assay shown in Figure 4-3, Figure 4-4 and Figure 4-5. A trend to increase in pseudoemperipolesis was observed with the addition of BCR stimulation (Figure 4-3); these findings were examined with reference to use of $F(ab')_2$ fragment stimulation (n=8) as opposed to anti-IgM stimulation with avidin crosslinking (n=3) and there were found to be no significant differences with BCR stimulation in either subgroup (Figure 4-4). Fresh sample use (n=6) when compared with thawed sample (n=7) pseudoemperipolesis did not affect statistical significance (Figure 4-4). Statistical analysis could not be extended to the ZAP70 negative subgroup (n=2) however ZAP70 positivity conferred a significant increase in CLL cell pseudoemperipolesis in response to BCR stimulation (Figure 4-5).

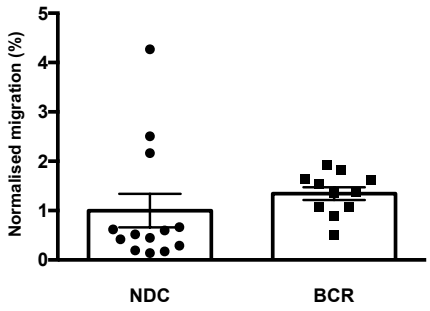

Figure 4-3 BCR stimulation effects on CLL cell pseudoemperipolesis
Normalised mean and SEM pseudoemperipolesis over 5 h with the effects of the addition of BCR stimulation in relation to untreated controls (n=13). Each dot plotted represents the average of three FACS measurements for wells which were performed in duplicate and fluorescence measurement of cells stained for CD19+ were compared by normalising BCR responses to the levels measured for unstimulated, untreated controls. A trend to increase in pseudoemperipolesis was observed with 15 h (overnight) BCR stimulation.

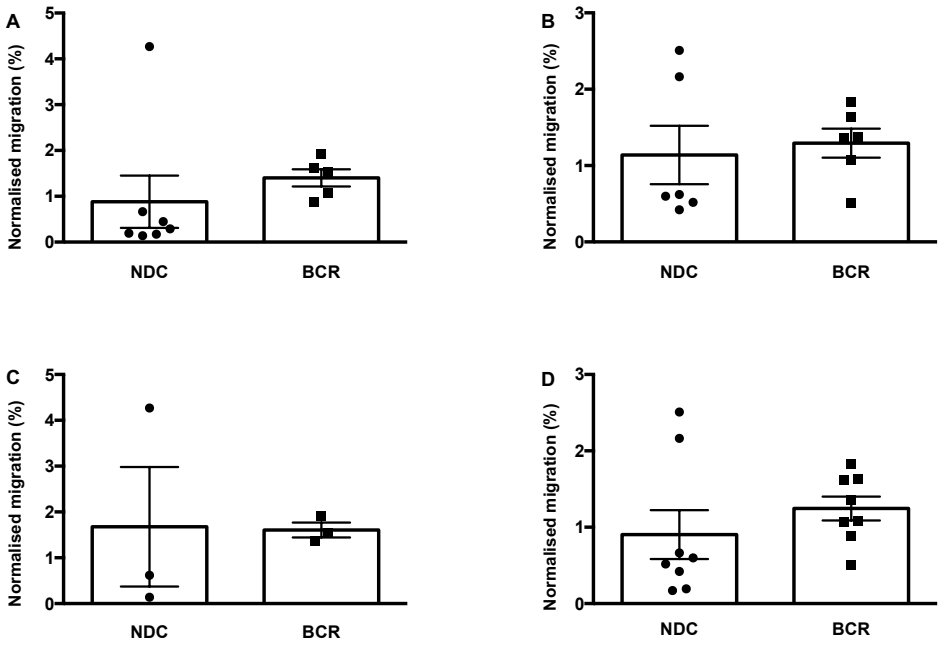

Figure 4-4 BCR stimulation effects on pseudoemperipolesis: subgroup analysis
Normalised mean and SEM pseudoemperipolesis over 5 h with the effects of the addition of BCR stimulation in relation to untreated controls. Samples were stratified by whether they were used fresh (A, n=7), thawed (B, n=6) and by method of BCR stimulation, either by anti-IgM stimulation with avidin crosslinking (C, n=3) or F(ab')$_2$ fragment stimulation (D).

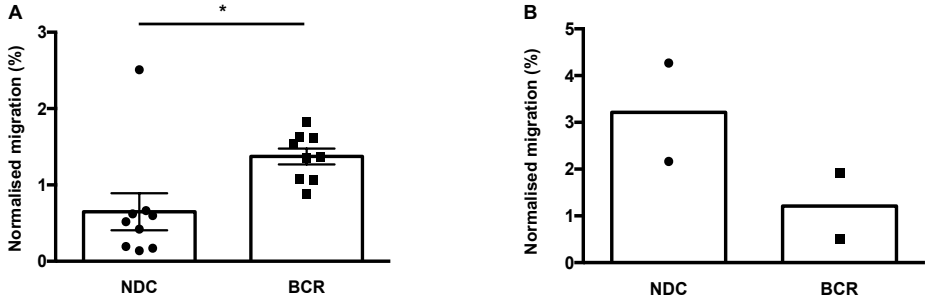

Figure 4-5 BCR stimulation effects on pseudoemperipolesis: influence of ZAP70
Normalised mean and SEM pseudoemperipolesis over 5 h with the effects of the addition of BCR stimulation in relation to untreated controls of (A) ZAP70 positive (n=9) and (B) ZAP70 negative samples (n=2). *=p≤0.05; **=p≤0.01; ***=p≤0.001; ****=p≤0.0001.

Analysis of the effect of mTOR inhibitors on migration in the presence or absence of BCR stimulation (n=3) revealed some samples with amplified pseudoemperipolesis effect which skew the combined raw data, however, there is a statistically apparent inhibition by 100 nM AZD8055 of pseudoemperipolesis (Figure 4-6). With removal of the outliers (classed as those samples exhibiting 5% pseudoemperipolesis in the unstimulated non-drug control), there is enhancement of statistical significance of the inhibition by AZD8055 100 nM. Furthermore, there is a significant increase in pseudoemperipolesis with the addition of BCR stimulation in the subset shown in (Figure 4-6 B).

Normalised data were compared in Figure 4-7 with graphs to display unstimulated drug effects (Figure 4-7 A) and those with the addition of BCR stimulation (Figure 4-7 B). A significant reduction in pseudoemperipolesis could be demonstrated in the BCR-stimulated cells, with the addition of 100 nM AZD8055 and ibrutinib 1 μM and with inhibition demonstrated to a greater degree by 300 nM AZD8055.

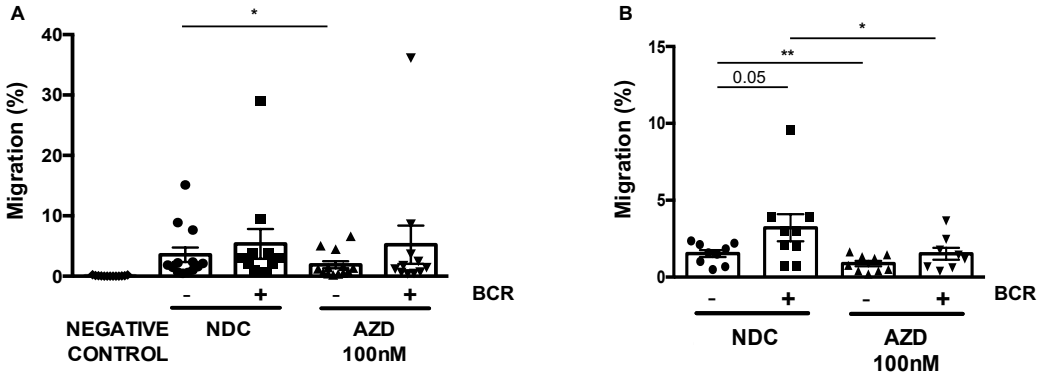

Figure 4-6 Primary CLL sample pseudoemperipolesis: raw data
Graphs display (A) pseudoemperipolesis effects over 5 h with non-drug control (NDC) or dual mTOR inhibitor AZD8055 100nM (AZD) +/- BCR stimulation (A) (n=13). Elimination of outliers by GraphPad software allows visualisation of statistical trends (B) (n=9). *=p≤0.05; **=p≤0.01; ***=p≤0.001; ****=p≤0.0001.

As per the experimental protocol, a wash control step was incorporated which involves 5 min incubation of M2-10B4 cells with a CLL cell suspension of the original cell concentration used at the beginning of the 5 h incubation period. The wash step condition is used to assess the stringency of the washing process throughout all of the experimental wells and a threshold of 0.05% CLL cells in the control well is used to determine the overall success of the washing process. On analysis after elimination of samples with a wash control >0.05%, the trends

in drug inhibitor effects on pseudoemperipolesis persist. However, the significant reduction in migration that was seen with overnight AZD8055 treatment at 100 nM and 300 nM and ibrutinib 1 μM are lost (Figure 4-8). More samples are required to repeat the experiment, in order to confirm the significance of the trends of drug inhibitor effects on pseudoemperipolesis. Interestingly, rapamycin appears to be less effective in migration inhibition of the samples studied, possibly due to loss of negative feedback regulation of the mTORC2 signalling complex and unregulated AKT signalling.

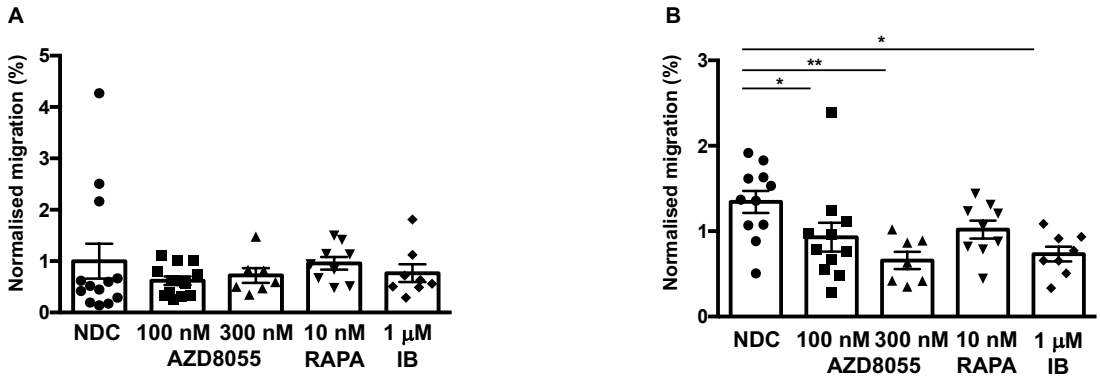

Figure 4-7 Primary CLL sample pseudoemperipolesis: normalised data (i)
Charts display normalised data with the effects of overnight addition of non-drug control (NDC), AZD8055 100 nM (AZD), rapamycin 10 nM (RAPA) and ibrutinib 1 μM (IB) prior to pseudoemperipolesis over 5 h, shown in (A) (n=13). The same drug conditions were replicated with 30 min pre-treatment with inhibitors, followed by overnight BCR stimulation displayed in (B), this time with significant inhibition by AZD8055 at both 100 nM and 300 nM, and by ibrutinib 1 μM (n=11). *=p≤0.05; **=p≤0.01; ***=p≤0.001; ****=p≤0.0001.

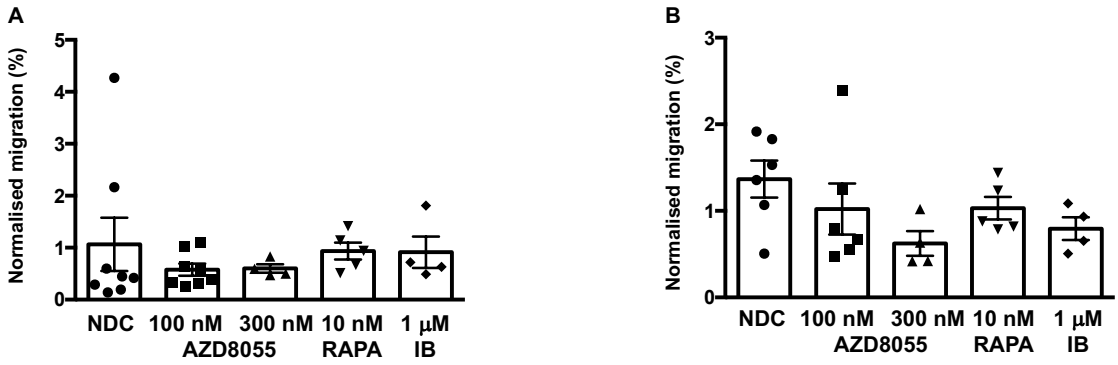

Figure 4-8 Primary CLL sample pseudoemperipolesis: normalised data (ii)
Pseudoemperipolesis over 5 h with the effects of overnight addition of non-drug control (NDC), AZD8055 100 nM (AZD), rapamycin 10 nM (RAPA) and ibrutinib 1 μM (IB) prior to experiments with data shown in (A), with removal of all samples with a wash control CLL cell content of >0.05% (n=8). The same drug conditions were replicated with 30 min pre-treatment with inhibitors, followed by overnight BCR stimulation displayed in (B) (n=7). *=p≤0.05; **=p≤0.01; ***=p≤0.001; ****=p≤0.0001.

4.3 The effects of mTOR inhibition on CLL cell transwell migration

I show that BCR stimulation follows a trend towards increased primary CLL sample transwell migration along a CXCL12 gradient, when compared with the unstimulated control (Figure 4-9). The effects of drug conditions upon transwell migration followed a similar pattern in the presence and absence of BCR stimulation however no significant inhibition of migration was observed (Figure 4-10 A&B). With the observation that some CLL samples respond negatively to BCR stimulation in terms of the percentage of migrated cells, a subset of samples were identified to exhibit an increase in migration with BCR stimulation, a subgroup termed "BCR responders" which may be contrasted with "non-responders" (Figure 4-11 A&B). For these 5 patient samples (CLL8, CLL42, CLL90, CLL113, CLL116) there is a significant increase in BCR stimulation within the drug conditions AZD8055 100 nM and ibrutinib 1 μM. There is a reduction in migration with 300 nM AZD8055 although this is not statistically significant however the loss of significant increase in BCR stimulation at the higher concentration of AZD8055 may represent an increased efficacy to overcome the pro-survival stimuli by these samples. Indeed when taking unstimulated and BCR-stimulated separately as in Figure 4-12, the BCR stimulation conditions reveal drug inhibition effects by dual mTOR inhibitor AZD8055 at both concentrations (Figure 4-12 B). As shown in both Figure 4-11 and Figure 4-12, there appears to be an increase in migration with rapamycin within the "BCR responders" group.

Overall analysis of the impact of drug exposure revealed no significant differences between drug conditions over the 11 samples utilised. More samples may be required from a range of prognostic subsets to try to establish the effects of the drug inhibitors. Another reason as to why the effects of mTOR inhibition could not be demonstrated by transwell migration could be due to the procedure used in the SDF-1 experiments described in chapter 3, as the samples were pre-treated with a period of serum starvation before the addition of drug inhibitors and subsequent BCR stimulation. The period of serum starvation creates a limit on the time period over which CLL cells may be exposed to the drug inhibitors. Therefore, an overnight drug exposure step could not be incorporated into the transwell assay, possibly preventing CLL cells from

sufficient exposure time to mTOR inhibition to facilitate changes affecting migration.

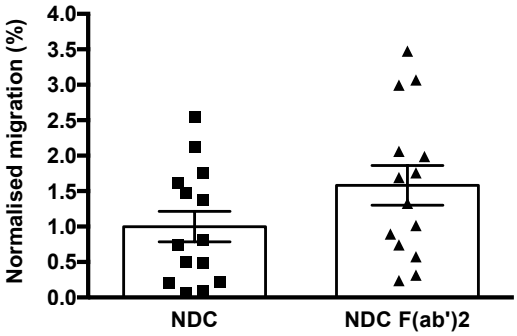

Figure 4-9 Effects of BCR stimulation on CXCL12 transwell migration of primary CLL samples
Mean and SEM transwell migration of primary CLL samples over 4 h, along a CXCL12 gradient after 1 h BCR stimulation (n=14). Data are normalised with individual data points each representing duplicate transwells with each transwell cell count being performed in triplicate *i.e.* each data point represents n=6 for an individual sample.

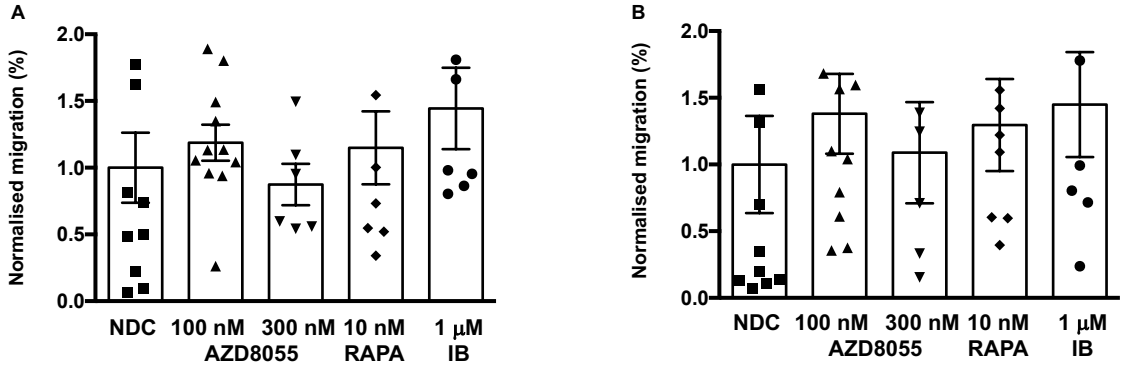

Figure 4-10 Transwell migration of primary CLL samples towards CXCL12
Mean and SEM of normalised transwell migration of primary CLL samples over 4 h, along a CXCL12 gradient after 30 min drug inhibition with non-drug control (NDC), AZD8055 100 nM (AZD), rapamycin 10 nM (RAPA) and ibrutinib 1 μM (IB), (A) in the absence and (B) with subsequent BCR stimulation for 1 h (n=11).

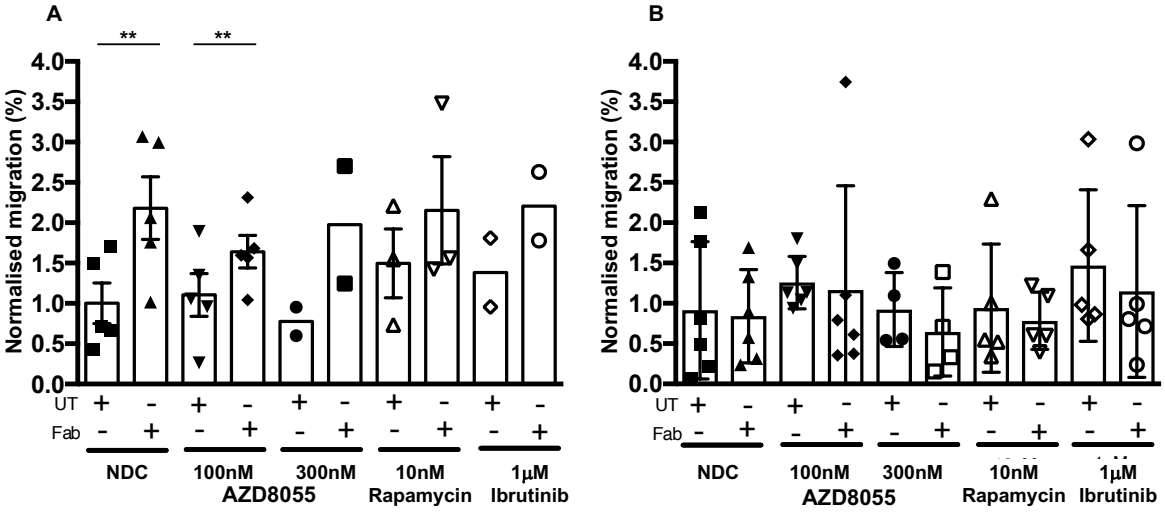

Figure 4-11 Transwell migration analysis by BCR responses
Normalised mean and SEM of cell counts generated as described previously. Transwell migration was conducted towards CXCL12 for 4 h after 30 min treatment with non-drug control (NDC), AZD8055 100 nM (AZD), rapamycin 10 nM (RAPA) and ibrutinib 1 μM (IB) and 1 h BCR stimulation. A subgroup was identified based upon samples responding positively to BCR stimulation in the transwell migration assay (A, n=5). The remaining samples which were non-responsive to BCR stimulation are shown (B, n=6). *=p≤0.05; **=p≤0.01; ***=p≤0.001; ****=p≤0.0001.

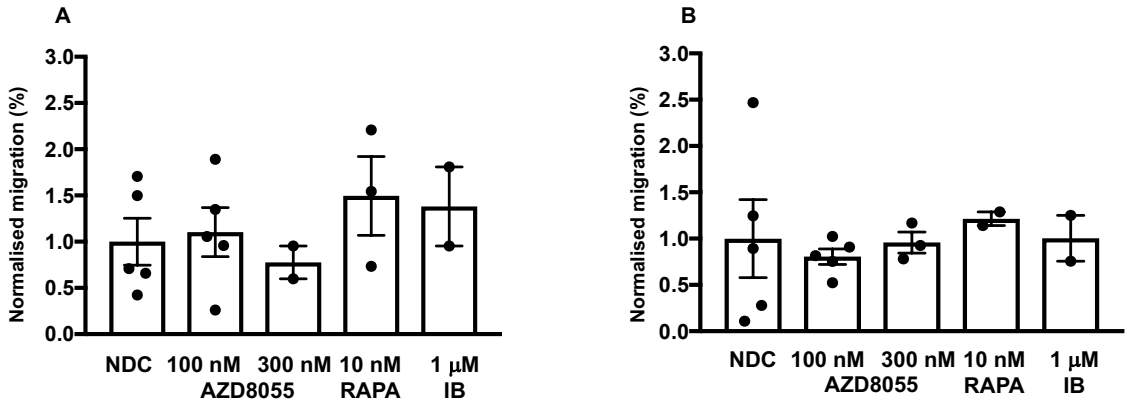

Figure 4-12 Transwell migration of "BCR responder" subgroup
Mean and SEM migration of a subgroup generated by isolation of samples responding positively to BCR stimulation in the transwell assay (CLL8, 42, 44, 113, 116, n=5). Data are normalised after generation of cell counts as described previously, following transwell migration towards CXCL12 for 4 h after 30 min treatment with non-drug control (NDC), AZD8055 100 nM (AZD), rapamycin 10 nM (RAPA) and ibrutinib 1 μM (IB), (A) without and (B) with subsequent BCR stimulation for 1 h.

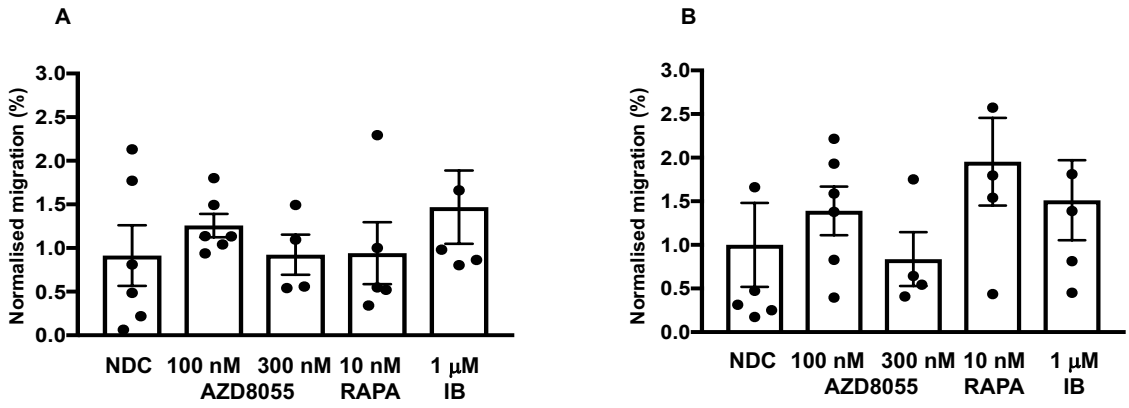

Figure 4-13 Transwell migration of "BCR non-responder" subgroup
Mean and SEM migration of a subgroup generated by isolation of samples with no response to BCR stimulation in the transwell assay (CLL80, 85, 90, 109, 119, 130, n=6). Data are normalised after generation of cell counts as described previously (2.2.5), following transwell migration towards CXCL12 for 4 h after 30 min treatment with non-drug control (NDC), AZD8055 100 nM (AZD), rapamycin 10 nM (RAPA) and ibrutinib 1 μM (IB), (A) without and (B) with subsequent BCR stimulation for 1 h.

Further evaluation of CLL cells and their response to chemokine ligand in the transwell migration assay was undertaken using CXCL13 as the stimulus for migration (Figure 4-14). Experimental conditions required optimisation as there data availability on the use of CXCL13 in transwell assays was limited with no specific references to its use in CLL cell migration studies to be found in published literature (263, 264). Therefore, a concentration gradient of CXCL13 was studied from 800 ng/ml to 1 μg/ml with the impact of BCR stimulation using $F(ab')_2$ fragments on levels of migration towards CXCL13 displayed in Figure 4-14. An increase in chemokine-mediated migration towards CXCL13 was observed with the addition of BCR stimulation, although the increase was not significant as more samples are required to confirm this trend.

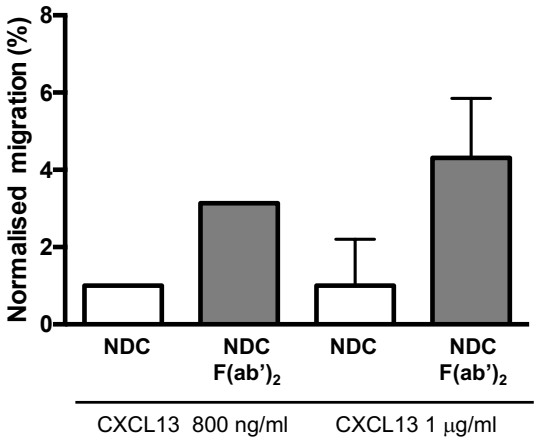

Figure 4-14 Effects of BCR stimulation on CXCL13 transwell migration of primary CLL samples
Mean and SEM of normalised transwell migration data of CLL samples along a chemokine gradient of 800 ng/ ml (CLL93, n=1) and of 1 μg/ ml CXCL13 (CLL42, 93, 109, n=3).

4.4 The effects of mTOR inhibition on PKCα-KR cell migration

Based upon the above results, I sought to consolidate the data regarding primary CLL sample migration responses, leading to the application of our *in vitro*-generated cellular model of CLL to the transwell assay. The biological similarity of the PKCα–KR mouse model to CLL *in vivo* with overlapping cellular immunophenotype characteristics with CLL is the basis for the use of our model. The PKCα–KR model has features in keeping with poor prognostic disease, with reliance upon the BCR signal, making it a useful model for the study of novel agents including mTOR inhibitors and BTK inhibitors (182). One such phenotypic similarity to CLL is the property of increased cell surface expression of CXCR4 making PKCα–KR suitable for use in the transwell assay (Figure 4-15). I completed the transwell assay which showed strongly significant inhibition of migration towards CXCL12 demonstrated by the incubation of PKCαKR cells with 100 nM AZD8055 and 1 μM ibrutinib, and even greater inhibition by 10 nM rapamycin (Figure 4-16).

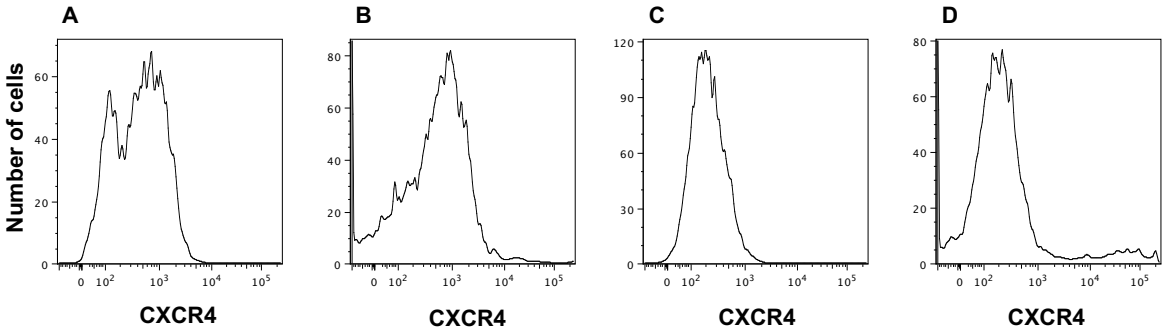

Figure 4-15 Histogram from FACS analysis of MIEV and PKCαKR cells
Graphs A & C are unstained controls and B & D represent live cells gated on CD19+ and stained for CXCR4. Cells are taken from day 9 of culture *in vitro* with MIEV and PKCαKR cells displaying a proportion of cells which stain strongly for CXCR4 in comparison with the unstained controls.

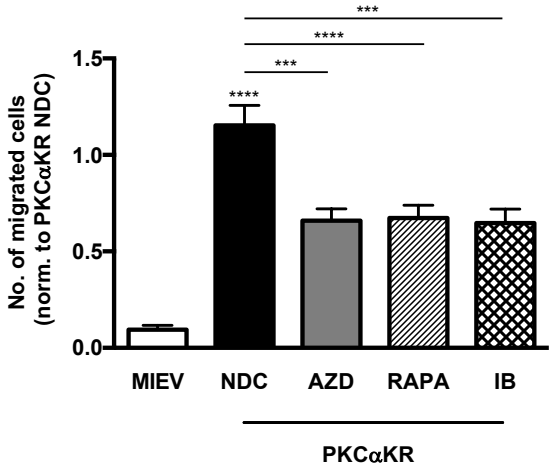

Figure 4-16 PKCαKR transwell assay migration studies
PKCαKR transwell assays with 6 technical replicates for each condition, as with the primary CLL sample transwells. There were 5 biological replicates combined to demonstrate the significant impact of mTOR and BTK inhibition on transwell migration. PKCαKR cells were incubated for 30 min with non-drug control (NDC), AZD8055 100 nM (AZD), rapamycin 10 nM (RAPA) and ibrutinib 1 μM (IB) with subsequent transwell migration for 4 hours. Effects were compared with the transwell migration results for MIEV. *=p≤0.05; **=p≤0.01; ***=p≤0.001; ****=p≤0.0001.

4.5 The effects of mTOR inhibition on actin polymerisation

4.5.1 Assessment of actin polymerisation by flow cytometry

The ability to construct the actin cytoskeleton relates directly to cellular migration potential, so we employed assays utilising flow cytometry and immunofluorescence staining to define how BCR crosslinking, SDF-1 stimulation and inhibitors may mediate changes in migration. Actin exists in an equilibrium of cellular forms from monomers to different organisational states of actin polymerisation. Peptide toxin phalloidin, derived from the fungus *amanita phalloides* was found to stabilise F-actin filament polymers and to stain these cell structures with high specificity (265). Therefore, phalloidin may be applied *in vitro* to study actin polymerisation in fixed cells such as our CLL samples and when phalloidin is labelled with a fluorophore, mean cellular fluorescence intensity, as measured by flow cytometry, may be used as a surrogate marker of actin polymerisation (180). After application of phalloidin to a CLL cell suspension *in vitro*, the polymerisation reaction may be studied over a range of time points with serial sampling to assess the extent of actin polymerisation, with variations in the degree of cytoskeletal formation and pattern over time with each sample which remain heterogeneous after data normalisation (Figure 4-17 A-C).

Although the limitations of the assay require data analysis to be conducted with the use of time as a categorical variable rather than as a continuous variable, peak cytoskeletal activation may be studied. Differences in actin polymerisation at each time point were compared with significant increase in fluorescence intensity, relating to cytoskeletal formation, at the 15 second time point with SDF-1 and at 30 and 60 seconds with $F(ab')_2$ and BCR crosslinking with avidin respectively (Figure 4-18 A-C).

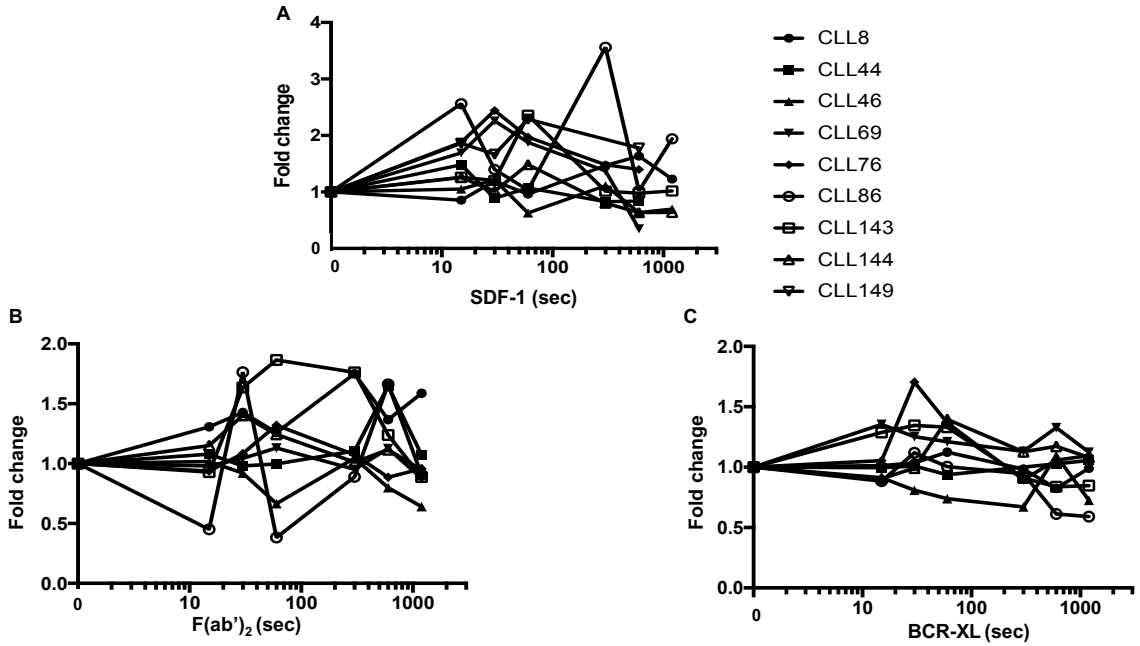

Figure 4-17 Actin polymerisation assay by individual CLL samples
Actin polymerisation studies combined (n=9) to demonstrate heterogeneity of CLL sample responses to stimuli. Each stimulation was performed on serum-starved, either fresh or thawed, CLL cells at 37°C with serial sampling, cell fixation, permeabilisation and phalloidin staining. Reactions were triggered by *in vitro* conditions: (A) 100 ng /ml SDF-1 (B) 10 μg /ml F(ab')$_2$ fragments and (C) 10 μg /ml anti-IgM with 25 μg /ml avidin crosslinking.

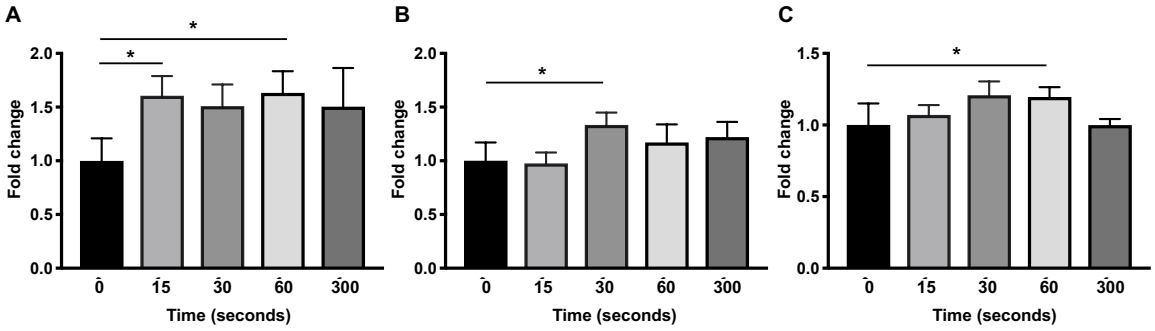

Figure 4-18 Actin polymerisation assay by time point
Mean and SEM actin polymerisation of both fresh and thawed CLL samples at each sampling time point in response to (A) 100 ng /ml SDF-1 (B) 10 μg /ml F(ab')$_2$ fragments and (C) 10 μg /ml anti-IgM with 25 μg /ml avidin crosslinking. Significant increases in actin polymerisation may be demonstrated at different time points with each type of stimulus. *=p≤0.05; **=p≤0.01; ***=p≤0.001; ****=p≤0.0001.

I used FITC-phalloidin for the majority of the actin polymerisation assays to mainly to restrict the measurement of fluorescence intensity to single channel to reduce the exposure of the data to another variable, however, there are data to suggest that the use of different fluorophores may be applied with different fluorescence intensity over time (266). Therefore, I explored the use of TRITC phalloidin in the actin polymerisation experiments to investigate for differential fluorescence intensity of this fluorophore and to optimise the use of the rhodamine fluorophore for our immunofluorescence imaging studies. Figure 4-19 demonstrates the responses to a range of stimuli of a freshly-obtained sample in comparison to a thawed sample from the same patient, CLL8. The effects of fluorophore on baseline fluorescence intensity levels in the same sample may also be observed, with minimal effect as may be observed. Both fresh and thawed samples display SDF-1-responsiveness whereas there are minimal effects of BCR-stimulation on actin polymerisation responses (Figure 4-20).

Next, the phenomenon of BCR-responsiveness was explored by subjecting further samples to actin polymerisation studies using BCR-stimulation. Figure 4-21 illustrates the variety of responses to BCR stimulation with CLL80 indicated in Figure 4-21 A with a late peak in BCR response in the untreated control condition and with greatest elevation in actin polymerisation with the addition of 10 nM rapamycin. There appear to be smaller increases with the addition of AZD8055 100 nM and ibrutinib 1 μM however these contrast with the overall absence of response to BCR in all conditions in Figure 4-21 B representing responses of sample CLL86. Further evidence of the heterogeneous response to drug inhibitors, and in support of the combination of fresh samples with thawed samples for analysis is given in Figure 4-22 with (A) demonstrating the responses of a fresh sample as opposed to (B) where a different but similarly poor prognosis sample is used thawed.

Actin polymerisation was studied with reference to responses for individual drug conditions. With SDF-1 stimulation, no statistically significant effects were demonstrated however peak inhibition by mTOR inhibitors and ibrutinib occurred at the 30 and 60 second time points (Figure 4-23 A-E). Dual mTOR inhibitor AZD8055 inhibited actin polymerisation at 15 and 300 seconds where BCR stimulation effects were studied, however at the 15 second time point it

increased actin polymerisation with a significant rise at 600 seconds. Rapamycin increased actin polymerisation at all time points except at 300 seconds whereas ibrutinib was inhibitory at 15 and 300 seconds (Figure 4-24 A-E).

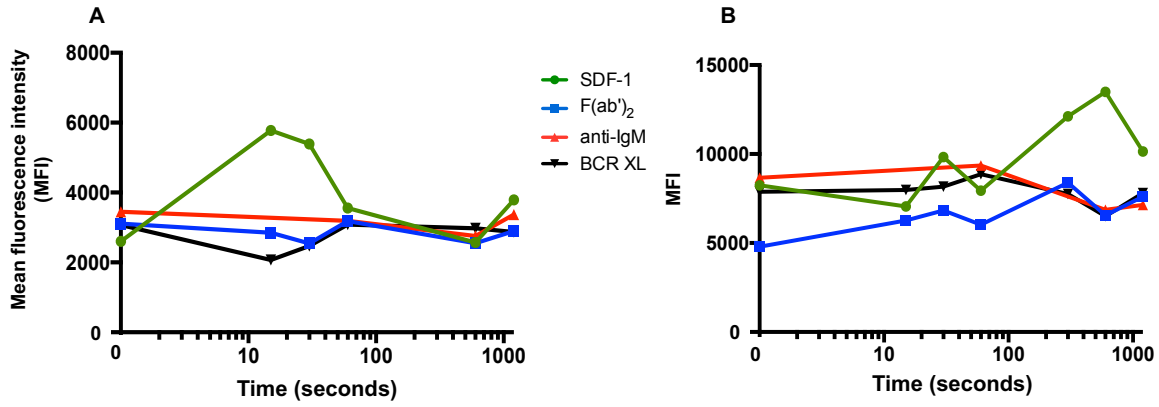

Figure 4-19 CLL8 actin polymerisation: analysis by stimulation
Actin polymerisation of a single patient sample with SDF-1, anti-IgM stimulation, BCR crosslinking or F(ab')$_2$ fragment stimulation. The sample (A) was obtained as a fresh sample and is stained with TRITC phalloidin whereas (B) is from a thawed sample and stained with FITC phalloidin.

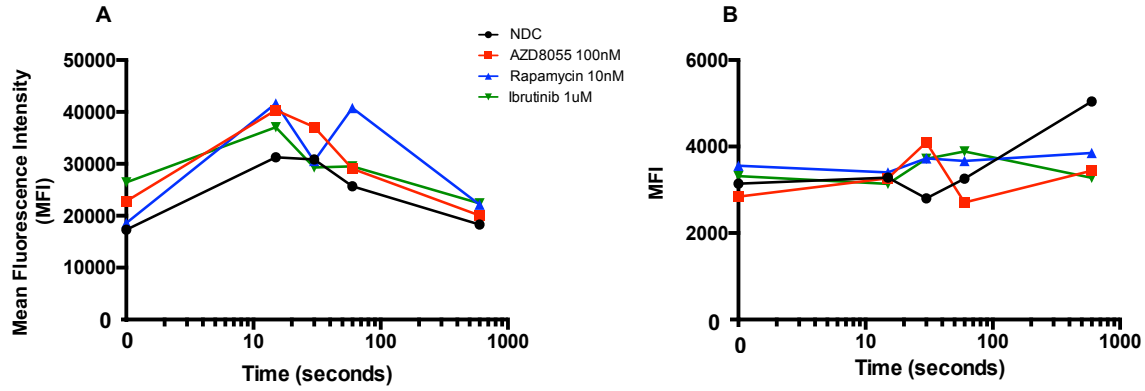

Figure 4-20 CLL8 actin polymerisation: effects of mTOR inhibition
CLL8 actin polymerisation from serial sampling after the administration of (A) SDF-1 and (B) F(ab')$_2$ fragment stimulation, each with 30 min pre-treatment with drug inhibitors as indicated.

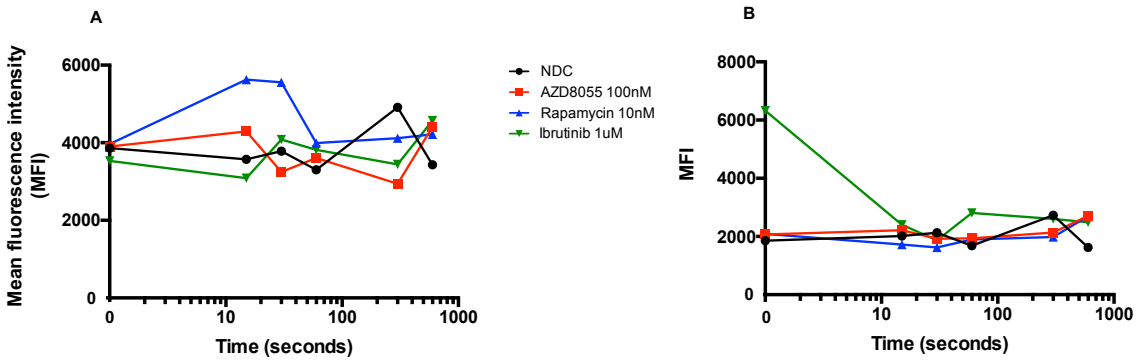

Figure 4-21 Actin polymerisation in response to BCR stimulation
Actin polymerisation from serial sampling after the administration of F(ab')$_2$ fragment stimulation with 30 min pre-treatment with drug inhibitors using (A) CLL80, known to harbour a 17p deletion and (B) CLL86, known to harbour an 11q deletion.

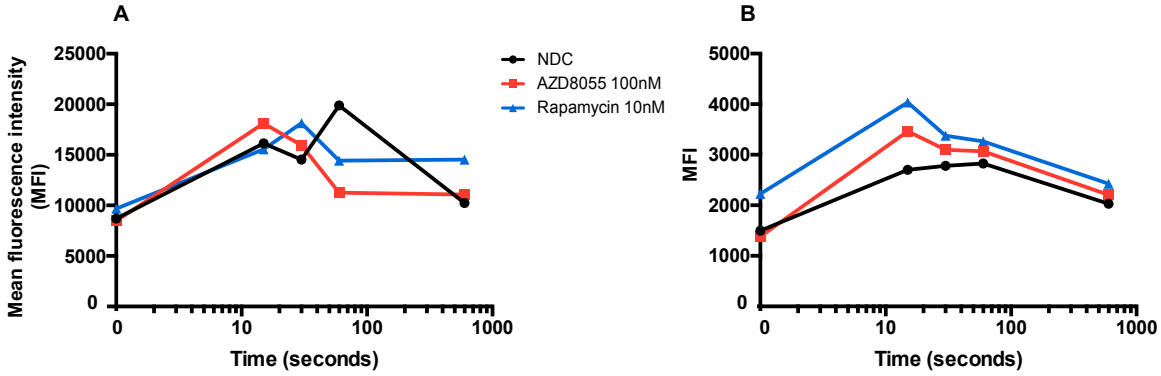

Figure 4-22 Actin polymerisation in response to SDF-1 stimulation
Actin polymerisation studies of samples harbouring a 17p deletion with 30 min pre-treatment with drug inhibitors using (A) fresh (CLL149) or (B) thawed (CLL113).

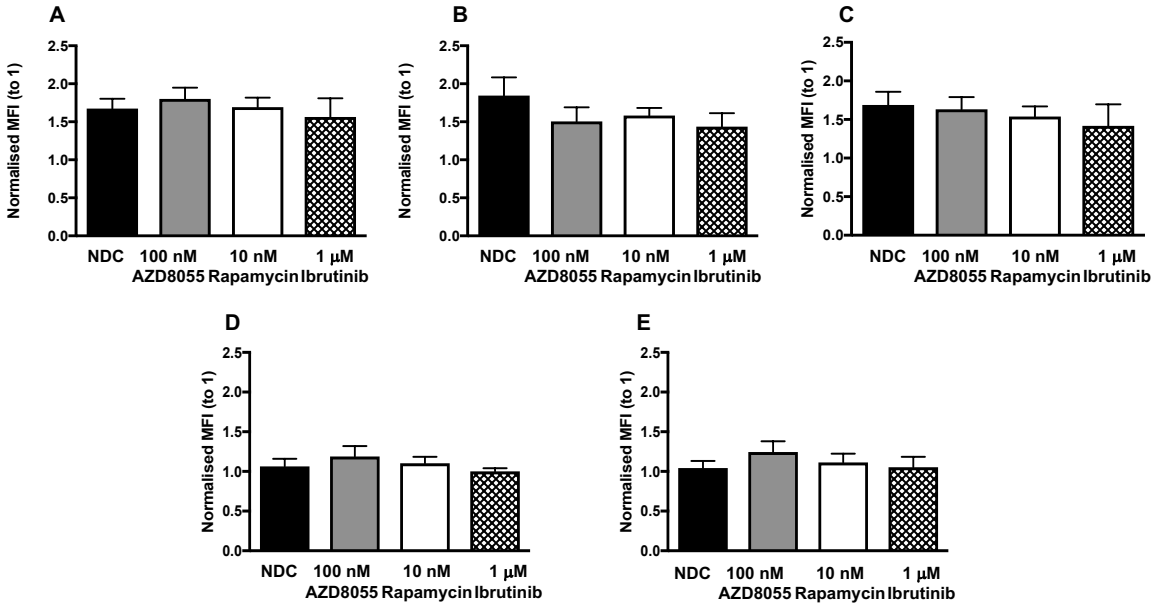

Figure 4-23 Actin polymerisation in response to SDF-1 stimulation
Mean and SEM of actin polymerisation for non-drug control (NDC) (n=12), 100 nM AZD8055 (AZD) (n=12), 10 nM rapamycin (RAPA) (n=12), 1 μM ibrutinib (IB) (n=6) at sampling time points (A) 15 seconds (B) 30 seconds (C) 60 seconds (D) 300 seconds and (E) 600 seconds.

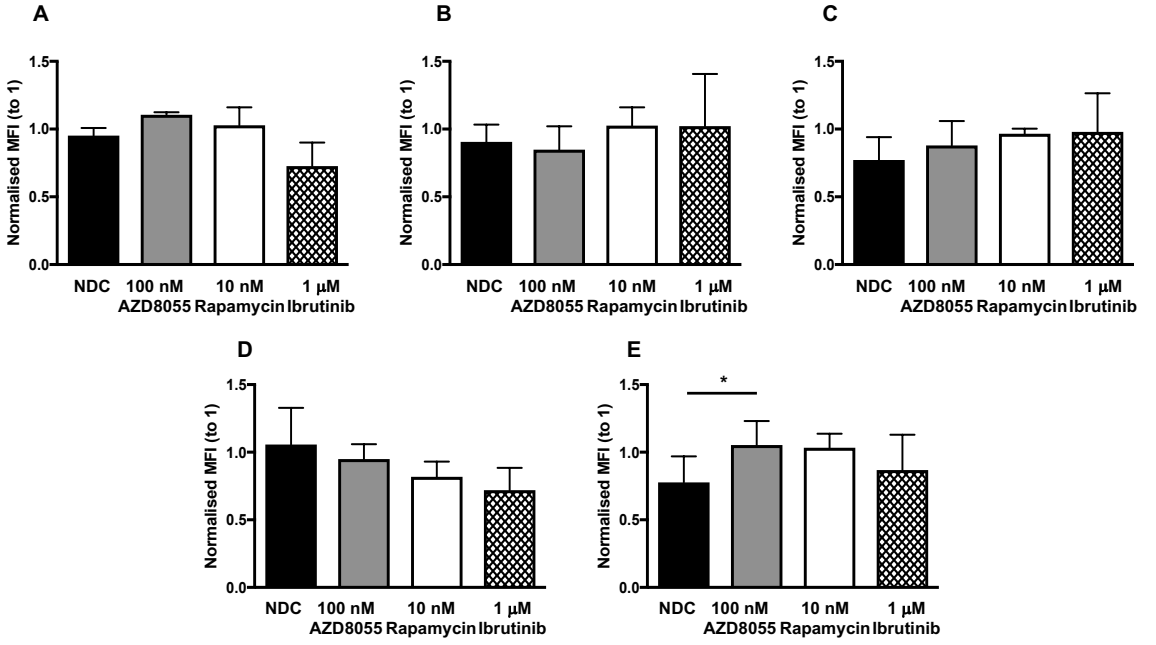

Figure 4-24 Actin polymerisation in response to BCR stimulation
Mean and SEM of actin polymerisation for non-drug control (NDC) (n=4), 100 nM AZD8055 (AZD) (n=4), 10 nM rapamycin (RAPA) (n=4), 1 μM ibrutinib (IB) (n=3) at sampling time points (A) 15 seconds (B) 30 seconds (C) 60 seconds (D) 300 seconds and (E) 600 seconds.

4.5.2 Assessment of actin polymerisation by immunofluorescence

Actin polymerisation was also evaluated by fluorescent microscopy and cells assessed for changes with drug inhibitors and with BCR or SDF-1 stimulation (Figure 4-25, Figure 4-26). Both stimulation conditions displayed evidence of spreading of the actin cytoskeleton with no consistent impact of mTOR inhibition or BTK inhibition on cell morphology. Cell stimulation effects were studied further by quantitation of intensity of cytoplasmic fluorescence using CellProfiler™ software and the subtraction method (2.5.6). A range of parameters were studied in order to quantitate cytoplasmic spreading, each of which should be interpreted with caution in view of the automatic nature of the software's analysis and the inherent deficiencies of assessing a 2-dimensional image of a 3-dimensional structure. Parameters such as mean and median nuclear: cytoplasmic intensity ratio; mean and median cytoplasmic intensity in the FITC channel of cells from individual samples at high power magnification were also measured as shown in Figure 4-28 and Figure 4-29. Mean data values were calculated from combining over 200 cells from each sample. Data from BCR-stimulated cells were compared for 7 samples to show a significant reduction in median cytoplasmic fluorescence intensity which may represent the increased cytoplasmic spreading seen with BCR stimulation, a phenomenon which may be studied in more detail with deconvolution of cellular images (Figure 4-27 and Figure 4-28). Images from an exemplary analysis by CellProfiler™ software are shown in Figure 2-4, 2.5.6.

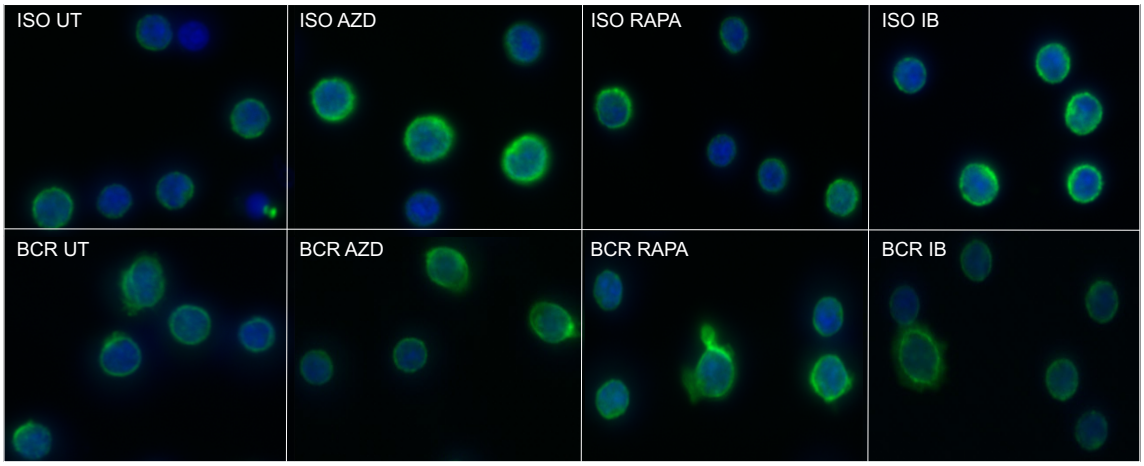

Figure 4-25 Immunofluorescence effects of BCR stimulation on CLL actin polymerisation
Fluorescent microscopic images of phalloidin staining in response to 30 min treatment with non-drug control (NDC), AZD8055 100 nM (AZD), rapamycin 10 nM (RAPA) and ibrutinib 1 μM (IB) then 1 h BCR stimulation on CLL155, a CLL sample known to harbour an 11q deletion (x 100 magnification).

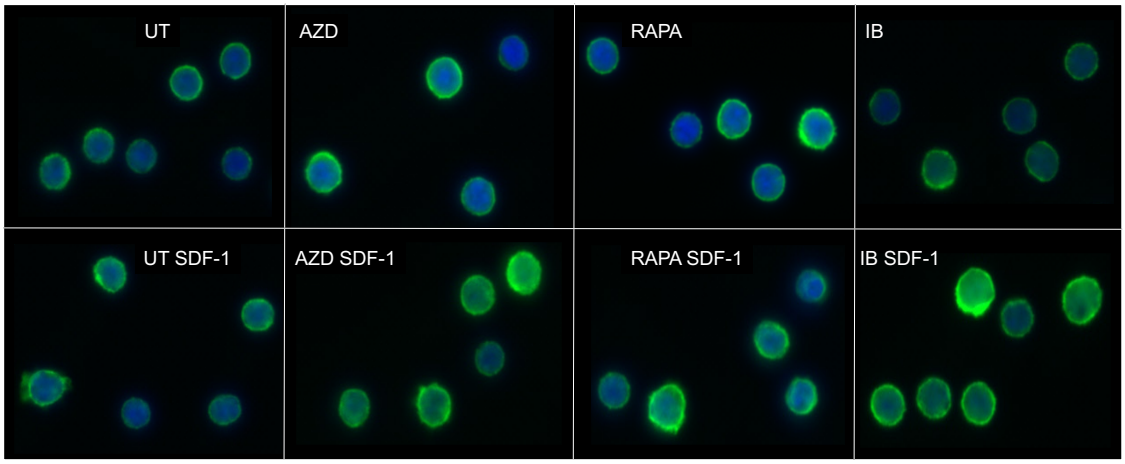

Figure 4-26 Immunofluorescence effects of SDF-1 stimulation on CLL actin polymerisation
Fluorescent microscopic images of phalloidin staining in response to 30 min treatment with non-drug control (NDC), AZD8055 100 nM (AZD), rapamycin 10 nM (RAPA) and ibrutinib 1 μM (IB) then 1 h SDF-1 stimulation on CLL155 (x 100 magnification).

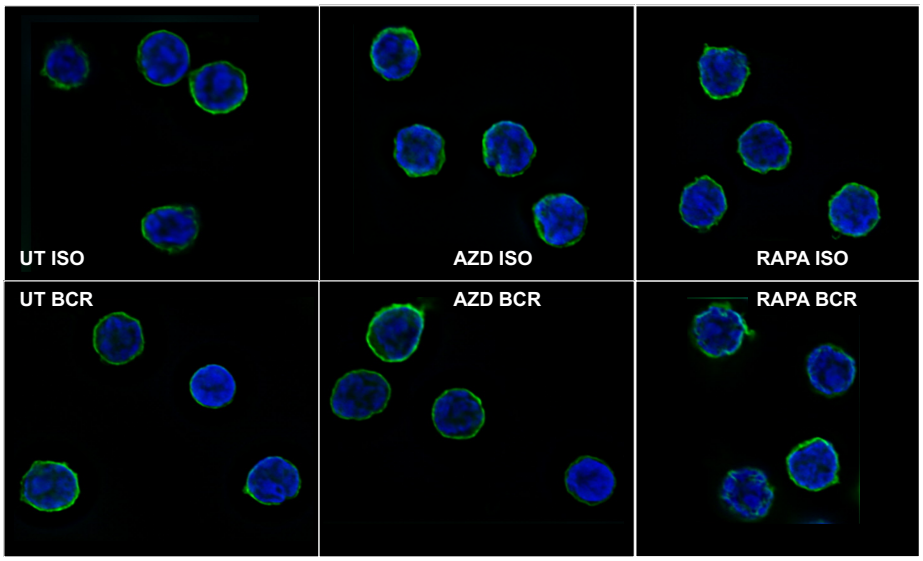

Figure 4-27 BCR stimulation effects on CLL actin polymerisation
Deconvoluted fluorescent microscopic images of actin polymerisation in response to 1 h BCR stimulation with effects of non-drug control (NDC), AZD8055 100 nM (AZD) and rapamycin 10 nM (RAPA) on CLL122, a CLL sample known to harbour a 17p deletion (x 100 magnification).

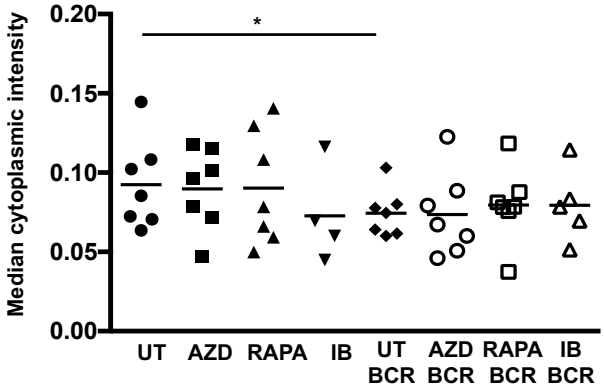

Figure 4-28 Quantitative analysis of immunofluorescence changes with BCR stimulation on actin polymerisation
Graphical representation of median cytoplasmic intensity for >200 cells from samples CLL46, 69, 80, 86, 143, 144 and 148, with distribution according to drug condition (non-drug control (NDC), AZD8055 100 nM (AZD), rapamycin 10 nM (RAPA) and ibrutinib 1 μM (IB)) and presence or absence of 1 h BCR stimulation. *=p≤0.05; **=p≤0.01; ***=p≤0.001; ****=p≤0.0001.

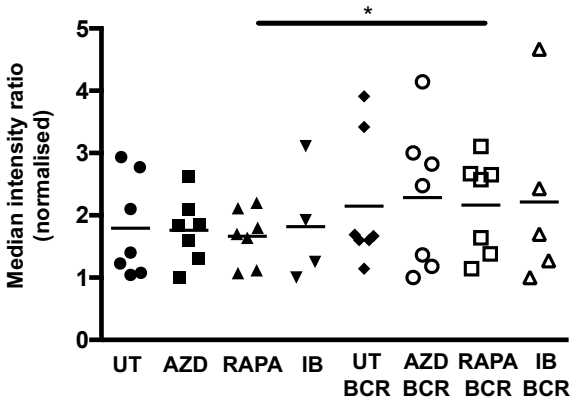

Figure 4-29 Quantitative analysis of actin polymerisation nuclear: cytoplasmic ratio changes
Nuclear: cytoplasmic (N:C) intensity ratio for >200 cells from samples CLL46, 69, 80, 86, 143, 144 and 148, with distribution according to condition (non-drug control (NDC), AZD8055 100 nM (AZD), rapamycin 10 nM (RAPA) and ibrutinib 1 μM (IB)) and presence or absence of 1 h BCR stimulation. Both mean and median N:C are significantly enhanced by BCR stimulation with the prior addition of rapamycin. *=p≤0.05; **=p≤0.01; ***=p≤0.001; ****=p≤0.0001.

4.6 Summary of chapter

In this chapter I demonstrate evidence of pseudoemperipolesis by CLL cells and show that it may be affected by drug inhibitors. These data show support for the use of dual mTOR inhibition as a more effective strategy to block pseudoemperipolesis than mTORC1 inhibition alone, with a trend to increase in this form of migration with the addition of rapamycin. My hypothesis that short-term exposure to mTOR inhibitors would be insufficient to affect pseudoemperipolesis is supported by data to compare 1 h drug inhibition with overnight exposure to drugs. I postulate that the underlying reason for the requirement for longer drug exposure may be that changes in pseudoemperipolesis effected by the mTOR inhibitors occur at the level of the cell nucleus. The primary CLL cell transwell migration study findings also suggest that the cellular changes which regulate migration and those changes which may be targeted by drug inhibitors may occur after longer-term drug exposure periods. Drug effects may be mediated at the level of receptor endocytosis and endocytic recycling, as changes in short-term cell surface receptor expression, or at the level of protein translation to alter the number of adhesion molecules being produced and trafficked to the cellular membrane. Further work is required to delineate the underlying processes in regulation of these effects in primary CLL samples. It is of note that significant reduction in transwell migration could be demonstrated by the addition of mTOR inhibitors to PKCα–KR mouse cells in culture over a short incubation time. These differences may relate to a differential response of the mouse model to the mTOR inhibitors or may be reflective of the heterogeneity present within the CLL samples used.

I assess functional analysis of mTOR inhibitors by their migratory effects in the actin polymerisation assay, however after data analysis, the only significant effects demonstrable were exhibited in response to *in vitro* stimuli; SDF-1 and BCR stimulation. There were no consistent responses to mTOR inhibition with the actin polymerisation assay, either by FACS or by immunofluorescence. Further work to study the responses of GTPases known to regulate migration effects via actin cytoskeletal remodelling and which are known to play a role in CLL cell chemokine responses will be explored in the next chapter.

Chapter 5 Regulation of CLL cell migration by small GTPases and the effects of mTOR inhibition

5.1 Introduction

There are myriad cellular processes involved in regulation of migration signals, of which potential candidates for further study include members of the small guanosine triphosphatase (GTPase) superfamily; containing 5 subfamilies each with multiple members possessing overlapping functions. GTPases all share a common feature in that they act as "molecular switches" in signal transduction as they cycle between active and inactive forms. The switching process is accelerated by regulatory guanine nucleotide exchange factors (GEF) which facilitate guanosine diphosphate (GDP) dissociation, Rho GDP dissociation inhibitors (Rho-GDI) and GTPase activating proteins (GAP), responsible for GTP hydrolysis (Figure 5-1).

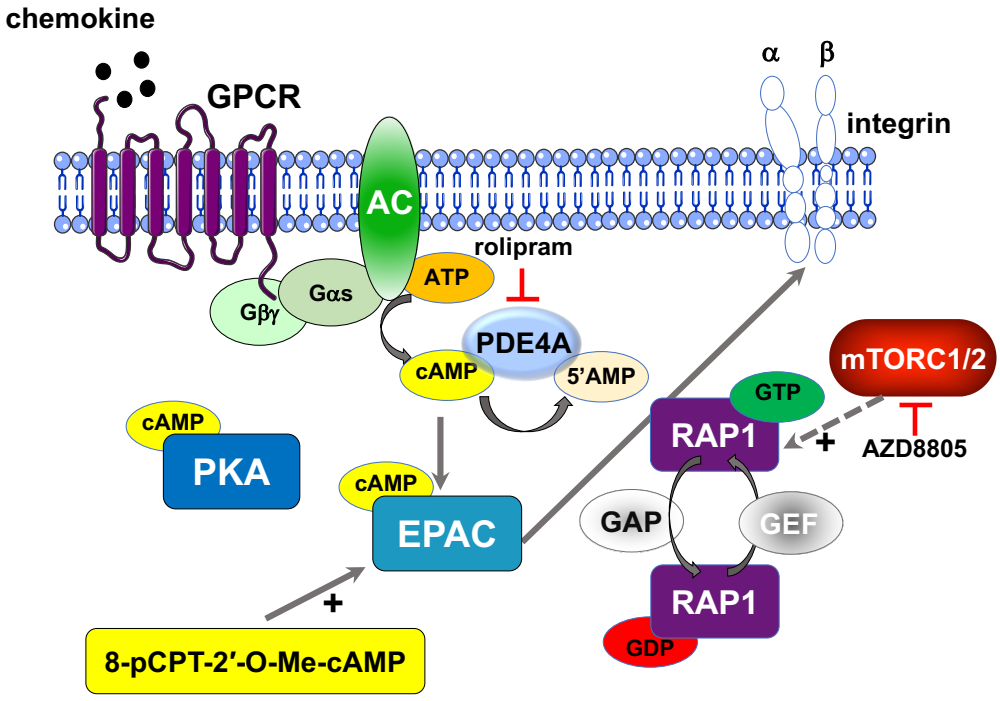

Figure 5-1 Diagram of Rap1 GTPase signalling with indication of downstream relationship to chemokine receptor and integrin signalling in normal B cells
Activator of the Rap1 signal 8-pCPT-2'-O-Me-cAMP along with pharmacological PDE4 inhibitor rolipram are shown. Dual mTORC1/2 inhibitor AZD8055 is displayed with along its site of action within the mTOR complex.

The originally discovered Ras subfamily and its members were strongly linked with oncogenesis, particularly in solid tumours. Rab and Arf subfamilies share functions in vesicle trafficking and membrane transport, with the sole Ran family member found to have roles in nuclear pore formation and in microtubule organisation (267). The Rho family and its members are implicated in actin cytoskeletal organisation; Rac1 and cdc42 initiate actin polymerisation through Arp2/3 complex activation, via WASp binding. Our experimental approach is focused on two GTPases: Rap1 and Rac1 proteins. The Ras family-member Rap1 has already been investigated in CLL with the regulation of its function found to be impaired (237, 238). Experimental strategies for investigation of GTPase activation rely upon the ability to delineate active from inactive forms of the protein under investigation, given the earlier findings which demonstrate consistent protein levels in the presence of drug inhibitions and *in vitro* stimulation. As these methods require a suitable positive control from which to assess relative proportions of active and inactive protein I refer to the Rap1 signalling pathway to look for exogenous means of activating Rap1.

As pictured in Figure 5-1, the Rap1 signalling axis is reliant upon phosphodiesterase (PDE) 4A-mediated generation of cyclic AMP (cAMP) which in turn, activates exchange protein directly activated by cAMP (EPAC). Pharmacological analogues are available, with their actions being to increase cellular activation of EPAC without concomitant increase in PKA activity, a by-product of PDE inhibition (268) and these EPAC activators may be exploited for the *in vitro* Rap1 activity assay in primary CLL samples. The EPAC activator may also be of use in IF assays as although antibodies for either Western blot or IF cannot distinguish between active and inactive forms of Rap1, EPAC activation may be utilised to promote Rap1 in its active form, to permit study of fluorescence pattern and localisation.

My hypothesis is that mTOR inhibition may block the active form of Rap1 GTPase, given the downstream location of Rap1 to the chemokine signalling pathway. Rap1 activity may also be reduced by ibrutinib, given that BTK is also positioned downstream of chemokine signalling pathways (269). There are putative effects on localisation of Rap1, based upon studies which show impaired endosomal recycling in CLL and one hypothesis is that these defects may

potentially be corrected by mTOR inhibition. IF offers a potential method of evaluation of protein localisation with co-staining for multiple cellular organelles.

The Rho family of GTPases has functions in actin re-organisation which places it central in regulation of cellular processes such as adhesion, cell polarity and membrane trafficking. Rac1 has specific functions in lamellipodia formation and clathrin-independent endocytosis, in these ways it has responsibility for mediation of downstream effects of focal adhesion kinase (FAK). There is evidence from *in vivo* studies of the importance of Rho family GTPases to the CLL microenvironment (189), identifying this family as being of interest for further study in CLL. Active Rac1 may also be measured by evaluating the relative quantities of active and inactive forms of the protein in an experimental condition, however there was no available pharmacological activator, therefore control conditions were limited to the concentrated samples of G-protein-activating GTP analogue, guanosine γ thio-phosphate ($GTP_{\gamma}S$) and GDP, which were added to positive and negative control cells, respectively.

5.2 Molecular effects of mTOR inhibition on GTPase activity

Immunoprecipitation assays were performed to explore changes in cellular protein levels under a range of drug inhibition and chemokine or BCR stimulation conditions.

5.2.1 **Rap1 by GTPase activity assay**

The initial Rap1 activity experiment using published conditions (237) was performed using a fresh CLL95 sample (normal karyotype CLL) and it yielded no Western blot signal in the sample conditions, however there was a weak signal in the GTPγS positive control lane. Molecular properties of GTPγS include its guanosine triphosphate (GTP) analogue function, G protein-activating and non-hydrolysable state which are exploited by the GTPase activity assay to provide a positive control condition. There was also no signal detected in the EPAC positive control cells, therefore we elected to include only the GTPγS and GDP controls. A representative example of the effects of mTOR inhibitors on Rap1

activity is shown upon SDF-1 and BCR stimulation demonstrated, along with positive and negative controls (Figure 5-2). There is a clear stimulation of Rap1 activity upon SDF-1 and BCR stimulation on sample CLL152, with pronounced effects of ibrutinib to inhibit Rap1 activity in the presence and absence of with either *in vitro* BCR or SDF-1 stimulation. The inhibition of Rap1 activity by AZD8055 is weaker and less consistently displayed, with a mild stimulation in Rap1 activity with rapamycin treatment in the presence and absence of SDF-1 or BCR ligation.

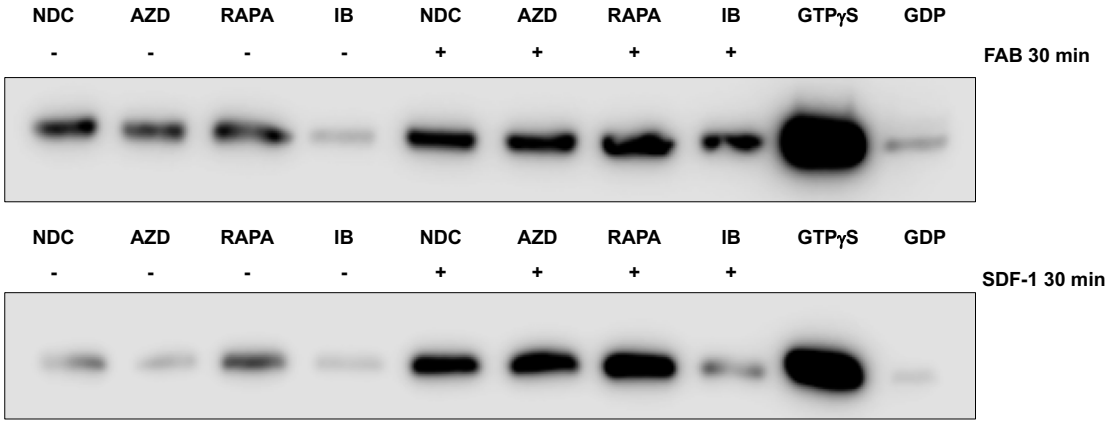

Figure 5-2 Rap1 activity assay
CLL152 (2 x 10^7 cells), a normal karyotype CLL sample was serum-starved for 2 h, treated for 30 min with non-drug control (NDC), AZD8055 100 nM (AZD), rapamycin 10 nM (RAPA) and ibrutinib 1 μM (IB) then stimulated with either $F(ab')_2$ fragment stimulation or SDF-1 for 30 min followed by immunoprecipitation for active Rap1. Rap1 levels are shown by Western blot along with positive and negative controls to confirm the success of the immunoprecipitation procedure.

5.2.2 **Rac1 activity in CLL cells**

The GTPase Rac-1, also involved in migration and its regulation, was found to show consistent protein expression levels under drug and stimulation conditions used (Figure 5-3), highlighting the need for study of activation status of this protein in investigation of the role that GTPases play downstream of mTOR signalling.

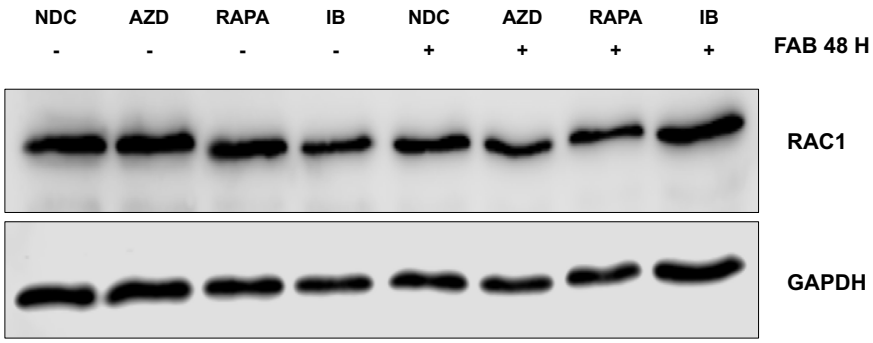

Figure 5-3 Total Rac1 protein levels after long-term mTOR inhibition and BCR stimulation
Patient sample CLL18, an 11q deletion patient, was treated for 30 min with non-drug control (NDC), AZD8055 100 nM (AZD), rapamycin 10 nM (RAPA) and ibrutinib 1 μM (IB) then exposed to 48 h F(ab')$_2$ fragment stimulation. The Western blot antibody to Rac1 cannot distinguish between active and inactive forms of the protein and the overall levels appear as unchanged in relation to the untreated control.

The availability of Rac1 activity assay with beads specific for active Rac1 allowed me to perform similar experiments as for Rap1 activity. The efficacy of the immunoprecipitation process was supported by the results of GTPγS and GDP controls and a representative sample result of Rac1 activity in response to either SDF-1 or BCR stimulation is shown (Figure 5-4). Inhibitors appear to have little effect in the unstimulated samples with no effect of ibrutinib overall. Rapamycin inhibits BCR-mediated Rac1 activity and AZD8055 has no effect in the sample shown in Figure 5-4. Direct comparison of Rac1 activity in SDF1 and BCR stimulated cells on the same Western blot for CLL147 (Figure 5-5) confirmed that the overall signal generated by BCR stimulation is greater than that with SDF-1 stimulation.

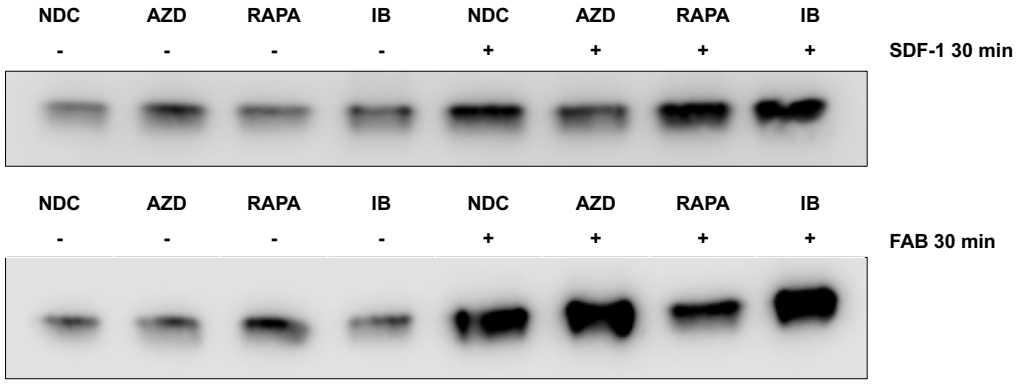

Figure 5-4 Rac1 activity assay of a single normal karyotype CLL sample
CLL147, a normal karyotype CLL sample was serum-starved for 2 h, pre-treated for 30 min with non-drug control (NDC), AZD8055 100 nM (AZD), rapamycin 10 nM (RAPA) and ibrutinib 1 μM (IB) then stimulated for 30 min with either F(ab')$_2$ fragment or 30 min SDF-1 followed by immunoprecipitation for active Rac1.

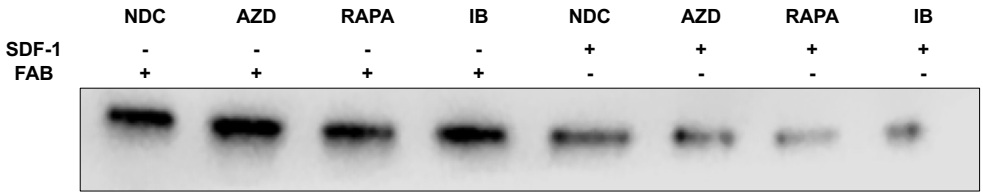

Figure 5-5 Comparison of Rac1 activity assay SDF-1 and BCR ligation conditions Samples of CLL147 were evaluated for levels of active Rac1 for drug conditions: non-drug control (NDC), AZD8055 100 nM (AZD), rapamycin 10 nM (RAPA) and ibrutinib 1 μM (IB). Residual lysates from the active Rac1 pull-down assay were run on Western blot to repeat earlier findings.

Although protein concentrations were assumed to be constant at the outset of the experiment, based upon the use of equal aliquots of the same cell suspension to provide individual drug and stimulation conditions and the use of equal sized aliquots of protein lysates in each lane of all Western blots performed. Also, based upon Western blot findings shown in 3.1.6 I have shown that total GTPase levels are unaffected by drug inhibitors or *in vitro* stimulation. However, additional control conditions were sought to prove that there was no change in protein expression of GTPases and that the protein concentration in the protein lysates obtained by immunoprecipitation was constant. To do this, I extracted eluate from stage of sample exposure to the Rac1 beads and assessed total Rac1 content using sample CLL147. The signals in Figure 5-6 exhibit consistency between total Rac1 levels and loading control, supportive of earlier data to demonstrate consistency in overall Rac1 levels in the presence and absence of drug inhibition and stimulation conditions. As the protein concentrations were consistent and because original published data in CLL refer only to raw data values in relation to GTPase activity, I compared Western blot of individual samples using densitometry values for uncorrected Rap1/Rac1 activity (237, 238).

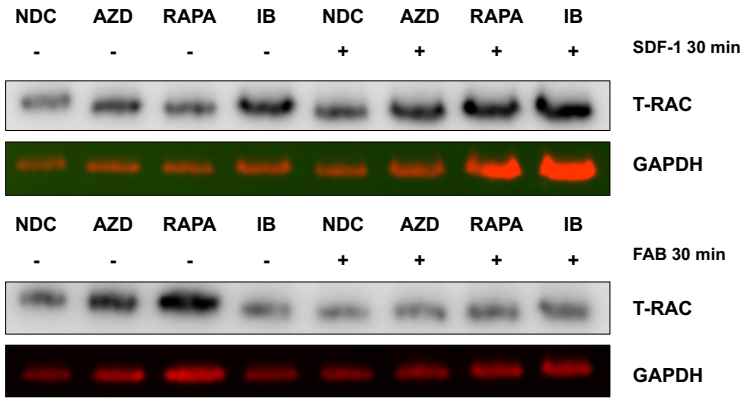

Figure 5-6 Analysis of Rac1 protein expression with drug inhibitors and SDF-1 or BCR stimulation
Patient samples CLL147 lysates were obtained from the pull-down assay for analysis, from both SDF-1 and BCR stimulation experiments for drug conditions: non-drug control (NDC), AZD8055 100 nM (AZD), rapamycin 10 nM (RAPA) and ibrutinib 1 μM (IB). All inactive and non-bound Rac1 and other proteins are eluted during the immunoprecipitation process and in the spin column below the filter cup the sample may be collected and maintained at -20°C for further analysis. Western blots were probed for total Rac1 protein (T-RAC) and a loading control.

The Rap1 densitometry findings most clearly demonstrate an increased activity with the addition of *in vitro* stimulation conditions (Figure 5-7). Both SDF-1 and BCR stimulation increase Rap1 activity, with significance in the SDF-1 experiments and a trend to significance with the addition of BCR stimulation. Ibrutinib blocks Rap1 activity more effectively than mTOR inhibitors, which appears to be overcome by SDF-1 stimulation (Figure 5-7 A) but not by BCR stimulation (Figure 5-7 B), which may reflect a greater dependence upon BTK for transduction of the BCR signal as opposed its role in chemokine signalling. Rapamycin appears to have minimal effects upon Rap1 activity with the inhibitory effects of AZD8055 displaying a trend to reduction in Rap1 activity in the absence of BCR or SDF-1 stimulation, suggesting that AZD8055 inhibition may be overcome by the addition of *in vitro* SDF-1 and BCR stimulation.

Densitometry of the active Rac1 signal also supports the effects of *in vitro* BCR and SDF-1 stimulation to cause increased Rac1 activity (Figure 5-8 A&B). However, there are minimal drug effects under all 3 drug conditions. More samples are required to be assessed by Rap1 and Rac1 activity assays, to confirm and to establish the effects of drug inhibitors.

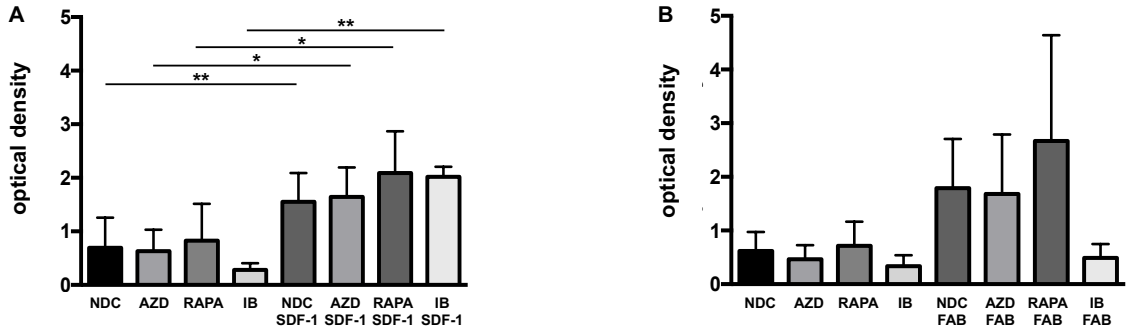

Figure 5-7 Rap1 activity assay Western blot densitometry
Raw mean and SEM densitometry values for Rap1 assay with n=4 samples treated for 30 min with non-drug control (NDC), AZD8055 100 nM (AZD), rapamycin 10 nM (RAPA) and ibrutinib 1 μM (IB) followed by 30 min (A) SDF-1 and (B) F(ab')$_2$ stimulation. *=p≤0.05; **=p≤0.01; ***=p≤0.001; ****=p≤0.0001.

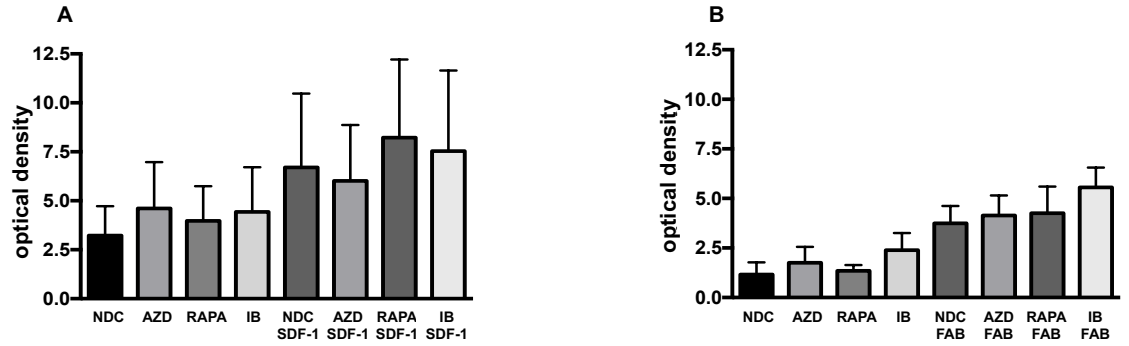

Figure 5-8 Rac1 activity assay Western blot densitometry
Raw mean and SEM densitometry values for Rac1 activity assay results are also shown with 30 min exposure to non-drug control (NDC), AZD8055 100 nM (AZD), rapamycin 10 nM (RAPA) and ibrutinib 1 μM (IB) then 30 min (A) SDF-1 (n=5) and (B) F(ab')$_2$ stimulation (n=3).

5.3 Chemokine stimulation effects on fluorescent staining for GTPase proteins

The effects of mTOR inhibition were explored further with an IF assay and stimulation techniques developed using signalling pathways shown earlier as their basis. Initially, a secondary control step was performed to compare the fluorescence of secondary bound to primary antibody and those of non-specific secondary antibody binding and fluorescence. Figure 5-9 A displays the unstained control cells which are to be contrasted with the raw image of CLL cells with Rap1 and LAMP1 co-staining (B).

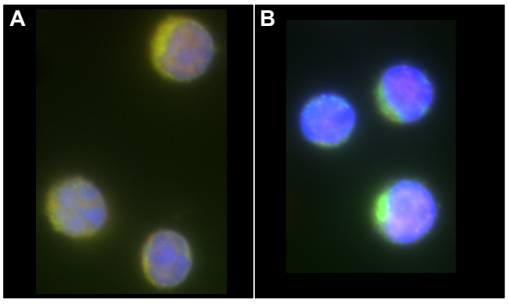

Figure 5-9 Secondary control for Rap1/ LAMP1 co-staining experiment
CLL132, a sample known to harbour a 17p deletion, was rested overnight in either (A) block containing 5% BSA and 0.1% Triton or (B) 1/200 anti-Rap1 rabbit antibody and anti-LAMP1 mouse antibody both in block, with subsequent exposure for 1 h to red and green secondary antibodies.

Figure 5-1 displays both Rap1 signalling and activation with the inclusion of mTOR and its posited role in the cascade and based upon this awareness of Rap1 signalling, I have validated an assay used in earlier studies (238) that exploits the availability of a pharmacological activator of Rap1 signalling EPAC agonist 8-(4-Chlorophenylthio)-2'-O-methyladenosine 3',5'-cyclic monophosphate monosodium hydrate and changes in distribution of Rap1 upon stimulation. Primary CLL cells were stimulated with EPAC agonist or SDF-1, each for 5 min, and the cells were then stained for Rap1 protein (238). In keeping with existing evidence, CLL is variably responsive to SDF-1 and EPAC agonist with a tendency for Rap1 redistribution to the plasma membrane and a more peripheral distribution within the cytoplasm in some cells. Figure 5-10 shows a patient sample in which there were minimal effects upon redistribution of Rap1 in response to SDF-1 and EPAC stimulation. These appearances may be consistent with anergic CLL (237). The effects of mTOR inhibitors on Rap1 distribution were introduced as experimental conditions (Figure 5-11 and Figure 5-12). There are minimal observable effects of mTOR inhibition on the protein distribution of Rap1 in this sample whereas there appears to be a redistribution of Rap1 to the plasma membrane with both EPAC and SDF-1 stimulation (Figure 5-11 A&D and Figure 5-12 A&D). Interestingly, the EPAC-stimulated redistribution effect appears to be overcome by both AZD8055 and rapamycin treatment and indicated by increased green fluorescence in the DAPI stained region of the cell (Figure 5-11 D-F) which may suggest that mTOR inhibition has specific effects to inhibit Rap1 activity. In contrast, Figure 5-12 demonstrates the effects of SDF-1 to redistribute Rap1 protein in the pictured sample (Figure 5-12 A&D), effects

which appear unaltered by mTOR inhibition (Figure 5-12 D-F) therefore mTOR inhibition does not demonstrably affect Rap1 redistribution in response to chemokine in this case.

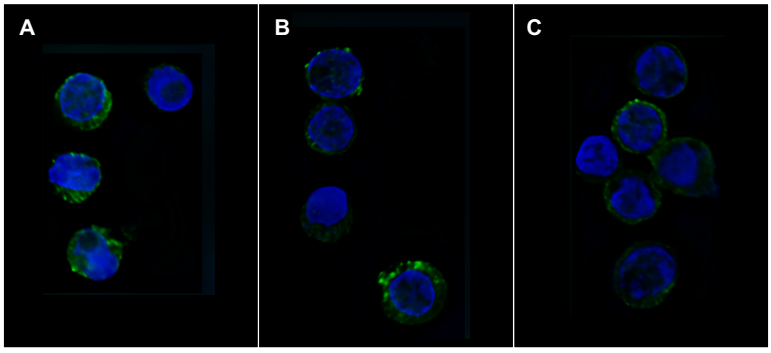

Figure 5-10 Comparison of effects of SDF-1 and EPAC stimulation on CLL cellular Rap1 distribution
CLL138, a sample with a normal karyotype was either (A) untreated (B) exposed to 100 ng/ml SDF-1 stimulation or (C) exposed to 10 μg/ ml EPAC stimulation for 5 min before cell fixation, permeabilisation, blocking steps. Slides were then stained with primary anti-Rap1 rabbit polyclonal antibody overnight with secondary antibody staining with green fluorescence and overnight exposure to DAPI, which stains the nuclear structures.

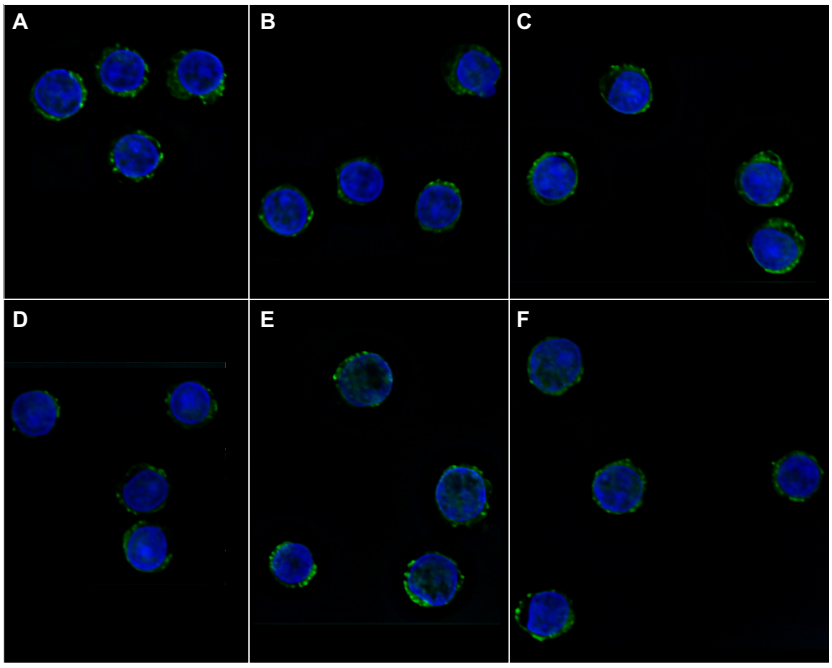

Figure 5-11 Effects of mTOR inhibition and EPAC stimulation on cellular Rap1 staining
CLL122, a sample known to have a 17p deletion, was pre-treated with mTOR inhibitors for 30 min and 10 μg/ml EPAC stimulation for 5 min before cell fixation, permeabilisation, blocking steps. Slides were then stained with primary anti-Rap1 rabbit polyclonal antibody overnight with secondary antibody staining with green fluorescence and overnight exposure to DAPI, which stains the nuclear structures. Experimental conditions are indicated by labels: (A) untreated control (B) 100 nM AZD8055 (C) 10 nM Rapamycin (D) EPAC stimulation alone (E) 100 nM AZD8055 + EPAC stimulation (F) 10 nM Rapamycin + EPAC stimulation.

The impact of SDF-1 stimulation on Rac1 distribution was also demonstrably altered in this CLL sample, with peripheral localisation of Rac1 when compared with the unstimulated cells (Figure 5-13 A&D). Figure 5-13 also incorporates the effects of mTOR inhibition with some cells displaying Rac1 localisation to the plasma membrane in both AZD8055 and rapamycin conditions although some cells maintain a more diffuse pattern of Rac1 distribution. The effects of AZD8055 are more clearly delineated using a different patient sample stained for Rac1 protein where there are more cells shown to have a peripheral Rac1 distribution in the AZD8055 condition when compared with untreated controls as demonstrated in Figure 5-14.

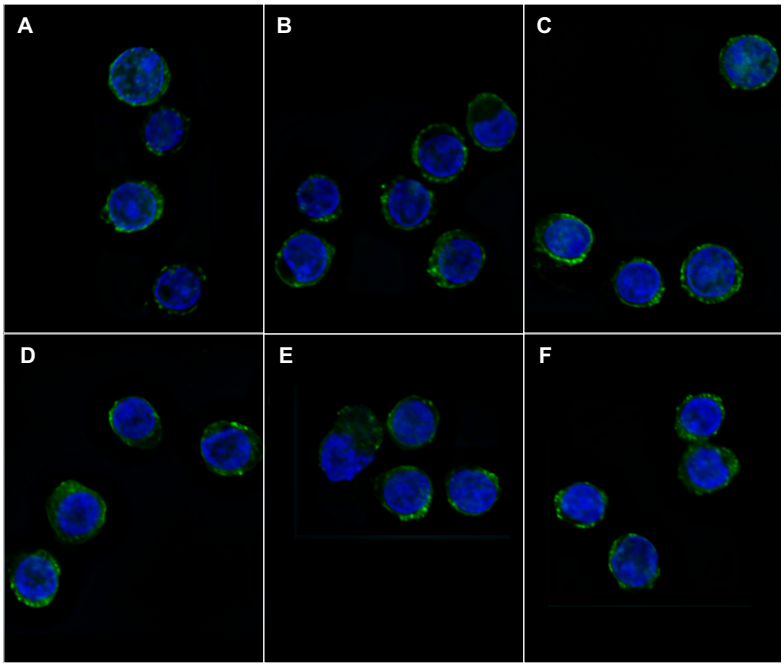

Figure 5-12 Effects of mTOR inhibition and SDF-1 stimulation on cellular Rap1 staining CLL122, a sample known to have a 17p deletion, was pre-treated with mTOR inhibitors for 30 min and 100 ng/ml SDF-1 stimulation for 5 min before cell fixation, permeabilisation and blocking steps. Slides were then stained with primary anti-Rap1 rabbit polyclonal antibody overnight with secondary antibody staining with green fluorescence and overnight exposure to DAPI, which stains the nuclear structures. Experimental conditions are indicated by labels: (A) untreated control (B) 100 nM AZD8055 (C) 10 nM Rapamycin (D) SDF-1 stimulation alone (E) 100 nM AZD8055 + SDF-1 stimulation (F) 10 nM Rapamycin + SDF-1 stimulation.

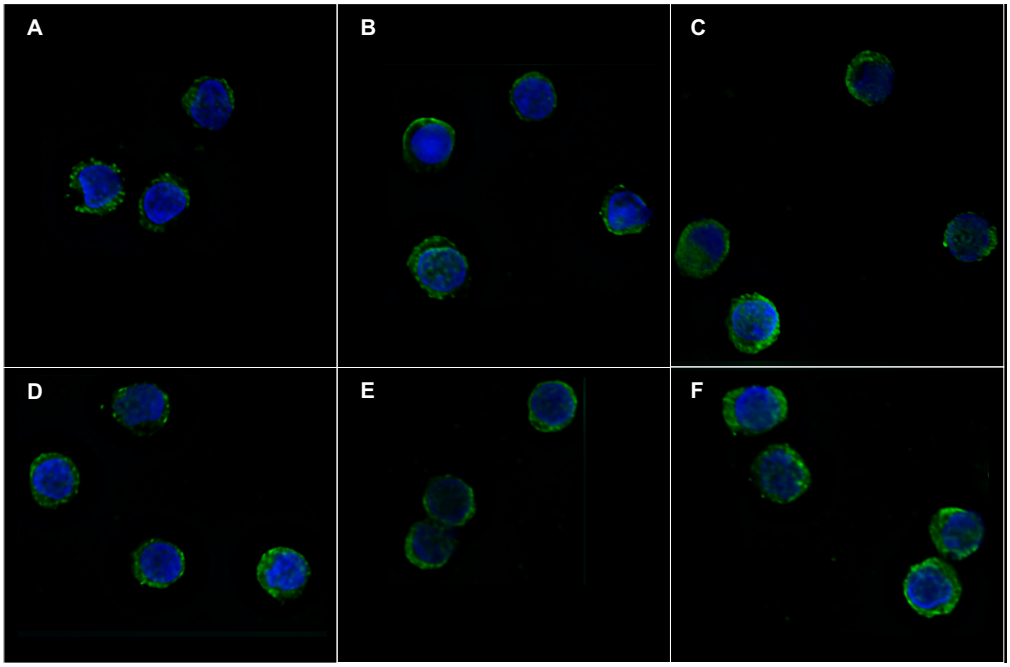

Figure 5-13 Effects of mTOR inhibition and SDF-1 stimulation on cellular Rac1 staining by IF
CLL149, a sample known to harbour a 17p deletion, was pre-treated with mTOR inhibitors for 30 min and 100 ng/ml SDF-1 stimulation for 5 min before cell fixation, permeabilisation and blocking steps. Slides were then stained with primary anti-Rac1 rabbit polyclonal antibody overnight with secondary antibody staining with green fluorescence and overnight exposure to DAPI, which stains the nuclear structures. Experimental conditions are indicated by labels: (A) untreated control (B) 100 nM AZD8055 (C) 10 nM Rapamycin (D) SDF-1 stimulation alone (E) 100 nM AZD8055 + SDF-1 stimulation (F) 10 nM Rapamycin + SDF-1 stimulation.

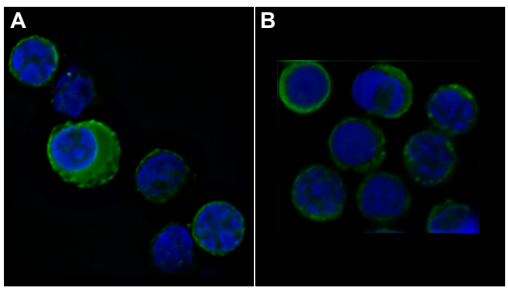

Figure 5-14 Effects of AZD8055 upon CLL cellular Rac1 distribution
CLL143, a sample known to have a 11q deletion, was pre-treated with AZD8055 before cell fixation, permeabilisation and blocking steps. Slides were then stained with primary anti-Rac1 rabbit polyclonal antibody overnight with secondary antibody staining with green fluorescence and overnight exposure to DAPI. Experimental conditions are indicated by labels: (A) untreated control (B) 100 nM AZD8055.

5.3.1 **Colocalisation studies with SDF-1 stimulation**

To investigate protein distribution further, colocalisation staining was performed for Early Endosomal Antigen-1 (EEA-1) and Lysosomal-Associated Marker Protein-1 (LAMP-1) together with Rap1 staining. The images show some evidence of

colocalisation of EEA1 (Figure 5-15) and LAMP1 (Figure 5-16) endosomal markers with Rap1 in CLL143 and give further support to the peripheral redistribution of Rap1 in response to SDF-1 and to a lesser extent with EPAC stimulation (Figure 5-17 A-C). Features which indicate colocalisation include the relative lack of Rap1 distribution throughout the cytoplasm and the orange staining of cytoplasmic structures, indicative of Rap1/ LAMP1 protein colocalisation.

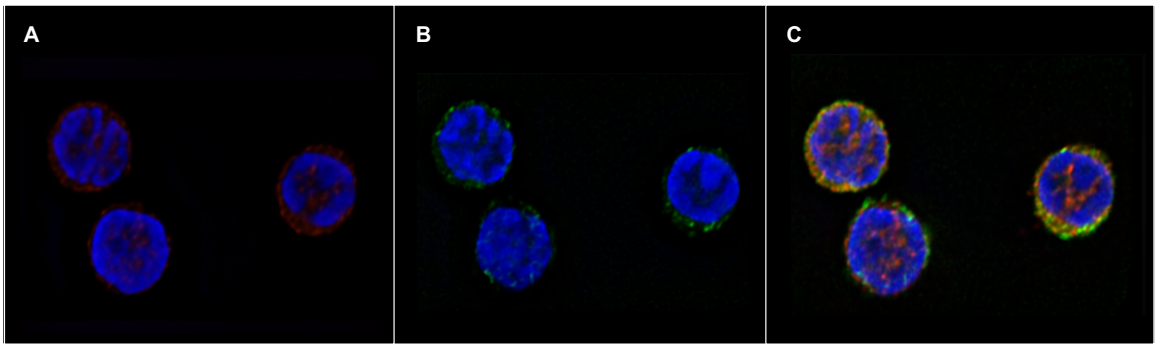

Figure 5-15 CLL cellular Rap1 distribution with co-staining for EEA1 endosomal marker CLL149, a sample with an 17p deletion was adhered to slides, then stained with primary anti-Rap1 rabbit polyclonal antibody and EEA1 mouse antibody overnight with secondary antibody staining Rap1 and EEA1. Slides were then exposed to DAPI overnight. DAPI stains nuclei blue and Rap1 protein in (A) stains with red fluorescence whereas EEA1 stains with green fluorescence (B). Images from 3 superimposed fluorescence channels are displayed (C).

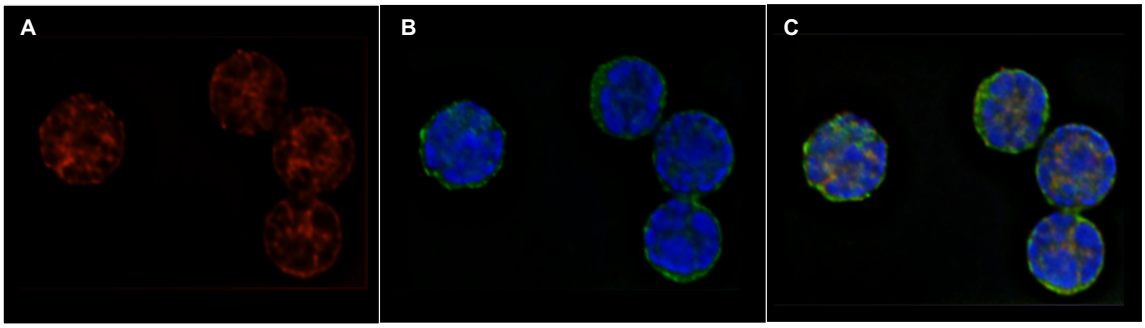

Figure 5-16 CLL cellular Rap1 distribution with co-staining for LAMP1 endosomal marker CLL149, a sample with a 17p deletion was adhered to slides, then stained with primary anti-Rap1 rabbit polyclonal antibody and LAMP1 mouse antibody overnight with secondary antibody staining Rap1 and LAMP1. Slides were then exposed to DAPI overnight. Rap1 protein in (A) stains with red fluorescence whereas LAMP1 stains with green fluorescence with nuclear DAPI shown (B). Images from 3 superimposed fluorescence channels are displayed (C).

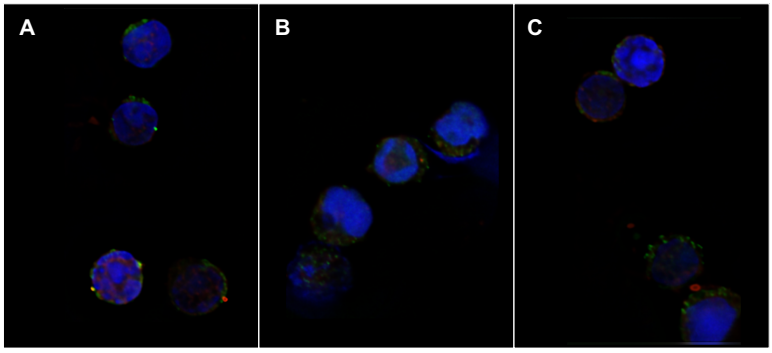

Figure 5-17 Comparison of effects of SDF-1 and EPAC stimulation on CLL cellular Rap1 distribution with co-staining for LAMP1 endosomal marker
CLL143, a sample with an 11q deletion was either (A) untreated (B) exposed to 100 ng/ml SDF-1 stimulation or (C) exposed to 10 μg/ml EPAC stimulation for 5 min before cell fixation, permeabilisation and blocking steps. Slides were then stained with primary anti-Rap1 rabbit polyclonal antibody and LAMP1 mouse antibody overnight. Rap1 antibody is bound by red fluorescent secondary antibody whereas LAMP1 is bound by green fluorescence. Slides were then exposed to DAPI overnight.

5.3.2 BCR stimulation effects on intracellular colocalisation of GTPase proteins

Given the evidence for defective chemokine responsiveness in CLL cells and the role of Rap1, we sought to explore the BCR stimulation effects upon Rap1 in primary CLL cells (237). An experimental method to integrate BCR stimulation into existing IF staining protocols was already established for use by our group. Slides were pre-coated with anti-IgM antibody after the poly-L-lysine preparation step which was prepared the night before the IF experiment. A blocking step to dampen non-specific binding signal is a requirement inherent to any antibody binding protocol and following previously tested protocols I blocked slide-bound antibody using 30 min incubation with 10% BSA/RPMI media at 37ºC. Unfortunately, there was repeated contamination of fluorescent images by non-specific signal which was not eliminated by media filtration. Therefore, the blocking step was abbreviated to 15 min which proved effective in removal of the non-cellular debris from the microscopic field.

The effects of BCR stimulation upon Rap1 cellular distribution are shown in Figure 5-18 with the effects of the prior addition of mTOR inhibitors and ibrutinib also demonstrated. Unlike the SDF-1 stimulation effects, BCR stimulation appears to have minimal effect upon Rap1 distribution in the CLL samples which were tested, although there does appear to be an elevated

concentration of Rap1 staining at the plasma membrane in BCR stimulated cells. Both mTOR inhibitors appear to be localising Rap1 to an intracellular compartment, with greater effects of rapamycin in the unstimulated cells whereas AZD8055 shows more effects with BCR stimulation. The difficulties encountered with ascertaining the effects of mTOR inhibitors on Rap1 localisation, along with differential responses to BCR stimulation led to the evaluation of Rap1 colocalisation. Cellular organelles and their relationship to Rap1 staining were studied in the presence and absence of BCR stimulation.

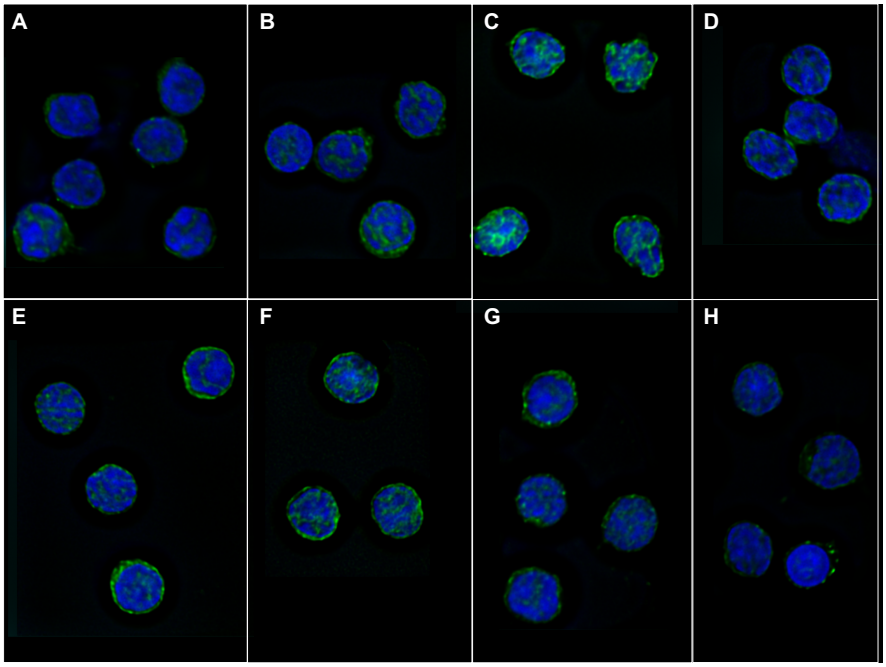

Figure 5-18 Effects of mTOR inhibition and BCR stimulation on cellular Rap1 staining CLL122, a sample known to harbour a 17p deletion, was pre-treated with mTOR inhibitors for 30 min and added to slides coated either with isotype control or anti-IgM antibody with incubation at 37°C for 30 min before cell fixation, permeabilisation and blocking steps. Slides were then stained with Rap1 rabbit polyclonal antibody overnight with secondary antibody staining with green fluorescence and overnight exposure to DAPI. Experimental conditions are indicated by labels: (A) untreated isotype control (B) 100 nM AZD8055 (C) 10 nM Rapamycin (D) 1 μM Ibrutinib (E) anti-IgM alone (F) 100 nM AZD8055 + BCR stimulation (G) 10 nM Rapamycin + BCR stimulation (H) 1 μM Ibrutinib + BCR stimulation.

First, it was confirmed that BCR stimulation has negligible effects on organelle distribution by comparison of LAMP1 staining pattern in the presence and absence of BCR stimulation as shown in Figure 5-19 A&B.

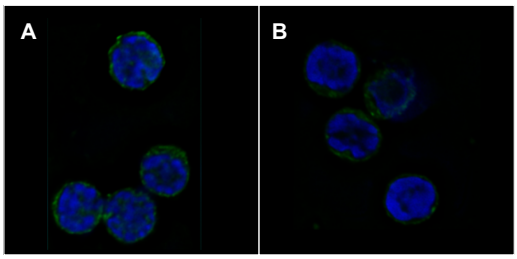

Figure 5-19 Effects of BCR stimulation on localisation of LAMP1 staining in CLL
CLL149 was treated with either (A) isotype control or (B) BCR stimulation by prior coating of slides with anti-IgM antibody and exposure to slides for 30 min before cell fixation, permeabilisation and antibody staining techniques. LAMP1 mouse antibody is indicated by green fluorescence with nuclear structures stained in blue. CHANGE FOR EEA1

In Figure 5-20 there is slightly greater peripheral localisation of the Rap1 with BCR stimulation, when a comparison is made between (A) unstimulated controls and (B) BCR stimulated cells. Evidence for colocalisation is provided by greater overlap of the dual staining as indicated by the orange colour created in (B) but not (A), and where present the orange colour is confined largely to the plasma membrane. Figure 5-21 displays the same sample, CLL149, stained for Rap1 alone as a comparison.

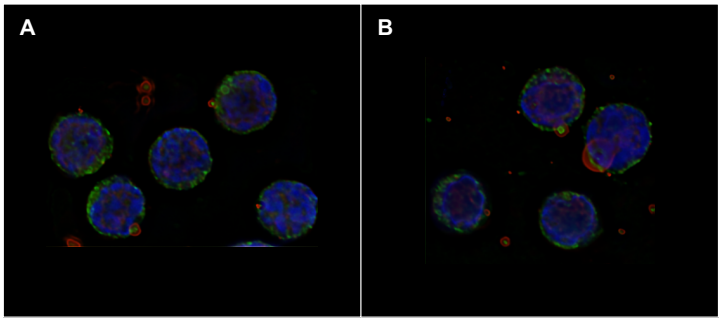

Figure 5-20 Effects of BCR stimulation on colocalisation of Rap1 with EEA1 staining
CLL149, a sample known to harbour a 17p deletion, was treated with either (A) isotype control or (B) BCR stimulation by prior coating of slides with anti-IgM antibody and exposure to slides for 30 min before cell fixation, permeabilisation and antibody staining techniques. Rap1 rabbit antibody is stained with secondary antibody with red fluorescence and EEA1 mouse antibody is bound by secondary antibody with green fluorescence.

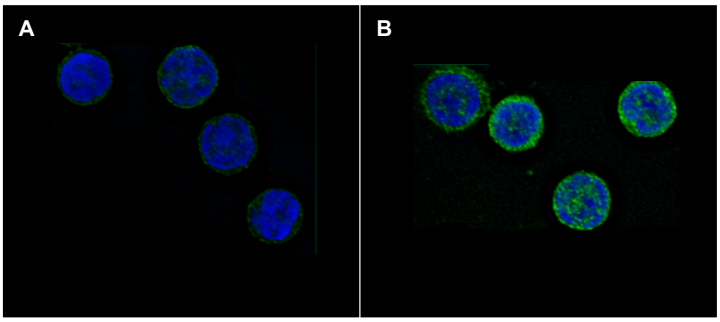

Figure 5-21 Effects of BCR stimulation on localisation of Rap1
CLL149, a sample known to harbour a 17p deletion, was treated with either (A) isotype control or (B) BCR stimulation by prior coating of slides with anti-IgM antibody and exposure to slides for 30 min before cell fixation, permeabilisation and antibody staining techniques. Rap1 rabbit antibody is stained with secondary antibody with green fluorescence.

Next, I analysed the impact of mTOR inhibition in combination with BCR stimulation in another poor prognostic CLL sample (Figure 5-22). There is evidence of Rap1 and LAMP1 colocalisation with BCR stimulation as cells stain peripherally with both red and green however Rap1 remains distributed throughout the cell cytoplasm (Figure 5-22 E-H). There appears to be some colocalisation in Figure 5-22 C and to a lesser extent in Figure 5-22 D, which suggests that rapamycin or ibrutinib are acting directly to redistribute Rap1 to CLL endosomes but not the dual mTOR inhibitor. Further images are required from the testing of additional samples to confirm this trend and to explore the drug effects further. More data are required due to the heterogeneity of responses of the primary CLL samples tested, in order to confirm the patterns

shown by IF staining in our cells. Quantitative analysis of colocalisation would be desirable to confirm the trends which are visible from the microscopic images.

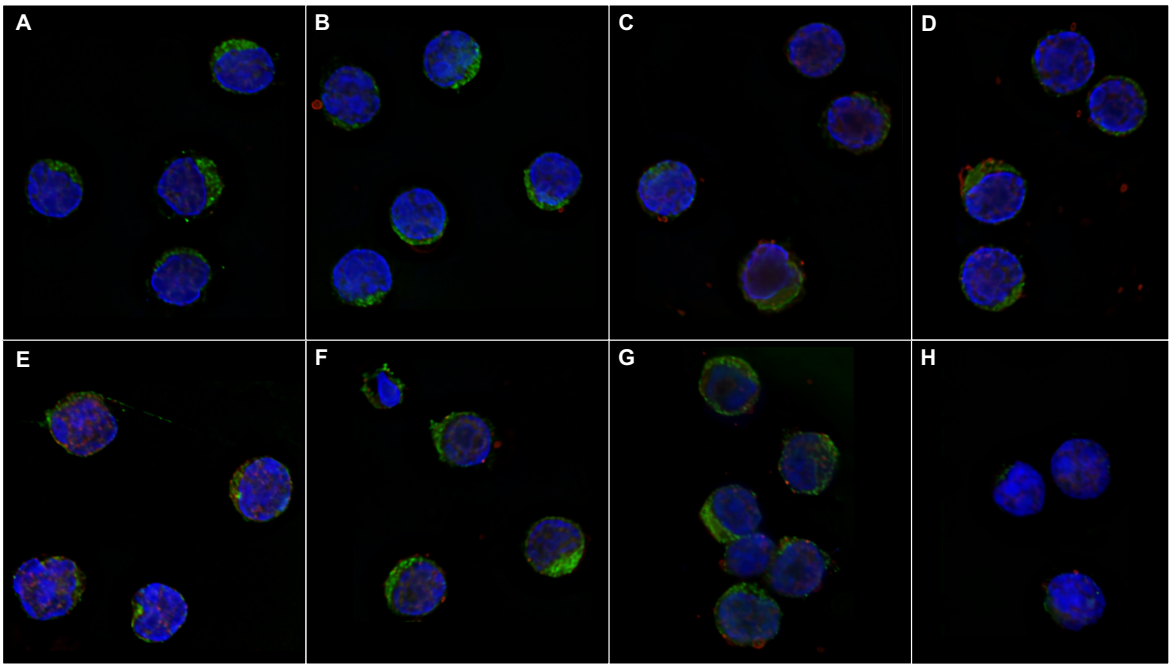

Figure 5-22 Effects of BCR stimulation on colocalisation of Rap1 with LAMP1 staining CLL132, a sample known to harbour a 17p deletion, was exposed to 30 min drug pre-treatment then added to slides previously coated with either isotype control or anti-IgM antibody. After 30 min cells were fixed, permeabilised and stained with Rap1 rabbit antibody (red) or LAMP1 mouse antibody (green). Experimental conditions are indicated by labels: (A) untreated isotype control (B) 100 nM AZD8055 (C) 10 nM Rapamycin (D) 1 μM Ibrutinib (E) anti-IgM alone (F) 100 nM AZD8055 + BCR stimulation (G) 10 nM Rapamycin + BCR stimulation (H) 1 μM Ibrutinib + BCR stimulation.

5.4 Summary of chapter

The regulation of signalling networks is integral to migration control in lymphocytes, as discussed in Chapter 1. GTPases both exert control and are themselves regulated both spatially and temporally by their associated GAPs and GEFs and by factors upstream of these. Rap1 is shown to be enriched at the plasma membrane but has dynamic localisation at the membrane in molecular complexes and within cellular endosomes (270). Initial evidence was available in support of a key role for Rap1 GTPase dysregulation in CLL cells however the role of other small GTPases remains unexamined in the disease (237, 238). Furthermore, it is known that Rap1 lies downstream of a range of kinase signalling pathways including PKC (271) however its relationship to mTOR kinase

signalling is not established. I now provide evidence from GTPase activity assays in support of a trend towards inhibition of Rap1 activity by mTOR inhibitors with the effects of dual mTOR inhibitor AZD8055 being more pronounced than those of rapamycin. Rap1 activity appears to be blocked effectively by ibrutinib which appears to have the most consistent effects and in relation to its striking clinical activity it represents a positive control drug however more data are required to confirm the trends. Although chemokine and BCR stimulation effects upon Rac1 activity could be demonstrated, no consistent drug effects were shown but in view of the low sample number and heterogeneity of individual responses this highlights an area for further study.

IF findings were consistent with the existing data to show CLL cell chemokine responses acting to redistribute Rap1 to the plasma membrane, a phenomenon which is variably present between different CLL samples. There is also some evidence of Rap1 redistribution in response to its specific activator, EPAC, to which our samples are variably responsive, indicative of the anergic status of these cells. Anergy in CLL has been mainly described with reference to its BCR responses and is an interesting property from a therapeutic perspective as the anergic population may represent a clonal reservoir of immunologically evasive cells. Such anergic cells have shown relative resistance to apoptosis, which is reversible once the anergy is overcome. The normal cellular responses to chemokine do not appear to be overcome by mTOR inhibition in our study however there do appear to be effects upon Rap1 activator, EPAC, responses which may represent specific mTOR-mediated effects upon Rap1 activity. The effects of BCR stimulation upon Rap1 distribution could not be demonstrated by Rap1 staining alone but the colocalisation of Rap1 and the endosomal marker, LAMP1 could be demonstrated with BCR stimulation. The effects of colocalisation of Rap1 and early endosomal marker, EEA1, were shown in response to SDF-1 stimulation. The effects of mTOR inhibition upon Rap1 and endosome colocalisation require further investigation. As Rac1 is also implicated in leukocyte chemotaxis (272) in processes of actin cytoskeletal activation and lamellipodia formation, its function and activity may also be spatially regulated. Rac1 protein localisation appears to be affected by dual mTOR inhibition, as Rac1 appears to be peripherally distributed in the samples studies but this

finding requires confirmation and further exploration using colocalisation studies.

Chapter 6 General Discussion

6.1 Migration control in CLL cells

The next few sections describe some of the recent research which has been undertaken to identify the mechanisms whereby microenvironmental inputs are abrogated by novel drug therapies in CLL. During the following sections, along with an explanation of the microenvironmental mechanisms, I address my own experimental results concurrently to base my explanations in the context of recent research findings.

6.1.1 Integrin signalling and GTPase regulation

Integrin signalling has been known to have a regulatory role in CLL migration for some time. Studies of both integrin expression and function have been performed and the main molecules to be implicated include heterodimers alpha 4 beta 1 (VLA-4) which binds VCAM-1 and fibronectin, and alpha L beta 2 (LFA-1) which binds ICAM. Integrins are responsible for lymphocyte entry into tissue and experimentally it was shown that endothelial stimulation enhanced binding of CLL cells via the VLA-4 heterodimer (273). Aberrant integrin signalling has been found in association with various cytogenetic defects in CLL cells. Firstly, deletions at the chromosome 11q locus have been associated with CLL presentation with bulky lymphadenopathy (106). An associated reduction in levels of functionally relevant adhesion molecules including integrins was attributed as the underlying cause of the characteristic clinical features (274). The study identified differential CD49d expression as a means of the altered disease pathophysiology, however it could not fully explain the integrin defect in the context of disease biology. Trisomy 12 has been more recently associated with a demonstrable increase in integrin signalling, in particular, LFA-1, VLA-4, Mac-1, CD49d and CD11a (107). The changes were modulated by *NOTCH1* expression with mutated *NOTCH1* being associated with lower levels of integrin signalling than UM-CLL cases. The increased integrin signalling was hypothesised to be responsible for increased cell motility and an increased capacity for CLL homing, supported with evidence from the disease biology of trisomy 12 cases. It was noted that the poorer prognosis attributed to the *NOTCH1* mutation could

not be explained by increased motility of this subset as *NOTCH1* mutation is found in association with inhibition of β2 signalling (107).

The influence of GTPases in regulation of integrin signalling has been examined, based upon an awareness of a defective activation of integrin signalling in CLL cells. Rap1 GTPase was found to regulate both VLA-4 and LFA-1 and a failure of Rap1 GTP-loading was implicated in the impaired activation of integrin in response to chemokine-induced activation (238). T cells from CLL cells also exhibit impaired integrin activation and the T cell defect is repaired with lenalidomide therapy. It was shown that Rho GTPase signalling defects were the underlying factor in the impaired LFA-1 activation which gives further definition to the role of integrin signalling in the CLL microenvironment (275, 276). The original study demonstrated defective actin polymerisation which resulted from the described integrin defects and as these were studied independently from GTPases in my project these shall be handled separately.

The role of mTOR signalling in relation to integrin and GTPase signalling was explored in Chapter 5 with specific reference to GTPase activity assays in 5.2.1 and 5.2.2. The trends in Rap1 activity suggest that mTOR inhibition reduced active Rap1 signalling and this is concordant with the effects of ibrutinib upon the Rap1 signal. Both chemokine and BCR signalling were shown to increase Rap1 and Rac1 signalling which suggests that the ability of the primary CLL samples tested to respond to chemokine and BCR signalling *in vitro* was unimpaired. AZD8055 treatment blocked active GTPase signalling and partially overcame the chemokine effects thus placing mTOR downstream of the chemokine signal and upstream of the active Rap1/Rac1 signal. The variation in Rap1 chemokine responsiveness by IF was explored in 5.3 but no conclusions could be drawn in relation to mTOR effects, due to limited sample numbers and the heterogeneity of sample responses.

6.1.2 **Cytoskeletal activation and mTOR signalling**

Cytoskeletal activation was studied in 4.5.1 using the actin polymerisation experimental technique. Stimulation of actin polymerisation was observed with both SDF-1 and BCR stimulation over a range of samples, each from

heterogeneous prognostic categories. There were no clear trends from the application of mTOR inhibitors to the assay when multiple samples were combined, however rapamycin appeared more often to increase actin polymerisation in CLL cells whereas there was a greater tendency to a reduction in actin polymerisation with AZD8055 or ibrutinib. Further work is required to determine the role of mTOR inhibition in regulation of the cellular cytoskeletal framework and its activation.

6.2 Advances in the understanding of CLL migration and microenvironment

The experimental findings outlined in chapters 3, 4 and 5 may be taken together with recent advances in the understanding of the CLL microenvironment. It appears that many novel therapies act to deprive CLL cells of the survival signals they may acquire in the LN and BM microenvironment, facilitating a potential "death by neglect" or *anoikis* (259). Taking the microenvironmental signals each in turn, I shall outline what I perceive to be the microenvironmental interactions of greatest interest in the recent study and application of therapeutic activity into within CLL research.

6.2.1 **CXCR4-CXCL12 axis**

Trafficking between lymphoid microenvironments has a pivotal role in CLL survival and growth. Our understanding of the CLL microenvironment is critical to our understanding of disease pathogenesis and we know that the normal germinal centre in secondary lymphoid tissue is distinctive from CLL germinal centres. Tissue homing of CLL cells is regulated by expression of chemokine receptors on CLL cells and it has been shown that peripheral blood CLL cells express increased CXCR4 and CXCR5 with these receptors being downregulated by receptor-mediated endocytosis (269). We can now define CLL cells which have recently exited the lymphoid tissue by their immunophenotype with expression of low surface CXCR4 and increased CD5 and it has been shown that microenvironmental mesenchymal stem cells (MSCs) (276) express and secrete CXCL12 (156). Effects of SDF-1 upon the immunophenotype of primary CLL samples were shown in 3.2.2. Primary CLL cells treated with SDF-1 for 48 h exhibiting a surface immunophenotype shift from $CXCR4^{hi}CD5^{dim}$ to a

predominantly $CXCR4^{dim}CD5^{hi}$ profile. The effects of SDF-1 upon CLL cells *in vitro* were similar in the presence of both mTOR inhibitors and of ibrutinib and appeared to be diminished.

The ability of CLL cells to respond to secreted CXCL12 has been explored *in vitro* using stromal cells lines but also using human MSCs using chemotaxis models whereby chemotaxis could be induced and then blocked using anti-CXCR4 antibody (277). Evidence for the effects of the CXCR4-CXCL12 in regulation of CLL cell migration can be obtained from the effects of ibrutinib in cell redistribution where peripheral blood lymphocytes display differential immunophenotype from LN-originated CLL cells, and ibrutinib is shown to block CLL cell chemotaxis (178, 186). My data confirm these effects in 4.2 and 4.3 with transwell and pseudoemperipolesis assays. The effects of AZD8055 to inhibit pseudoemperipolesis mirror those of ibrutinib, supportive of AZD8055 as another agent to act via lymphocyte redistribution. The data from the transwell migration assay demonstrate similar trends between AZD8055 and ibrutinib however the sample size in the ibrutinib condition was small. The effects of AZD8055 in comparison to control appear to be more marked over a longer term drug incubation phase. In consideration of the basis for the AZD8055 effects, it may be that differences in the timescale of drug effects are representative of drug activity at different loci within the CLL cell.

Our primary CLL cell transwell migration study findings also suggest that the cellular changes which regulate migration, and those changes which may be targeted by drug inhibitors, may occur after longer-term drug exposure periods. There were less pronounced effects of AZD8055 demonstrated by the transwell assay compared with those observed in the pseudoemperipolesis assay. All migration assay results must also be taken into consideration alongside my data shown in 3.2.5 which appears to conflict with the idea that AZD8055-mediated effects are mediated over long-term timescales, as a 30 min drug pre-treatment phase followed by 30 min SDF-1 exposure exhibits effects upon mTOR substrates and may overcome SDF-1 elicited effects upon mTOR substrates in addition.

Rapamycin does not inhibit migration to the same extent in either the pseudoemperipolesis or transwell migration assays compared with AZD8055. It is

known that rapamycin has an ability to regulate cellular migration which is a 4EBP1 and S6K1- dependent function (278). However, mTORC1 has fewer functions in cellular migration and when rapamycin therapy has been shown to inhibit migration it has been in settings of prolonged exposure to the drug which may elicit mTORC2 inhibition in addition to mTORC1 blockade (279). Thus, rapamycin effects on migration in the context of my migration assays are minimal by comparison with those of AZD8055 and ibrutinib.

In consideration of any apparent conflict of my experimental findings it is helpful to consider the experimental designs each in turn. Whilst the migration assays may each be affected by differential effects upon CLL cell survival, I have already analysed the survival effects of the drug inhibitors over these timescales and found the contribution of apoptotic effects to be minimal. However, the fact that changes in mTOR substrate levels can appear over such short time-scales indicate that the initiation of the intracellular events which lead ultimately to changes in CXCR4 and CD62L surface expression caused by mTOR substrates are early events. Effects upon migration in response to AZD8055 must therefore be considered as later events, as the overnight effects of the drug were more pronounced, and may be initiated by earlier changes in mTOR substrate levels. Drug effects may be mediated at the level of receptor endocytosis and endocytic recycling, manifesting as changes in short-term cell surface receptor expression, or at the level of protein translation to alter the number of adhesion molecules being produced and trafficked to the cellular membrane. It has already been shown that SDF-1 alone may trigger CXCR4 receptor endocytosis in CLL cells in a dose-dependent fashion (148) and it may be that with a longer drug incubation pre-phase that AZD8055 may accentuate this response, whereas the time-scale for demonstration of these effects with the transwell assay may be insufficient.

Pseudoemperipolesis and transwell assays performed in parallel with drug incubation studies and concomitant measurement of cell surface CXCR4 levels by flow cytometry could provide corroborative evidence for alterations in cell surface expression of CXCR4 via receptor endocytosis as the means of drug effect.

6.2.2 **T cells and the tumour cell niche**

T cells play an instrumental role in the CLL microenvironment as evidenced by IHC co-staining where serial section analysis of pseudo-follicles revealed co-segregation of CD3 and Ki67 staining regions (280). Indeed it has been shown that BCR stimulation leads to production of CCL3-secreting T cells which implicates T cells as a feature of progressive CLL disease conditions (281). In other studies, the existence of a "BCR-activation" signature within the CLL microenvironment was identified whereby genes implicated in chemotaxis such as *CCL3* and *CCL4* displayed an increased expression level in the CLL LN and in NLC co-culture conditions in association with gene expression phenotyping which was consistent with BCR signalling activity (157). It has become apparent that CCL3 and CLL4 secretion are one of myriad ways that T cells engage in microenvironmental crosstalk. On further examination, it appears that CCL3 and CCL4 protein secretion is inducible in CLL NLC co-culture settings after BCR stimulation, a phenomenon which is differentially activated by IgM but not IgD signalling (282). Also IgM production leads to a selective reduction in protein expression of BCL-6, a known tumour repressor, whereas IgD stimulation does not.

Dependence on one or other molecular isotype for individual patient disease biology may explain some of the differences in response in migration assays and may be one underlying cause of the generation of a BCR response subgroup as shown in 4.3. As described earlier, the transwell migration study which utilised CXCL12 to create a chemokine ligand gradient showed significant migration responses to BCR stimulation. However, the significant effects were only demonstrated after identification of a subgroup of CLL samples which responded positively to BCR stimulation. Analysis of the basis for inter-sample variations revealed that the majority of transwell experiments were performed after stimulation with $F(ab')_2$ fragments rather than by anti-IgM stimulation with avidin crosslinking, negating the likelihood of method of BCR stimulation as the underlying cause of differential responses. Next, we referred to the traditional definitions of prognostic risk category, *i.e.* CLL karyotype and ZAP70 status. No common features are shared by the 5 samples listed above, apart from ZAP70 positivity although ZAP70 positivity and "BCR response" are not mutually

exclusive. Further experiments to examine the significance of ZAP70 positive status on migration potential are required to explore this possibility. Another more basic feature of CLL biology may be at play for as previously discussed, both IgM and IgD are functionally expressed in CLL however I have limited my experiments to use of anti-IgM without the use of anti-IgD, based upon the experience of our group (180). However, stimulation of the CLL BCR via IgM and via IgD have been compared by Haerzschel *et al*. to show differential migratory responses of CLL according to the target molecule (283). Cells stimulated via anti-IgD retained the ability to migrate in the context of chemotaxis assay findings, whereas stimulation via IgM affected CLL cells to reduce migratory potential.

As already discussed, CCL3 protein expression varies in the CLL microenvironment however it has also been CCL3 staining density correlates with staining for T cell markers in the CLL LN and it is variation in the localisation of CCL3 secretion which may regulate the trafficking of CLL cells within these structures (284). Evidence for CCL3 and CCL4 as biomarkers of BCR-signal mediated migration effects come from the drug trials of ibrutinib and idelalisib, BCR signalling inhibitors, which act downstream of the BCR and display pronounced effects upon levels of these chemokines (186). As with many pathogenic processes in CLL the chemokine effects are reflective of underlying normal lymphocyte biology as normal GC B cells engage in competition for T cell help via CCL3 and CCL4.

6.2.3 **IL4R-IL4 axis**

Recent study has shown the IL4R-IL4 axis to play a pivotal part in the CLL microenvironment. Disruption of IL4R-IL4 by ibrutinib therapy predisposes UM-CLL to destruction as they show greater dependence upon this microenvironmental input. IL4 a is key survival factor which predisposes to a reduction in CLL cell surface CXCR4 levels and it enhances levels and function of surface membrane IgM, particularly in UM-CLL. Ibrutinib blocks IL4 secreted by T cells, leading to a lymphocytosis in M-CLL and increased cell death in UM-CLL. B cell survival in UM-CLL, promoted by T cells, may be blocked by pre-treatment of those T cells with ibrutinib and is attenuated similarly by the addition of IL4-

neutralising antibodies. Extension of the culture conditions to M-CLL subsets did not have any effect upon the survival of B cells, lending further support to the specificity of the IL4 axis in its UM-CLL effects. As a result of the co-culture conditions of T cells with ibrutinib, expression of sIL4R and pSTAT6 were also diminished (285).

The loss of IL-4 expression with ibrutinib therapy leads to a reduction in IL4R signalling in both UM-CLL and M-CLL. Furthermore, *ex vivo* analysis of ibrutinib-treated CLL patients displayed a B cell lymphocytosis and T lymphocytosis in ibrutinib therapy in UM-CLL but less so with M-CLL.

Further study revealed that T cells are impaired after ibrutinib therapy with a significant reduction in IL-4 production, manifesting in a reduction of T cell proliferation upon stimulation. The effects of ibrutinib were examined using mouse xenograft experiments into which patient samples were transplanted, each of whom were treated for 24 h with ibrutinib (n = 3 for each patient sample). The mice were then sacrificed and CD3+ T cells obtained from xenografts derived from ibrutinib-treated patients were found to be unable to home to the spleen upon secondary transplantation. Furthermore, IL4R was present at reduced levels in UM-CLL and M-CLL patients treated with ibrutinib. The dysfunctional CXCR4 signalling induced by ibrutinib therapy of CLL B cells leads to a loss of phosphoCXCR4 and a greater inhibition of its activity in UM-CLL as opposed to M-CLL, as these cells fail to respond to SDF-1 (269).

Ibrutinib also causes a reduction in BCL-2 levels in CLL cells which is a more pronounced effect when observed in UM-CLL over M-CLL clones (286). There is a consequent reduction in CLL B cell survival in tissue niches as a result of the BCL-2 effects particularly in UM-CLL cases.

In summary, ibrutinib causes a dual loss in environmental prosurvival signals; it causes a reduction in IL4 production by T cells and subsequent blocking of IL4-ILR4 axis with a reduced cell survival because of BCL-2 reduction leading to vulnerability of UM-CLL B cells which die in tissue niches (286).

These findings relate to my experimental results as the overwhelming majority of my samples in the pseudoemperipolesis assay were representative of CLL with high ZAP70 expression which is concordant with UM-CLL. As it is shown by the data demonstrated in 4.2, correlation between ZAP70 positive/UM-CLL and the BCR effects in the pseudoemperipolesis assay may be understood in terms of IL-4 changes. Also, as shown by my pseudoemperipolesis findings, there was concordance between ibrutinib and AZD8055 in their effects upon BCR-stimulated pseudoemperipolesis levels suggestive that the dual mTOR inhibitor AZD8055 may also act in this way. There were minimal effects of rapamycin upon migration in the pseudoemperipolesis, both in the presence and absence of BCR stimulation. As both ibrutinib and AZD8055 inhibit the mTOR signal effectively whereas rapamycin is directed at mTORC1, differential drug responses in the migration studies may be ascribed to mTORC2-mediated effects. However, a notable study of migration using endothelial cells was supportive of the ability of rapamycin to inhibit mTORC2 using downstream markers of mTORC2 inhibition. Indeed, rapamycin was shown to alter GTPase signalling and subsequently inhibited cytoskeletal activation in the endothelial cell experiments. Therefore it may be that a more prolonged exposure of CLL cells to rapamycin would elicit effects upon migration in the assays described in this project (279).

6.2.4 **BCR signalling**

BCR stimulation impacts CXCR4 surface expression although there has been some debate regarding the direction of effect as there are apparently conflicting reports (252, 253). Initial reports described that BCR ligation caused downregulation of CLL cell CXCR4 and CD62L levels on the cell surface and my data in 3.2.1 are supportive of these effects. However, an almost simultaneous report observed the opposite phenomenon: BCR ligation led to an increase in surface CXCR4 and these discrepancies are attributed to variation in the modality of BCR ligation and cell type studied however the same conclusions were drawn from each study, that long-term BCR ligation causes induction of an adhesive phenotype in CLL cells.

The mechanisms which underpin the reduction in sCXCR4 expression and changes in CXCR4 signalling have been studied with respect to functional responses of CLL cells in response to ibrutinib (269). I have shown that changes in sCXCR4 as mediated by anti-IgM responses are inhibited by mTOR inhibitor AZD8055 and ibrutinib but not by rapamycin (3.2.1). On further exploration of the ibrutinib mechanism of activity, functional changes are mediated by phosphorylation of CXCR4 at Serine 339 with downstream inhibition of the pathway at the level of the BTK protein after ligand binding (269). Further detail regarding the mechanism of ibrutinib activity involved another study with a focus on migration, utilising heavy water labelling of CLL cells prior to ibrutinib therapy to study their birth and death rates (287). Patients drank deuterated water with subsequent measurement of labelled CLL cell percentage. It was found that once the CLL cells reach a plateau there is a continuous proliferation rate and where one would expect a reduction in the percentage of CLL cells due to dilution effects, a plateau occurs when the birth rate is abrogated with a concomitant increase in the CLL death rate. Ibrutinib therefore inhibits proliferation and accelerates CLL cell death in two ways; firstly by death of BCR signal-dependent cells and by deprivation of CLL cells from other tissue survival signals.

The migration effects of ibrutinib were explored in my data in 3.2.3 with study of the *in vivo* effects of ibrutinib in a single patient. Whilst any effects from a single patient study must be interpreted with caution, there are trends in chemokine receptor surface expression which implicate CXCR4 surface changes as some of the initial means of cell redistribution. In 3.2.1, the CXCR4 surface changes that occur on the context of BCR stimulation occur both with ibrutinib and AZD8055 over the same timescale, indicating that parallels may be drawn with AZD8055 and ibrutinib as to the potential effects of AZD8055 *in vivo*. Exploration of the role of AZD8055 *in vivo* is beyond the scope of this project but support for its *in vivo* application is offered by these findings.

The mechanism underlying the BCR-mediated effects upon CLL cell surface marker expression may be understood further by the BCR effects upon miRNAs and may more likely relate to BCR-mediated changes over long-term incubation such as were shown in 3.1.6. MiRNAs mediate regulation of BCR and microenvironmental interactions (288). From the initial finding that miR15-16 is

integral to CLL pathogenesis, to the increased awareness of the function of miRNAs in participation in negative feedback loops, the details of the functional significance of miRNAs have not yet been worked out. As already stated, miRNAs are short complementary binding sequences which regulate stability of protein translation and individual sequences can regulate between 10 to greater than 100 miRNAs. CLL may exhibit both negative and positive BCR regulation and there is evidence that malignant cells may be dependent upon the BCR signal from both *in vitro* studies and clinical data regarding BTK inhibitors (289). From exome and genome profiling studies there are no specific BCR mutations responsible for CLL pathogenesis however it may be that non-coding RNAs are involved.

Microenvironmental interactions affect miRNA expression as shown in studies of recent LN emigrant CLL cells which were sorted by CXCR4 and CD5 levels (290). $CXCR4^{lo}$ $CD5^{hi}$ cells have low SHIP1 levels which correlates with a higher BCR signalling propensity and it has been identified that miR155 is a relevant regulator of SHIP1 as in CLL cells with higher levels of SHIP1 correlating with miR155 inhibition. In the CD40L co-culture setting there is an upregulation of miR155 and a downregulation of SHIP1. Other signals such as BAFF ligand confer a similar phenotype to CD40L, which is likely to originate from either follicular dendritic cells or stromal cells. Evidence from ibrutinib studies confirms that effects upon miRNAs relate to treatment response as miR155 is demonstrably reduced over time with ibrutinib therapy; it is known that higher miR155 levels over time confer shorter OS duration (291). Therapeutic targeting of miRNAs therefore offers an attractive opportunity to exploit the important role that is played in by miRNAs in CLL pathogenesis.

BCR signalling effects may be relayed to the cell nucleus in addition to the immediate effects at the plasma membrane and at the cytoplasmic level. A family of transcriptional regulators, Forkhead box O (FOXO) proteins, are known to have signalling interactions with mTOR kinase and are responsible for signal transduction to the cell nucleus. There 4 mammalian FOXO family members with FOXO1 being the first to be identified and found to be located on chromosome 13 in humans. It was originally implicated in the biology of rhabdomysarcoma with the t(2;13) translocation as part of the oncogenic process in the disease

(292). FOXO4 was next to be discovered and has been implicated in acute leukaemias, in particular, those leukaemias found to contain MLL gene rearrangements. It is of note that FOXO3 shares high homology with FOXO1 whereas FOXO6, the most recently discovered family-member is also the most distinct (293).

Some of the earliest information in relation to FOXO regulation by came from a study where three phosphorylation sites were identified which AKT may bind FOXO1; T24, S256 and S319, thus regulating its transcriptional effects (260). The mechanistic aspects of FOXO activation by AKT are complex and not fully understood. Both nuclear and cytoplasmic pools of FOXO proteins are present, and dependent upon the cell and specific isoform of FOXO there may be phosphorylation by AKT in either location (260). However much of the nuclear FOXO may be found without phosphorylation at the AKT sites. Phosphorylation of FOXO serves as a docking site for 14-3-3 protein binding and this mediates the effects upon FOXO DNA binding in inhibition of transcription by facilitating its degradation. Therefore, FOXO proteins act downstream of the mTOR signal offering a means of transcriptional regulation which may be modulated by mTOR inhibition.

In sections 3.2.4 and 3.2.5, I have demonstrated by Western blot for protein levels of FOXO1 that it may be upregulated by either form of stimulation and with the addition of short-term BCR stimulation, phosphorylation levels of the FOXO1 transcription factor follow the pattern of mTORC2 substrate AKT^{S473} with demonstrably reduced levels in the presence of either AZD8055 or ibrutinib. However, further work is required to confirm that the effects shown over 1 h BCR stimulation may be related to changes in nuclear FOXO1 phosphorylation and not cytoplasmic levels of FOXO1 which may offer an insight into the spatial and temporal regulation of FOXO1.

6.2.5 **Myeloid compartment and CLL progression**

The myeloid cellular contribution to the CLL microenvironment is derived from BM progenitors which are able to modulate lymphoid cell responses whereby immature myeloid derived cells promote differentiation of lymphoid cells.

Evidence from *in vitro* co-culture experiments demonstrate the survival support from myeloid derived cells given to CLL cells to prevent apoptosis even at low myeloid cell proportions. As previously described, monocytes which harbour TAM phenotypes exist to influence the tumour microenvironment (294, 295) and in CLL it is apparent that the leukaemic cells induce a TAM phenotype via chemokine production. There is also evidence that myeloid cells are immunosuppressive in CLL with evidence from clinical cases that display downregulation of immune regulatory genes from gene expression profiling.

The myeloid cell compartment has been examined experimentally in the EμTCL-1 mouse model which was first analysed for its myeloid component by removing splenocytes and injecting them into immature wild-type syngeneic mice, known as the adoptive transfer (AT) model. The AT model facilitates study of the influence of CLL upon the myeloid microenvironment as CLL-induced changes may be compared and contrasted. The AT model also permits study of the immune effects and effects upon disease development of myeloid cell depletion (296). Cytokine antibody arrays of the AT model display an overlap between 174 human and 144 murine cytokines elevated expression of many similar proteins in serum of individuals with inflammatory disease when compared with controls. Monocyte distribution control as a means of disease pathogenesis has been studied with an accumulation of patrolling monocytes as opposed to inflammatory monocytes with respect to Ly6C or CD43 status in mice affected by CLL. Peritoneal macrophages in the TCL-1 mouse model display a skew towards a TAM-like phenotype and monocytes from the same model have both an inflammatory and immunosuppressive phenotype.

Factors such as TREM-1 and PD-L1 have been implicated in the regulation of the inflammatory myeloid phenotype and these findings were explored further using the TCL-1 AT model (297). The development of CLL was studied over 3 weeks in mice treated with antagonists of PD1 or PD-L1 with the effect of slowing the onset of CLL without curing the disease in this model. It appears that PD-L1 blockade controls inflammation and restores myeloid and T cell effector dysfunction in CLL, laying the foundation for the use of such checkpoint inhibitors in clinical practice. Another strategy was to exploit the myeloid effects of sodium clodronate in the CLL mouse model with effects to deplete the

myeloid compartment resulting in attenuated CLL development, also controlling inflammation and restoring myeloid and T cell effector dysfunction in CLL (298).

CLL exosomes are known to influence the microenvironmental cross-talk with monocytes in CLL (299). On further study of the basis for the tumour-supportive phenotype in the myeloid cells, exosomes were isolated from CLL cell culture supernatant and these were applied to monocytes. Purification of exosomes was undertaken from plasma or cell lines and ultracentrifugation to pellet extracellular vesicles. Then nanoparticle tracking of labelled exosomes could be performed with uptake of MEC-1 cell exosomes in myeloid cells or to murine cell line J774 cells to be visualised by immunofluorescence (300). Small RNA sequencing of CLL exosomes and comparison with MEC-1 cells revealed up to 200 sequences which were enriched in CLL. The regions of enriched RNA were non-coding in nature and were described as “y4RNA”, appearing to induce PD-L1 in monocytes and macrophages and causing an increase in inflammatory cytokines. It appears that the response to hY4 RNAs is TLR7-dependent. A TLR7-knockout mouse to which exosomes or yRNAs were applied demonstrated that the upregulation of PD-L1 was lost in these mice. The effects of chloroquine were also to decrease exosome-mediated effects upon TLR7 and also showed attenuated disease development in the AT model (300).

Another CLL exosome purification study monitored the accumulation of labelled exosomes in CLL cytoplasm which were associated with a concomitant reduction in CCR2, an increase in PD-L1 and in monocyte production of CCL2, CCL4 and IL-6 (301). Using IF imaging and flow cytometry it is also possible to show that exosomes may be stimulated by the BCR signal (302), with activated B cells being able to produce exosomes which are blocked by ibrutinib.

6.2.6 **Mesenchymal stem cells in the BM microenvironment**

A greater understanding of the centrality of the CLL microenvironment to disease pathogenesis has formed the basis for many of the recent advances in CLL therapeutics and alongside this there has been an increased appreciation for CLL as a clonal entity with competing subclones, each with variation in genetic composition (137). Much of the research focus has been on the BCR signalling

pathway and its contribution to the CLL microenvironment, particularly with the development of specific inhibitors of the pathway. Indeed, it has become apparent that active participants in the constitution of CLL microenvironment comprises more than the cells of haemopoietic origin and that the MSC offer disease-defining interactions in their molecular interaction in the instance of incipient CLL. Genes regulated by MSC interactions with an importance for CLL pathogenesis include those relating to the PI3K signalling pathway, cellular metabolic and adhesion pathways such as XIAP, MCL-1 and BCL-2 (303).

Evidence for the protective effects of the microenvironment upon CLL cells originates from study of the cells in the peripheral circulation to show increased Bim, indicative of their tendency for programmed cell death. BM resident CLL cells, however, demonstrate a significant reduction in Bim levels. Also, in stromal cell co-culture, CLL cells demonstrate increased BCL-2 and increased BCL2A1, both of which offer relative resistance to BCL-2 inhibition *in vitro*. When MSC are cultured *in vitro* with CLL there is an increased proportion of CD38-positive CLL cells which may represent a predilection for these cells to home and bind to MSC cells in the *in vivo* setting (105). MSCs within the CLL microenvironment also play a key role in protecting the CLL cells from oxidative stress and subsequent apoptosis and this reliance upon oxidative phosphorylation CLL may be exploited therapeutically (304). In turn, CLL cells appear to exert an influence upon MSC cell signalling with an increase in levels of AKT and PI3K activity. Evidence from other diseases such as lymphoma and solid tumour-associated fibroblasts suggest an upregulated signal via the NFκB pathway as a basis for these effects.

A recent study of microenvironmental interactions downstream of chemokine signalling has revealed PIM kinases as one of the mediators of these signals (305). PIM kinases are a family of serine/threonine kinases which play a role in cellular processes of cell cycle initiation, apoptosis and DNA damage repair pathways among others. Levels of PIM kinases have been shown to be inducible under conditions of hypoxic stress and act in mediation of drug resistance, a phenomenon first observed in pancreatic ductal adenocarcinoma (306). However it has now been shown that PIM kinases may be targeted in CLL under conditions which mimic the hypoxic tumour environment and that strategies which combine

PIM kinase inhibition with the effects of PI3K inhibition may offer efficacy *in vitro* (307). The concept of targeting the aspects of the microenvironmental conditions which are known to be conducive to disease development and progression may be explored as a potential therapeutic strategy in CLL. The use of mTOR inhibitors in combination with current novel therapies which are already available for routine use may be applied in some cases of CLL. As the mTOR signal regulates the metabolic pathways of the cell it is thought that this may be why mTOR is so routinely dysregulated in oncogenesis. Therefore, mTOR inhibition may be applied as a means of depriving the tumour cell of nutrient and metabolic signals which may enhance disease progression, thereby attacking the malignant cells on two fronts.

The TCL-1 CLL mouse model has also offered further insights into the microenvironmental MSC contribution as the introduction of PKCβ gene knockout attenuates disease development when co-cultured with stromal cells, in relation to wild-type PKCβ TCL-1 models (308). It seems therefore that the MSC contribution is dependent upon cell-cell contact and further investigation has implicated Notch ligand which appears also to be constitutionally expressed upon the MSC cell surface, as well as on CLL cells. Evidence for the importance of Notch in MSCs, and Notch2 in particular, comes from Nestin^{GFP+} mice which are neural cells which are expressed to retain a "stemness" capacity for study of differentiation in these lineages. It appears that Notch activates the promoter in these cells and in the small population of MSCs which these mice (309).

Further study of Notch2 function in MSCs from Notch2-deficient floxed mice indicate that Notch2 is largely responsible for repression of other genes and those which are upregulated fall into categories of collagen formation or inflammatory response-mediators. Interestingly, somatic mutations which are known drivers of disease in CLL are often found to affect the Wnt/β-catenin signalling pathway by its aberrant activation. However, a robust increase in β-catenin within CLL cells may be exerted by culture of CLL cells on a layer of MSCs and this finding has been confirmed through IF studies to display increased β-catenin expression. From the use of CRISPR-Cas9 gene editing studies it was found that the elimination of Notch2 expression in MSC cells leads to a stabilisation of β-catenin through GSK3β binding. Therefore, therapeutic

approaches to target the Wnt signal may offer cytotoxic effects in CLL and may represent an indirect approach to target stromal Notch2 activity within the microenvironment. A range of approaches to target components of the disease microenvironment have already been discussed earlier in this chapter and include BTK inhibition to target the fibronectin – VCAM1 interaction, AMD3100 to target the CXCL12-CXCR4 axis sodium clodronate and checkpoint inhibitors, however other approaches which target the stromal cells associated with CLL cells may include Nox-A12 which inhibits migration of CLL cells via CXCL12 inhibition and permit CLL chemo-sensitisation (310). Furthermore, the immunomodulatory effects of lenalidomide may be applied to the CLL disease milieu with efficacy against CLL *in vivo* (311).

6.3 Advances in CLL pathogenesis

The next section is intended to summarise the latest advances in the understanding of CLL biology with a focus on discoveries made in relation to the underlying pathogenic process.

6.3.1 **Clonal evolution in CLL**

Whole exome sequencing was applied to 149 cases of CLL for study of disease clones, intra-tumoural heterogeneity and the factors associated with disease response to therapy and subsequent disease progression (138). Such sequencing studies serve to demonstrate the properties of CLL as a clonal disease within which clonal evolution occurs as a key feature of disease progression. The awareness of the existence of clones in CLL has been present for some time however until recently, the significance of the existence of disease clones was not clear. Features of CLL which make it amenable for study of clonal evolution include the relative slow-growing nature of the malignant cell population and as any changes may progress slowly over time. Therefore there is a greater chance of capturing a cross-section of the clonal populations when the disease is undertaking population shifts. Furthermore, the relative ease of sampling patients with CLL means that aliquots of blood may be sampled and stored for later analysis at disease progression. At stages of progression, novel genetic changes may be searched for within historical serial samples to identify their presence at very low levels.

Given the limitations of FISH evaluation in detection of somatic mutations in CLL, whole exome sequencing was used on 160 CLL cases and normal pairs; the CLL samples were selected to reflect the range of clinical features that occur in CLL (312). Twenty putative CLL cancer genes were detected at an increased rate with 9 (in bold) potential CLL driver mutations: *TP53, ATM, MYD88, SF3B1, NOTCH1, DDX3X, ZMYM3, FBXW7, XPO1, CHD2, POT1,* ***NRAS, KRAS, BCOR, EGR2, MED12, RIPK1, SAMHD1, ITPKB, HIST1H1E***. There were also 5 cytogenetic aberrations implicated in the cohort studied each of which are well-established contributors to CLL biology; deletions of 8p, 11q, 13q and 17p were found in addition to trisomy 12. All mutations or cytogenetic defects were found to be involved in a limited range of intracellular signalling pathways each of which play a role in CLL biology, these were DNA/ cell cycle regulation, Notch signalling, Wnt signalling, RNA processing/splicing and inflammatory pathways. Of note, increased age and UM IgV_H heavy chain status were associated with an increased number of subclonal mutations and the rate of such mutations increased with CLL therapy. Mutations were stratified by their clonal or subclonal status and temporal ordering of mutations was then inferred. Evolution patterns with chemotherapy were then studied and the negative prognostic influence of subclonal driver mutations was identified. These findings lay the basis for targeted therapies directed at subclonal driver mutations to prevent the expansion of such subclone, and may help to guide sequencing of available therapies with the knowledge of the evolutionary process of the disease (138).

6.3.2 Functional evaluation of somatic mutations contributing to CLL

Recent study has focused on the role of key recurrent somatic mutations in CLL as we seek to understand how specific mutations lead to disease progression. As an example, *SF3B1* is known as the catalytic core of the spliceosome and mutations affecting this gene independently predicts poor prognosis (138). To improve understanding of the contribution of SF3B1 to CLL development and progression, investigative strategies were employed to integrate transcriptome and functional analysis; gene set enrichment analysis identified multiple CLL pathways as being affected by mutation of SF3B1 and downstream signal alterations (313). Notch pathway activation was discovered in association with

mutation of SF3B1 by the study of overexpression of wild-type and mutated SF3B1 in multiple isogenic cell lines.

Notch signalling has been implicated in CLL cell migration and survival and is constitutively activated in the pathogenic process (116, 118). It was also discovered that subtle changes in DNA telomerase and in-frame deletion in DVL2 is associated with SF3B1 mutation and can inhibit Notch signalling *in vivo*. DVL2 is a Dishevelled protein family member; such proteins are implicated in the Wnt signalling pathway and are upregulated in multiple malignant diseases (73). Altered DVL2 is present in CLL with associated mutation of SF3B1 and it modulates the Notch signalling pathway but does not appear to affect Wnt signalling in progressive CLL. Furthermore, study of activating coding and non-coding mutations in CLL have led to the conclusion that somatic mutations are only one mechanism of genetic alteration in CLL and a range of changes occur including subclonal somatic copy number alterations and subclonal somatic single nucleotide variations, epigenetic changes, miRNAs and non-coding region affecting splice variants (313, 314).

Further study of the role of SF3B1 in CLL was undertaken with generation of a mouse line with conditional expression of SF3B1-K700E mutation. The mouse model was generated by $CD19^{+}$-$cre^{+/+}$ crossed with $SF3B1^{flox/+}$ mice and produced equivalent levels of protein between wild-type and mutant mice. The model gave evidence of oncogene-induced cellular senescence with SF3B1-K700E and a PCR array revealed 84 cellular senescence-associated genes. All such genes were upregulated in the mutant B cells, and 18 demonstrated a significant increase in expression. Of note, there was no evidence of leukaemia by B cell profiling over a 1 month period in the studied mice to aid with the conclusion that SF3B1 is predominantly a subclonal event, however cellular senescence appeared to be overturned in the mice with the combination of monoclonal B220+CD5+ cell infiltration in BM and spleen (313). Other work on CLL genetics has been conducted to address how somatic mutations contribute to natural progression of CLL, with a particular focus on genetic features of CLL with a poor prognostic phenotype. Based upon the described findings we appear to be moving towards a more comprehensive understanding of the genetic characteristics of CLL and are

now shifting focus to a review of somatic mutations to identify their critical oncogenic effects to determine the risk of individual defects (313).

6.3.3 Complex karyotype as a negative prognostic marker in CLL

Genomic complexity has been discovered as an independent predictor of a negative prognosis in CLL. Complex karyotype in CLL has been defined as the presence of 3 or more karyotypic abnormalities (315). Studies with venetoclax have demonstrated a poorer PFS in patients harbouring a complex karyotype and was an indicator of progressive disease (316). A complication of the study of genomic complexity has been a lack of standardisation of methods for its evaluation. Some studies employ lipopolysaccharide-stimulated metaphase cytogenetic analysis whereas others use multiple interphase FISH probes with whole genome array and whole genome sequencing are also in use. A recent study assessed the role of complex karyotype with a focus on FISH and lipopolysaccharide-stimulated metaphase cytogenetic analysis which found there to be a significant failure rate of the analysis (317). Also, complex karyotype was predictive of a negative prognosis independently of 17p deletion. Further studies to integrate different methods of chromosomal analysis with each with greater numbers of patients may provide a consensus on the role of genomic complexity to inform clinical decision-making.

6.4 BCR signalling inhibitors and other novel therapies: clinical trial data updated

6.4.1 BTK inhibitors in clinical trial

There has been a plethora of clinical trials undertaken to explore the use of BTK inhibitors since the commencement of my project. I aim to summarise some of the trials which have been completed and to outline some of those still in operation at the time of writing. The randomised, open-label phase 3 trial, RESONATE-2, was initiated to explore the role of ibrutinib in treatment of the elderly patients (median age 73) comparing ibrutinib with chlorambucil in previously untreated patients with CLL or SLL (318). Ibrutinib offered superior responses to chlorambucil across all outcomes with median PFS on ibrutinib not reached as opposed to 18.9 months with chlorambucil, and 2-year OS for

ibrutinib was 98% compared with 85% for chlorambucil. Interestingly, ibrutinib outcome was unaffected by high-risk prognostic features in the cohort of 296 patients studied, unlike chlorambucil. The HELIOS trial studied the effects of the addition of ibrutinib to regimens containing bendamustine and rituximab by randomising relapsed/refractory CLL patients to either ibrutinib and BR or placebo plus BR with significant benefits of ibrutinib across all progression and survival-based outcomes and with an MRD rate of 9% with ibrutinib as opposed to 2% without. However, the combination of BR and ibrutinib has not been adopted into treatment recommendations as cross-trial comparison fails to support the superiority of ibrutinib and BR over ibrutinib alone (319).

Building upon the initial safety and efficacy data (49), there are studies underway using acalabrutinib including a phase III study to compare acalabrutinib alone, acalabrutinib and obinutuzumab against chlorambucil with obinutuzumab in previously untreated elderly patients and those with lower performance status (NCT02475681). As chlorambucil and obinutuzumab is already a recognised treatment option for this category of patients, the performance of acalabrutinib alone and with obinutuzumab will be of great interest. There is a phase II trial to study the administration of acalabrutinib for those patients that are unsuitable for chemotherapy and received but were intolerant of ibrutinib (NCT02717611). The premise upon which acalabrutinib is indicated in the study population is that the relative low number of off-target effects in comparison with ibrutinib suggest an improved side effect profile and increased tolerability (320). Finally, a phase II comparison of ibrutinib and acalabrutinib is underway with the intext of demonstrating non-inferiority of acalabrutinib in the relapsed/refractory CLL patient (NCT02477696). Study outcomes include tolerability measures and there is potential study power to demonstrate superiority of acalabrutinib.

With regard to other BTK inhibitors in current clinical trial, GS-4059 is currently in phase I/II studies either alone or in combinations including obinutuzumab, SYK inhibitors or idelalisib and early indications are that it has tolerability and efficacy (NCT02968563). Indeed, long-term follow up of phase I studies confirms the tolerability of GS-4059 (321). SNS-062 is a non-covalent inhibitor of BTK which offers a means of inhibiting BTK where there is a C481S mutation. This

second generation BTK inhibitor has progressed through phase Ia with combined safety and efficacy studies are underway (322). Furthermore, BGB-3111, which is a covalent BTK inhibitor, is being studied in phase III comparisons with ibrutinib to see if it offers a difference in outcomes from the first-generation BTK inhibitor (*e.g.* NCT03336333).

Some questions remain: are there any novel agents with greater efficacy either alone or in combination when compared to current front-line chemoimmunotherapeutic options? Do second generation BTK inhibitors offer superior outcomes to ibrutinib in CLL and are there any agents which may overcome BTK resistance mutations? Also, are there any other BCR signalling inhibitors which offer a safe and efficacious combination with venetoclax? The aforementioned and following trials aim to address the outstanding clinical problems in CLL.

6.4.2 **SYK and PI3K inhibitors in clinical trial**

Strategies to target SYK in CLL more recently have focused on an oral, selective SYK inhibitor known as GS-9973, or entospletinib. At the time of writing, entospletinib had reached phase II studies and may offered as part of a trial either to be administered alone or in combination with other drugs such as obinutuzumab or idelalisib. Published data support the tolerability and efficacy of entospletinib in a population of pre-treated CLL patients (323). Also, dual SYK/JAK inhibitors have emerged such as PRT062070 (cerdulatinib) offer dual targeting of BCR and IL-4 signalling pathways which was originally shown *in vitro* (324). Interestingly, there has been some success *in vitro* with the combination of cerdulatinib and ibrutinib with specific applications for cases of ibrutinib resistance (325). A phase I/IIa dose escalation study of the selective anti-SYK/JAK agent cerdulatinib in CLL, SLL or NHL is currently in progress (NCT01994382).

The safety and efficacy of duvelisib has now been explored with results indicating that duvelisib may be applied in both treatment-naïve and relapsed/refractory CLL/SLL populations. Targeting of both PI3Kδ and γ is efficacious and causes minimal adverse effect with only mild elevation in

transaminases observed (326). Therefore, duvelisib has been identified as an eligible candidate for phase III testing and phase II study has also commenced for duvelisib in combination with venetoclax (NCT03534323).

6.4.3 **mTOR inhibitors in clinical trial**

First-in-human studies have now been performed to show the safety and efficacy of AZD2014 in solid tumours (327). At the time of writing, the only active clinical trial including a dual mTOR inhibitor is the TORCH study for evaluation of AZD2014 alone and with the addition of rituximab for relapsed/refractory DLBCL (NCT02752204). The phase II study in DLBCL which includes 36 patients, is estimated to complete in April 2019.

6.4.4 **CAR T cells**

Perhaps the most innovative therapy for haematological malignancies which has become clinically available as a treatment of CLL are chimaeric antigen receptor (CAR) T cells. A type of immunotherapy, known as adoptive cell transfer (ACT), the CAR T cell technology has been in existence for decades but has been refined to produce a greater and more sustainable yield of modified T cells for application in haematological disease.

Comprising 3 generations of molecular design, first generation CAR T cells only possessed an extracellular domain which generally takes the form of an antigen recognition molecule from the T cell receptor (TCR) or a cell surface receptor ligand directed at targets such as CD19. The intracellular component of the first generation molecules was merely an intracellular component of the CD3 molecule. Later versions of the molecule possess co-stimulatory domains including molecules such as CD28, CD134 and/or CD137 to provide the signal for T cell activation. Phase I/II trials show responses of 50 – 90 % overall responses in B cell malignancies which have not responded to standard therapies, with a curative outcome in some cases studied. The therapeutic approach requires harvest of the patient's T cells for adoptive transfer of the CAR construct. Thereafter, cells are expanded *in vitro* which takes a period of around 4 weeks, which may limit its utility in acute leukaemias but poses less difficulty for chronic malignancies such as CLL. Issues which may limit its therapeutic

application in CLL including the cytokine-release syndrome, which may be related to specific construct- or conditioning-related issues. Other complications may include B cell aplasia in the case of anti-CD19 CAR T cells, antigen-shedding of target cells which may be addressed by dual targeting of malignant cell-associated antigens and insertional mutagenesis originating from the viral vectors used to introduce the construct to the patients' T cell population. An understanding of the frequency of complications of CAR T cells, with the subsequent development of technologies to manage these adverse effects, may enhance the utility of CAR T cells and other immunotherapies in the treatment of haematological malignancies such as CLL (328).

6.5 Conclusions

Situated downstream of BCR signalling and exhibiting upregulated activity in CLL pathogenesis, the mTOR signalling pathway comprises two inter-linked kinase complexes: mTORC1 and mTORC2 (190). Selective mTORC1 therapeutic strategies utilising rapalogues have elicited only modest clinical responses with potential limitation due to consequential upregulation of AKT signalling. Ibrutinib and idelalisib, inhibitors of BCR-mediated signals, elicit a peripheral blood lymphocytosis indicative of CLL cell redistribution from the LN and BM niche; a characteristic clinical effect of mTORC1 inhibitors. Dual mTORC1/2 offers a mechanistic advantage over mTORC1 inhibition in closure of the mTORC1-mTORC2 negative feedback loop whilst providing an alternative means of BCR signal blockade. The aim of this study was to examine the functional and molecular impact of mTOR kinase inhibition on BCR- and chemokine-mediated CLL migration. Treatment with mTOR inhibitors for patients with CLL is supported by the data I have shown with dual mTOR inhibitor AZD8055 exhibiting superior efficacy of inhibition of the mTOR kinase complex over rapamycin *in vitro*. There are greater effects of AZD8055 upon CLL cell viability, upon cell surface markers which relate to CLL cell migration, there is more significant impact upon migration studies and upon downstream markers of migration including GTPases. Further work is required to elucidate the differential effects of mTOR inhibition upon colocalisation of GTPases and intracellular organelles by IF studies. AZD8055 offers greater depth of inhibition of the AKT signal than rapamycin thus from my work and that of others *in vitro* it may be supposed that

the effects of AZD8055 to target these molecules and signals *in vivo* would also be greater. The study of the effects of AZD8055 and its clinical analogue, AZD2014, are underway *in vivo* using the mouse model developed in our laboratory.

With a view to potential clinical uses for AZD2014, parallels may be drawn from *in vitro* data for solid tumours and their outcomes. Activity of the dual mTOR kinase inhibitor against ovarian cancer and breast cancer has been shown to overcome resistance mechanisms in disease models to paclitaxel or hormone therapy (329, 330). Studies such as these suggest putative roles for mTOR inhibition in targeting disease resistance to other agents or in targeting of multiple pathways simultaneously, so as to reduce “escape mechanisms” for the pro-survival signals that facilitate CLL progression, such as in the studies of cerdulatinib in combination with ibrutinib, for example (325).

One study which explored the combination of AZD2014 with BCL-2 inhibition by a small molecule inhibitor (ABT-737) demonstrated efficacy in combination against head and neck squamous cell carcinoma (331). Findings obtained from studies such as these may be applied to venetoclax as it is an orally bioavailable agent of the same class of ABT-737. However, the study of venetoclax in the treatment of acute myeloid leukaemia (AML) may be of greater relevance to CLL therapeutics (332). Both BCL-2 and MCL-1 are implicated in AML although the only available specific inhibitors are directed at BCL-2. The described study in AML focused on the efficacy of venetoclax in the inhibition of BCL-2 but demonstrated synergy with conventional chemotherapeutics. The study also utilised an AML xenograft model and found that selective targeting of BCL-2 and MCL-1 was sufficient to eliminate leukaemia from diseased mice. Therefore, the ability of AZD2014 and AZD8055 to inhibit MCL-1 as shown in 3.1.6 identifies the dual mTOR inhibitor as a potential agent for therapeutic approaches in combination with venetoclax (332).

In conclusion, I show functional and molecular studies supporting mTOR inhibition as a strategy for attenuating downstream BCR signalling. Microenvironmental modelling demonstrates similarity between AZD8055 and ibrutinib in their effects on CLL cell viability, CXCR4 levels, targeting of mTOR

kinase substrates and in changes in transwell migration with the addition of BCR. As ibrutinib targets upstream of mTOR activation, AZD8055 may circumvent the emerging resistance mutational changes in BTK or PLCγ that render ibrutinib ineffective in CLL (333, 334).

List of References

1. Schetelig J, de Wreede LC, Andersen NS, Moreno C, van Gelder M, Vitek A, et al. Centre characteristics and procedure-related factors have an impact on outcomes of allogeneic transplantation for patients with CLL: a retrospective analysis from the European Society for Blood and Marrow Transplantation (EBMT). Br J Haematol. 2017;178(4):521-33.
2. Delgado J, Villamor N. Chronic lymphocytic leukemia in young individuals revisited. Haematologica. 2014;99(1):4-5.
3. Cancer Research UK. Chronic lymphocytic leukaemia (CLL) incidence [URL]. http://www.cancerresearchuk.org/health-professional/cancer-statistics/statistics-by-cancer-type/leukaemia-cll#heading-Zero: Cancer Research UK; 2015 [Chronic lymphocytic leukaemia (CLL) statistics].
4. Cancer Research UK. Chronic lymphocytic leukaemia (CLL) mortality http://www.cancerresearchuk.org/health-professional/cancer-statistics/statistics-by-cancer-type/leukaemia-cll#heading-One: Cancer Research UK; 2015 [Chronic lymphocytic leukaemia (CLL) statistics].
5. Goldin LR, Pfeiffer RM, Li X, Hemminki K. Familial risk of lymphoproliferative tumors in families of patients with chronic lymphocytic leukemia: results from the Swedish Family-Cancer Database. Blood. 2004;104(6):1850-4.
6. Brown JR. Inherited susceptibility to chronic lymphocytic leukemia: evidence and prospects for the future. Ther Adv Hematol. 2013;4(4):298-308.
7. Tsimberidou AM, Wen S, McLaughlin P, O'Brien S, Wierda WG, Lerner S, et al. Other malignancies in chronic lymphocytic leukemia/small lymphocytic lymphoma. J Clin Oncol. 2009;27(6):904-10.
8. Parikh SA, Rabe KG, Kay NE, Call TG, Ding W, Schwager SM, et al. Chronic lymphocytic leukemia in young (≤ 55 years) patients: a comprehensive analysis of prognostic factors and outcomes. Haematologica. 2014;99(1):140-7.
9. Yang SM, Li JY, Gale RP, Huang XJ. The mystery of chronic lymphocytic leukemia (CLL): Why is it absent in Asians and what does this tell us about etiology, pathogenesis and biology? Blood Rev. 2015;29(3):205-13.
10. Matutes E, Owusu-Ankomah K, Morilla R, Garcia Marco J, Houlihan A, Que TH, et al. The immunological profile of B-cell disorders and proposal of a scoring system for the diagnosis of CLL. Leukemia. 1994;8(10):1640-5.
11. Moreau EJ, Matutes E, A'Hern RP, Morilla AM, Morilla RM, Owusu-Ankomah KA, et al. Improvement of the chronic lymphocytic leukemia scoring system with the monoclonal antibody SN8 (CD79b). Am J Clin Pathol. 1997;108(4):378-82.
12. Kohnke T, Wittmann VK, Bucklein VL, Lichtenegger F, Pasalic Z, Hiddemann W, et al. Diagnosis of CLL revisited: increased specificity by a modified five-marker scoring system including CD200. Br J Haematol. 2017;179(3):480-7.
13. Agathangelidis A, Darzentas N, Hadzidimitriou A, Brochet X, Murray F, Yan XJ, et al. Stereotyped B-cell receptors in one-third of chronic lymphocytic leukemia: a molecular classification with implications for targeted therapies. Blood. 2012;119(19):4467-75.
14. Visco C, Barcellini W, Maura F, Neri A, Cortelezzi A, Rodeghiero F. Autoimmune cytopenias in chronic lymphocytic leukemia. Am J Hematol. 2014;89(11):1055-62.

15. Hall AM, Vickers MA, McLeod E, Barker RN. Rh autoantigen presentation to helper T cells in chronic lymphocytic leukemia by malignant B cells. Blood. 2005;105(5):2007-15.
16. Efremov DG, Ivanovski M, Siljanovski N, Pozzato G, Cevreska L, Fais F, et al. Restricted immunoglobulin VH region repertoire in chronic lymphocytic leukemia patients with autoimmune hemolytic anemia. Blood. 1996;87(9):3869-76.
17. Weiss RB, Freiman J, Kweder SL, Diehl LF, Byrd JC. Hemolytic anemia after fludarabine therapy for chronic lymphocytic leukemia. J Clin Oncol. 1998;16(5):1885-9.
18. Pangalis GA, Roussou PA, Kittas C, Mitsoulis-Mentzikoff C, Matsouka-Alexandridis P, Anagnostopoulos N, et al. Patterns of bone marrow involvement in chronic lymphocytic leukemia and small lymphocytic (well differentiated) non-Hodgkin's lymphoma. Its clinical significance in relation to their differential diagnosis and prognosis. Cancer. 1984;54(4):702-8.
19. Mauro FR, Foa R, Cerretti R, Giannarelli D, Coluzzi S, Mandelli F, et al. Autoimmune hemolytic anemia in chronic lymphocytic leukemia: clinical, therapeutic, and prognostic features. Blood. 2000;95(9):2786-92.
20. Visco C, Novella E, Peotta E, Paolini R, Giaretta I, Rodeghiero F. Autoimmune hemolytic anemia in patients with chronic lymphocytic leukemia is associated with IgVH status. Haematologica. 2010;95(7):1230-2.
21. Visco C, Ruggeri M, Laura Evangelista M, Stasi R, Zanotti R, Giaretta I, et al. Impact of immune thrombocytopenia on the clinical course of chronic lymphocytic leukemia. Blood. 2008;111(3):1110-6.
22. Tsimberidou AM, Keating MJ. Richter syndrome: biology, incidence, and therapeutic strategies. Cancer. 2005;103(2):216-28.
23. Jamroziak K, Tadmor T, Robak T, Polliack A. Richter syndrome in chronic lymphocytic leukemia: updates on biology, clinical features and therapy. Leuk Lymphoma. 2015;56(7):1949-58.
24. Bruzzi JF, Macapinlac H, Tsimberidou AM, Truong MT, Keating MJ, Marom EM, et al. Detection of Richter's transformation of chronic lymphocytic leukemia by PET/CT. J Nucl Med. 2006;47(8):1267-73.
25. Jain N, Keating MJ. Richter transformation of CLL. Expert Rev Hematol. 2016;9(8):793-801.
26. Swerdlow SH, Campo E, Pileri SA, Harris NL, Stein H, Siebert R, et al. The 2016 revision of the World Health Organization classification of lymphoid neoplasms. Blood. 2016;127(20):2375-90.
27. Rai KR, Sawitsky A, Cronkite EP, Chanana AD, Levy RN, Pasternack BS. Clinical staging of chronic lymphocytic leukemia. Blood. 1975;46(2):219-34.
28. Binet JL, Auquier A, Dighiero G, Chastang C, Piguet H, Goasguen J, et al. A new prognostic classification of chronic lymphocytic leukemia derived from a multivariate survival analysis. Cancer. 1981;48(1):198-206.
29. Durig J, Nuckel H, Cremer M, Fuhrer A, Halfmeyer K, Fandrey J, et al. ZAP-70 expression is a prognostic factor in chronic lymphocytic leukemia. Leukemia. 2003;17(12):2426-34.
30. Molica S, Alberti A. Prognostic value of the lymphocyte doubling time in chronic lymphocytic leukemia. Cancer. 1987;60(11):2712-6.
31. Moreton P, Kennedy B, Lucas G, Leach M, Rassam SM, Haynes A, et al. Eradication of minimal residual disease in B-cell chronic lymphocytic leukemia after alemtuzumab therapy is associated with prolonged survival. J Clin Oncol. 2005;23(13):2971-9.
32. Rawstron AC, de Tute R, Jack AS, Hillmen P. Flow cytometric protein expression profiling as a systematic approach for developing disease-specific

assays: identification of a chronic lymphocytic leukaemia-specific assay for use in rituximab-containing regimens. Leukemia. 2006;20(12):2102-10.
33. Bottcher S, Ritgen M, Fischer K, Stilgenbauer S, Busch RM, Fingerle-Rowson G, et al. Minimal residual disease quantification is an independent predictor of progression-free and overall survival in chronic lymphocytic leukemia: a multivariate analysis from the randomized GCLLSG CLL8 trial. J Clin Oncol. 2012;30(9):980-8.
34. Dimier N, Delmar P, Ward C, Morariu-Zamfir R, Fingerle-Rowson G, Bahlo J, et al. A model for predicting effect of treatment on progression-free survival using MRD as a surrogate end point in CLL. Blood. 2018;131(9):955-62.
35. Molica S, Shanafelt TD, Giannarelli D, Gentile M, Mirabelli R, Cutrona G, et al. The chronic lymphocytic leukemia international prognostic index predicts time to first treatment in early CLL: Independent validation in a prospective cohort of early stage patients. Am J Hematol. 2016;91(11):1090-5.
36. Rai KR, Peterson BL, Appelbaum FR, Kolitz J, Elias L, Shepherd L, et al. Fludarabine compared with chlorambucil as primary therapy for chronic lymphocytic leukemia. N Engl J Med. 2000;343(24):1750-7.
37. Catovsky D, Richards S, Matutes E, Oscier D, Dyer MJ, Bezares RF, et al. Assessment of fludarabine plus cyclophosphamide for patients with chronic lymphocytic leukaemia (the LRF CLL4 Trial): a randomised controlled trial. Lancet. 2007;370(9583):230-9.
38. Keating MJ, O'Brien S, Albitar M, Lerner S, Plunkett W, Giles F, et al. Early results of a chemoimmunotherapy regimen of fludarabine, cyclophosphamide, and rituximab as initial therapy for chronic lymphocytic leukemia. J Clin Oncol. 2005;23(18):4079-88.
39. Hallek M, Fischer K, Fingerle-Rowson G, Fink AM, Busch R, Mayer J, et al. Addition of rituximab to fludarabine and cyclophosphamide in patients with chronic lymphocytic leukaemia: a randomised, open-label, phase 3 trial. Lancet. 2010;376(9747):1164-74.
40. Tam CS, O'Brien S, Plunkett W, Wierda W, Ferrajoli A, Wang X, et al. Long-term results of first salvage treatment in CLL patients treated initially with FCR (fludarabine, cyclophosphamide, rituximab). Blood. 2014;124(20):3059-64.
41. Knauf WU, Lissichkov T, Aldaoud A, Liberati A, Loscertales J, Herbrecht R, et al. Phase III randomized study of bendamustine compared with chlorambucil in previously untreated patients with chronic lymphocytic leukemia. J Clin Oncol. 2009;27(26):4378-84.
42. Fischer K, Cramer P, Busch R, Stilgenbauer S, Bahlo J, Schweighofer CD, et al. Bendamustine combined with rituximab in patients with relapsed and/or refractory chronic lymphocytic leukemia: a multicenter phase II trial of the German Chronic Lymphocytic Leukemia Study Group. J Clin Oncol. 2011;29(26):3559-66.
43. Goede V, Fischer K, Busch R, Engelke A, Eichhorst B, Wendtner CM, et al. Obinutuzumab plus chlorambucil in patients with CLL and coexisting conditions. N Engl J Med. 2014;370(12):1101-10.
44. Byrd JC, Furman RR, Coutre SE, Flinn IW, Burger JA, Blum KA, et al. Targeting BTK with ibrutinib in relapsed chronic lymphocytic leukemia. N Engl J Med. 2013;369(1):32-42.
45. Byrd JC, Furman RR, Coutre SE, Burger JA, Blum KA, Coleman M, et al. Three-year follow-up of treatment-naive and previously treated patients with CLL and SLL receiving single-agent ibrutinib. Blood. 2015;125(16):2497-506.
46. Rushworth SA, MacEwan DJ, Bowles KM. Ibrutinib in relapsed chronic lymphocytic leukemia. N Engl J Med. 2013;369(13):1277-8.

47. Brown JR, Hillmen P, O'Brien S, Barrientos JC, Reddy NM, Coutre SE, et al. Extended follow-up and impact of high-risk prognostic factors from the phase 3 RESONATE study in patients with previously treated CLL/SLL. Leukemia. 2018;32(1):83-91.
48. Ding W, LaPlant BR, Call TG, Parikh SA, Leis JF, He R, et al. Pembrolizumab in patients with CLL and Richter transformation or with relapsed CLL. Blood. 2017;129(26):3419-27.
49. Byrd JC, Harrington B, O'Brien S, Jones JA, Schuh A, Devereux S, et al. Acalabrutinib (ACP-196) in Relapsed Chronic Lymphocytic Leukemia. N Engl J Med. 2016;374(4):323-32.
50. Brown JR, Byrd JC, Coutre SE, Benson DM, Flinn IW, Wagner-Johnston ND, et al. Idelalisib, an inhibitor of phosphatidylinositol 3-kinase p110delta, for relapsed/refractory chronic lymphocytic leukemia. Blood. 2014;123(22):3390-7.
51. Furman RR, Sharman JP, Coutre SE, Cheson BD, Pagel JM, Hillmen P, et al. Idelalisib and rituximab in relapsed chronic lymphocytic leukemia. N Engl J Med. 2014;370(11):997-1007.
52. Jones JA, Robak T, Brown JR, Awan FT, Badoux X, Coutre S, et al. Efficacy and safety of idelalisib in combination with ofatumumab for previously treated chronic lymphocytic leukaemia: an open-label, randomised phase 3 trial. Lancet Haematol. 2017;4(3):e114-e26.
53. O'Brien SM, Lamanna N, Kipps TJ, Flinn I, Zelenetz AD, Burger JA, et al. A phase 2 study of idelalisib plus rituximab in treatment-naive older patients with chronic lymphocytic leukemia. Blood. 2015;126(25):2686-94.
54. Balakrishnan K, Peluso M, Fu M, Rosin NY, Burger JA, Wierda WG, et al. The phosphoinositide-3-kinase (PI3K)-delta and gamma inhibitor, IPI-145 (Duvelisib), overcomes signals from the PI3K/AKT/S6 pathway and promotes apoptosis in CLL. Leukemia. 2015;29(9):1811-22.
55. Flinn IW, O'Brien S, Kahl B, Patel M, Oki Y, Foss FF, et al. Duvelisib, a novel oral dual inhibitor of PI3K-delta,gamma, is clinically active in advanced hematologic malignancies. Blood. 2018;131(8):877-87.
56. Advani PP, Paulus A, Masood A, Sher T, Chanan-Khan A. Pharmacokinetic evaluation of oblimersen sodium for the treatment of chronic lymphocytic leukemia. Expert Opin Drug Metab Toxicol. 2011;7(6):765-74.
57. Durig J, Duhrsen U, Klein-Hitpass L, Worm J, Hansen JB, Orum H, et al. The novel antisense Bcl-2 inhibitor SPC2996 causes rapid leukemic cell clearance and immune activation in chronic lymphocytic leukemia. Leukemia. 2011;25(4):638-47.
58. Wilson WH, O'Connor OA, Czuczman MS, LaCasce AS, Gerecitano JF, Leonard JP, et al. Navitoclax, a targeted high-affinity inhibitor of BCL-2, in lymphoid malignancies: a phase 1 dose-escalation study of safety, pharmacokinetics, pharmacodynamics, and antitumour activity. Lancet Oncol. 2010;11(12):1149-59.
59. Souers AJ, Leverson JD, Boghaert ER, Ackler SL, Catron ND, Chen J, et al. ABT-199, a potent and selective BCL-2 inhibitor, achieves antitumor activity while sparing platelets. Nat Med. 2013;19(2):202-8.
60. Seymour JF, Ma S, Brander DM, Choi MY, Barrientos J, Davids MS, et al. Venetoclax plus rituximab in relapsed or refractory chronic lymphocytic leukaemia: a phase 1b study. Lancet Oncol. 2017;18(2):230-40.
61. van Gelder M, de Wreede LC, Bornhauser M, Niederwieser D, Karas M, Anderson NS, et al. Long-term survival of patients with CLL after allogeneic transplantation: a report from the European Society for Blood and Marrow Transplantation. Bone Marrow Transplant. 2017;52(3):372-80.

62. Kramer I, Stilgenbauer S, Dietrich S, Bottcher S, Zeis M, Stadler M, et al. Allogeneic hematopoietic cell transplantation for high-risk CLL: 10-year follow-up of the GCLLSG CLL3X trial. Blood. 2017;130(12):1477-80.
63. Decker DJ, Boyle NE, Koziol JA, Klinman NR. The expression of the Ig H chain repertoire in developing bone marrow B lineage cells. J Immunol. 1991;146(1):350-61.
64. Schamel WW, Reth M. Monomeric and oligomeric complexes of the B cell antigen receptor. Immunity. 2000;13(1):5-14.
65. Hardy RR. B cell ontogeny and B cell subsets. Curr Opin Immunol. 1989;2(2):189-98.
66. Hardy RR, Kincade PW, Dorshkind K. The protean nature of cells in the B lymphocyte lineage. Immunity. 2007;26(6):703-14.
67. Maier H, Ostraat R, Gao H, Fields S, Shinton SA, Medina KL, et al. Early B cell factor cooperates with Runx1 and mediates epigenetic changes associated with mb-1 transcription. Nat Immunol. 2004;5(10):1069-77.
68. Blyth K, Cameron ER, Neil JC. The RUNX genes: gain or loss of function in cancer. Nat Rev Cancer. 2005;5(5):376-87.
69. Hardy RR, Hayakawa K. B cell development pathways. Annu Rev Immunol. 2001;19:595-621.
70. Merrell KT, Benschop RJ, Gauld SB, Aviszus K, Decote-Ricardo D, Wysocki LJ, et al. Identification of anergic B cells within a wild-type repertoire. Immunity. 2006;25(6):953-62.
71. Lam KP, Rajewsky K. B cell antigen receptor specificity and surface density together determine B-1 versus B-2 cell development. J Exp Med. 1999;190(4):471-7.
72. Matthews AG, Oettinger MA. RAG: a recombinase diversified. Nat Immunol. 2009;10(8):817-21.
73. Khan AS, Hojjat-Farsangi M, Daneshmanesh AH, Hansson L, Kokhaei P, Osterborg A, et al. Dishevelled proteins are significantly upregulated in chronic lymphocytic leukaemia. Tumour Biol. 2016;37(9):11947-57.
74. Kim S, Davis M, Sinn E, Patten P, Hood L. Antibody diversity: somatic hypermutation of rearranged VH genes. Cell. 1981;27(3 Pt 2):573-81.
75. Kraal G, Weissman IL, Butcher EC. Germinal centre B cells: antigen specificity and changes in heavy chain class expression. Nature. 1982;298(5872):377-9.
76. Lanasa MC, Weinberg JB. Immunoglobulin class switch recombination in chronic lymphocytic leukemia. Leuk Lymphoma. 2011;52(7):1398-400.
77. Fais F, Sellars B, Ghiotto F, Yan XJ, Dono M, Allen SL, et al. Examples of in vivo isotype class switching in IgM+ chronic lymphocytic leukemia B cells. J Clin Invest. 1996;98(7):1659-66.
78. Radbruch A, Burger C, Klein S, Muller W. Control of immunoglobulin class switch recombination. Immunol Rev. 1986;89:69-83.
79. Muramatsu M, Sankaranand VS, Anant S, Sugai M, Kinoshita K, Davidson NO, et al. Specific expression of activation-induced cytidine deaminase (AID), a novel member of the RNA-editing deaminase family in germinal center B cells. J Biol Chem. 1999;274(26):18470-6.
80. Durandy A. Activation-induced cytidine deaminase: a dual role in class-switch recombination and somatic hypermutation. Eur J Immunol. 2003;33(8):2069-73.
81. Oppezzo P, Vuillier F, Vasconcelos Y, Dumas G, Magnac C, Payelle-Brogard B, et al. Chronic lymphocytic leukemia B cells expressing AID display dissociation between class switch recombination and somatic hypermutation. Blood. 2003;101(10):4029-32.

82. Morande PE, Sivina M, Uriepero A, Seija N, Berca C, Fresia P, et al. Ibrutinib therapy downregulates AID enzyme and proliferative fractions in chronic lymphocytic leukemia. Blood. 2019.
83. Rawstron AC, Bennett FL, O'Connor SJ, Kwok M, Fenton JA, Plummer M, et al. Monoclonal B-cell lymphocytosis and chronic lymphocytic leukemia. N Engl J Med. 2008;359(6):575-83.
84. Landgren O, Albitar M, Ma W, Abbasi F, Hayes RB, Ghia P, et al. B-cell clones as early markers for chronic lymphocytic leukemia. N Engl J Med. 2009;360(7):659-67.
85. Totterman TH, Carlsson M, Simonsson B, Bengtsson M, Nilsson K. T-cell activation and subset patterns are altered in B-CLL and correlate with the stage of the disease. Blood. 1989;74(2):786-92.
86. Fazi C, Scarfo L, Pecciarini L, Cottini F, Dagklis A, Janus A, et al. General population low-count CLL-like MBL persists over time without clinical progression, although carrying the same cytogenetic abnormalities of CLL. Blood. 2011;118(25):6618-25.
87. Casabonne D, Almeida J, Nieto WG, Romero A, Fernandez-Navarro P, Rodriguez-Caballero A, et al. Common infectious agents and monoclonal B-cell lymphocytosis: a cross-sectional epidemiological study among healthy adults. PLoS One. 2012;7(12):e52808.
88. Landgren O, Gridley G, Check D, Caporaso NE, Morris Brown L. Acquired immune-related and inflammatory conditions and subsequent chronic lymphocytic leukaemia. Br J Haematol. 2007;139(5):791-8.
89. Solomon BM, Chaffee KG, Moreira J, Schwager SM, Cerhan JR, Call TG, et al. Risk of non-hematologic cancer in individuals with high-count monoclonal B-cell lymphocytosis. Leukemia. 2016;30(2):331-6.
90. Hamblin TJ, Davis Z, Gardiner A, Oscier DG, Stevenson FK. Unmutated Ig V(H) genes are associated with a more aggressive form of chronic lymphocytic leukemia. Blood. 1999;94(6):1848-54.
91. Haslinger C, Schweifer N, Stilgenbauer S, Dohner H, Lichter P, Kraut N, et al. Microarray gene expression profiling of B-cell chronic lymphocytic leukemia subgroups defined by genomic aberrations and VH mutation status. J Clin Oncol. 2004;22(19):3937-49.
92. Kulis M, Heath S, Bibikova M, Queiros AC, Navarro A, Clot G, et al. Epigenomic analysis detects widespread gene-body DNA hypomethylation in chronic lymphocytic leukemia. Nat Genet. 2012;44(11):1236-42.
93. Jain P, Nogueras Gonzalez GM, Kanagal-Shamanna R, Rozovski U, Sarwari N, Tam C, et al. The absolute percent deviation of IGHV mutation rather than a 98% cut-off predicts survival of chronic lymphocytic leukaemia patients treated with fludarabine, cyclophosphamide and rituximab. Br J Haematol. 2018;180(1):33-40.
94. Wiestner A, Rosenwald A, Barry TS, Wright G, Davis RE, Henrickson SE, et al. ZAP-70 expression identifies a chronic lymphocytic leukemia subtype with unmutated immunoglobulin genes, inferior clinical outcome, and distinct gene expression profile. Blood. 2003;101(12):4944-51.
95. Marantidou F, Dagklis A, Stalika E, Korkolopoulou P, Saetta A, Anagnostopoulos A, et al. Activation-induced cytidine deaminase splicing patterns in chronic lymphocytic leukemia. Blood Cells Mol Dis. 2010;44(4):262-7.
96. Ghiotto F, Fais F, Valetto A, Albesiano E, Hashimoto S, Dono M, et al. Remarkably similar antigen receptors among a subset of patients with chronic lymphocytic leukemia. J Clin Invest. 2004;113(7):1008-16.

97. Messmer BT, Albesiano E, Efremov DG, Ghiotto F, Allen SL, Kolitz J, et al. Multiple distinct sets of stereotyped antigen receptors indicate a role for antigen in promoting chronic lymphocytic leukemia. J Exp Med. 2004;200(4):519-25.
98. Forconi F, Potter KN, Wheatley I, Darzentas N, Sozzi E, Stamatopoulos K, et al. The normal IGHV1-69-derived B-cell repertoire contains stereotypic patterns characteristic of unmutated CLL. Blood. 2010;115(1):71-7.
99. Anderson LA, Landgren O, Engels EA. Common community acquired infections and subsequent risk of chronic lymphocytic leukaemia. Br J Haematol. 2009;147(4):444-9.
100. Vergani S. CLL Stereotyped IGHV-D--J Rearrangements Can Be Detected in Normal B---Cell Populations Using Ultra--Deep, Next Generation Sequencing Techniques. XVII International Workshop on Chronic Lymphocytic Leukemia. 2017.
101. Darzentas N, Hadzidimitriou A, Murray F, Hatzi K, Josefsson P, Laoutaris N, et al. A different ontogenesis for chronic lymphocytic leukemia cases carrying stereotyped antigen receptors: molecular and computational evidence. Leukemia. 2010;24(1):125-32.
102. Damle RN, Wasil T, Fais F, Ghiotto F, Valetto A, Allen SL, et al. Ig V gene mutation status and CD38 expression as novel prognostic indicators in chronic lymphocytic leukemia. Blood. 1999;94(6):1840-7.
103. Ibrahim S, Keating M, Do KA, O'Brien S, Huh YO, Jilani I, et al. CD38 expression as an important prognostic factor in B-cell chronic lymphocytic leukemia. Blood. 2001;98(1):181-6.
104. Durig J, Naschar M, Schmucker U, Renzing-Kohler K, Holter T, Huttmann A, et al. CD38 expression is an important prognostic marker in chronic lymphocytic leukaemia. Leukemia. 2002;16(1):30-5.
105. Zucchetto A, Benedetti D, Tripodo C, Bomben R, Dal Bo M, Marconi D, et al. CD38/CD31, the CCL3 and CCL4 chemokines, and CD49d/vascular cell adhesion molecule-1 are interchained by sequential events sustaining chronic lymphocytic leukemia cell survival. Cancer Res. 2009;69(9):4001-9.
106. Dohner H, Stilgenbauer S, James MR, Benner A, Weilguni T, Bentz M, et al. 11q deletions identify a new subset of B-cell chronic lymphocytic leukemia characterized by extensive nodal involvement and inferior prognosis. Blood. 1997;89(7):2516-22.
107. Riches JC, O'Donovan CJ, Kingdon SJ, McClanahan F, Clear AJ, Neuberg DS, et al. Trisomy 12 chronic lymphocytic leukemia cells exhibit upregulation of integrin signaling that is modulated by NOTCH1 mutations. Blood. 2014;123(26):4101-10.
108. Dohner H, Stilgenbauer S, Fischer K, Bentz M, Lichter P. Cytogenetic and molecular cytogenetic analysis of B cell chronic lymphocytic leukemia: specific chromosome aberrations identify prognostic subgroups of patients and point to loci of candidate genes. Leukemia. 1997;11 Suppl 2:S19-24.
109. Rigolin GM, Cavallari M, Quaglia FM, Formigaro L, Lista E, Urso A, et al. In CLL, comorbidities and the complex karyotype are associated with an inferior outcome independently of CLL-IPI. Blood. 2017;129(26):3495-8.
110. Schaffner C, Stilgenbauer S, Rappold GA, Dohner H, Lichter P. Somatic ATM mutations indicate a pathogenic role of ATM in B-cell chronic lymphocytic leukemia. Blood. 1999;94(2):748-53.
111. Starostik P, Manshouri T, O'Brien S, Freireich E, Kantarjian H, Haidar M, et al. Deficiency of the ATM protein expression defines an aggressive subgroup of B-cell chronic lymphocytic leukemia. Cancer Res. 1998;58(20):4552-7.
112. Stankovic T, Stewart GS, Fegan C, Biggs P, Last J, Byrd PJ, et al. Ataxia telangiectasia mutated-deficient B-cell chronic lymphocytic leukemia occurs in

pregerminal center cells and results in defective damage response and unrepaired chromosome damage. Blood. 2002;99(1):300-9.
113. Pospisilova S, Gonzalez D, Malcikova J, Trbusek M, Rossi D, Kater AP, et al. ERIC recommendations on TP53 mutation analysis in chronic lymphocytic leukemia. Leukemia. 2012;26(7):1458-61.
114. Rossi D, Fangazio M, Rasi S, Vaisitti T, Monti S, Cresta S, et al. Disruption of BIRC3 associates with fludarabine chemorefractoriness in TP53 wild-type chronic lymphocytic leukemia. Blood. 2012;119(12):2854-62.
115. Rossi D, Spina V, Bomben R, Rasi S, Dal-Bo M, Bruscaggin A, et al. Association between molecular lesions and specific B-cell receptor subsets in chronic lymphocytic leukemia. Blood. 2013;121(24):4902-5.
116. Rosati E, Sabatini R, Rampino G, Tabilio A, Di Ianni M, Fettucciari K, et al. Constitutively activated Notch signaling is involved in survival and apoptosis resistance of B-CLL cells. Blood. 2009;113(4):856-65.
117. Rossi D, Rasi S, Fabbri G, Spina V, Fangazio M, Forconi F, et al. Mutations of NOTCH1 are an independent predictor of survival in chronic lymphocytic leukemia. Blood. 2012;119(2):521-9.
118. Lopez-Guerra M, Xargay-Torrent S, Rosich L, Montraveta A, Roldan J, Matas-Cespedes A, et al. The gamma-secretase inhibitor PF-03084014 combined with fludarabine antagonizes migration, invasion and angiogenesis in NOTCH1-mutated CLL cells. Leukemia. 2015;29(1):96-106.
119. Di Bernardo MC, Crowther-Swanepoel D, Broderick P, Webb E, Sellick G, Wild R, et al. A genome-wide association study identifies six susceptibility loci for chronic lymphocytic leukemia. Nat Genet. 2008;40(10):1204-10.
120. Kandaswamy R, Sava GP, Speedy HE, Bea S, Martin-Subero JI, Studd JB, et al. Genetic Predisposition to Chronic Lymphocytic Leukemia Is Mediated by a BMF Super-Enhancer Polymorphism. Cell Rep. 2016;16(8):2061-7.
121. Ramsay AJ, Quesada V, Foronda M, Conde L, Martinez-Trillos A, Villamor N, et al. POT1 mutations cause telomere dysfunction in chronic lymphocytic leukemia. Nat Genet. 2013;45(5):526-30.
122. Speedy HE, Kinnersley B, Chubb D, Broderick P, Law PJ, Litchfield K, et al. Germ line mutations in shelterin complex genes are associated with familial chronic lymphocytic leukemia. Blood. 2016;128(19):2319-26.
123. Andersson EI, Putzer S, Yadav B, Dufva O, Khan S, He L, et al. Discovery of novel drug sensitivities in T-PLL by high-throughput ex vivo drug testing and mutation profiling. Leukemia. 2018;32(3):774-87.
124. Clifford R, Louis T, Robbe P, Ackroyd S, Burns A, Timbs AT, et al. SAMHD1 is mutated recurrently in chronic lymphocytic leukemia and is involved in response to DNA damage. Blood. 2014;123(7):1021-31.
125. Tsujimoto Y, Finger LR, Yunis J, Nowell PC, Croce CM. Cloning of the chromosome breakpoint of neoplastic B cells with the t(14;18) chromosome translocation. Science. 1984;226(4678):1097-9.
126. Tsujimoto Y, Jaffe E, Cossman J, Gorham J, Nowell PC, Croce CM. Clustering of breakpoints on chromosome 11 in human B-cell neoplasms with the t(11;14) chromosome translocation. Nature. 1985;315(6017):340-3.
127. Tsujimoto Y, Croce CM. Analysis of the structure, transcripts, and protein products of bcl-2, the gene involved in human follicular lymphoma. Proc Natl Acad Sci U S A. 1986;83(14):5214-8.
128. Delbridge AR, Grabow S, Strasser A, Vaux DL. Thirty years of BCL-2: translating cell death discoveries into novel cancer therapies. Nat Rev Cancer. 2016;16(2):99-109.
129. Barbarotto E, Schmittgen TD, Calin GA. MicroRNAs and cancer: profile, profile, profile. Int J Cancer. 2008;122(5):969-77.

130. Aqeilan RI, Calin GA, Croce CM. miR-15a and miR-16-1 in cancer: discovery, function and future perspectives. Cell Death Differ. 2010;17(2):215-20.
131. Klein U, Lia M, Crespo M, Siegel R, Shen Q, Mo T, et al. The DLEU2/miR-15a/16-1 cluster controls B cell proliferation and its deletion leads to chronic lymphocytic leukemia. Cancer Cell. 2010;17(1):28-40.
132. Calin GA, Ferracin M, Cimmino A, Di Leva G, Shimizu M, Wojcik SE, et al. A MicroRNA signature associated with prognosis and progression in chronic lymphocytic leukemia. N Engl J Med. 2005;353(17):1793-801.
133. O'Brien SM, Cunningham CC, Golenkov AK, Turkina AG, Novick SC, Rai KR. Phase I to II multicenter study of oblimersen sodium, a Bcl-2 antisense oligonucleotide, in patients with advanced chronic lymphocytic leukemia. J Clin Oncol. 2005;23(30):7697-702.
134. Rassenti LZ, Balatti V, Ghia EM, Palamarchuk A, Tomasello L, Fadda P, et al. MicroRNA dysregulation to identify therapeutic target combinations for chronic lymphocytic leukemia. Proc Natl Acad Sci U S A. 2017;114(40):10731-6.
135. Balatti V, Rizzotto L, Miller C, Palamarchuk A, Fadda P, Pandolfo R, et al. TCL1 targeting miR-3676 is codeleted with tumor protein p53 in chronic lymphocytic leukemia. Proc Natl Acad Sci U S A. 2015;112(7):2169-74.
136. Pekarsky Y, Balatti V, Palamarchuk A, Rizzotto L, Veneziano D, Nigita G, et al. Dysregulation of a family of short noncoding RNAs, tsRNAs, in human cancer. Proc Natl Acad Sci U S A. 2016;113(18):5071-6.
137. Landau DA, Carter SL, Stojanov P, McKenna A, Stevenson K, Lawrence MS, et al. Evolution and impact of subclonal mutations in chronic lymphocytic leukemia. Cell. 2013;152(4):714-26.
138. Landau DA, Tausch E, Taylor-Weiner AN, Stewart C, Reiter JG, Bahlo J, et al. Mutations driving CLL and their evolution in progression and relapse. Nature. 2015;526(7574):525-30.
139. Rasi S, Khiabanian H, Ciardullo C, Terzi-di-Bergamo L, Monti S, Spina V, et al. Clinical impact of small subclones harboring NOTCH1, SF3B1 or BIRC3 mutations in chronic lymphocytic leukemia. Haematologica. 2016;101(4):e135-8.
140. Rossi D, Khiabanian H, Spina V, Ciardullo C, Bruscaggin A, Fama R, et al. Clinical impact of small TP53 mutated subclones in chronic lymphocytic leukemia. Blood. 2014;123(14):2139-47.
141. Dameshek W. Chronic lymphocytic leukemia--an accumulative disease of immunolgically incompetent lymphocytes. Blood. 1967;29(4):Suppl:566-84.
142. Messmer BT, Messmer D, Allen SL, Kolitz JE, Kudalkar P, Cesar D, et al. In vivo measurements document the dynamic cellular kinetics of chronic lymphocytic leukemia B cells. J Clin Invest. 2005;115(3):755-64.
143. Van den Hove LE, Van Gool SW, Vandenberghe P, Bakkus M, Thielemans K, Boogaerts MA, et al. CD40 triggering of chronic lymphocytic leukemia B cells results in efficient alloantigen presentation and cytotoxic T lymphocyte induction by up-regulation of CD80 and CD86 costimulatory molecules. Leukemia. 1997;11(4):572-80.
144. Kern C, Cornuel JF, Billard C, Tang R, Rouillard D, Stenou V, et al. Involvement of BAFF and APRIL in the resistance to apoptosis of B-CLL through an autocrine pathway. Blood. 2004;103(2):679-88.
145. Pontikoglou C, Kastrinaki MC, Klaus M, Kalpadakis C, Katonis P, Alpantaki K, et al. Study of the quantitative, functional, cytogenetic, and immunoregulatory properties of bone marrow mesenchymal stem cells in patients with B-cell chronic lymphocytic leukemia. Stem Cells Dev. 2013;22(9):1329-41.

146. Burger JA, Tsukada N, Burger M, Zvaifler NJ, Dell'Aquila M, Kipps TJ. Blood-derived nurse-like cells protect chronic lymphocytic leukemia B cells from spontaneous apoptosis through stromal cell-derived factor-1. Blood. 2000;96(8):2655-63.
147. Butcher EC, Picker LJ. Lymphocyte homing and homeostasis. Science. 1996;272(5258):60-6.
148. Burger JA, Burger M, Kipps TJ. Chronic lymphocytic leukemia B cells express functional CXCR4 chemokine receptors that mediate spontaneous migration beneath bone marrow stromal cells. Blood. 1999;94(11):3658-67.
149. Burkle A, Niedermeier M, Schmitt-Graff A, Wierda WG, Keating MJ, Burger JA. Overexpression of the CXCR5 chemokine receptor, and its ligand, CXCL13 in B-cell chronic lymphocytic leukemia. Blood. 2007;110(9):3316-25.
150. Till KJ, Lin K, Zuzel M, Cawley JC. The chemokine receptor CCR7 and alpha4 integrin are important for migration of chronic lymphocytic leukemia cells into lymph nodes. Blood. 2002;99(8):2977-84.
151. Calpe E, Codony C, Baptista MJ, Abrisqueta P, Carpio C, Purroy N, et al. ZAP-70 enhances migration of malignant B lymphocytes toward CCL21 by inducing CCR7 expression via IgM-ERK1/2 activation. Blood. 2011;118(16):4401-10.
152. Malavasi F, Deaglio S, Damle R, Cutrona G, Ferrarini M, Chiorazzi N. CD38 and chronic lymphocytic leukemia: a decade later. Blood. 2011;118(13):3470-8.
153. Girbl T, Hinterseer E, Grossinger EM, Asslaber D, Oberascher K, Weiss L, et al. CD40-mediated activation of chronic lymphocytic leukemia cells promotes their CD44-dependent adhesion to hyaluronan and restricts CCL21-induced motility. Cancer Res. 2013;73(2):561-70.
154. Burgess M, Gill D, Singhania R, Cheung C, Chambers L, Renyolds BA, et al. CD62L as a therapeutic target in chronic lymphocytic leukemia. Clinical cancer research : an official journal of the American Association for Cancer Research. 2013;19(20):5675-85.
155. Redondo-Munoz J, Escobar-Diaz E, Samaniego R, Terol MJ, Garcia-Marco JA, Garcia-Pardo A. MMP-9 in B-cell chronic lymphocytic leukemia is up-regulated by alpha4beta1 integrin or CXCR4 engagement via distinct signaling pathways, localizes to podosomes, and is involved in cell invasion and migration. Blood. 2006;108(9):3143-51.
156. Pasikowska M, Walsby E, Apollonio B, Cuthill K, Phillips E, Coulter E, et al. Phenotype and immune function of lymph node and peripheral blood CLL cells are linked to transendothelial migration. Blood. 2016;128(4):563-73.
157. Herishanu Y, Perez-Galan P, Liu D, Biancotto A, Pittaluga S, Vire B, et al. The lymph node microenvironment promotes B-cell receptor signaling, NF-kappaB activation, and tumor proliferation in chronic lymphocytic leukemia. Blood. 2011;117(2):563-74.
158. Calissano C, Damle RN, Hayes G, Murphy EJ, Hellerstein MK, Moreno C, et al. In vivo intraclonal and interclonal kinetic heterogeneity in B-cell chronic lymphocytic leukemia. Blood. 2009;114(23):4832-42.
159. Minici C, Gounari M, Ubelhart R, Scarfo L, Duhren-von Minden M, Schneider D, et al. Distinct homotypic B-cell receptor interactions shape the outcome of chronic lymphocytic leukaemia. Nat Commun. 2017;8:15746.
160. Rickert RC. New insights into pre-BCR and BCR signalling with relevance to B cell malignancies. Nat Rev Immunol. 2013;13(8):578-91.
161. Zhang M, Srivastava G, Lu L. The pre-B cell receptor and its function during B cell development. Cell Mol Immunol. 2004;1(2):89-94.

162. Damm F, Mylonas E, Cosson A, Yoshida K, Della Valle V, Mouly E, et al. Acquired initiating mutations in early hematopoietic cells of CLL patients. Cancer Discov. 2014;4(9):1088-101.
163. Kikushige Y, Ishikawa F, Miyamoto T, Shima T, Urata S, Yoshimoto G, et al. Self-renewing hematopoietic stem cell is the primary target in pathogenesis of human chronic lymphocytic leukemia. Cancer Cell. 2011;20(2):246-59.
164. Landau DA, Clement K, Ziller MJ, Boyle P, Fan J, Gu H, et al. Locally disordered methylation forms the basis of intratumor methylome variation in chronic lymphocytic leukemia. Cancer Cell. 2014;26(6):813-25.
165. Duhren-von Minden M, Ubelhart R, Schneider D, Wossning T, Bach MP, Buchner M, et al. Chronic lymphocytic leukaemia is driven by antigen-independent cell-autonomous signalling. Nature. 2012;489(7415):309-12.
166. Refaeli Y, Young RM, Turner BC, Duda J, Field KA, Bishop JM. The B cell antigen receptor and overexpression of MYC can cooperate in the genesis of B cell lymphomas. PLoS Biol. 2008;6(6):e152.
167. Apollonio B, Scielzo C, Bertilaccio MT, Ten Hacken E, Scarfo L, Ranghetti P, et al. Targeting B-cell anergy in chronic lymphocytic leukemia. Blood. 2013;121(19):3879-88, S1-8.
168. Coulter EM, Pepper A, Mele S, Folarin N, Townsend W, Cuthill K, et al. In vitro and in vivo evidence for uncoupling of B-cell receptor internalization and signaling in chronic lymphocytic leukemia. Haematologica. 2018;103(3):497-505.
169. Lam KP, Kuhn R, Rajewsky K. In vivo ablation of surface immunoglobulin on mature B cells by inducible gene targeting results in rapid cell death. Cell. 1997;90(6):1073-83.
170. Monroe JG. ITAM-mediated tonic signalling through pre-BCR and BCR complexes. Nat Rev Immunol. 2006;6(4):283-94.
171. Honigberg LA, Smith AM, Sirisawad M, Verner E, Loury D, Chang B, et al. The Bruton tyrosine kinase inhibitor PCI-32765 blocks B-cell activation and is efficacious in models of autoimmune disease and B-cell malignancy. Proc Natl Acad Sci U S A. 2010;107(29):13075-80.
172. Herman SE, Gordon AL, Hertlein E, Ramanunni A, Zhang X, Jaglowski S, et al. Bruton tyrosine kinase represents a promising therapeutic target for treatment of chronic lymphocytic leukemia and is effectively targeted by PCI-32765. Blood. 2011;117(23):6287-96.
173. Liu P, Cheng H, Roberts TM, Zhao JJ. Targeting the phosphoinositide 3-kinase pathway in cancer. Nat Rev Drug Discov. 2009;8(8):627-44.
174. Friedberg JW, Sharman J, Sweetenham J, Johnston PB, Vose JM, Lacasce A, et al. Inhibition of Syk with fostamatinib disodium has significant clinical activity in non-Hodgkin lymphoma and chronic lymphocytic leukemia. Blood. 2010;115(13):2578-85.
175. Weinblatt ME, Kavanaugh A, Genovese MC, Musser TK, Grossbard EB, Magilavy DB. An oral spleen tyrosine kinase (Syk) inhibitor for rheumatoid arthritis. N Engl J Med. 2010;363(14):1303-12.
176. Hoellenriegel J, Meadows SA, Sivina M, Wierda WG, Kantarjian H, Keating MJ, et al. The phosphoinositide 3'-kinase delta inhibitor, CAL-101, inhibits B-cell receptor signaling and chemokine networks in chronic lymphocytic leukemia. Blood. 2011;118(13):3603-12.
177. Hoellenriegel J, Coffey GP, Sinha U, Pandey A, Sivina M, Ferrajoli A, et al. Selective, novel spleen tyrosine kinase (Syk) inhibitors suppress chronic lymphocytic leukemia B-cell activation and migration. Leukemia. 2012;26(7):1576-83.
178. de Rooij MF, Kuil A, Geest CR, Eldering E, Chang BY, Buggy JJ, et al. The clinically active BTK inhibitor PCI-32765 targets B-cell receptor- and chemokine-

controlled adhesion and migration in chronic lymphocytic leukemia. Blood. 2012;119(11):2590-4.
179. Buchner M, Baer C, Prinz G, Dierks C, Burger M, Zenz T, et al. Spleen tyrosine kinase inhibition prevents chemokine- and integrin-mediated stromal protective effects in chronic lymphocytic leukemia. Blood. 2010;115(22):4497-506.
180. McCaig AM, Cosimo E, Leach MT, Michie AM. Dasatinib inhibits CXCR4 signaling in chronic lymphocytic leukaemia cells and impairs migration towards CXCL12. PLoS One. 2012;7(11):e48929.
181. Nakagawa R, Soh JW, Michie AM. Subversion of protein kinase C alpha signaling in hematopoietic progenitor cells results in the generation of a B-cell chronic lymphocytic leukemia-like population in vivo. Cancer Res. 2006;66(1):527-34.
182. Nakagawa R, Vukovic M, Tarafdar A, Cosimo E, Dunn K, McCaig AM, et al. Generation of a poor prognostic chronic lymphocytic leukemia-like disease model: PKCalpha subversion induces up-regulation of PKCbetaII expression in B lymphocytes. Haematologica. 2015;100(4):499-510.
183. Abrams ST, Lakum T, Lin K, Jones GM, Treweeke AT, Farahani M, et al. B-cell receptor signaling in chronic lymphocytic leukemia cells is regulated by overexpressed active protein kinase CbetaII. Blood. 2007;109(3):1193-201.
184. Johnson AJ, Lucas DM, Muthusamy N, Smith LL, Edwards RB, De Lay MD, et al. Characterization of the TCL-1 transgenic mouse as a preclinical drug development tool for human chronic lymphocytic leukemia. Blood. 2006;108(4):1334-8.
185. Shukla V, Ma S, Hardy RR, Joshi SS, Lu R. A role for IRF4 in the development of CLL. Blood. 2013;122(16):2848-55.
186. Ponader S, Chen SS, Buggy JJ, Balakrishnan K, Gandhi V, Wierda WG, et al. The Bruton tyrosine kinase inhibitor PCI-32765 thwarts chronic lymphocytic leukemia cell survival and tissue homing in vitro and in vivo. Blood. 2012;119(5):1182-9.
187. Suljagic M, Longo PG, Bennardo S, Perlas E, Leone G, Laurenti L, et al. The Syk inhibitor fostamatinib disodium (R788) inhibits tumor growth in the Eμ-TCL1 transgenic mouse model of CLL by blocking antigen-dependent B-cell receptor signaling. Blood. 2010;116(23):4894-905.
188. ten Hacken E, Scielzo C, Bertilaccio MT, Scarfò L, Apollonio B, Barbaglio F, et al. Targeting the LYN/HS1 signaling axis in chronic lymphocytic leukemia. Blood. 2013;121(12):2264-73.
189. Troeger A, Johnson AJ, Wood J, Blum WG, Andritsos LA, Byrd JC, et al. RhoH is critical for cell-microenvironment interactions in chronic lymphocytic leukemia in mice and humans. Blood. 2012;119(20):4708-18.
190. Guertin DA, Sabatini DM. Defining the role of mTOR in cancer. Cancer Cell. 2007;12(1):9-22.
191. Wang L, Harris TE, Roth RA, Lawrence JC, Jr. PRAS40 regulates mTORC1 kinase activity by functioning as a direct inhibitor of substrate binding. J Biol Chem. 2007;282(27):20036-44.
192. Oshiro N, Takahashi R, Yoshino K, Tanimura K, Nakashima A, Eguchi S, et al. The proline-rich Akt substrate of 40 kDa (PRAS40) is a physiological substrate of mammalian target of rapamycin complex 1. J Biol Chem. 2007;282(28):20329-39.
193. Pearce LR, Huang X, Boudeau J, Pawlowski R, Wullschleger S, Deak M, et al. Identification of Protor as a novel Rictor-binding component of mTOR complex-2. Biochem J. 2007;405(3):513-22.

194. Heitman J, Movva NR, Hall MN. Targets for cell cycle arrest by the immunosuppressant rapamycin in yeast. Science. 1991;253(5022):905-9.
195. Kunz J, Henriquez R, Schneider U, Deuter-Reinhard M, Movva NR, Hall MN. Target of rapamycin in yeast, TOR2, is an essential phosphatidylinositol kinase homolog required for G1 progression. Cell. 1993;73(3):585-96.
196. Feng J, Park J, Cron P, Hess D, Hemmings BA. Identification of a PKB/Akt hydrophobic motif Ser-473 kinase as DNA-dependent protein kinase. J Biol Chem. 2004;279(39):41189-96.
197. Phillips RJ, Mestas J, Gharaee-Kermani M, Burdick MD, Sica A, Belperio JA, et al. Epidermal growth factor and hypoxia-induced expression of CXC chemokine receptor 4 on non-small cell lung cancer cells is regulated by the phosphatidylinositol 3-kinase/PTEN/AKT/mammalian target of rapamycin signaling pathway and activation of hypoxia inducible factor-1alpha. J Biol Chem. 2005;280(23):22473-81.
198. Saucedo LJ, Gao X, Chiarelli DA, Li L, Pan D, Edgar BA. Rheb promotes cell growth as a component of the insulin/TOR signalling network. Nat Cell Biol. 2003;5(6):566-71.
199. Sarbassov DD, Guertin DA, Ali SM, Sabatini DM. Phosphorylation and regulation of Akt/PKB by the rictor-mTOR complex. Science. 2005;307(5712):1098-101.
200. Jacinto E, Facchinetti V, Liu D, Soto N, Wei S, Jung SY, et al. SIN1/MIP1 maintains rictor-mTOR complex integrity and regulates Akt phosphorylation and substrate specificity. Cell. 2006;127(1):125-37.
201. Laplante M, Sabatini DM. mTOR signaling in growth control and disease. Cell. 2012;149(2):274-93.
202. Choo AY, Yoon SO, Kim SG, Roux PP, Blenis J. Rapamycin differentially inhibits S6Ks and 4E-BP1 to mediate cell-type-specific repression of mRNA translation. Proc Natl Acad Sci U S A. 2008;105(45):17414-9.
203. Henske EP, Jozwiak S, Kingswood JC, Sampson JR, Thiele EA. Tuberous sclerosis complex. Nat Rev Dis Primers. 2016;2:16035.
204. Guertin DA, Stevens DM, Saitoh M, Kinkel S, Crosby K, Sheen JH, et al. mTOR complex 2 is required for the development of prostate cancer induced by Pten loss in mice. Cancer Cell. 2009;15(2):148-59.
205. Julien LA, Carriere A, Moreau J, Roux PP. mTORC1-activated S6K1 phosphorylates Rictor on threonine 1135 and regulates mTORC2 signaling. Molecular and cellular biology. 2010;30(4):908-21.
206. Dibble CC, Asara JM, Manning BD. Characterization of Rictor phosphorylation sites reveals direct regulation of mTOR complex 2 by S6K1. Molecular and cellular biology. 2009;29(21):5657-70.
207. Vezina C, Kudelski A, Sehgal SN. Rapamycin (AY-22,989), a new antifungal antibiotic. I. Taxonomy of the producing streptomycete and isolation of the active principle. J Antibiot (Tokyo). 1975;28(10):721-6.
208. Martel RR, Klicius J, Galet S. Inhibition of the immune response by rapamycin, a new antifungal antibiotic. Can J Physiol Pharmacol. 1977;55(1):48-51.
209. Eng CP, Sehgal SN, Vezina C. Activity of rapamycin (AY-22,989) against transplanted tumors. J Antibiot (Tokyo). 1984;37(10):1231-7.
210. Hudes G, Carducci M, Tomczak P, Dutcher J, Figlin R, Kapoor A, et al. Temsirolimus, interferon alfa, or both for advanced renal-cell carcinoma. N Engl J Med. 2007;356(22):2271-81.
211. Witzig TE, Geyer SM, Ghobrial I, Inwards DJ, Fonseca R, Kurtin P, et al. Phase II trial of single-agent temsirolimus (CCI-779) for relapsed mantle cell lymphoma. J Clin Oncol. 2005;23(23):5347-56.

212. Decker T, Sandherr M, Goetze K, Oelsner M, Ringshausen I, Peschel C. A pilot trial of the mTOR (mammalian target of rapamycin) inhibitor RAD001 in patients with advanced B-CLL. Annals of hematology. 2009;88(3):221-7.
213. Zent CS, LaPlant BR, Johnston PB, Call TG, Habermann TM, Micallef IN, et al. The treatment of recurrent/refractory chronic lymphocytic leukemia/small lymphocytic lymphoma (CLL) with everolimus results in clinical responses and mobilization of CLL cells into the circulation. Cancer. 2010;116(9):2201-7.
214. Chresta CM, Davies BR, Hickson I, Harding T, Cosulich S, Critchlow SE, et al. AZD8055 is a potent, selective, and orally bioavailable ATP-competitive mammalian target of rapamycin kinase inhibitor with in vitro and in vivo antitumor activity. Cancer Res. 2010;70(1):288-98.
215. Mi W, Ye Q, Liu S, She QB. AKT inhibition overcomes rapamycin resistance by enhancing the repressive function of PRAS40 on mTORC1/4E-BP1 axis. Oncotarget. 2015;6(16):13962-77.
216. Thoreen CC, Kang SA, Chang JW, Liu Q, Zhang J, Gao Y, et al. An ATP-competitive mammalian target of rapamycin inhibitor reveals rapamycin-resistant functions of mTORC1. J Biol Chem. 2009;284(12):8023-32.
217. Blunt MD, Carter MJ, Larrayoz M, Smith LD, Aguilar-Hernandez M, Cox KL, et al. The PI3K/mTOR inhibitor PF-04691502 induces apoptosis and inhibits microenvironmental signaling in CLL and the Emicro-TCL1 mouse model. Blood. 2015;125(26):4032-41.
218. Thijssen R, Ter Burg J, van Bochove GG, de Rooij MF, Kuil A, Jansen MH, et al. The pan phosphoinositide 3-kinase/mammalian target of rapamycin inhibitor SAR245409 (voxtalisib/XL765) blocks survival, adhesion and proliferation of primary chronic lymphocytic leukemia cells. Leukemia. 2016;30(9):1963.
219. Thijssen R, Ter Burg J, Garrick B, van Bochove GG, Brown JR, Fernandes SM, et al. Dual TORK/DNA-PK inhibition blocks critical signaling pathways in chronic lymphocytic leukemia. Blood. 2016;128(4):574-83.
220. Liu L, Chen L, Chung J, Huang S. Rapamycin inhibits F-actin reorganization and phosphorylation of focal adhesion proteins. Oncogene. 2008;27(37):4998-5010.
221. Fong S, Mounkes L, Liu Y, Maibaum M, Alonzo E, Desprez PY, et al. Functional identification of distinct sets of antitumor activities mediated by the FKBP gene family. Proc Natl Acad Sci U S A. 2003;100(24):14253-8.
222. Parasuraman P, Mulligan P, Walker JA, Li B, Boukhali M, Haas W, et al. Interaction of p190A RhoGAP with eIF3A and Other Translation Preinitiation Factors Suggests a Role in Protein Biosynthesis. J Biol Chem. 2017;292(7):2679-89.
223. Chen L, Xu B, Liu L, Liu C, Luo Y, Chen X, et al. Both mTORC1 and mTORC2 are involved in the regulation of cell adhesion. Oncotarget. 2015;6(9):7136-50.
224. Guba M, von Breitenbuch P, Steinbauer M, Koehl G, Flegel S, Hornung M, et al. Rapamycin inhibits primary and metastatic tumor growth by antiangiogenesis: involvement of vascular endothelial growth factor. Nat Med. 2002;8(2):128-35.
225. Liu L, Luo Y, Chen L, Shen T, Xu B, Chen W, et al. Rapamycin inhibits cytoskeleton reorganization and cell motility by suppressing RhoA expression and activity. J Biol Chem. 2010;285(49):38362-73.
226. Jacinto E, Loewith R, Schmidt A, Lin S, Ruegg MA, Hall A, et al. Mammalian TOR complex 2 controls the actin cytoskeleton and is rapamycin insensitive. Nat Cell Biol. 2004;6(11):1122-8.

227. Sarbassov DD, Ali SM, Kim DH, Guertin DA, Latek RR, Erdjument-Bromage H, et al. Rictor, a novel binding partner of mTOR, defines a rapamycin-insensitive and raptor-independent pathway that regulates the cytoskeleton. Curr Biol. 2004;14(14):1296-302.
228. Aubry L, Maeda M, Insall R, Devreotes PN, Firtel RA. The Dictyostelium mitogen-activated protein kinase ERK2 is regulated by Ras and cAMP-dependent protein kinase (PKA) and mediates PKA function. J Biol Chem. 1997;272(7):3883-6.
229. Leve F, de Souza W, Morgado-Diaz JA. A cross-link between protein kinase A and Rho-family GTPases signaling mediates cell-cell adhesion and actin cytoskeleton organization in epithelial cancer cells. J Pharmacol Exp Ther. 2008;327(3):777-88.
230. Scavello M, Petlick AR, Ramesh R, Thompson VF, Lotfi P, Charest PG. Protein kinase A regulates the Ras, Rap1 and TORC2 pathways in response to the chemoattractant cAMP in Dictyostelium. J Cell Sci. 2017;130(9):1545-58.
231. He Y, Li D, Cook SL, Yoon MS, Kapoor A, Rao CV, et al. Mammalian target of rapamycin and Rictor control neutrophil chemotaxis by regulating Rac/Cdc42 activity and the actin cytoskeleton. Mol Biol Cell. 2013;24(21):3369-80.
232. McDonald PC, Oloumi A, Mills J, Dobreva I, Maidan M, Gray V, et al. Rictor and integrin-linked kinase interact and regulate Akt phosphorylation and cancer cell survival. Cancer Res. 2008;68(6):1618-24.
233. Chen MY, Long Y, Devreotes PN. A novel cytosolic regulator, Pianissimo, is required for chemoattractant receptor and G protein-mediated activation of the 12 transmembrane domain adenylyl cyclase in Dictyostelium. Genes Dev. 1997;11(23):3218-31.
234. Helliwell SB, Schmidt A, Ohya Y, Hall MN. The Rho1 effector Pkc1, but not Bni1, mediates signalling from Tor2 to the actin cytoskeleton. Curr Biol. 1998;8(22):1211-4.
235. Liu L, Das S, Losert W, Parent CA. mTORC2 regulates neutrophil chemotaxis in a cAMP- and RhoA-dependent fashion. Dev Cell. 2010;19(6):845-57.
236. Agarwal NK, Chen CH, Cho H, Boulbes DR, Spooner E, Sarbassov DD. Rictor regulates cell migration by suppressing RhoGDI2. Oncogene. 2013;32(20):2521-6.
237. Pye DS, Rubio I, Pusch R, Lin K, Pettitt AR, Till KJ. Chemokine unresponsiveness of chronic lymphocytic leukemia cells results from impaired endosomal recycling of Rap1 and is associated with a distinctive type of immunological anergy. J Immunol. 2013;191(3):1496-504.
238. Till KJ, Harris RJ, Linford A, Spiller DG, Zuzel M, Cawley JC. Cell motility in chronic lymphocytic leukemia: defective Rap1 and alphaLbeta2 activation by chemokine. Cancer Res. 2008;68(20):8429-36.
239. Sutherland HJ, Eaves CJ, Lansdorp PM, Thacker JD, Hogge DE. Differential regulation of primitive human hematopoietic cells in long-term cultures maintained on genetically engineered murine stromal cells. Blood. 1991;78(3):666-72.
240. Adler J, Parmryd I. Colocalization analysis in fluorescence microscopy. Methods Mol Biol. 2013;931:97-109.
241. Nimmagadda SC, Frey S, Edelmann B, Hellmich C, Zaitseva L, Konig GM, et al. Bruton's tyrosine kinase and RAC1 promote cell survival in MLL-rearranged acute myeloid leukemia. Leukemia. 2018;32(3):846-9.
242. Herman SE, Niemann CU, Farooqui M, Jones J, Mustafa RZ, Lipsky A, et al. Ibrutinib-induced lymphocytosis in patients with chronic lymphocytic leukemia: correlative analyses from a phase II study. Leukemia. 2014.

243. Yang H, Rudge DG, Koos JD, Vaidialingam B, Yang HJ, Pavletich NP. mTOR kinase structure, mechanism and regulation. Nature. 2013;497(7448):217-23.
244. Pike KG, Malagu K, Hummersone MG, Menear KA, Duggan HM, Gomez S, et al. Optimization of potent and selective dual mTORC1 and mTORC2 inhibitors: the discovery of AZD8055 and AZD2014. Bioorg Med Chem Lett. 2013;23(5):1212-6.
245. Laprevotte E, Voisin G, Ysebaert L, Klein C, Daugrois C, Laurent G, et al. Recombinant human IL-15 trans-presentation by B leukemic cells from chronic lymphocytic leukemia induces autologous NK cell proliferation leading to improved anti-CD20 immunotherapy. J Immunol. 2013;191(7):3634-40.
246. Weinberg A, Zhang L, Brown D, Erice A, Polsky B, Hirsch MS, et al. Viability and functional activity of cryopreserved mononuclear cells. Clin Diagn Lab Immunol. 2000;7(4):714-6.
247. Garcia-Pineres AJ, Hildesheim A, Williams M, Trivett M, Strobl S, Pinto LA. DNAse treatment following thawing of cryopreserved PBMC is a procedure suitable for lymphocyte functional studies. J Immunol Methods. 2006;313(1-2):209-13.
248. Ma XM, Blenis J. Molecular mechanisms of mTOR-mediated translational control. Nat Rev Mol Cell Biol. 2009;10(5):307-18.
249. O'Hayre M, Salanga CL, Kipps TJ, Messmer D, Dorrestein PC, Handel TM. Elucidating the CXCL12/CXCR4 signaling network in chronic lymphocytic leukemia through phosphoproteomics analysis. PLoS One. 2010;5(7):e11716.
250. Munk R, Ghosh P, Ghosh MC, Saito T, Xu M, Carter A, et al. Involvement of mTOR in CXCL12 mediated T cell signaling and migration. PLoS One. 2011;6(9):e24667.
251. Quiroga MP, Balakrishnan K, Kurtova AV, Sivina M, Keating MJ, Wierda WG, et al. B-cell antigen receptor signaling enhances chronic lymphocytic leukemia cell migration and survival: specific targeting with a novel spleen tyrosine kinase inhibitor, R406. Blood. 2009;114(5):1029-37.
252. Vlad A, Deglesne PA, Letestu R, Saint-Georges S, Chevallier N, Baran-Marszak F, et al. Down-regulation of CXCR4 and CD62L in chronic lymphocytic leukemia cells is triggered by B-cell receptor ligation and associated with progressive disease. Cancer Res. 2009;69(16):6387-95.
253. Quiroga MP, Burger JA. BCR-mediated decrease of CXCR4 and CD62L in CLL. Cancer Res. 2010;70(12):5194; author reply 5.
254. Rombout A, Lust S, Offner F, Naessens E, Verhasselt B, Philippe J. Mimicking the tumour microenvironment of chronic lymphocytic leukaemia in vitro critically depends on the type of B-cell receptor stimulation. Br J Cancer. 2016;114(6):704-12.
255. Kimby E, Rincon J, Patarroyo M, Mellstedt H. Expression of adhesion molecules CD11/CD18 (Leu-CAMs, beta 2-integrins), CD54 (ICAM-1) and CD58 (LFA-3) in B-chronic lymphocytic leukemia. Leuk Lymphoma. 1994;13(3-4):297-306.
256. Bulian P, Shanafelt TD, Fegan C, Zucchetto A, Cro L, Nuckel H, et al. CD49d is the strongest flow cytometry-based predictor of overall survival in chronic lymphocytic leukemia. J Clin Oncol. 2014;32(9):897-904.
257. Deneys V, Thiry V, Hougardy N, Mazzon AM, Leveugle P, De Bruyere M. Impact of cryopreservation on B cell chronic lymphocytic leukaemia phenotype. J Immunol Methods. 1999;228(1-2):13-21.
258. Deglesne PA, Chevallier N, Letestu R, Baran-Marszak F, Beitar T, Salanoubat C, et al. Survival response to B-cell receptor ligation is restricted to progressive chronic lymphocytic leukemia cells irrespective of Zap70 expression. Cancer Res. 2006;66(14):7158-66.

259. Burger JA, Li KW, Keating MJ, Sivina M, Amer AM, Garg N, et al. Leukemia cell proliferation and death in chronic lymphocytic leukemia patients on therapy with the BTK inhibitor ibrutinib. JCI Insight. 2017;2(2):e89904.
260. Brunet A, Bonni A, Zigmond MJ, Lin MZ, Juo P, Hu LS, et al. Akt promotes cell survival by phosphorylating and inhibiting a Forkhead transcription factor. Cell. 1999;96(6):857-68.
261. Lemoine FM, Humphries RK, Abraham SD, Krystal G, Eaves CJ. Partial characterization of a novel stromal cell-derived pre-B-cell growth factor active on normal and immortalized pre-B cells. Exp Hematol. 1988;16(8):718-26.
262. D'Apuzzo M, Rolink A, Loetscher M, Hoxie JA, Clark-Lewis I, Melchers F, et al. The chemokine SDF-1, stromal cell-derived factor 1, attracts early stage B cell precursors via the chemokine receptor CXCR4. Eur J Immunol. 1997;27(7):1788-93.
263. Estes JD, Thacker TC, Hampton DL, Kell SA, Keele BF, Palenske EA, et al. Follicular dendritic cell regulation of CXCR4-mediated germinal center CD4 T cell migration. J Immunol. 2004;173(10):6169-78.
264. Park SH, Kim HR, Jun CD, Song WK, Park SG. Spin90 deficiency increases CXCL13-mediated B cell migration. Scand J Immunol. 2014;80(3):191-7.
265. Wehland J, Osborn M, Weber K. Phalloidin-induced actin polymerization in the cytoplasm of cultured cells interferes with cell locomotion and growth. Proc Natl Acad Sci U S A. 1977;74(12):5613-7.
266. Chazotte B. Labeling cytoskeletal F-actin with rhodamine phalloidin or fluorescein phalloidin for imaging. Cold Spring Harb Protoc. 2010;2010(5):pdb prot4947.
267. Carazo-Salas RE, Gruss OJ, Mattaj IW, Karsenti E. Ran-GTP coordinates regulation of microtubule nucleation and dynamics during mitotic-spindle assembly. Nat Cell Biol. 2001;3(3):228-34.
268. Tiwari S, Felekkis K, Moon EY, Flies A, Sherr DH, Lerner A. Among circulating hematopoietic cells, B-CLL uniquely expresses functional EPAC1, but EPAC1-mediated Rap1 activation does not account for PDE4 inhibitor-induced apoptosis. Blood. 2004;103(7):2661-7.
269. Chen SS, Chang BY, Chang S, Tong T, Ham S, Sherry B, et al. BTK inhibition results in impaired CXCR4 chemokine receptor surface expression, signaling and function in chronic lymphocytic leukemia. Leukemia. 2016;30(4):833-43.
270. Bivona TG, Philips MR. Analysis of Ras and Rap activation in living cells using fluorescent Ras binding domains. Methods. 2005;37(2):138-45.
271. Zheng Y, Liu H, Coughlin J, Zheng J, Li L, Stone JC. Phosphorylation of RasGRP3 on threonine 133 provides a mechanistic link between PKC and Ras signaling systems in B cells. Blood. 2005;105(9):3648-54.
272. Sun CX, Downey GP, Zhu F, Koh AL, Thang H, Glogauer M. Rac1 is the small GTPase responsible for regulating the neutrophil chemotaxis compass. Blood. 2004;104(12):3758-65.
273. Vincent AM, Cawley JC, Burthem J. Integrin function in chronic lymphocytic leukemia. Blood. 1996;87(11):4780-8.
274. Sembries S, Pahl H, Stilgenbauer S, Dohner H, Schriever F. Reduced expression of adhesion molecules and cell signaling receptors by chronic lymphocytic leukemia cells with 11q deletion. Blood. 1999;93(2):624-31.
275. Ramsay AG, Johnson AJ, Lee AM, Gorgun G, Le Dieu R, Blum W, et al. Chronic lymphocytic leukemia T cells show impaired immunological synapse formation that can be reversed with an immunomodulating drug. J Clin Invest. 2008;118(7):2427-37.

276. Ramsay AG, Evans R, Kiaii S, Svensson L, Hogg N, Gribben JG. Chronic lymphocytic leukemia cells induce defective LFA-1-directed T-cell motility by altering Rho GTPase signaling that is reversible with lenalidomide. Blood. 2013;121(14):2704-14.
277. Stamatopoulos B, Meuleman N, De Bruyn C, Pieters K, Mineur P, Le Roy C, et al. AMD3100 disrupts the cross-talk between chronic lymphocytic leukemia cells and a mesenchymal stromal or nurse-like cell-based microenvironment: pre-clinical evidence for its association with chronic lymphocytic leukemia treatments. Haematologica. 2012;97(4):608-15.
278. Liu L, Parent CA. Review series: TOR kinase complexes and cell migration. J Cell Biol. 2011;194(6):815-24.
279. Moss SC, Lightell DJ, Jr., Marx SO, Marks AR, Woods TC. Rapamycin regulates endothelial cell migration through regulation of the cyclin-dependent kinase inhibitor p27Kip1. J Biol Chem. 2010;285(16):11991-7.
280. Stevenson FK, Caligaris-Cappio F. Chronic lymphocytic leukemia: revelations from the B-cell receptor. Blood. 2004;103(12):4389-95.
281. Burger JA, Quiroga MP, Hartmann E, Burkle A, Wierda WG, Keating MJ, et al. High-level expression of the T-cell chemokines CCL3 and CCL4 by chronic lymphocytic leukemia B cells in nurselike cell cocultures and after BCR stimulation. Blood. 2009;113(13):3050-8.
282. Ten Hacken E, Sivina M, Kim E, O'Brien S, Wierda WG, Ferrajoli A, et al. Functional Differences between IgM and IgD Signaling in Chronic Lymphocytic Leukemia. J Immunol. 2016;197(6):2522-31.
283. Haerzschel A, Catusse J, Hutterer E, Paunovic M, Zirlik K, Eibel H, et al. BCR and chemokine responses upon anti-IgM and anti-IgD stimulation in chronic lymphocytic leukaemia. Annals of hematology. 2016;95(12):1979-88.
284. Hartmann EM, Rudelius M, Burger JA, Rosenwald A. CCL3 chemokine expression by chronic lymphocytic leukemia cells orchestrates the composition of the microenvironment in lymph node infiltrates. Leuk Lymphoma. 2016;57(3):563-71.
285. Chen SS RP, Ferrer G, Mazzarello AN, Palacios F, Ibrahim M, Kieso Y, Barrientos JC, Clark E, Sherry B, Burger JA, Rai K and Chiorazzi N. Ibrutinib Disrupts IL-4R - IL-4 Axis By Inhibiting IL-4R Signaling and Reversing Th2/Th1 Polarization through Diminished CLECL1 in CLL B Cells. Blood. 2017(130):387.
286. Chen SS. IL-4R – IL-4 axis Disruption by Ibrutinib Therapy Contributes to the Greater Vulnerability of U-CLL Clones to Loss of Microenvironmental Inputs. XVII International Workshop on Chronic Lymphocytic Leukemia. 2017.
287. Wodarz D, Garg N, Komarova NL, Benjamini O, Keating MJ, Wierda WG, et al. Kinetics of CLL cells in tissues and blood during therapy with the BTK inhibitor ibrutinib. Blood. 2014;123(26):4132-5.
288. Mraz M, Kipps TJ. MicroRNAs and B cell receptor signaling in chronic lymphocytic leukemia. Leuk Lymphoma. 2013;54(8):1836-9.
289. Burger JA, Montserrat E. Coming full circle: 70 years of chronic lymphocytic leukemia cell redistribution, from glucocorticoids to inhibitors of B-cell receptor signaling. Blood. 2013;121(9):1501-9.
290. Cui B, Ghia EM, Chen L, Rassenti LZ, DeBoever C, Widhopf GF, 2nd, et al. High-level ROR1 associates with accelerated disease progression in chronic lymphocytic leukemia. Blood. 2016;128(25):2931-40.
291. Guinn D, Ruppert AS, Maddocks K, Jaglowski S, Gordon A, Lin TS, et al. miR-155 expression is associated with chemoimmunotherapy outcome and is modulated by Bruton's tyrosine kinase inhibition with Ibrutinib. Leukemia. 2015;29(5):1210-3.

292. Galili N, Davis RJ, Fredericks WJ, Mukhopadhyay S, Rauscher FJ, 3rd, Emanuel BS, et al. Fusion of a fork head domain gene to PAX3 in the solid tumour alveolar rhabdomyosarcoma. Nat Genet. 1993;5(3):230-5.
293. Jacobs FM, van der Heide LP, Wijchers PJ, Burbach JP, Hoekman MF, Smidt MP. FoxO6, a novel member of the FoxO class of transcription factors with distinct shuttling dynamics. J Biol Chem. 2003;278(38):35959-67.
294. Mantovani A, Marchesi F, Malesci A, Laghi L, Allavena P. Tumour-associated macrophages as treatment targets in oncology. Nat Rev Clin Oncol. 2017;14(7):399-416.
295. Allavena P, Mantovani A. Immunology in the clinic review series; focus on cancer: tumour-associated macrophages: undisputed stars of the inflammatory tumour microenvironment. Clin Exp Immunol. 2012;167(2):195-205.
296. Hanna BS, McClanahan F, Yazdanparast H, Zaborsky N, Kalter V, Rossner PM, et al. Depletion of CLL-associated patrolling monocytes and macrophages controls disease development and repairs immune dysfunction in vivo. Leukemia. 2016;30(3):570-9.
297. McClanahan F, Hanna B, Miller S, Clear AJ, Lichter P, Gribben JG, et al. PD-L1 checkpoint blockade prevents immune dysfunction and leukemia development in a mouse model of chronic lymphocytic leukemia. Blood. 2015;126(2):203-11.
298. Galletti G, Scielzo C, Barbaglio F, Rodriguez TV, Riba M, Lazarevic D, et al. Targeting Macrophages Sensitizes Chronic Lymphocytic Leukemia to Apoptosis and Inhibits Disease Progression. Cell Rep. 2016;14(7):1748-60.
299. Paggetti J, Haderk F, Seiffert M, Janji B, Distler U, Ammerlaan W, et al. Exosomes released by chronic lymphocytic leukemia cells induce the transition of stromal cells into cancer-associated fibroblasts. Blood. 2015;126(9):1106-17.
300. Haderk F, Schulz R, Iskar M, Cid LL, Worst T, Willmund KV, et al. Tumor-derived exosomes modulate PD-L1 expression in monocytes. Sci Immunol. 2017;2(13).
301. Haderk F, Hanna B, Richter K, Schnolzer M, Zenz T, Stilgenbauer S, et al. Extracellular vesicles in chronic lymphocytic leukemia. Leuk Lymphoma. 2013;54(8):1826-30.
302. Yeh YY, Ozer HG, Lehman AM, Maddocks K, Yu L, Johnson AJ, et al. Characterization of CLL exosomes reveals a distinct microRNA signature and enhanced secretion by activation of BCR signaling. Blood. 2015;125(21):3297-305.
303. Herishanu Y, Katz BZ, Lipsky A, Wiestner A. Biology of chronic lymphocytic leukemia in different microenvironments: clinical and therapeutic implications. Hematol Oncol Clin North Am. 2013;27(2):173-206.
304. Jitschin R, Hofmann AD, Bruns H, Giessl A, Bricks J, Berger J, et al. Mitochondrial metabolism contributes to oxidative stress and reveals therapeutic targets in chronic lymphocytic leukemia. Blood. 2014;123(17):2663-72.
305. Decker S, Finter J, Forde AJ, Kissel S, Schwaller J, Mack TS, et al. PIM kinases are essential for chronic lymphocytic leukemia cell survival (PIM2/3) and CXCR4-mediated microenvironmental interactions (PIM1). Mol Cancer Ther. 2014;13(5):1231-45.
306. Blanco FF, Jimbo M, Wulfkuhle J, Gallagher I, Deng J, Enyenihi L, et al. The mRNA-binding protein HuR promotes hypoxia-induced chemoresistance through posttranscriptional regulation of the proto-oncogene PIM1 in pancreatic cancer cells. Oncogene. 2016;35(19):2529-41.
307. Crassini K, Shen Y, O'Dwyer M, O'Neill M, Christopherson R, Mulligan S, et al. The dual inhibitor of the phosphoinositol-3 and PIM kinases, IBL-202, is effective against chronic lymphocytic leukaemia cells under conditions that

mimic the hypoxic tumour microenvironment. Br J Haematol. 2018;182(5):654-69.
308. Lutzny G, Kocher T, Schmidt-Supprian M, Rudelius M, Klein-Hitpass L, Finch AJ, et al. Protein kinase c-beta-dependent activation of NF-kappaB in stromal cells is indispensable for the survival of chronic lymphocytic leukemia B cells in vivo. Cancer Cell. 2013;23(1):77-92.
309. Fazeli Z, Omrani MD, Ghaderian SM. Down-regulation of nestin in mesenchymal stem cells derived from peripheral blood through blocking bone morphogenesis pathway. J Cell Commun Signal. 2016;10(4):273-82.
310. Hoellenriegel J, Zboralski D, Maasch C, Rosin NY, Wierda WG, Keating MJ, et al. The Spiegelmer NOX-A12, a novel CXCL12 inhibitor, interferes with chronic lymphocytic leukemia cell motility and causes chemosensitization. Blood. 2014;123(7):1032-9.
311. Ramsay AG, Clear AJ, Fatah R, Gribben JG. Multiple inhibitory ligands induce impaired T-cell immunologic synapse function in chronic lymphocytic leukemia that can be blocked with lenalidomide: establishing a reversible immune evasion mechanism in human cancer. Blood. 2012;120(7):1412-21.
312. Gnirke A, Melnikov A, Maguire J, Rogov P, LeProust EM, Brockman W, et al. Solution hybrid selection with ultra-long oligonucleotides for massively parallel targeted sequencing. Nat Biotechnol. 2009;27(2):182-9.
313. Wang L, Brooks AN, Fan J, Wan Y, Gambe R, Li S, et al. Transcriptomic Characterization of SF3B1 Mutation Reveals Its Pleiotropic Effects in Chronic Lymphocytic Leukemia. Cancer Cell. 2016;30(5):750-63.
314. Landau DA, Wu CJ. Chronic lymphocytic leukemia: molecular heterogeneity revealed by high-throughput genomics. Genome Med. 2013;5(5):47.
315. Stamatopoulos K, Agathangelidis A, Rosenquist R, Ghia P. Antigen receptor stereotypy in chronic lymphocytic leukemia. Leukemia. 2017;31(2):282-91.
316. Anderson MA, Tam C, Lew TE, Juneja S, Juneja M, Westerman D, et al. Clinicopathological features and outcomes of progression of CLL on the BCL2 inhibitor venetoclax. Blood. 2017;129(25):3362-70.
317. Thompson PA, O'Brien SM, Wierda WG, Ferrajoli A, Stingo F, Smith SC, et al. Complex karyotype is a stronger predictor than del(17p) for an inferior outcome in relapsed or refractory chronic lymphocytic leukemia patients treated with ibrutinib-based regimens. Cancer. 2015;121(20):3612-21.
318. Burger JA, Tedeschi A, Barr PM, Robak T, Owen C, Ghia P, et al. Ibrutinib as Initial Therapy for Patients with Chronic Lymphocytic Leukemia. N Engl J Med. 2015;373(25):2425-37.
319. Chanan-Khan A, Cramer P, Demirkan F, Fraser G, Silva RS, Grosicki S, et al. Ibrutinib combined with bendamustine and rituximab compared with placebo, bendamustine, and rituximab for previously treated chronic lymphocytic leukaemia or small lymphocytic lymphoma (HELIOS): a randomised, double-blind, phase 3 study. Lancet Oncol. 2016;17(2):200-11.
320. Robak P, Robak T. Novel synthetic drugs currently in clinical development for chronic lymphocytic leukemia. Expert Opin Investig Drugs. 2017;26(11):1249-65.
321. Walter HS, Jayne S, Rule SA, Cartron G, Morschhauser F, Macip S, et al. Long-term follow-up of patients with CLL treated with the selective Bruton's tyrosine kinase inhibitor ONO/GS-4059. Blood. 2017;129(20):2808-10.
322. Thompson PA, Burger JA. Bruton's tyrosine kinase inhibitors: first and second generation agents for patients with Chronic Lymphocytic Leukemia (CLL). Expert Opin Investig Drugs. 2018;27(1):31-42.

323. Sharman J, Hawkins M, Kolibaba K, Boxer M, Klein L, Wu M, et al. An open-label phase 2 trial of entospletinib (GS-9973), a selective spleen tyrosine kinase inhibitor, in chronic lymphocytic leukemia. Blood. 2015;125(15):2336-43.
324. Blunt MD, Koehrer S, Dobson RC, Larrayoz M, Wilmore S, Hayman A, et al. The Dual Syk/JAK Inhibitor Cerdulatinib Antagonizes B-cell Receptor and Microenvironmental Signaling in Chronic Lymphocytic Leukemia. Clinical cancer research : an official journal of the American Association for Cancer Research. 2017;23(9):2313-24.
325. Guo A, Lu P, Coffey G, Conley P, Pandey A, Wang YL. Dual SYK/JAK inhibition overcomes ibrutinib resistance in chronic lymphocytic leukemia: Cerdulatinib, but not ibrutinib, induces apoptosis of tumor cells protected by the microenvironment. Oncotarget. 2017;8(8):12953-67.
326. O'Brien S, Patel M, Kahl BS, Horwitz SM, Foss FM, Porcu P, et al. Duvelisib, an oral dual PI3K-delta,gamma inhibitor, shows clinical and pharmacodynamic activity in chronic lymphocytic leukemia and small lymphocytic lymphoma in a Phase 1 study. Am J Hematol. 2018.
327. Basu B, Dean E, Puglisi M, Greystoke A, Ong M, Burke W, et al. First-in-Human Pharmacokinetic and Pharmacodynamic Study of the Dual m-TORC 1/2 Inhibitor AZD2014. Clinical cancer research : an official journal of the American Association for Cancer Research. 2015;21(15):3412-9.
328. Neelapu SS, Tummala S, Kebriaei P, Wierda W, Gutierrez C, Locke FL, et al. Chimeric antigen receptor T-cell therapy - assessment and management of toxicities. Nat Rev Clin Oncol. 2018;15(1):47-62.
329. Wong Te Fong AC, Thavasu P, Gagrica S, Swales KE, Leach MO, Cosulich SC, et al. Evaluation of the combination of the dual m-TORC1/2 inhibitor vistusertib (AZD2014) and paclitaxel in ovarian cancer models. Oncotarget. 2017;8(69):113874-84.
330. Guichard SM, Curwen J, Bihani T, D'Cruz CM, Yates JW, Grondine M, et al. AZD2014, an Inhibitor of mTORC1 and mTORC2, Is Highly Effective in ER+ Breast Cancer When Administered Using Intermittent or Continuous Schedules. Mol Cancer Ther. 2015;14(11):2508-18.
331. Li Y, Cui JT. Inhibition of Bcl-2 potentiates AZD-2014-induced anti-head and neck squamous cell carcinoma cell activity. Biochem Biophys Res Commun. 2016;477(4):607-13.
332. Teh TC, Nguyen NY, Moujalled DM, Segal D, Pomilio G, Rijal S, et al. Enhancing venetoclax activity in acute myeloid leukemia by co-targeting MCL1. Leukemia. 2018;32(2):303-12.
333. Cheng S, Guo A, Lu P, Ma J, Coleman M, Wang YL. Functional characterization of BTK(C481S) mutation that confers ibrutinib resistance: exploration of alternative kinase inhibitors. Leukemia. 2015;29(4):895-900.
334. Liu TM, Woyach JA, Zhong Y, Lozanski A, Lozanski G, Dong S, et al. Hypermorphic mutation of phospholipase C, gamma2 acquired in ibrutinib-resistant CLL confers BTK independency upon B-cell receptor activation. Blood. 2015;126(1):61-8.